MEASUREMENT-BASED PARAMETER ESTIMATION AND ANALYSIS OF POWER SYSTEM

Presented to
The Academic Faculty

by

Omer Lateef

In Partial Fulfillment
of the Requirements for the Degree
Doctor of Philosophy in the
Electrical Engineering

Georgia Institute of Technology
August 2020

Measurement-based Parameter Estimation and Analysis of Power System

Approved by:

Dr. Thomas G Habetler, Advisor
School of Electrical and Computer Engineering
Georgia Institute of Technology

Dr. Lukas Graber
School of Electrical and Computer Engineering
Georgia Institute of Technology

Dr. Daniel Molzahn
School of Electrical and Computer Engineering
Georgia Institute of Technology

Dr. Haomin Zhou
School of Mathematics
Georgia Institute of Technology

Dr. Santiago Carlos Grijalva
School of Electrical and Computer Engineering
Georgia Institute of Technology

Date Approved: May 14, 2020

==========

TABLE OF CONTENTS

ACKNOWLEDGMENT

As any work of intellect is seldom an outcome of an individual effort, this work is also made possible from the help of many. I am blessed with people, from family members and friends to my mentors and teachers, who always wanted the best for me. Without the comfort and guidance provided by them, this thesis could not have seen the light of the day.

If not impossible, it is almost next to impossible for me to mention all the people who have, somehow, helped me to embark on and complete my PhD (doing that would require a separate book). Therefore, I am mentioning those people whose help, I think, was indispensable.

Firstly, I would like to thank the Fulbright scholarship program for selecting me and providing me with an opportunity to study at one of the best universities in the world.

At Georgia Institute of Technology, I would like to appreciate many people. Most importantly, I would like to thank my first advisor, Prof. Ron G. Harley (April 27, 1940 - October 30, 2017), for guiding me during the initial years of my PhD studies. Long meetings with him had a lasting impact on me. The compassion with which he used to treat his students was exemplary. My interactions with him taught me that the most conducive environment for learning is the one in which the most attention is paid to the student-advisor relation. He always asked about my health and family before enquiring about research. He was always very welcoming. Whenever I encountered any difficulty, regardless of whether it was about research, I used to discuss it with him. He always listened patiently and did everything possible for him to resolve the issue. He used to advice

his students on topics ranging from current research, marriage, friendship, to parenting. And regardless of the domain, I was always amazed from his knowledge and wisdom. Meeting with him always kindled a new fire in me to explore new avenues of thoughts both within and outside my research area. This helped in preventing me from the provincialism that doing a PhD often entails. Unfortunately, Prof. Harley was diagnosed with terminal cancer soon after his 75th birthday was celebrated. It was a very painful and difficult time for all his students. He was so much committed that even during his last painful days, he was worried what his students would do in his absence. And, therefore, requested Prof. Thomas G. Habetler, his dearest friend, to take care of them after he is gone.

I would like to thank Prof. Habetler for accepting me as a student after the demise of Prof. Harley. If it was difficult time for me, it was a lot more difficult for him to lose a lifelong friend. Though being transferred to a new professor is not easy for any graduate student, especially when your relationship with the previous advisor is like it was between me and Prof. Harley, but Prof. Habetler did everything to make the transition effortless. It helped me that I already knew a lot about him as Prof. Harley often used to talk about his friendship with him.

I would like to thank Prof. Daniel Molzahn, who joined the department when I was preparing my proposal presentation. He was always very generous with his time. Though he was very busy adjusting to a new workplace, he always guided and helped me even when I approached him without an appointment. He gave me many suggestions which helped me a lot in resolving the problems I encountered during my research. His feedback helped me improve my thesis. I wish I could have spent more time with him and attended more of his courses.

I am also thankful to Prof. Santiago Grijalva for the valuable feedback he provided on my proposal and initial drafts of thesis.

I am indebted to Prof. Zhou for his guidance. I was fortunate enough to be his student in the class of Numerical Linear Algebra. Although I learnt a lot in the class, it was nothing compared to what I learned in the countless hours I spent with him outside the class. His enthusiasm about mathematics was contagious. We used to talk not only about Linear Algebra, but also about mathematicians and other branches of mathematics like functional analysis, set theory and real analysis. It was, primarily, due to the enthusiasm he instilled in me that I started reading various mathematics texts during my free time. The knowledge I gained from reading such texts helped me a lot in approaching the problems from different perspectives which helped me a lot in my research.

I am also thankful to Prof. Stephen Boyd of Stanford University. Although I have not attended any of his class in person, his online lectures on convex optimization and the accompanying book, that he has freely provided, helped me a lot.

I was fortunate to have many friends who helped me in all domains of life during my PhD studies. I would like to thank Dr. Ahmad Usman for receiving and accommodating me when I came to US. He was very hospitable and made every effort to ease the transition from my home country to a foreign land. I would like to thank Dr. Muhammad Ali Murtaza for being with me throughout my PhD. We shared many memorable moments and did discussion ranging from comics to latest research in many domains. I would also like to thank Dr. Usman Ali who mentored me during my initial years of PhD before completing his studies and returning to Pakistan. Dr. Aqeel Anwar and I took many courses together

and did many late-night discussions ranging from simulations to mathematical proofs. These discussions were very insightful as they always offered new perspective and helped me to consolidate the concepts. I want to thank Dr. Hamza, Dr. Rizwan and all the members of Pakistan house – Dr. Zaheer, Dr. Jawad, Mr. Ahmad Nawaz, Mr. Mubeen Ahmad, Mr. Adnan, Mr. Usama and Dr. Mutee – for their help during my stay there. I would also like to extend my thanks to Dr. Arslan with whom I stayed during the last days before leaving USA. I learnt a lot from him and had many fruitful discussions with him.

Last, but not-by-any-means the least, I would like to thank my family members: my parents, my brothers, my sisters-in-law and my wife. My parents always provided me with the best and instilled, early on, in me the importance of education. Without their help, I could not have achieved anything worthwhile. I am thankful to my brothers and their spouses for being always there for me during every thick and thin. They helped me a lot during the final stages of my PhD as I had to leave US, and therefore, complete some last parts of the thesis in Pakistan. They ensured my comfort and helped me complete my thesis timely. I would also like to thank my wife for all the encouragement and help she offered during my PhD. Without her, this long journey of PhD would have been a lot more difficult and lonelier.

LIST OF TABLES

LIST OF FIGURES

LIST OF SYMBOLS AND ABBREVIATIONS

PMU	Phasor Measurement Unit
Y_{bus}	Power system bus admittance matrix
Z_{bus}	Power system bus impedance matrix
EMS	Energy Management System
IED	Intelligent Electronic Device
RTU	Remote Terminal Unit

CHAPTER 1. BACKGROUND AND LITERATURE REVIEW

1.1 Background

Electricity is an essential component of the modern society. Therefore, power systems must reliably provide electricity. However, modern power systems are complex dynamic systems that can span countries and, in some cases, even subcontinents, and maintaining a reliable operation of such vast and complex systems can be challenging [1], [2]. Furthermore, the complexity of power systems will increase in the future due to several factors. Therefore, a novel set of tools will be required to meet the new technical challenges these systems will bring about [3]. Some tools that can be used to meet a few of such new challenges are proposed in the thesis.

Although electricity is an essential component of modern society, its production from the conventional energy sources is also one of the biggest sources of pollution. In future, the pollution caused by the production of electricity is likely to decrease as renewable energy sources will gradually replace their conventional counterparts [4]. Additionally, with the addition of prosumers and the incentive of net metering, small consumers with the facilities for energy production from a renewable source will also provide surplus power to the system [5], [6]. All these factors will contribute in increasing the proportion of renewable energy in electricity production.

This increased proportion of renewable energy in the production of electricity will shift the design-paradigm of power systems [7]. A conventional power system consists of a few large generating units connected through transmission lines to the load centers. However, in the future power systems, these large thermal units will be replaced by a set

of distributed and small generating units, most of which will be based on renewable energy sources. Though the increased proportion of renewable energy for electricity production will help in reducing the pollution, this shift will also introduce a new set of technical challenges in maintaining a reliable and secure operation of power systems [8].

Renewable sources, unlike their conventional thermal counterparts, are much more variable sources of energy. Moreover, renewable energy sources provide a far less control over the produced electricity compared to the conventional sources. Therefore, the increased participation of renewable energy sources in electricity production will introduce much more variability in power systems. To accommodate this increased variability in power production, future power systems must be more flexible [9]–[12] than the existing power systems. Additionally, under specific conditions, this increased variation of power injected into the power system buses will congest certain power lines [13]. Therefore, future power systems must also have the adaptability to change their topology to address the issue of congestion. Such an adaptability is necessary for power systems of future to operate economically and reliably [3], [14]–[16].

All these factors will cause future power systems to be far more complex than those currently in use. This increased complexity will make it difficult to maintain a secure and efficient operation of such systems [17]. Recent blackouts [18], [19] have highlighted drawbacks in the current operating practices of power systems. These drawbacks show, among other things, that the current practices will not be able to meet the reliability criteria for the much more variable and far more complex power systems of the future. Therefore, to meet the reliability criteria, the techniques currently used for the analysis of power systems, suited to centralized and static systems, need to be replaced with novel ones suited

to distributed and dynamic power systems of the future [3], [20]. In this study, various such techniques are proposed.

1.2 Model-Based Power System Analysis

Presently, all of power system analysis is carried out in a centralized Energy Management System (EMS) based on offline models [21]. The offline models of the components of a power system are derived during their design. The parameters of these models are calculated using the physical attributes of the components and are thereafter stored in a database in the EMS. In an EMS, the topology of a power system is decided from the statuses of its circuit breakers communicated by the Remote Terminal Units (RTUs) installed at the substations [22]. The topology, thereby derived, is used along with the offline parameters, stored in the database, to generate a power system model in the EMS. This scheme of power system modeling is illustrated in Figure 1.1.

This offline, model-based approach to modeling can result in an erroneous model and, therefore, is not recommended [3] in future power systems. The errors in the model may be due to some human miscalculation [21], difficulty in modeling a component (e.g., the junction between a cable and a transmission line), or variations in the parameter values of the components due to the changes in the loading and atmospheric conditions [23]. These variations are often neglected in the offline approach to mathematical modeling of power systems which results in the erroneous parameters.

Additionally, in a conventional power system, the status of a circuit breaker is decided, in an EMS, through a signal communicated from an RTU installed in the corresponding substation. If, somehow, this signal has the wrong status of the underlying

breaker, the topology of the system thereby decided will be erroneous. This erroneous topology results in a lack of the situational awareness of a power system. Such a lack of situational awareness can [3] and has contributed [24] in a blackout of a power system.

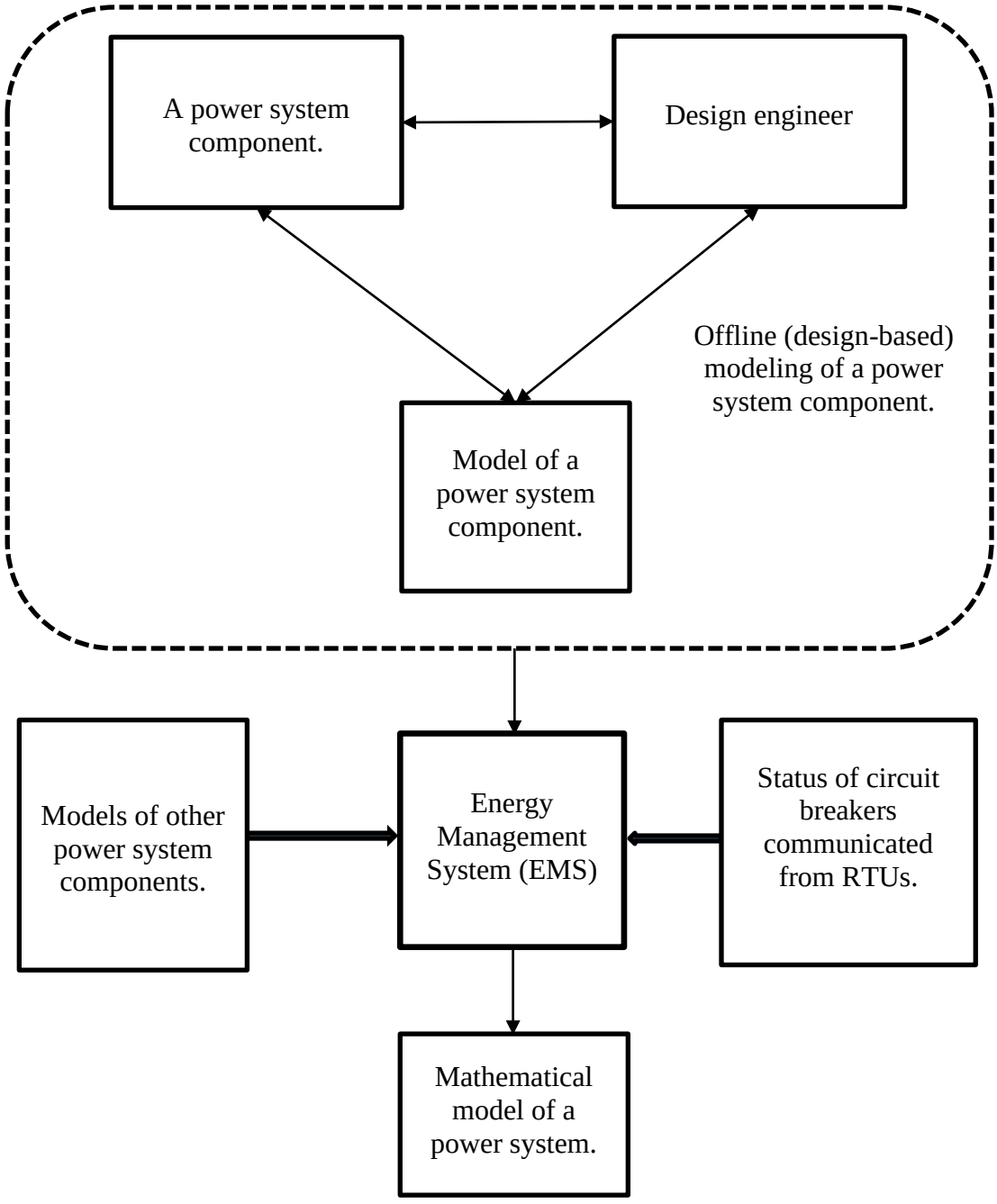

Figure 1.1 - Offline (design-based) modeling paradigm of a power system.

Due to all the above-mentioned drawbacks of the current modeling approach, some other scheme should be adapted for the mathematical modeling of future power systems. An alternative to the model-based (offline) approach to modeling is the measurement-based (online) approach [3], [25].

1.3 Measurement-Based Power System Analysis

In the measurement-based approach to mathematical modeling, an algorithm generates a model of system using the measurements taken by the instruments installed in the system. The measurement-based modeling paradigm for a power system is illustrated in Figure 1.2. As an algorithm is used for the modeling, the factor of human miscalculation reduces substantially. Additionally, using such an approach, the drawbacks of the offline, model-based, modeling of a power system can be resolved.

The accuracy of a measurement-based model depends on two factors: the robustness of the algorithm used for modeling, the accuracy and the precision of the metering devices being used. Therefore, to use measurement-based methods for estimation and modeling, the installation of highly accurate metering devices is recommended. For power systems, Phasor Measurement Units (PMUs) belong to such a class of accurate metering devices.

A PMU [26], installed at any bus, can accurately measure many variables, including the current phasors in the attached lines and the voltage phasors at the bus of installation. The accuracy of these measurements primarily depends on the quality of the transducers and can, therefore, be further improved by using high quality transducers. In the future, high quality transducers such as electronic or optical potential and current transformers will be used instead of their magnetic counterparts [3] which will further improve the

accuracy of the measurements. This increase in the accuracy of measurements will further improve the results of measurement-based techniques of modeling in power systems.

For accurate modeling of the components of power systems, many measurement-based techniques have already been presented [27]. Almost all such techniques assume the availability of highly accurate phasor measurements provided by PMUs. For example, [28] proposes an online technique to estimate the temperature, sag and ABCD parameters of a line using PMUs' measurements at both the ends of the transmission line. The errors in the model-based parameters values of power lines are discussed in [21]. Additionally, using the PMUs measurements, a method for the real-time evaluation of line parameters is presented. Using the phasor measurements at a generator's terminals, [29] proposes a technique based on the Kalman filter to simultaneously estimate the parameters of a synchronous generator, governor and exciter. In [30], the bus admittance matrix is estimated by assuming that the bus injection currents are signals produced from a random process. The corresponding voltages of the buses are also assumed to be random signals related to the injection currents through a cross-covariance matrix. Using statistical signal processing technique, the cross-covariance matrix is evaluated and shown to be equal to the bus admittance matrix of the underlying system. However, the % variations in the loads are not are not mentioned for the various sets of measurements. The technique not only requires a large variation in the loads connected to the power system but also is not shown to be robust against the fault measurements. The measurement-based distribution factors are evaluated in [31], [32] with the assumption that phasor measurements are available at each bus of the power system. Lastly, [33] discusses the practical experience of real-time identifications of the parameters of transmission lines in the Southern Power Grid of China.

It is high time, due to the advantages offered, that the conventional model-based offline approaches for the modeling of power systems be replaced by their measurement-based counterparts. Although the hardware required for this replacement has been available for some time, the algorithms needed for its realization have not yet been adopted or proposed [20]. In this regard, many measurement-based algorithms are proposed in this work for the accurate estimation of the parameters of a power system's components.

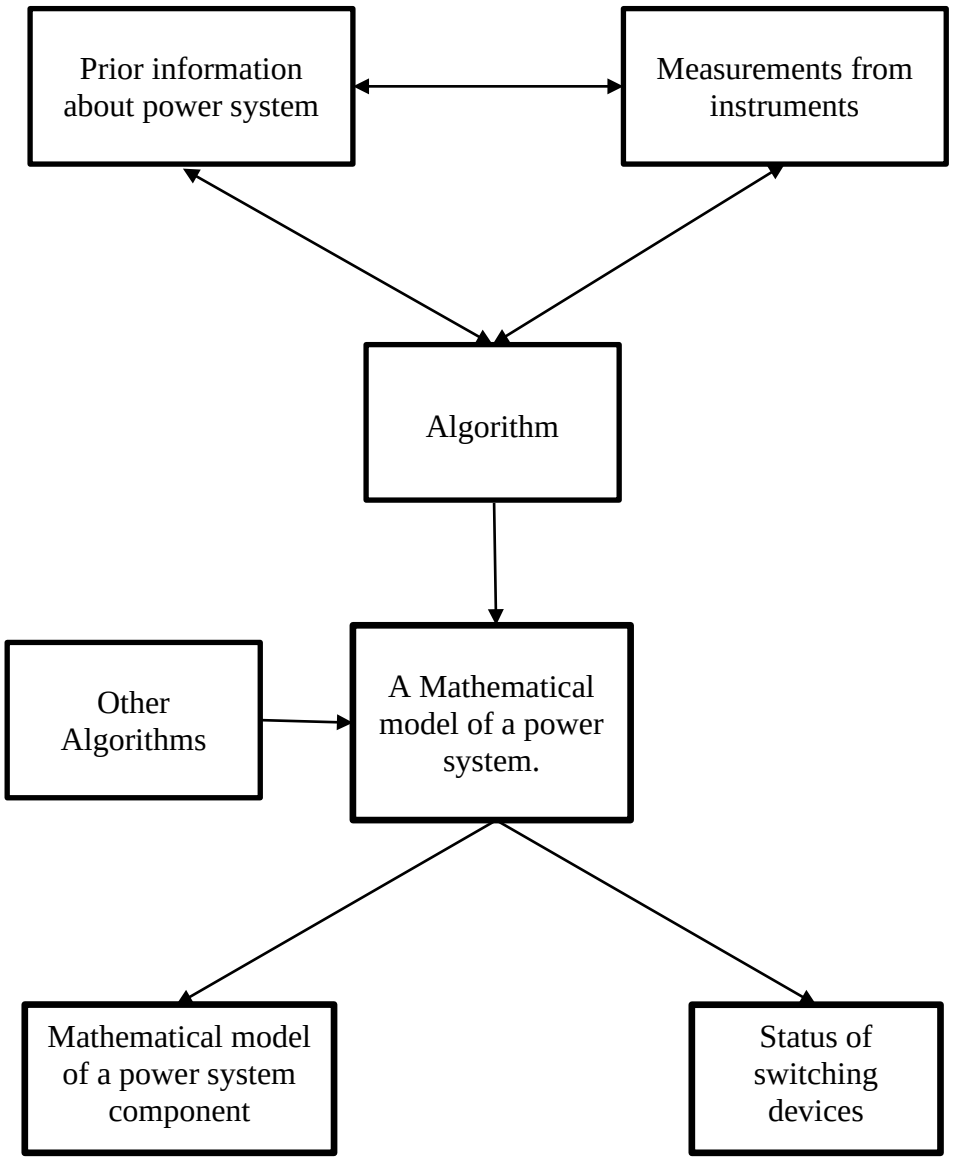

Figure 1.2 - Measurement-based (Online) modeling paradigm of a power system.

The proposed algorithms estimate the power system matrices i.e., the bus admittance matrix and the bus impedance matrix of a power system through the phasor measurements. From the bus admittance matrix, the topology of the underlying power system can be assessed. Moreover, using the matrix entries, the parameters of the components can be estimated. This measurement-based approach for the estimation of system topology and parameters is preferable as it is less prone to errors. Additionally, the approach accommodates any changes in the parameters of the components of a power system unlike the offline model presently in use.

The connections for each line are presently decided through signals, transmitted by an RTU, communicating the status of the corresponding circuit breakers [22]. If, somehow, the signal has the wrong status of a circuit breaker, the topology of the power system derived in the control center will be erroneous. This discrepancy will result in the lack of situational awareness of the system and may contribute towards a blackout as has happened in California in 2003 [24].

In the algorithms presented in the thesis, the status of a circuit breaker is decided through multiple measurements obtained from various instruments. Even if some of the signals are erroneous, the algorithm will be able to assess the correct statuses of the circuit breakers. Therefore, by using the algorithms presented, the true topology of a power system can be derived with a high probability. Had this facility been available to the system operators, the California-blackout of 2003 might have been prevented [24], [34].

1.4 Power System Matrices[1]

Modern power system operation is mostly based on node-based analysis techniques [35]. All such techniques are based on two matrices: the bus admittance matrix, Y_{bus}, and the bus impedance matrix, Z_{bus}. Although the two matrices, the Y_{bus} and the Z_{bus}, are related, i.e., one is the inverse of other, they provide very different insights into the corresponding power system and are, therefore, used in different applications.

The bus admittance matrix of a power system is primarily used in the load flow analysis and the state estimation. Whereas, the bus impedance matrix of a power system is used in the fault calculations and contingency analysis. Both power system matrices are derived using the two key attributes of a power system: system's topology and the admittances (impedances) of the components.

1.4.1 Bus Admittance Matrix

The information regarding the topology and the components' admittances of a power system are succinctly represented in its bus admittance matrix. The topology of a power system is usually represented through its node incidence matrix, A, that contains the information regarding which branches of the system are connected to which of its buses[2]. Dimension of a node incidence matrix is $b \times n$, where b is the total number of branches

[1]The theory presented here is applicable, without any loss of generality, to all the sequence networks of a power system: positive, negative, or zero sequence. However, the discussion is done with respect to positive-sequence networks and the corresponding bus admittance and impedance matrices. If the positive-sequence quantities are replaced by the corresponding negative or zero-sequence quantities, the results still hold.

[2] The terms nodes and buses are used interchangeably throughout the thesis.

and n is the total number of non-reference buses in the corresponding power system. So, in a node incidence matrix, there is one row for each branch and one column for each non-reference node. To form the node incidence matrix of a power system, its nodes and branches are numbered[3]; an arbitrary direction of flow is associated with each branch of the power system, and the entry corresponding to i^{th} row and j^{th} column is given by,

$$A_{(i,j)} = \left\{ \begin{array}{rl} 0; & if\ branch\ i\ is\ not\ connected\ to\ the\ bus\ j\ of\ power\ system \\ 1; & if\ branch\ i\ is\ connected\ to\ bus\ j\ with\ flow\ towards\ bus\ j \\ -1; & if\ branch\ i\ is\ connected\ to\ bus\ j\ with\ flow\ away\ from\ bus\ j \end{array} \right\}$$

The information regarding the branch admittances of a power system is stored in the admittance matrix, Y. The dimension of Y is $b \times b$ where b is the number of branches in the network as there is one row and one column corresponding to each branch of the network.

Along the diagonal, the admittance matrix is filled with the admittances of the branches of a power system. The i^{th} diagonal entry of the matrix is filled with the admittance of branch numbered i. If branches i and j have mutual admittance y_{ij}, the value of the off-diagonal entry $Y_{(i,j)}$ is given by,

$$Y_{(i,j)} = \left\{ \begin{array}{ll} 0\ ; & if\ there\ is\ no\ mutual\ admittance\ between\ branches\ i\ and\ j \\ y_{ij}; & if\ there\ is\ mutual\ admittance\ admittance\ between\ branches\ i\ and\ j \end{array} \right\}$$

Under the balanced system conditions, the mutual admittances can be accommodated

[3] Although, theoretically, the ultimate results are not dependent on the way the nodes are numbered, in practice, various algorithms are used to achieve an efficient node-numbering. Using an efficient node-numbering scheme guarantees that the sparsity of the matrices (obtained while performing the analysis on the system) is maintained.

into equivalent self-admittances [35], and the resulting bus admittance matrix, Y_{eq}, will be a diagonal matrix.

As mentioned above, the information regarding the topology of a power system is stored in its node incidence matrix, A, whereas the information regarding the admittances of the branches of a power system is stored in the admittance matrix, Y. As only these two attributes of a power system are required for the formation of its bus admittance matrix, the bus admittance matrix of a power system is related with the corresponding node incidence matrix and the admittance matrix as [35],

$$Y_{bus} = A^T Y A \tag{1.1}$$

If, however, the equivalent admittance matrix, Y_{eq}, which is a diagonal matrix, is used in equation 1.1, then $Y_{bus(i,j)}$ is non-zero if and only if $A_{(i,j)}$ is non-zero. And, therefore, the topology of a power system determines the sparsity pattern of the corresponding Y_{bus}. If bus i and bus j of a power system are not directly connected by any element, then the entries $Y_{bus(i,j)}$ and $Y_{bus(j,i)}$ of the resulting Y_{bus} will be zero whereas if buses i and j are connected by some component, $Y_{bus(i,j)}$ and $Y_{bus(j,i)}$ will be equal to the negative admittance of the connecting component. The diagonal entry $Y_{bus(i,i)}$ will be equal to the sum of the admittances of the components directly connected to the bus i. So, as the topology of a power system determines the sparsity pattern of its bus admittance matrix, the admittances of its components determine the values of the non-zero entries of the corresponding bus admittance matrix. Therefore, the information regarding both the key attributes (topology and admittances) of a power system are present in its bus admittance matrix.

Even more, given its bus admittance matrix, the impedance diagram of the corresponding power system can be easily determined, as illustrated in Figure 1.3. In the thesis, various algorithms will be presented to estimate the bus admittance matrix of a power system using the phasor measurements. Thereupon, the parameters and the topology of the power system will be derived from the estimated matrix.

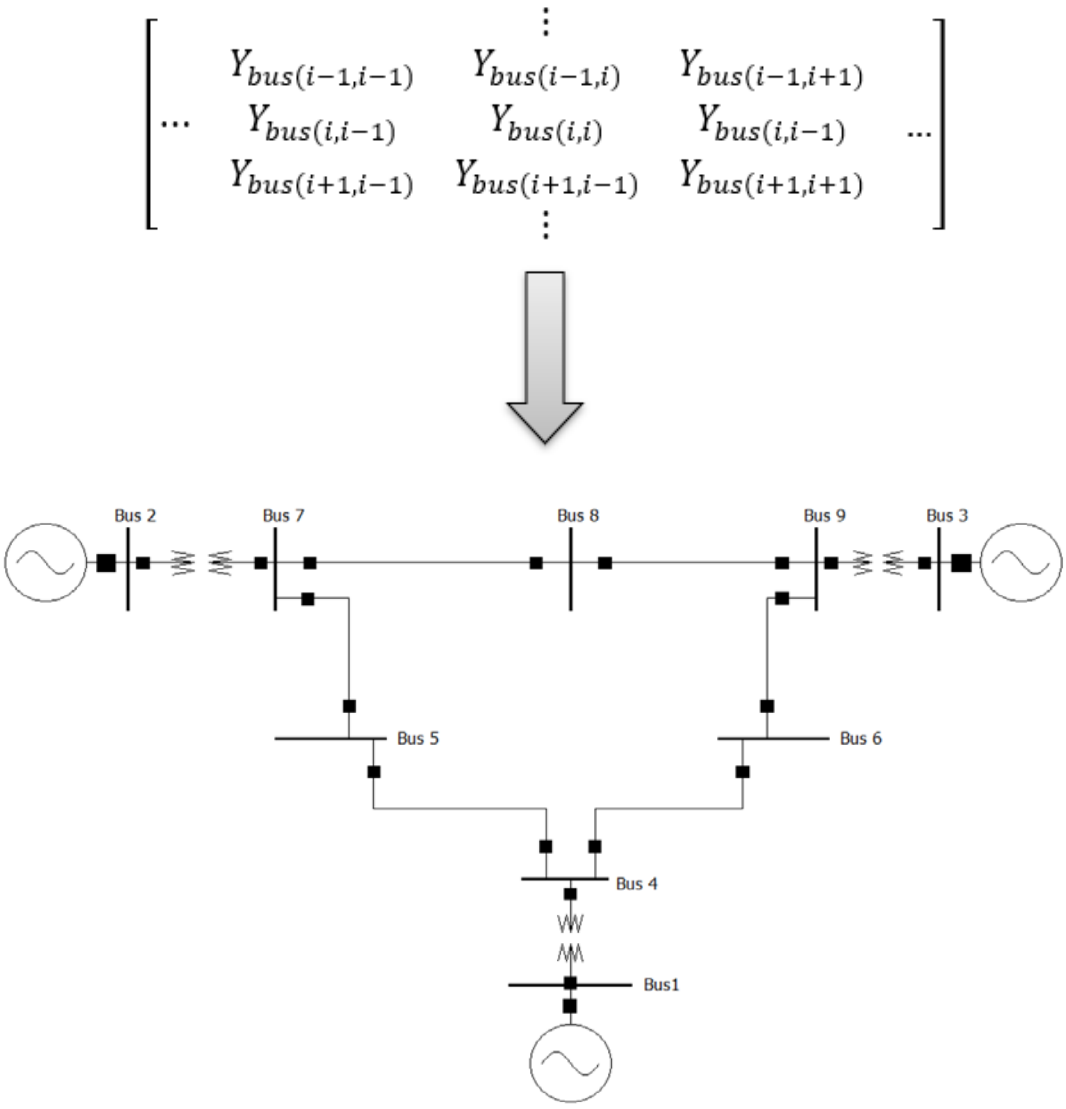

Figure 1.3 – Reactance diagram of a power system can be derived from the corresponding Y_{bus}.

Owing to the topology of power systems, each bus is directly connected only to few other buses; these buses are called the neighboring buses of the bus. In a typical power system, the average number of neighboring buses is 1.5 [35]. This intrinsic structure results in a high sparsity (the ratio of the number of zero elements of a matrix to its total number of elements) for the bus admittance matrix of a practical power system. For illustration, the sparsity pattern of various systems used for simulation in the thesis are shown in Figure 1.4.

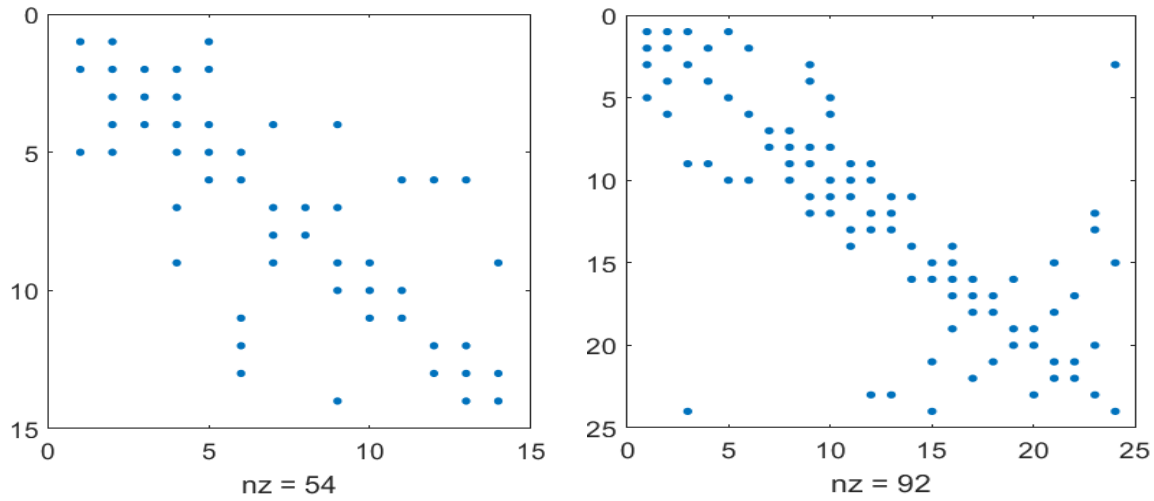

a) IEEE 14-bus power system
b) IEEE 24-bus power system
c) IEEE 30-bus power system
d) IEEE 118-bus power system

Figure 1.4 – Sparsity pattern of various IEEE systems (dots are representing nonzero values).

1.4.2 Bus impedance Matrix

Unlike the bus admittance matrix, the entries of the bus impedance matrix involve a different set of calculations and provide a much different information about the underlying power system. The diagonal element of a bus impedance matrix, $Z_{bus(k,k)}$, is the Thevenin impedance of the corresponding power system at the k^{th} bus, as illustrated in Figure 1.5, which provides information regarding the short-circuit capacity at the k^{th} bus of a power system.

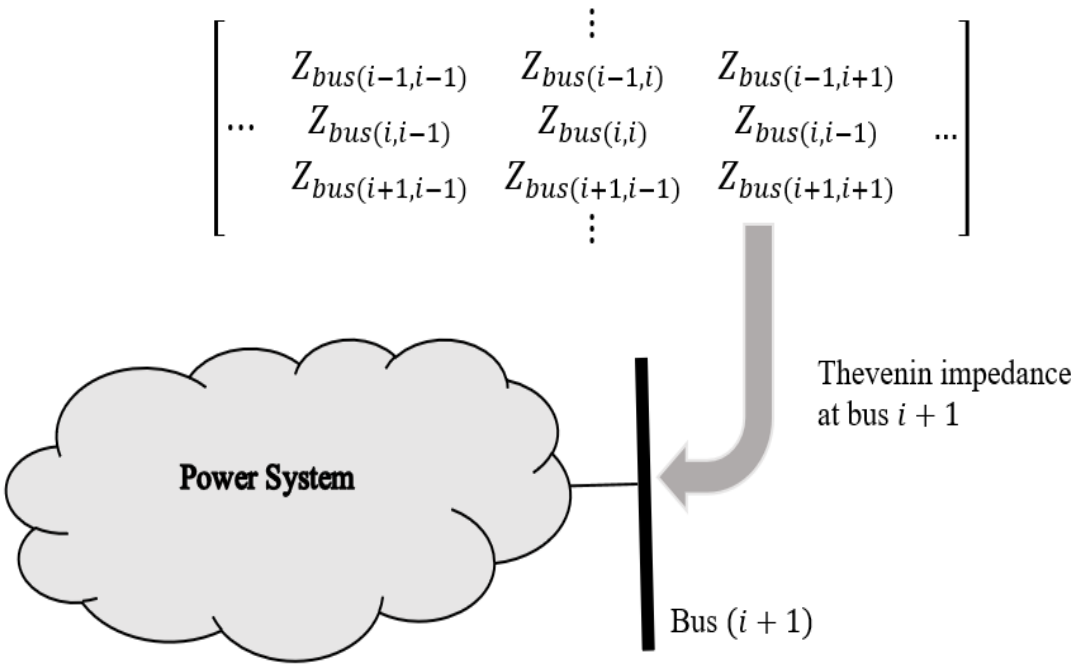

Figure 1.5 - Diagonal elements of the Z_{bus} of a power system are the Thevenin impedances at the respective buses.

One of the many uses of the bus impedance matrix is in the fault calculations of power systems. The results from these calculations are used in the settings of power system relays. Currently, the off-line models are used in deriving the entries of Z_{bus}. Such methods

can result in erroneous settings of the relays, as off-line methods do not update the relays' settings with changes in the system [23].

The diagonal entries of a bus impedance matrix are used in the fault analysis to calculate the fault currents. For example, the symmetrical fault current at any given bus *k* is

$$I_{f,k} = \frac{prefault\ voltage\ at\ bus\ k}{k^{th}\ diagonal\ entry\ of\ Z_{bus}} = \frac{V_{f,k}}{Z_{bus(k,k)}} \tag{1.2}$$

The off-diagonal element, $Z_{bus(j,k)}$, is the transfer impedance between nodes *j* and *k* of a system which indicates the change in the per-unit voltage at bus *j* due to the injection of one per-unit current at the k^{th} bus of the power system as,

$$\underbrace{\Delta V_{k\leftarrow 1pu}}_{\substack{Change\ in\ pu\ voltages\\ of\ power\ system\ buses\ due\ to\\ an\ injection\ of\ 1\ pu\ current\ at\ bus\ k}} = k^{th}\ column\ of\ Z_{bus} = \begin{bmatrix} Z_{bus(1,k)} \\ Z_{bus(2,k)} \\ \vdots \\ Z_{bus(k,k)} \\ \vdots \\ Z_{bus(n-1,k)} \\ Z_{bus(n,k)} \end{bmatrix} \tag{1.3}$$

As the bus impedance matrix is a linear model of power transmission or distribution system, the changes in the voltages of the buses of the system due to a symmetrical fault at bus k is given by,

$$\begin{matrix} changes\ in\ the \\ voltages \\ of\ buses\ of \\ power\ system\ due \\ to\ fault\ at\ bus\ k \end{matrix} = \underbrace{\Delta V_{k\leftarrow -I_f}}_{\substack{Change\ in\ the\ pu\ volatges\\ of\ power\ system\ buses\ due\ to\\ injection\ of\ -I_f\ current\ at\ bus\ k}} = \begin{bmatrix} Z_{bus(1,k)} \\ Z_{bus(2,k)} \\ \vdots \\ Z_{bus(k,k)} \\ \vdots \\ Z_{bus(n-1,k)} \\ Z_{bus(n,k)} \end{bmatrix} \times -I_{f,k} \tag{1.4}$$

Therefore, to perform the fault analysis at bus k of a power system, only the k^{th} column from the bus impedance matrix, $Z_{bus(:,k)}$, is needed. If, somehow, the respective column of the bus impedance matrix corresponding to the current operating condition is available at each bus of a power system, it can be used to perform fault analysis and update the relay settings according to the real-time conditions of power system. An algorithm which will do just that is presented in the thesis.

1.5 Phasor Measurements

Conventionally, the state variables of a power system (the complex voltages of the buses of a power system) are not measured directly. Although the magnitudes of the bus voltages are measured, the corresponding angles of the voltages are not measured directly in a conventional metering. Rather, the voltage angles are estimated indirectly through a state estimator using a set of large number of scalar measurements.

In the phasor measurements, a synchronized set of measurements are used to determine the phasor voltages of the buses and the phasor line currents. The synchronization is achieved by time stamping using the clock synchronized with the GPS. Since the implementation of phasor measurements, numerous algorithms have been proposed for various applications [27], [36], [37]. These applications can be broadly classified in the following broad areas:

i. State estimation [38], [39].

ii. Model formation, calibration and validation [40]–[44].

iii. Detection and finding location of fault [45], [46].

iv. Prediction and monitoring of dynamic stability [17].

v. Power system protection [23].

The recent failures of reliably operating a power system [18] and a huge loss that a blackout can incur [47] has surged an interest in coming up with new and better practices for operating power systems. Various recommendations [24], [48] have been made in this regard. One of these recommendations is to replace the offline models, currently in use, with the online models of power systems. This paradigm change requires installation of numerous high accuracy instruments across power systems. The recent recommendation [49] to take a large number of phasor measurements across power systems is a conformation to this requirement.

Many of the algorithms in power systems become much easier, faster, direct, as well as more reliable and accurate with the assumption that the synchronized set of measurements are available [50]. The algorithms presented in the current thesis assumes that these measurements are available at all the buses of the power system. One way to make these measurements available is by installing PMUs at all the buses, but currently, the high installation cost of PMUs makes this strategy economically unviable. Presently, a limited number of PMUs are used at the optimal location [51]–[55] to increase the situational awareness of power systems.

In the future, the number of PMUs installed across a power system, however, will increase considerably due to 1) the recommendations provided in the wake of recent blackouts [49]; 2) the advantages offered by them in power system operations [36], [17]; and 3) the decrease in their cost due to the advancement of technology.

Note that to measure the phasors at a bus of a power system, PMU need not be installed at the bus. Almost all modern protection relays have the ability to measure voltage and current phasors at the point of installation [56], [57]. Therefore, phasor measurement can be taken at a bus even without the installation of PMU if this feature of the relay installed at the bus is used.

Although the phasors at all the buses may not be measured in current power systems, the advantages of measuring the phasors, and the fact that many of these can be obtained through already installed relays implies that phasors at all the buses of a future power system will be measured [3], [31]. And therefore, in the future, power system analysis will be performed using these measurements [3]. Algorithms, using these measurements, will model the components and set the relays of power system. Some algorithms which can be used to serve this purpose are proposed in the current work.

The algorithms provide the estimates of power system matrices using phasor measurements. Once the estimate of these matrices is available, the parameters of various power system elements can be evaluated. For example, the parameter of the branches of a power system can be obtained from the corresponding bus admittance matrix whereas the Thevenin impedances of a power system can be obtained through its bus impedance matrix. As the power system models based on such matrices will be based on the real-time measurements, the models thus obtained will be more accurate and, therefore, will result in better analysis and situational awareness of the system.

1.6 Thesis Organization

In this section, a brief overview of the chapters of the thesis is presented.

Although an attempt has been made to keep the repetition to the minimum, the effort to design each chapter such that it can be read independently (without the need to read any other chapter) and the fact that the theory developed in some later chapters depends on the earlier chapters has made some repetition inevitable. For example, the setup of the simulation for each chapter varies only slightly from the setup for other chapters; however, the setup is repeated in each chapter for the ease of the reader.

Additionally, the experimental results for the cases of IEEE 14-bus and IEEE 24-bus systems are described relatively in more detail. This special treatment is for no reason other than their manageable size for the discussion of results in greater details. For example, the bus admittance and bus impedance matrices of these systems are such that they can be printed in the thesis with ease. Additionally, the numbers of branches in the systems are also not so much to be cumbersome to be discussed.

If the underlying assumptions of the algorithms are satisfied, the results obtained, for the IEEE 14 and 24-bus systems, apply to larger systems as well.

CHAPTER 1:

Chapter 1 provides the background material, the scope and the applications of the research undertaken.

CHAPTER 2:

A measurement-based algorithm (Algorithm 2.1) for the estimation of the bus admittance matrix of a power system is presented. The algorithm assumes no prior information regarding the topology or the parameters of the components of power system.

The proposed algorithm is tested on various IEEE systems. For each system, noisy phasor measurements are simulated by adding noise to the bus voltages and line currents obtained by running the load flow analysis under various operating conditions. The bus admittance matrix is estimated by running the algorithm on the resulting phasor measurements, and the corresponding errors are evaluated. From the resulting bus admittance matrix, the topology of the system and the parameters of the components are estimated.

Furthermore, the conditions, that a power system must satisfy, for the estimated bus admittance matrix to converge near the actual bus admittance matrix are discussed. For the power systems satisfying these conditions, the estimated matrix will be accurate enough for the parameter estimation. In the future, with the prevalence of renewable and distributed generation, most of the systems will satisfy these conditions.

If, however, somehow the conditions are not satisfied by a power system, the estimated bus admittance matrix obtained may not be accurate enough. The cases under which the algorithm fails to provide an accurate estimate of the bus admittance matrix are presented. The causes of the failure and the modification of the problem formulation to resolve the issue is suggested which has served as the basis for the next chapter.

CHAPTER 3:

A multi-criteria optimization-based algorithm, Algorithm 3.1, is presented for the estimation of the bus admittance matrix of a power system. If some prior information about the topology of a part or complete power system is available, the algorithm has the capability to accommodate this information. This accommodation will reduce the

computational and storage complexity of the algorithm. Moreover, the algorithm also provides the capability to take into account the prior estimates regarding any or all of the parameters of power system's components. If the prior estimates are good, the algorithm will be able to converge in a lesser number of measurements (and time).

The proposed algorithm is tested on various IEEE systems. For each system, the noisy phasor measurements are simulated by adding noise to the bus voltages and line currents obtained by running the load flow analysis for different operating conditions. The prior estimates of the parameters are generated by adding random errors to the actual parameters such that the resulting parameters are accurate up to 20%; such parameters are used as the offline parameters of the power system's components [58]. The algorithm is tested on the resulting measurements and data, and the results are compared with the algorithm presented in the previous chapter.

The algorithms presented in this and the previous chapters work fine if there are only a few faulty measurements. However, if the number of faulty measurements increase beyond a certain threshold (which depends on the state and the parameters of the underlying system), the accuracies of the algorithms are affected severely. In the future, with the advancement in the instrumentation and communication technology, the probability of faulty measurements is going to decrease, and therefore, the algorithms will work fine.

However, if, due to some reason, the measurements contain numerous faulty measurements, then such an algorithm should be used which is robust against the faulty measurements. In the subsequent chapter, such an algorithm is presented.

CHAPTER 4:

In this chapter, it is assumed that a substantial percentage of the measurements are faulty. To address the problem of faulty measurements, a new optimization problem is formulated whose solution is robust against the faulty measurements.

The proposed algorithm is tested on various IEEE systems. For each system, the noisy phasor measurements are simulated by adding noise to the variables obtained by running the load flow analysis for different operating conditions.

Faulty measurements are simulated at random instants of time by taking the samples from a Normal probability distribution having a large standard deviation and adding the results to the phasor measurements at the buses chosen randomly. The algorithm is run on measurements obtained thereby, and the results are compared with the results obtained from the algorithm derived in chapter 3.

CHAPTER 5:

A measurement-based algorithm, Algorithm 5.1, for the estimation of the bus impedance matrix of a power system is presented. The algorithm is recursive, and, therefore, the computation is done by processing only one set of measurements as it is received.

The proposed algorithm is tested on various IEEE systems. For each system, the noisy phasor measurements are simulated by adding noise to the variables obtained by running the load flow analysis for different operating conditions. The algorithm is run on the measurements, and the results are discussed.

As mentioned previously, one major application of the elements of a bus impedance matrix is the settings of the relays in the underlying power system. Therefore, if somehow, at each bus, the elements of the bus impedance matrix required for the settings of the corresponding relay are available, they can be used for the settings of the relays. For this purpose, a decentralized and distributed algorithm, that can update the elements of the bus impedance matrix with changes in the corresponding power system is better suited. In the next chapter, such an algorithm is presented.

CHAPTER 6:

A measurement-based decentralized algorithm for the estimation of the bus impedance matrix of a power system is presented. The conditions for the convergence of the algorithm are presented. The algorithm is tested on various IEEE power systems and the results are discussed. After the algorithm has run, the respective columns of the bus impedance matrix will be available at each bus of a power system which can be used to set the relays for power system protection.

CHAPTER 7:

The thesis is concluded with a discussion of various applications and possible extensions of the work presented

CHAPTER 2. ESTIMATION OF BUS ADMITTANCE MATRIX

2.1 Introduction

In this chapter, an online measurement-based method for the estimation of the bus admittance matrix of a power system is presented. As described in the previous chapter, such an online method is preferable to the conventional off-line model-based method as it can accommodate any changes in the system.

No prior information regarding the components' parameters and the topology of the underlying power system is used in the problem formulation. The algorithm relies only on the phasor measurements taken at various times samples across the power system. The algorithm assumes that phasors are measured at all the buses of the power system. Due to various reasons, mentioned in the previous chapter, this assumption is likely to hold for future power system.

The parameters of power system components are evaluated from the estimated bus admittance matrix obtained by running the algorithm on the phasor measurements. The proposed algorithm is tested on various IEEE power systems, and the results are discussed. The conditions for the convergence of the algorithm are discussed in the last section. With the increased penetration of renewable energies, most of the future power systems will meet these conditions. However, for the systems that do not meet the conditions, a modification of the algorithm is suggested. The modification forms the basis for the algorithm presented in the next chapter.

2.2 Mathematical Theory

Buses' voltage phasors, v_{bus}, and buses' injection current phasors, i_{bus}, of an $n+1$-bus power system (assuming one bus to be reference) are related through an $n \times n$ bus admittance matrix, defined in equation 1.1, as

$$Y_{bus} v_{bus} - i_{bus} = 0 \tag{2.1}$$

where v_{bus} is a complex-valued n-vector of actual bus voltages, and i_{bus} is a complex-valued n-vector of actual current injections at the respective buses. Voltage and current injection measurements taken at time t_i at bus j are $v_j(t_i)$ and $i_j(t_i)$ respectively. Buses' voltages and injection currents at time sample t_i are represented by the n-dimensional vectors, $v(t_i)$ and $i(t_i)$ respectively as, $v(t_i) \coloneqq [v_1(t_i)\ v_2(t_i)\ \dots\ v_n(t_i)]^T$ and $i(t_i) \coloneqq [i_1(t_i)\ i_2(t_i)\ \dots\ i_n(t_i)]^T$ where $^{\mathrm{T}}$ represents the transpose operation. The matrices V_{bus} and I_{bus} are $n \times m$ voltage and current measurement matrices defined as,

$$V_{bus} \coloneqq [v(t_1) \mid v(t_2) \mid v(t_3)\ \dots\ v(t_m)] \tag{2.2}$$

and

$$I_{bus} \coloneqq [i(t_1) \mid i(t_2) \mid i(t_3)\ \dots\ i(t_m)]. \tag{2.3}$$

All the phasor measurements will have some errors due to random measurement noise. Therefore, equation 2.1 will hold only approximately for the actual measurements. So, the measurement matrices, V_{bus} and I_{bus}, will be related as,

$$Y_{bus} V_{bus} - I_{bus} \approx 0. \tag{2.4}$$

$\dot{r}$ is the $n \times m$ residual matrix defined as,

$$\dot{r} \coloneqq Y_{bus}V_{bus} - I_{bus}. \tag{2.5}$$

The magnitude of the elements in $\dot{r}$ will depend on the errors in the measurement matrices. Note that the residual matrix, $\dot{r}$, is simply the concatenation of the n-dimensional residual vectors r_i taken at the m different samples i.e., $\dot{r} = [r_1 \mid r_2 \mid r_3 \ldots \mid r_m]$ where $r_i = Y_{bus}v(t_i) - i(t_i)$.

Compared to conventional measurements, phasor measurements (whether taken through PMUs or modern digital relays) have much better accuracy[4]. Therefore, the errors in the measurements will be relatively much smaller. When the errors in the measurements are small, a reasonable estimate of the bus admittance matrix, $\dot{Y}_{bus}$, can be obtained by minimizing the Frobenius norm[5] of the residual matrix [59] as,

$$\dot{Y}_{bus} \coloneqq \underset{\dot{Y}_{bus}}{minimize} \; ||(\dot{Y}_{bus}V_{bus} - I_{bus})||_f^2 \tag{2.6}$$

where $_f$ represents the Frobenius norm. Therefore, the solution of the optimization problem in equation 2.6 i.e., the estimated bus admittance matrix, $\dot{Y}_{bus}$, is the one with the lowest norm of $\dot{r}$. The solution to the optimization problem of equation 2.6 exists for all current measurement matrices if the bus voltage measurement matrix is full-rank.

Assuming V_{bus} to be a full-rank matrix, the closed-form solution of equation 2.6 is

$$\dot{Y}_{bus} = I_{bus} \times V_{bus}^{*}(V_{bus}V_{bus}^{*})^{-1}. \tag{2.7}$$

It is worth noting that $\dot{Y}_{bus}$ is not calculated using equation 2.7. As, not only, the direct

[4] All the technical requirements related to the phasor measurements are mentioned in the standard IEEE C37.118-2005 [76].

[5] Frobenius norm of a matrix is the sum of the squares of the magnitudes of its entries.

evaluation of the inverse, $(V_{bus}V_{bus}^{*})^{-1}$, is computationally intensive, rather, more importantly, the use of equation 2.7 reduces the accuracy of the estimated bus admittance matrix, $\dot{Y}_{bus}$, due to the increased condition number[6] [60] of the matrix $(V_{bus}V_{bus}^{*})$. By resorting to the *QR* factorization, the solution of the problem 2.6 can be obtained without the calculation of the inverse of the matrix $(V_{bus}V_{bus}^{*})$. The solution thereby obtained is, therefore, more accurate and computationally less demanding.

2.2.1 Regularization

The full-rank assumption of the voltage measurement matrix, V_{bus}, in equation 2.7 can be relaxed by using regularization [59] in which, instead of the optimization problem mentioned in equation 2.6, the following modified problem is solved,

$$\tilde{Y}_{bus} = \underset{\dot{Y}_{bus}}{minimize}\ ||(\dot{Y}_{bus}V_{bus} - I_{bus})||_f^2 + \underbrace{\delta||\dot{Y}_{bus}||_f^2}_{Regularization-term} \tag{2.8}$$

where δ is usually a small real number[7] and $\delta||\dot{Y}_{bus}||_f^2$ is a regularization-term. The use of the regularization-term in equation 2.8 can be justified for various reasons [59]–[62]. Some of these are:

i. The voltage measurement matrix, V_{bus}, has measurement errors. These errors are ignored in the estimate of the bus admittance matrix, $\dot{Y}_{bus}$, obtained through the solution of the optimization problem expressed in equation 2.6. The optimization problem assumes that only the current measurements are noisy and treats the corresponding voltage measurements as ideal (without any noise).

[6] The condition number of a matrix is the ratio of its largest singular value to its lowest singular value. The condition number of the matrix $(V_{bus}V_{bus}^{*})$ is the square of the condition number of the matrix V_{bus}.

[7] The selection of δ is highly dependent on the underlying system.

The estimation of the bus admittance matrix, $\tilde{Y}_{bus}$, through the regularized objective function, expressed in equation 2.8, accommodates these errors in the voltage measurements. The value of δ, in equation 2.8, should be decided by using the information about the magnitude of errors (if we have any) in the voltage measurements [61].

If a judicious value of δ is selected in the optimization problem 2.8, the solution, unlike the solution obtained from problem 2.6, will update to counter the effects of the errors in the voltage measurements. Therefore, a reasonable value of δ in the problem formulation will provide a relatively more accurate estimate of the bus admittance matrix compared to the one obtained by the solution of problem 2.6.

ii. When a linear system of equations is solved, the accuracy of the solution is related to the condition number of the underlying coefficient matrix. For a square matrix, the condition number of a matrix is a quantitative assessment of its nearness to the singularity. A perfectly invertible matrix (e.g., an orthogonal matrix[8]) has the condition number of 1 whereas all singular matrices have a condition number of ∞. A system of with an orthogonal coefficient matrix can be solved without any loss of accuracy whereas a coefficient matrix with a very large condition number will result in the loss of accuracy of the solution.

The concept of the condition number of a matrix can be extended to non-square matrices by using the Singular Value Decomposition (SVD). Roughly,

[8] Matrix A is orthogonal if $A^{-1} = A^{T}$. Orthogonal matrices are perfectly invertible in the sense that no accuracy is lost in the operation of transposition.

a large condition number of a matrix corresponds to a loss of accuracy in the solution of the Frobenius-norm estimation problem [63]. Therefore, the accuracy of the estimated bus admittance matrix depends on the condition number of the voltage measurement matrix, V_{bus}.

The regularization, essentially, adds δ to all the singular values of the matrix. Therefore, the addition of the regularization-term in the optimization problem, as is done in equation 2.8, ensures that the minimum singular value of the matrix in a system of equations is at least δ.

A linear system of equations is well-conditioned if the ratio of the magnitude of the largest and the smallest singular values of the corresponding coefficient matrix is small. The problem of a linear system of equations is well-scaled if not all the singular values of the underlying coefficient matrix are large or small in magnitude.

For a well-scaled problem, the effect of regularization on a well-conditioned problem is negligible [64]. However, if the condition number of the matrix is poor (large), the presence of the regularization-term in the objective guarantees that the smallest singular value is greater than or equal to δ [64]. This ensures that the condition number of the resulting coefficient matrix is not too low. And, therefore, the addition of regularization ensures that the accuracy of the result doesn't degrade too much.

So, when the condition number of the voltage measurement matrix will be poor, the regularization will ensure that the condition number of the corresponding coefficient matrix in the system of equation doesn't increase

much. This is achieved by keeping the minimum singular value at least δ. However, when the condition number of the voltage measurement matrix will be good, the regularization will minimally affect the result.

The closed-form solution of the regularized optimization problem in equation 2.8 is given by,

$$\tilde{Y}_{bus} = I_{bus} \times V_{bus}^{*}(V_{bus}V_{bus}^{*} + \delta I)^{-1} \tag{2.9}$$

where I is an n-dimensional identity matrix. Because of the additional regularization-term, $\delta||\grave{Y}_{bus}||_f^2$, the solution to equation 2.8 always exists, regardless of the rank of V_{bus}. As previously mentioned, the inverse in equation 2.9 is symbolic and is never actually computed. Instead, the solution in equation 2.9 of optimization problem expressed in equation 2.8 can be obtained by extending equation 2.4 as,

$$\grave{Y}_{bus}\left[\, V_{bus} \mid \sqrt{\delta} I \,\right] - \left[\, I_{bus} \mid \mathbf{0} \,\right] \approx 0 \tag{2.10}$$

where I and $\mathbf{0}$ are the $n \times n$ identity and zero matrices respectively. The extensions in the voltage and current matrices are to accommodate the regularization term, $\delta||\grave{Y}_{bus}||_f^2$, in equation 2.8. Now, taking the transpose of equation 2.10 results in,

$$\begin{matrix} m \\ n \end{matrix} \left\{ \underbrace{\begin{bmatrix} V_{bus}^{T} \\ \hline \sqrt{\delta} I \end{bmatrix}}_{n} \acute{Y}_{bus}^{T} - \begin{bmatrix} I_{bus}^{T} \\ \hline \mathbf{0} \end{bmatrix} \right. \approx 0. \tag{2.11}$$

An interpretation of the equation 2.11 can be made by seeing the partitions in the equation as two separate approximate equations.

The first partition, $V_{bus}^{T}\acute{Y}_{bus}^{T} - I_{bus}^{T} \approx 0$, is simply the transposed version of

equation 2.4 which is the approximate version of the equation 2.1 that defines the bus admittance matrix.

The second partition of the equation 2.11 is $\sqrt{\delta} I \, \acute{Y}_{bus}^{T} \approx 0$. As a bus admittance matrix is typically highly sparse, most of its entries will be zero. Therefore, this partition can be interpreted as the prior estimate in the Bayesian framework[9] of modeling which means that without any measurements, the bus admittance matrix will be estimated as the zero matrix.

With the accumulation of independent measurements corresponding to different operating conditions of the system, the estimate of the bus admittance matrix, $\tilde{Y}_{bus}$, will keep on updating and depart from the initial estimate depending on the rate determined by δ. The value of δ is related to the strength of belief in the prior estimate. The greater the value of δ, the greater will be the emphasis of the solver to keep the estimate near the prior estimate and vice versa[10]. In our case, since the prior estimate is very crude, the value of δ will be kept very small i.e., of the order of 10^{-4}.

Defining $\tilde{r}$ as the residual matrix of the extended problem as

[9] Prior estimate, in Bayesian framework of estimation, corresponds to our initial belief about the unknown. After receiving the measurements, a Bayesian estimator updates the estimate using the combinations of both the prior estimate and the measurements. The estimate derived depends on the corresponding weights assigned to the prior estimate and the measurements. If no weight is given to the measurements (or no measurements are received), the unknown will simply conform to our initial belief and will be equal to prior estimate.

[10] This interpretation fits nicely with idea that the magnitude of δ should be representative of the noise magnitude in the voltage measurement matrix. If the magnitude of the noise is large, a relatively large value of the δ should be used in the estimator. This high value of δ will compel the estimator to put relatively less emphasis to update the estimate according to the received measurements.

$$\tilde{r} := \begin{bmatrix} V_{bus}^T \\ \sqrt{\delta} I \end{bmatrix} \tilde{Y}_{bus}^T - \begin{bmatrix} I_{bus}^T \\ \mathbf{0} \end{bmatrix} \tag{2.12}$$

$$\tilde{r} \; = \; \tilde{V}_{bus} \tilde{Y}_{bus}^T - \; \tilde{I}_{bus} \tag{2.13}$$

where $\tilde{V}_{bus} = \; \left[V_{bus} \; \sqrt{\delta} I \; \right]^T$ and $\tilde{I}_{bus} = \; [I_{bus} \; \mathbf{0} \;]^T$. $\tilde{Y}_{bus}$ in equation 2.8 can be obtained as,

$$\tilde{Y}_{bus} = \; \underset{\tilde{Y}_{bus}}{minimize} \; ||\tilde{r}\,||_f^2. \tag{2.14}$$

The optimization problem in equation 2.14 is a tractable convex problem and, therefore, can be solved in polynomial time [61]. In the next section, a numerically stable algorithm to estimate $\tilde{Y}_{bus}$ along with its computational complexity is presented.

2.3 Algorithm 2.1

1) The reduced-QR factors[11] of $\tilde{V}_{bus} = \left[V_{bus} \; \sqrt{\delta} I \; \right]^T$ are evaluated. As per the definition of the factorization, Q consists of n $(m + n)$-dimensional vectors that are mutually orthogonal (i.e., $Q^* Q \; = I$) and R is an upper triangular matrix.
2) The solution of the systems of equations,

$$R \tilde{Y}_{bus}^T = \; Q^* \acute{I}_{bus} \tag{2.15}$$

is solved for $\tilde{Y}_{bus}^T$ as,

i) The product $Q^* \acute{I}_{bus}$ is evaluated.

[11] In the full-QR factorization, Q is a unitary matrix (i.e., $Q^* Q \; = I = Q Q^*$) and R is a rectangular, upper triangular matrix whereas in the reduced-QR factorization, Q is a thin rectangular matrix whose vectors are mutually orthogonal (i.e., $Q^* Q \; = I$) and R is a square, upper triangular matrix. If the full factors are not required explicitly, as in our case, the reduced factorization can result in considerable storage and computational savings.

ii) $\tilde{Y}_{bus}^{T}$ is evaluated by performing back-substitutions ($\because R$ is upper-triangular matrix) on the systems of equations $R\tilde{Y}_{bus}^{T} = Q^{*}\acute{I}_{bus}$ (the product from the first step).

3) The matrix $\tilde{Y}_{bus}^{T}$ obtained at the end of step 2 is transposed to obtain $\tilde{Y}_{bus}$.

The proposed algorithm, as used in the simulation for validation, is presented in the block diagram of Figure 2.1.

2.3.1 Computational complexity of the Algorithm 2.1

A rough estimate of the time to carry out an algorithm can be obtained by estimating the required number of floating-point operations (FLOPs) [12]. It is only a rough estimate as the actual time required by the algorithm is highly dependent on many other factors e.g., computer hardware and software. As FLOPs provide a very crude estimate of the time required, various simplifications are allowed [65].

The bounds on the number of FLOPs required by various steps of the algorithm are described below.

1) The number of FLOPs required in the first step (the QR factorization of the extended voltage measurement matrix, $\tilde{V}_{bus}$, can be bounded by[13] $c_1(m +$

[12] The processing speed of a typical modern computer is in the range 1-10 GFLOPS/s [59].

[13] A complex number is isomorphic to $\mathbb{R}^2$; similarly, an $m \times n$ complex matrix is isomorphic to a $2m \times 2n$ dimensional real matrix. The additional factor of 8 introduced, due to this doubling of the size, in the computations of QR factorization compared to factorization performed on a real matrix of same size, is accommodated in the coefficient c_1. This practice of accommodating the increase in the number of computations because of complex arithmetic will be adapted throughout the rest of the thesis.

$n)\ n^2$ [60] where $c_1 \in \mathbb{R}_{++}$.

2) The second step of the algorithm has two parts. The bounds on the number of FLOPs required to carry out both of them are mentioned below.

   i) The number of computations required to carry out the product $Q^* \acute{I}_{bus}$ can be bounded by $c_2 \times (m+n)\ n^2$ where $c_2 \in \mathbb{R}_{++}$.

   ii) The number of FLOPs required to carry out the back-substitutions on the systems of equations $R\tilde{Y}_{bus}^T = Q^* \acute{I}_{bus}$ (to find the estimate of the bus admittance matrix) can be bounded by $c_3 n^3$ where $c_3 \in \mathbb{R}_{++}$.

   Hence, the number of FLOPs needed to carry out the second step can be bounded by $c_2(m+n)\ n^2 + c_3 n^3$.

3) The number of operations required for step 3 is highly dependent on the architecture of the processor being used. However, this step has no primitive operations of addition or multiplication and can be carried out only by changing the order of access. Therefore, it is assumed that it requires zeros FLOPS.

Consequently, the number of FLOPs in the Algorithm 2.1 can be bounded by the addition of all the above-mentioned bounds as,

$$\begin{aligned} number\ of\ FLOPs\ for\ \text{Algorithm 2.1} &\leq c_1(m+n)n^2 + c_2(m+n)n^2 + c_3 n^3 \\ &= c_1 mn^2 + c_1 n^3 + c_2 mn^2 + c_2 n^3 + c_3 n^3 \\ &= (c_1 + c_2)\ mn^2 + (c_1 + c_2 + c_3)\ n^3 \\ &= c_4 mn^2 + cn^3;\ where\ c_4 \coloneqq c_1 + c_2\ and\ c \coloneqq c_3 + c_4. \\ &\leq c(mn^2 + n^3). \end{aligned}$$

Therefore, the computational complexity of the Algorithm 2.1 is $O(mn^2 + n^3)$.

2.4 Experimental Results

The algorithm is validated via simulations performed on various IEEE systems [66]. Simulations are performed in MATLAB using MATPOWER [67]. Slight modifications are made in the systems for the simulations.

For each new measurement, loads at all the buses are varied within $\pm 10\%$ of the nominal load. The difference in power, $\Delta P_G(t_k)$, between the total power generation at previous sampling time, $P_G(t_{k-1})$, and the sum of the total updated load at the current time, $P_L(t_k)$, with the system losses at previous sample, $P_{Loss}(t_{k-1})$, is distributed in all of the generators using participation factors according to the following equations

$$\Delta P_G(t_k) = P_L(t_k) + P_{Loss}(t_{k-1}) - P_G(t_{k-1}) \tag{2.16}$$

The additional power generated by the i^{th}generator at the k^{th}time sample is given by,

$$\Delta P_G^i(t_k) = \Delta P_G(t_k) \times PF^i \tag{2.17}$$

where, PF^i is the participation factor of the i^{th} generator defined as the ratio of the total MW capacity of the i^{th} generator to the sum of the total MW capacities of all the generators of the system.

Load flow analysis is then performed for the new system conditions. The residual power of the system (difference between total generation and total consumption) is provided by the slack-bus generator. The voltages and the injected current phasors are calculated at all the buses. Noise following a normal probability density function is added to all the phasors to simulate phasor measurements. The algorithm mentioned in section 2.3 is used to calculate the bus admittance matrix from measurements, $\tilde{Y}_{bus}$.

The error matrix, ΔY_{bus}, is defined as

$$\Delta Y_{bus} = Y_{bus} - \tilde{Y}_{bus} \tag{2.18}$$

The accuracy and convergence of the algorithm is estimated [68] through the evaluation of following terms

$$e_f = ||\Delta Y_{bus}||_f / ||Y_{bus}||_f \tag{2.19}$$

and

$$e_\infty = ||\Delta Y_{bus}||_\infty / ||Y_{bus}||_\infty \tag{2.20}$$

where f is representing the Frobenius norm and the ∞ is representing the infinity norm (the maximum value of the absolute row sum of a matrix). The magnitudes of the errors, e_f and e_∞, provide an estimate of the average error in the entries of the estimated matrix. For example, if the errors, e_f and e_∞, are around 10%, the error in the entries of the estimated bus admittance matrix will be on average 10% [68].

2.4.1 IEEE 14-bus system

A one-line diagram of the system is shown in Figure 2.2. The system has five generators connected at buses 1, 2, 3, 6, and 8 with the slack bus connected at bus 1. The system has 20 branches and 14 buses. The parameters and the connection information are provided in the appendix.

The scheme of Figure 2.1 is executed on the system, and the values of the errors e_f and e_∞ for the algorithm 2.1 at various numbers of measurements are tabulated in Table 2.1.

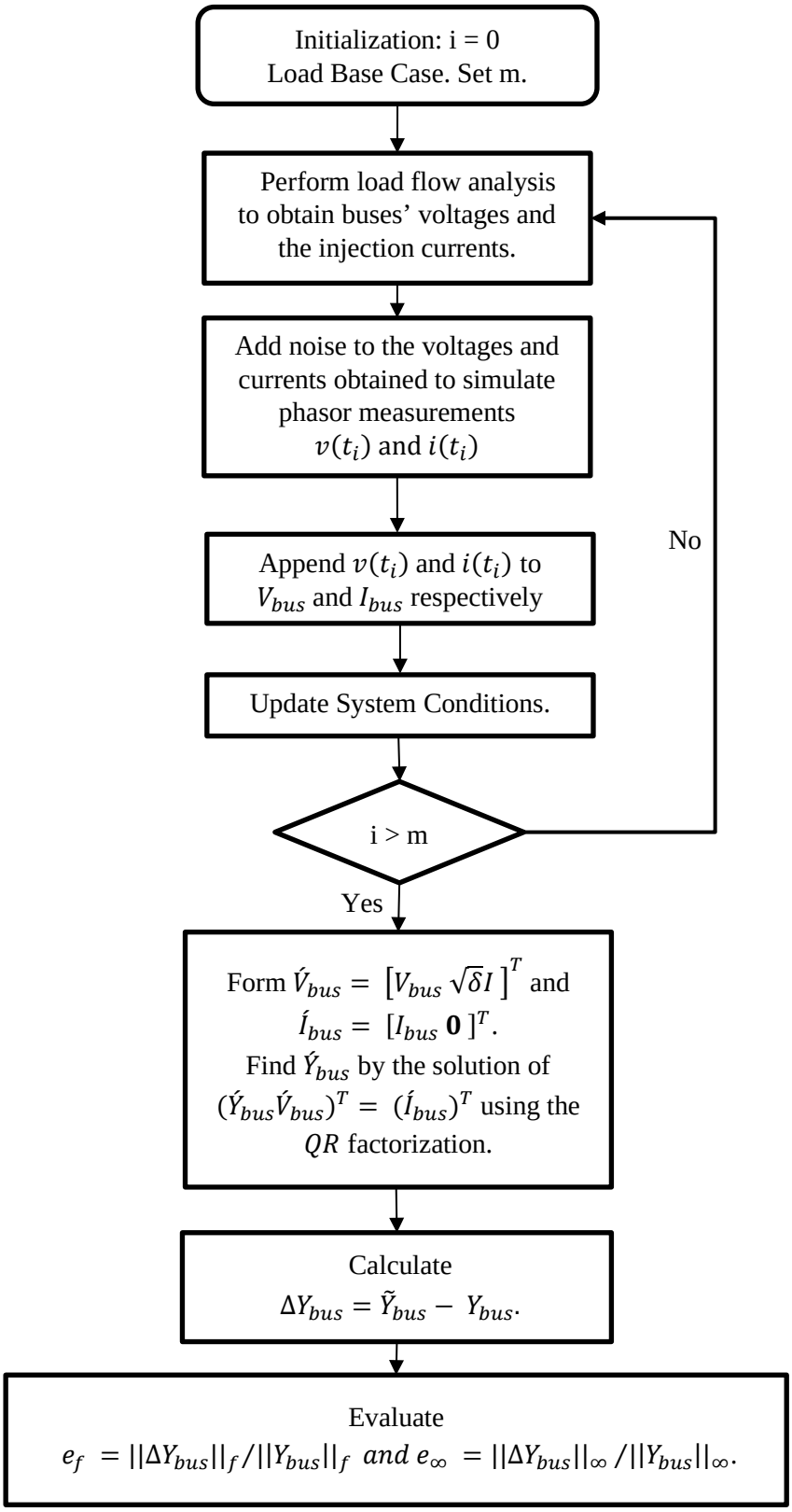

Figure 2.1 - Scheme used for the validation of the Algorithm 2.1.

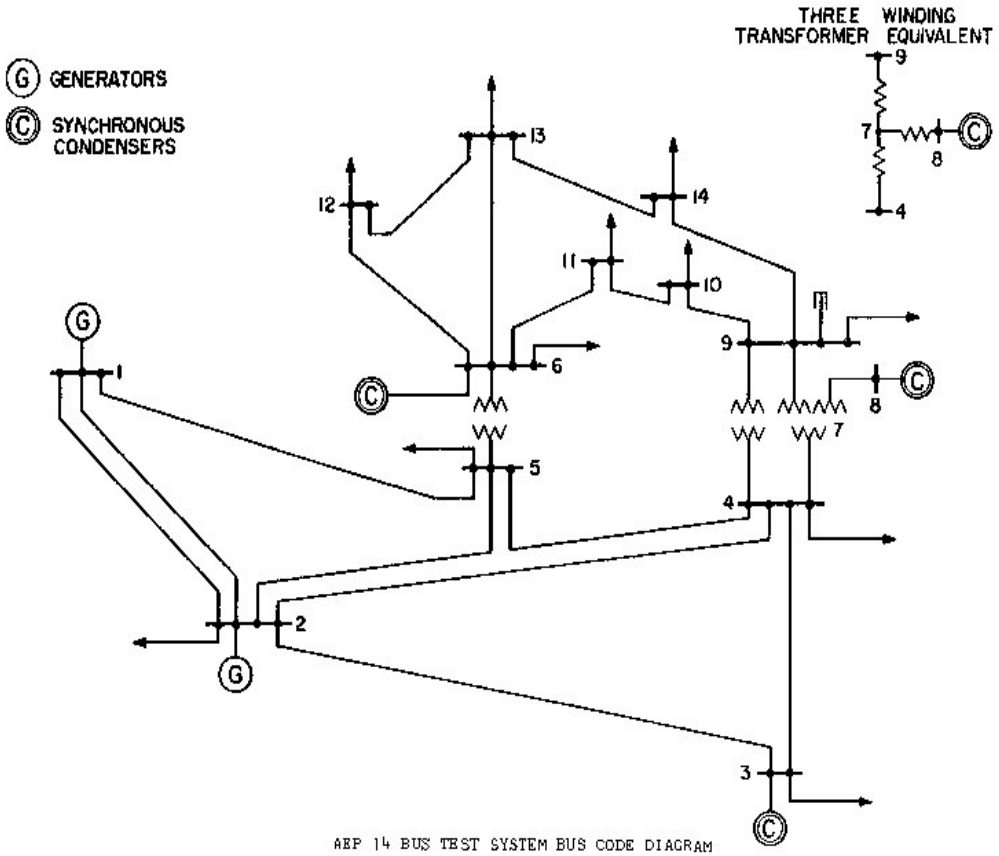

Figure 2.2 - A one-line diagram of IEEE 14-bus power system.

The errors, e_f and e_∞, for the algorithm 2.1, are plotted against the number of measurements in Figure 2.3. The actual bus admittance matrix, Y_{bus}, and the estimated bus admittance matrix, $\tilde{Y}_{bus}$, calculated from the algorithm are shown in the Table 2.3 and Table 2.4 respectively.

Table 2.1 - Errors in the bus admittance matrix estimated through Algorithm 2.1 at various number of measurements for the IEEE-14 bus power system.

No. of sets of measurements	**100**	**200**	**300**	**400**	**500**	**600**
e_f	0.0705	0.0579	0.0535	0.0529	0.0523	0.0511
e_∞	0.0570	0.0463	0.0439	0.0429	0.0433	0.0427

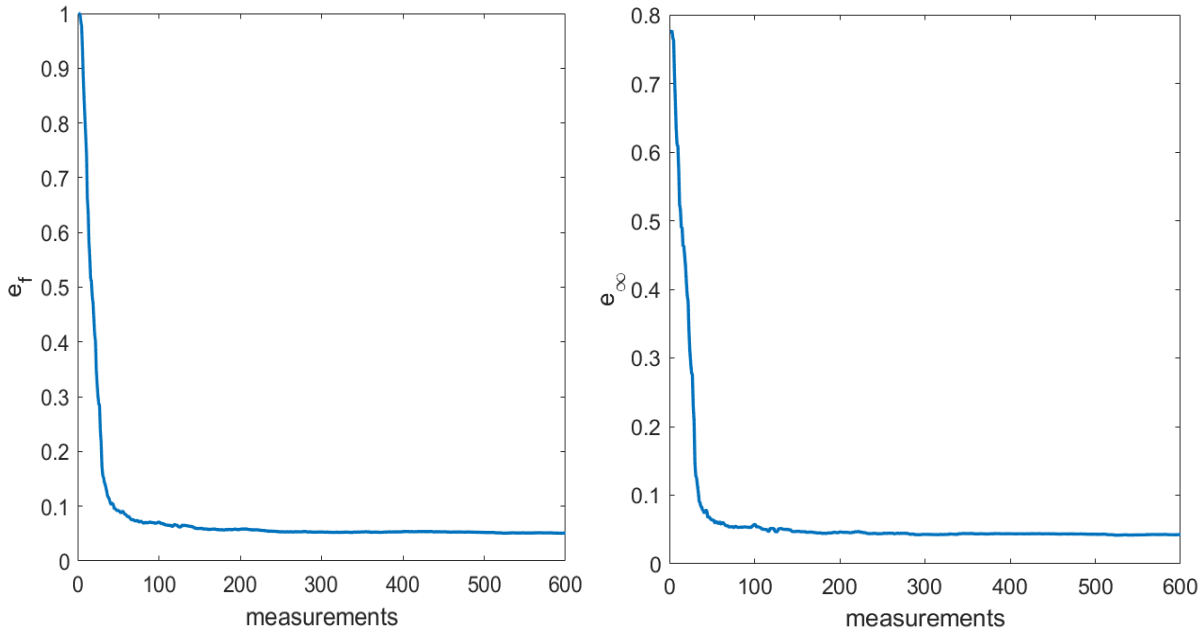

Figure 2.3 - Plot of the errors in the bus admittance matrix estimated through Algorithm 2.1 for the IEEE 14-bus power system.

The parameters of the lines (i.e., line impedance) can be evaluated from the entries of the estimated bus admittance matrix, $\tilde{Y}_{bus}$. For example, the impedance of the branch connecting bus 1 and bus 2 can be estimated[14] by the negative reciprocal of the mean of $\tilde{Y}_{bus}(1,2)$ and $\tilde{Y}_{bus}(2,1)$. That is, $\tilde{z}_{(1,2)} = -\frac{1}{(-4.83 + 14.93i - 4.89 + 14.87i)/2} = 0.0198 + 0.0607i$. The actual impedance of the branch 1-2 is 0.01938 + 0.05917i. Similarly, the estimated and the actual impedances of other branches are shown in the Table 2.2 along with the % error of the estimated impedance.

The histogram showing the number of elements falling within certain ranges of the errors is shown in Figure 2.5. Note that the errors for most of the estimated parameters are

[14] Here the assumption is that the component connecting bus 1 and bus 2 is not a tap changing transformer. If the component is a tap changing transformer with off-nominal tap settings, then $\tilde{z}_{(1,2)} = -\frac{1}{\tilde{Y}_{bus}(1,2)}$ and $\tilde{z}_{(2,1)} = -\frac{1}{\tilde{Y}_{bus}(2,1)}$.

less than 10% range.

Table 2.2 – Actual branch parameters along with the parameters estimated through Algorithm 2.1 for the IEEE 14-bus power system.

Branch		Actual Impedance z_{ij}	Estimated Impedance $\tilde{z}_{ij}$	% error = $\left\|\frac{\tilde{z}_{ij}-z_{ij}}{z_{ij}}\right\| \times 100$
From bus i	To bus j			
1	2	0.0194 + 0.0592i	0.0198 + 0.0607i	2.504
1	5	0.054 + 0.223i	0.0499 + 0.2268i	2.4575
2	3	0.047 + 0.198i	0.0472 + 0.2017i	1.8424
2	4	0.0581 + 0.1763i	0.0517 + 0.1795i	3.87
2	5	0.0569 + 0.1739i	0.0607 + 0.1776i	2.8837
3	4	0.067 + 0.171i	0.0684 + 0.1734i	1.4816
4	5	0.0133 + 0.0421i	0.0135 + 0.0443i	4.9856
4	7	0.2045i	0.00410 + 0.2129i	4.5823
4	9	0.5389i	0.00890 + 0.5637i	4.8809
5	6	0.2349i	0.00150 + 0.2555i	8.8125
6	11	0.095 + 0.1989i	0.1003 + 0.209i	5.1868
6	12	0.1229 + 0.2558i	0.130 + 0.2755i	7.3822
6	13	0.0662 + 0.1303i	0.0714 + 0.1353i	4.9604
7	8	0.1762i	-0.0014 + 0.182i	3.3956
7	9	0.11i	-0.0003 + 0.1173i	6.6712
9	10	0.0318 + 0.0845i	0.0373 + 0.0936i	11.7241
9	14	0.1271 + 0.2704i	0.1335 + 0.2794i	3.7069
10	11	0.0821 + 0.1921i	0.0855 + 0.2095i	8.4934
12	13	0.2209 + 0.1999i	0.2295 + 0.2066i	3.6603
13	14	0.1709 + 0.348i	0.1714 + 0.3558i	2.0043

Table 2.3 – Actual bus admittance matrix, Y_{bus}, of the IEEE 14-bus power system.

Bus No	1	2	3	4	5	6	7	8	9	10	11	12	13	14
1	6.03 - 19.45i	-5 + 15.26i	-	-	-1.03 + 4.23i	-	-	-	-	-	-	-	-	-
2	-5 + 15.26i	9.52 - 30.27i	-1.14 + 4.78i	-1.69 + 5.12i	-1.70 + 5.19i	-	-	-	-	-	-	-	-	-
3	-	-1.14 + 4.78i	3.12 - 9.82i	-1.99 + 5.07i	-	-	-	-	-	-	-	-	-	-
4	-	-1.69 + 5.12i	-1.99 + 5.07i	10.51 - 38.65i	-6.84 + 21.58i	-	4.89i	-	1.86i	-	-	-	-	-
5	-1.03 + 4.23i	-1.70 + 5.19i	-	-6.84 + 21.58i	9.57 - 35.53i	4.26i	-	-	-	-	-	-	-	-
6	-	-	-	-	4.26i	6.58 - 17.34i	-	-	-	-	-1.96 + 4.09i	-1.53 + 3.18i	-3.10 + 6.10i	-
7	-	-	-	4.89i	-	-	- 19.55i	5.68i	9.09i	-	-	-	-	-
8	-	-	-	-	-	-	5.68i	5.68i	-	-	-	-	-	-
9	-	-	-	1.86i	-	-	9.09i	-	5.33 - 24.09i	-3.90 + 10.37i	-	-	-	-1.42 + 3.03i
10	-	-	-	-	-	-	-	-	-3.90 + 10.37i	5.78 - 14.77i	-1.88 + 4.40i	-	-	-
11	-	-	-	-	-	-1.96 + 4.09i	-	-	-	-1.88 + 4.40i	3.84 - 8.50i	-	-	-
12	-	-	-	-	-	-1.53 + 3.18i	-	-	-	-	-	4.01 - 5.43i	-2.49 + 2.25i	-
13	-	-	-	-	-	-3.10 + 6.10i	-	-	-	-	-	-2.49 + 2.25i	6.72 - 10.67i	-1.14 + 2.31i
14	-	-	-	-	-	-	-	-	-1.42 + 3.03i	-	-	-	-1.14 + 2.31i	2.56 - 5.34i

Table 2.4 – Bus admittance matrix, $\widetilde{Y}_{bus}$, of IEEE 14-bus power system estimated through Algorithm 2.1[15].

Bus No	1	2	3	4	5	6	7	8	9	10	11	12	13	14
1	5.98 - 19.16i	-4.83 + 14.93i	-	-	-0.840 + 4.31i	-	-	-	-	-	-	-	-	-
2	-4.89 + 14.87i	9.19 - 29.73i	-1.14 + 4.68i	-1.23 + 5.36i	-1.90 + 4.87i	-	-	-	-	-	-	-	-	-
3	-	-1.06 + 4.72i	3.13 - 9.80i	-1.95 + 4.97i	-	-	-	-	-	-	-	-	-	-
4	-	-1.73 + 4.93i	-1.98 + 5.01i	9.97 - 37.67i	-6.23 + 20.64i	-	-0.100 + 4.67i	-	0.01 + 1.77i	-	-	-	-	-
5	-1.01 + 4.11i	-1.54 + 5.22i	-	-6.38 + 20.65i	9.02 - 34.45i	-0.0100 + 3.74i	-	-	-	-	-	-	-	-
6	-	-	-	-	-0.0400 + 4.09i	6.41 - 16.53i	-	-	-	-	-1.85 + 3.90i	-1.39 + 2.94i	-3.04 + 5.79i	-
7	-	-	-	-0.0800 + 4.72i	-	-	-0.0800 - 19.01i	0.05 + 5.48i	-0.01 + 8.46i	-	-	-	-	-
8	-	-	-	-	-	-	0.0300 + 5.51i	-0.01 - 5.60i	-	-	-	-	-	-
9	-	-	-	-0.0600 + 1.78i	-	-	0.0600 + 8.58i	-	5.18 - 22.66i	-3.74 + 9.02i	-	-	-	-1.35 + 2.97i
10	-	-	-	-	-	-	-	-	-3.60 + 9.43i	5.35 - 13.72i	-1.70 + 4.09i	-	-	-
11	-	-	-	-	-	-1.88 + 3.88i	-	-	-	-1.64 + 4.09i	3.73 - 8.33i	-	-	-
12	-	-	-	-	-	-1.41 + 3.00i	-	-	-	-	-	3.86 - 5.21i	-2.42 + 2.16i	-
13	-	-	-	-	-	-3.06 + 5.77i	-	-	-	-	-	-2.39 + 2.18i	6.56 - 10.34i	-1.12 + 2.26i
14	-	-	-	-	-	-	-	-	-1.44 + 2.86i	-	-	-	-1.07 + 2.30i	2.55 - 5.31i

[15] The entries which are very small in magnitude are shown by '-'. These small entries are due to the errors in the measurements. A very small admittance represents a very high impedance (effectively an open-circuit). This practice of replacing very small admittances by zero will be used throughout the rest of the thesis.

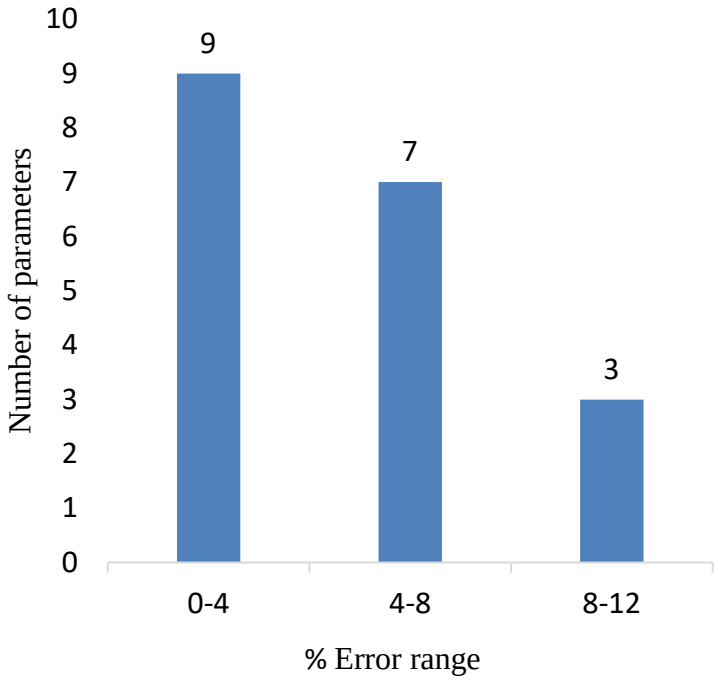

Figure 2.4 - Histogram of the errors in the parameters of IEEE 14-bus power estimated through Algorithm 2.1.

2.4.2 IEEE 24-bus system

The system has generators connected at buses 1, 2, 7, 13, 14, 15, 16, 18, 21, 22, and 23 with the slack-bus connected at bus 13. The system has 38 branches and 24 buses. The parameters and the connection information are provided in the appendix. The scheme of Figure 2.1 is executed on the system and the errors of the algorithm are tabulated in the Table 2.5.

Table 2.5 - Errors in the bus admittance matrix estimated through Algorithm 2.1 at various number of measurements for the IEEE 24-bus power system.

No. of sets of measurements	**100**	**200**	**300**	**400**	**500**	**600**
$\boldsymbol{e_f}$	0.1092	0.0788	0.0708	0.063	0.0583	0.0559
$\boldsymbol{e_\infty}$	0.1255	0.0924	0.0836	0.0744	0.068	0.0663

The errors in the estimated bus admittance matrix are also plotted in the Figure 2.5

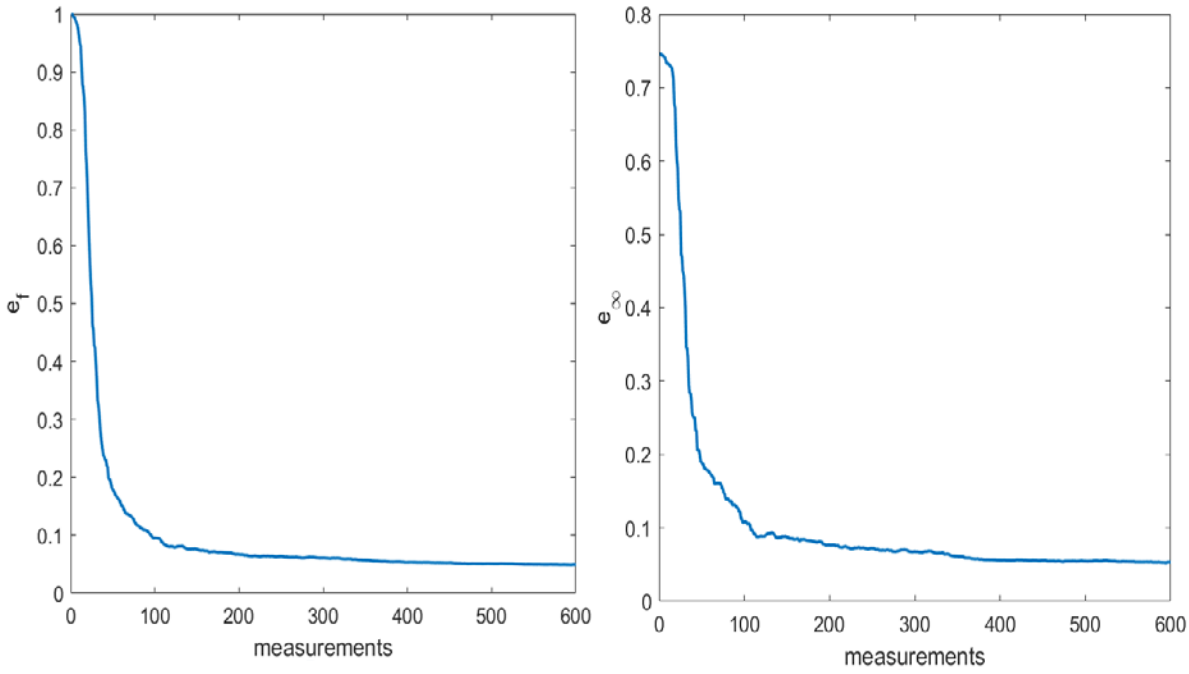

Figure 2.5 - Plot of the errors in the bus admittance matrix estimated through Algorithm 2.1 for the IEEE 24-bus power system.

The actual bus admittance matrix, Y_{bus}, and the estimated bus admittance matrix, $\tilde{Y}_{bus}$, calculated from the algorithm are shown in the Table 2.7 and Table 2.8 respectively. The estimated impedances along with the errors for the IEEE 24-bus system are mentioned in the Table 2.6.

Table 2.6 - Actual parameters of various branches along with parameters estimated through Algorithm 2.1 for the IEEE-24 bus power system.

Branch		Actual Impedance z_{ij}	Estimated Impedance $\tilde{z}_{ij}$	% error = $\left\|\frac{\tilde{z}_{ij}-z_{ij}}{z_{ij}}\right\| \times 100$
From bus i	To bus j			
1	2	0.0026 + 0.0139i	0.0027 + 0.0147i	6.0087
1	3	0.0546 + 0.2112i	0.0512 + 0.2137i	1.9291
1	5	0.0218 + 0.0845i	0.0217 + 0.0873i	3.2541

2	4	0.0328 + 0.1267i	0.0345 + 0.1324i	4.5538
2	6	0.0497 + 0.192i	0.0512 + 0.1983i	3.2674
3	9	0.0308 + 0.119i	0.0313 + 0.1196i	0.6347
3	24	0.0024 + 0.0864i	0.0023 + 0.0875i	1.2451
4	9	0.0268 + 0.1037i	0.0275 + 0.1044i	0.9461
5	10	0.0228 + 0.0883i	0.023 + 0.0889i	0.727
6	10	0.0139 + 0.0605i	0.0141 + 0.0607i	0.4407
7	8	0.0159 + 0.0614i	0.0158 + 0.0615i	0.2036
8	9	0.0427 + 0.1651i	0.0428 + 0.1656i	0.2832
8	10	0.0427 + 0.1651i	0.0427 + 0.1655i	0.2552
9	11	0.0024 + 0.0864i	0.0031 + 0.0874i	1.448
9	12	0.0024 + 0.0864i	0.0025 + 0.0915i	5.8765
10	11	0.0023 + 0.0856i	0.0026 + 0.087i	1.7362
10	12	0.0023 + 0.0856i	0.0044 + 0.0897i	5.3863
11	13	0.0061 + 0.0476i	0.0064 + 0.0482i	1.487
11	14	0.0054 + 0.0418i	0.0055 + 0.0424i	1.5296
12	13	0.0061 + 0.0476i	0.0064 + 0.0499i	4.8394
12	23	0.0124 + 0.0966i	0.0113 + 0.1032i	6.9006
13	23	0.0111 + 0.0865i	0.0095 + 0.0885i	2.8585
14	16	0.005 + 0.0389i	0.0046 + 0.0412i	6.0223
15	16	0.0022 + 0.0173i	0.0021 + 0.0186i	7.286
15	21	0.0031 + 0.0245i	0.0032 + 0.0252i	2.6627
15	24	0.0067 + 0.0519i	0.0066 + 0.0539i	3.735
16	17	0.0033 + 0.0259i	0.0037 + 0.028i	8.0179
16	19	0.003 + 0.0231i	0.0033 + 0.0249i	7.7201
17	18	0.0018 + 0.0144i	0.0018 + 0.0148i	3.0744
17	22	0.0135 + 0.1053i	0.0149 + 0.1091i	3.7979
18	21	0.0017 + 0.013i	0.0018 + 0.0136i	5.1058
19	20	0.0026 + 0.0198i	0.0030 + 0.0212i	7.2268

20	23	0.0014 + 0.0108i	0.0014 + 0.0117i	8.2622
21	22	0.0087 + 0.0678i	0.0062 + 0.0734i	9.0431

The histogram showing the number of estimated parameters falling within various error ranges is shown in the Figure 2.5. From the figure and the Table 2.6, it is clear that none of the estimated parameter has error > 10%, and most of the parameters are estimated with < 5% error.

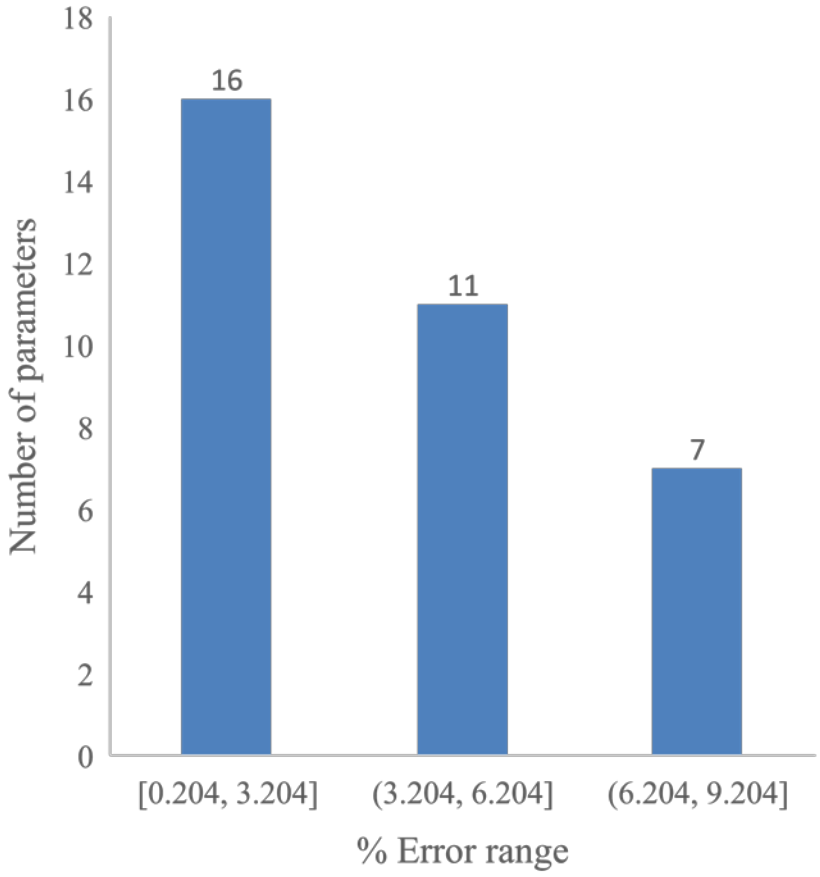

Figure 2.6 - Histogram of the errors in the parameters of IEEE 24-bus power estimated through Algorithm 2.1.

Table 2.7 - Actual bus admittance matrix, Y_{bus}, of the IEEE 24-bus power system.

Bus No	1	2	3	4	5	6	7	8	9	10	11	12	13	14	15	16	17	18	19	20	21	22	23	24
1	17.01 - 84.98i	-13.0 + 69.51i	-1.15 + 4.44i	-	-2.86 + 11.1i	-	-	-	-	-	-	-	-	-	-	-	-	-	-	-	-	-	-	-
2	-13.0 + 69.51i	16.18 - 81.72i	-	-1.91 + 7.40i	-	-1.26 + 4.88i	-	-	-	-	-	-	-	-	-	-	-	-	-	-	-	-	-	-
3	-1.15 + 4.44i	-	3.49 - 23.5i	-	-	-	-	-	-2.04 + 7.88i	-	-	-	-	-	-	-	-	-	-	-	-	-	-	-0.320 + 11.56i
4	-	-1.91 + 7.40i	-	4.25 - 16.41i	-	-	-	-	-2.34 + 9.04i	-	-	-	-	-	-	-	-	-	-	-	-	-	-	-
5	-2.86 + 11.1i	-	-	-	5.60 - 21.69i	-	-	-	-	-2.74 + 10.62i	-	-	-	-	-	-	-	-	-	-	-	-	-	-
6	-	-1.26 + 4.88i	-	-	-	4.87 - 20.33i	-	-	-	-3.61 + 15.7i	-	-	-	-	-	-	-	-	-	-	-	-	-	-
7	-	-	-	-	-	-	3.95 - 15.25i	-3.95 + 15.26i	-	-	-	-	-	-	-	-	-	-	-	-	-	-	-	-
8	-	-	-	-	-	-	-3.95 + 15.26i	6.89 - 26.56i	-1.47 + 5.68i	-1.47 + 5.68i	-	-	-	-	-	-	-	-	-	-	-	-	-	-
9	-	-	-2.04 + 7.88i	-2.34 + 9.04i	-	-	-	-1.47 + 5.68i	6.46 - 44.99i	-	-0.320 + 11.56i	-0.320 + 11.56i	-	-	-	-	-	-	-	-	-	-	-	-
10	-	-	-	-	-2.74 + 10.62i	-3.61 + 15.7i	-	-1.47 + 5.68i	-	8.44 - 53.63i	-0.320 + 11.68i	-0.320 + 11.68i	-	-	-	-	-	-	-	-	-	-	-	-
11	-	-	-	-	-	-	-	-	-0.320 + 11.56i	-0.320 + 11.68i	6.34 - 67.93i	-	-2.65 + 20.67i	-3.04 + 23.53i	-	-	-	-	-	-	-	-	-	-
12	-	-	-	-	-	-	-	-	-0.320 + 11.56i	-0.320 + 11.68i	-	4.61 - 54.52i	-2.65 + 20.67i	-	-	-	-	-	-	-	-	-	-1.31 + 10.18i	-
13	-	-	-	-	-	-	-	-	-	-	-2.65 + 20.67i	-2.65 + 20.67i	6.76 - 52.52i	-	-	-	-	-	-	-	-	-	-1.46 + 11.37i	-
14	-	-	-	-	-	-	-	-	-	-	-3.04 + 23.53i	-	-	6.29 - 48.74i	-	-3.25 + 25.29i	-	-	-	-	-	-	-	-
15	-	-	-	-	-	-	-	-	-	-	-	-	-	-	14.84 - 115.81i	-7.23 + 56.88i	-	-	-	-	-5.16 + 40.15i	-	-	-2.45 + 18.95i
16	-	-	-	-	-	-	-	-	-	-	-	-	-	-3.25 + 25.29i	-7.23 + 56.88i	20.85 - 162.63i	-4.84 + 37.99i	-	-5.53 + 42.57i	-	-	-	-	-
17	-	-	-	-	-	-	-	-	-	-	-	-	-	-	-	-4.84 + 37.99i	14.59 - 115.56i	-8.55 + 68.38i	-	-	-	-1.20 + 9.34i	-	-
18	-	-	-	-	-	-	-	-	-	-	-	-	-	-	-	-	-8.55 + 68.38i	18.23 - 144.29i	-	-	-9.68 + 75.99i	-	-	-
19	-	-	-	-	-	-	-	-	-	-	-	-	-	-	-	-5.53 + 42.57i	-	-	11.93 - 92.15i	-6.40 + 49.68i	-	-	-	-
20	-	-	-	-	-	-	-	-	-	-	-	-	-	-	-	-	-	-	-6.40 + 49.68i	18.2 - 140.61i	-	-	-11.8 + 91.06i	-
21	-	-	-	-	-	-	-	-	-	-	-	-	-	-	-5.16 + 40.15i	-	-	-9.68 + 75.99i	-	-	16.71 - 130.42i	-1.86 + 14.51i	-	-
22	-	-	-	-	-	-	-	-	-	-	-	-	-	-	-	-	-1.20 + 9.34i	-	-	-	-1.86 + 14.51i	3.06 - 23.67i	-	-
23	-	-	-	-	-	-	-	-	-	-	-	-1.31 + 10.18i	-1.46 + 11.37i	-	-	-	-	-	-	-11.8 + 91.06i	-	-	14.57 - 112.38i	-
24	-	-	-0.320 + 11.56i	-	-	-	-	-	-	-	-	-	-	-	-2.45 + 18.95i	-	-	-	-	-	-	-	-	2.77 - 30.81i

Table 2.8 - Bus admittance matrix, $\tilde{Y}_{bus}$, of IEEE 14-bus power system estimated through Algorithm 2.1.

Bus No	1	2	3	4	5	6	7	8	9	10	11	12	13	14	15	16	17	18	19	20	21	22	23	24
1	16.22 - 81.03i	-12.28 + 65.54i	-1.31 + 4.37i	-	-2.54 + 10.89i	-	-	-	-	-	-	-	-	-	-	-	-	-	-	-	-	-	-	-
2	-12.07 + 65.64i	15.32 - 77.78i	-	-1.86 + 7.1i	-	-1.16 + 4.74i	-	-	-	-	-	-	-	-	-	-	-	-	-	-	-	-	-	-
3	-0.81 + 4.48i	-	3.48 - 23.43i	-	-	-	-	-	-2.09 + 7.79i	-	-	-	-	-	-	-	-	-	-	-	-	-	-	-	-0.30 + 11.45i
4	-	-1.82 + 7.05i	-	4.25 - 16.33i	-	-	-	-	-2.35 + 8.98i	-	-	-	-	-	-	-	-	-	-	-	-	-	-	-
5	-2.81 + 10.69i	-	-	-	5.54 - 21.61i	-	-	-	-	-2.76 + 10.55i	-	-	-	-	-	-	-	-	-	-	-	-	-	-
6	-	-1.28 + 4.71i	-	-	-	4.87 - 20.29i	-	-	-	-3.64 + 15.62i	-	-	-	-	-	-	-	-	-	-	-	-	-	-
7	-	-	-	-	-	-	3.93 - 15.24i	-3.91 + 15.26i	-	-	-	-	-	-	-	-	-	-	-	-	-	-	-	-
8	-	-	-	-	-	-	-3.93 + 15.25i	6.84 - 26.56i	-1.48 + 5.65i	-1.42 + 5.67i	-	-	-	-	-	-	-	-	-	-	-	-	-	-
9	-	-	-2.0 + 7.86i	-2.37 + 8.93i	-	-	-	-1.44 + 5.67i	6.56 - 44.71i	-	-0.51 + 11.39i	-0.38 + 10.73i	-	-	-	-	-	-	-	-	-	-	-	-
10	-	-	-	-	-2.69 + 10.53i	-3.61 + 15.65i	-	-1.5 + 5.66i	-	8.56 - 53.3i	-0.42 + 11.4i	-0.70 + 11.04i	-	-	-	-	-	-	-	-	-	-	-	-
11	-	-	-	-	-	-	-	-	-0.31 + 11.46i	-0.26 + 11.56i	6.33 - 67.06i	-	-2.75 + 20.32i	-2.87 + 23.17i	-	-	-	-	-	-	-	-	-	-
12	-	-	-	-	-	-	-	-	-0.21 + 11.11i	-0.39 + 11.2i	-	4.42 - 52.25i	-2.51 + 19.82i	-	-	-	-	-	-	-	-	-	-1.72 + 9.52i	-
13	-	-	-	-	-	-	-	-	-	-	-2.68 + 20.42i	-2.56 + 19.61i	6.6 - 51.97i	-	-	-	-	-	-	-	-	-	-0.90 + 11.27i	-
14	-	-	-	-	-	-	-	-	-	-	-3.11 + 23.19i	-	-	6.19 - 48.33i	-	-2.82 + 23.76i	-	-	-	-	-	-	-	-
15	-	-	-	-	-	-	-	-	-	-	-	-	-	-	14.25 - 113.39i	-4.91 + 53.33i	-	-	-	-	-5.45 + 38.93i	-	-	-2.34 + 18.03i
16	-	-	-	-	-	-	-	-	-	-	-	-	-	-2.55 + 24.14i	-7.27 + 52.98i	18.78 - 152.64i	-4.43 + 35.74i	-	-4.45 + 39.83i	-	-	-	-	-
17	-	-	-	-	-	-	-	-	-	-	-	-	-	-	-	-4.77 + 34.58i	14.13 - 113.7i	-8.19 + 66.2i	-	-	-	-1.4 + 8.87i	-	-
18	-	-	-	-	-	-	-	-	-	-	-	-	-	-	-	-	-7.79 + 66.59i	18.01 - 140.66i	-	-	-9.58 + 71.69i	-	-	-
19	-	-	-	-	-	-	-	-	-	-	-	-	-	-	-	-5.91 + 39.21i	-	-	12.23 - 89.81i	-7.19 + 45.99i	-	-	-	-
20	-	-	-	-	-	-	-	-	-	-	-	-	-	-	-	-	-	-	-6.06 + 46.62i	16.32 - 131.95i	-	-	-10.22 + 84.02i	-
21	-	-	-	-	-	-	-	-	-	-	-	-	-	-	-4.55 + 39.3i	-	-	-9.13 + 72.87i	-	-	15.59 - 125.87i	-0.78 + 13.09i	-	-
22	-	-	-	-	-	-	-	-	-	-	-	-	-	-	-	-	-1.06 + 9.13i	-	-	-	-1.5 + 13.95i	2.84 - 23.35i	-	-
23	-	-	-	-	-	-	-	-	-	-	-	-0.38 + 9.63i	-1.51 + 11.08i	-	-	-	-	-	-	-9.48 + 84.63i	-	-	12.59 - 106.77i	-
24	-	-	-0.30 + 11.4i	-	-	-	-	-	-	-	-	-	-	-	-2.12 + 18.57i	-	-	-	-	-	-	-	-	2.7 - 30.47i

2.4.3 IEEE 30-bus system

The system has generators connected at buses 1, 2, 22, 27, 23 and the slack bus as 13. The system has 41 branches and 30 buses. The parameters and the connection information are provided in the appendix. The algorithm of Figure 2.1 is executed on the system and the errors are plotted in Figure 2.7.

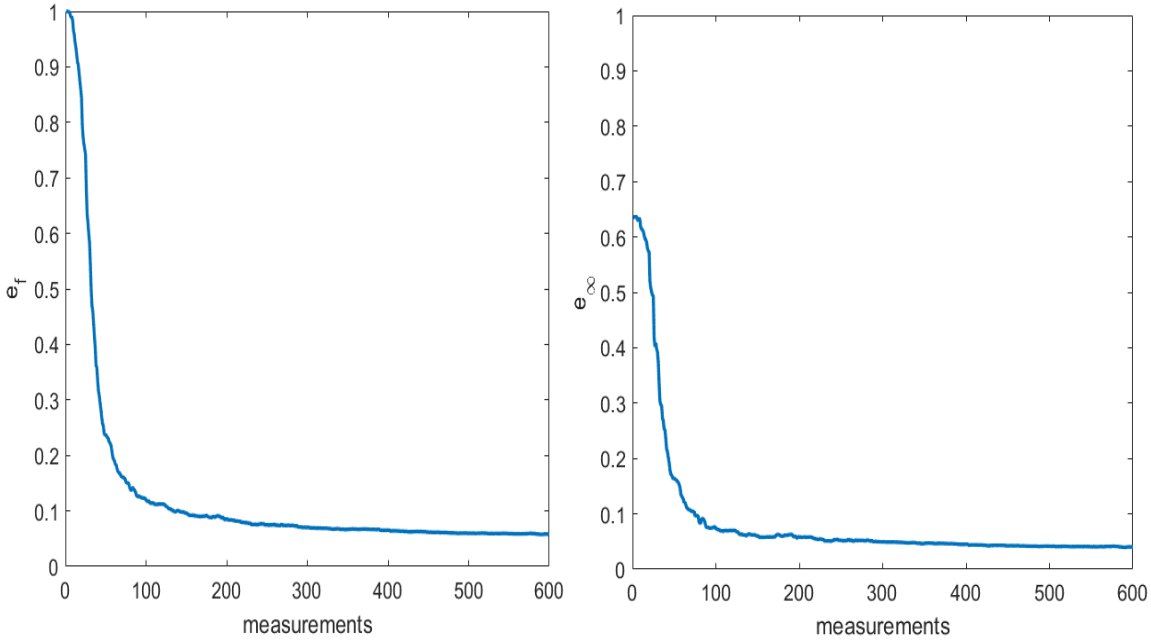

Figure 2.7 - Plot of the errors in the bus admittance matrix estimated through Algorithm 2.1 for the IEEE 30-bus power system.

The values of the errors at various numbers of measurements are mentioned in Table 2.9.

Table 2.9 - Errors in the bus admittance matrix estimated through Algorithm 2.1 at various number of measurements for the IEEE 30-bus power system.

No. of sets of measurements	**100**	**200**	**300**	**400**	**500**	**600**
e_f	0.1201	0.0854	0.0703	0.0653	0.0597	0.0581
e_∞	0.0735	0.0585	0.0496	0.0451	0.0415	0.0400

2.4.4 IEEE 118-bus system

The system has generators connected at 54 of its buses and bus 69 is the slack bus. The system has 186 branches and 118 buses. The parameters and the connection information are provided in the appendix. The algorithm of Figure 2.1 is executed on the system and the errors are plotted in Figure 2.8.

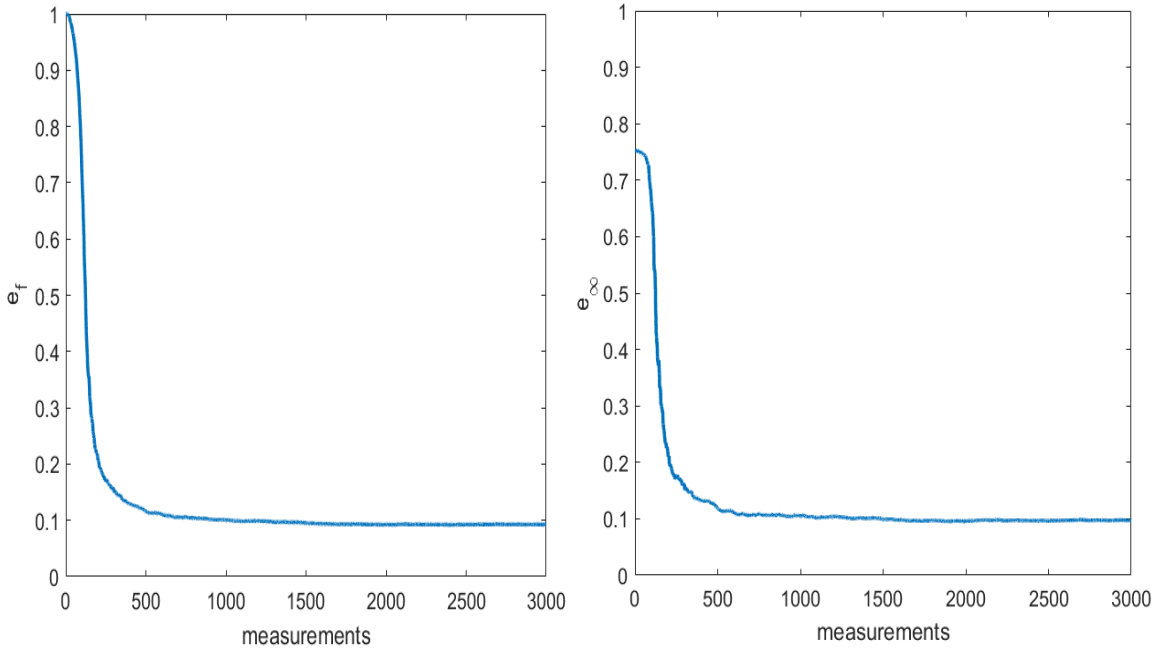

Figure 2.8 - Plot of the errors in the bus admittance matrix estimated through Algorithm 2.1 for the IEEE 118-bus power system.

The values of the errors at various numbers of measurements are shown in Table 2.10**.**

Table 2.10 - Errors in the bus admittance matrix estimated through Algorithm 2.1 at various number of measurements for the IEEE 118-bus power system.

No. of sets of measurements	**1**	**500**	**1000**	**1500**	**2000**
$\boldsymbol{e_f}$	1	0.1157	0.1002	0.0947	0.0923
$\boldsymbol{e_\infty}$	0.7526	0.1179	0.1048	0.0988	0.0963

2.5 Discussion

The plots and the tables of section 2.4 show that the errors in the estimated bus admittance matrix, $\tilde{Y}_{bus}$, decrease with the increase in the number of measurements. However, a system needs to satisfy certain conditions for the estimated bus admittance matrix to converge near the actual bus admittance matrix.

The algorithm will converge if the condition number of the voltage measurement matrix is good (< ~10^5). In other words, for the algorithm to converge near the actual bus admittance matrix, the voltage measurement matrix should have sufficient number of independent measurements. For power systems, this condition is satisfied if there are sufficient variations in the connected loads. Such variations result in independent measurements, and the voltage measurement matrix thereby obtained will have a relatively low condition number.

Such type of condition (or its slight variations) need to be satisfied for all the measurement-based algorithms [69] if no prior information about the unknowns is available. As the results obtained for the cases considered for IEEE 14 and 24-bus power systems in section 2.4 have small errors, the cases must have satisfied the condition mentioned above. The condition number of the cases considered for both the systems are mentioned in Table 2.11.

Table 2.11 – The condition number of the voltage measurement matrix of IEEE 14 and 24-bus systems for the cases considered in section 2.4.

System	Condition number	Final Error
IEEE 14-bus	2603.71	0.0511
IEEE 24-bus	3533.47	0.0559

The condition number of the voltage measurement matrix of a power system increases with a decrease in the variations of the loads connected to its buses. This increase in the condition number results in an increased error of the estimated bus admittance matrix. As an illustration, the condition number along with the final errors of the IEEE 14-bus power system is shown in Table 2.12 for various values of the permissible variations in the loads connected to each bus.

It is clear from Table 2.12 that with the increase in the variations of loads, both the condition number of the voltage measurement matrix as well as the final errors are reducing.

Table 2.12 – Errors in the estimated bus admittance matrix of the IEEE 14-bus power system for various condition numbers of the voltage measurement matrix.

Max. % load change at each bus	Condition number of voltage measurement matrix	Errors		Max. % load change at each bus	Condition number of voltage measurement matrix	Errors	
		e_f	e_{inf}			e_f	e_{inf}
0.75	38919.29	0.8535	0.6730	8.25	3675.48	0.0726	0.0582
1.5	19334.91	0.6543	0.5158	9	3366.82	0.0654	0.0516
2.25	12782.43	0.4622	0.3539	9.75	3104.33	0.0580	0.0464
3	9814.86	0.3281	0.2497	10.5	2935.39	0.0524	0.0435
3.75	7735.08	0.2365	0.1728	11.25	2759.35	0.0475	0.0390
4.5	6560.92	0.1897	0.1388	12	2600.89	0.0430	0.0360
5.25	5645.06	0.1482	0.1123	12.75	2471.64	0.0408	0.0350
6	4927.07	0.1205	0.0891	13.5	2363.17	0.0383	0.0327
6.75	4363.76	0.0978	0.0766	14.25	2248.00	0.0372	0.0322
7.5	3987.44	0.0827	0.0656	15	2106.75	0.0359	0.0317

Therefore, with the assumption of no faulty measurements and the variance of the measurement errors being constant, the % error for the Algorithm 2.1 depends on the variations in the load. With the increase in the variations of the connected loads, the condition number of the voltage measurement matrix will decrease which will result in a more accurate estimate of the bus admittance matrix from the algorithm.

A fat matrix (number of columns > number of rows) has a low condition number if its rows are sufficiently independent[16]. Similarly, a thin matrix (number of columns < number of rows) has a low condition number if its columns are independent by a sufficient margin. One scenario that results in a high condition number of a fat matrix is that two of its rows are almost linearly related. For the voltage measurement matrix, only this scenario can result in a high condition number of the matrix. This scenario can occur for the voltage measurement matrix if there exists, at least, one pair of buses such that the voltage measurements for all time samples at one of the buses can be approximated (in a very good manner) by a scalar multiplication of the voltage measurements of the other. This scenario can occur in a power system under following two circumstances:

i) When the buses are joined by a very short equivalent impedance line, as illustrated in the Figure 2.9, the voltages at the buses *tend* to be equal. If I_{ij} is the current flowing through a line with a very short impedance, $z_{ij} = \epsilon$, connecting bus i with bus j, then the voltage difference, V_{ij}, will be given by,

$$V_i - V_j = V_{ij} = I_{ij} \times z_{ij} = I_{ij} \times \epsilon$$

[16] Sufficiently independent here means that at least one of the components of the orthogonal complement of each row vector in the space spanned by the rest of the rows in the matrix has a magnitude that is sufficiently greater than the epsilon of the machine used for computations.

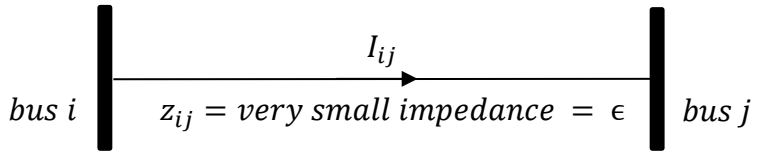

Figure 2.9 - A short impedance line connecting buses *i* and *j*.

Unless the current, I_{ij}, is very large in magnitude, the voltage difference, V_{ij}, will tend to be zero, and the voltages of buses *i* and *j* will be almost the same. Such a scenario will result in an almost identical i^{th} and j^{th} rows of the voltage measurement matrix, and, therefore, the condition number of the matrix will increase which will negatively affect the accuracy of the estimated bus admittance matrix.

ii) In Figure 2.10, if the variations in the load at bus *j*, ΔS_j, are very small, then during normal operation of power system, the variation in the line current, ΔI_{ij}, will be very small as well. As a result, the voltage difference, $V_i - V_j = V_{ij}$, will be nearly constant, and the voltages of the buses *i* and *j* will be approximately linearly related. Such a scenario will result in a poor condition number of the voltage measurement matrix, and, therefore, the accuracy of the resulting estimated bus admittance matrix will degrade.

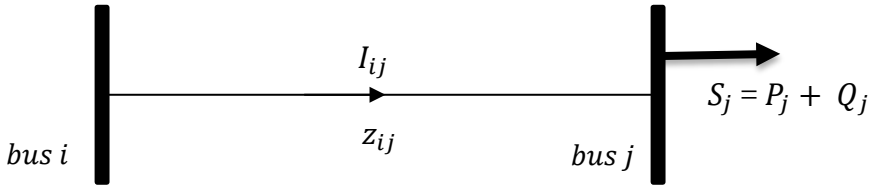

Figure 2.10 – Current I_{ij} flowing through the branch connecting bus *i* with bus *j*.

If the condition number of the voltage measurement matrix is low, then, as shown in the plots and the tables of section 2.4, the errors in the estimated bus admittance matrix reduce as more measurements are accumulated,. Initially, the errors decrease rapidly with the accumulation of measurements, reducing to some threshold (the knee of the curve). However, the rate of reduction in the errors with further accumulation of measurements is extremely low.

Error in the estimated bus admittance matrix never drops to zero due to the noise considered in the measurements of currents and voltage phasors; with perfect (noiseless) measurements, the algorithm, eventually, converges extremely[17] near to the actual bus admittance matrix of the power system. The errors in the phasor measurements are essentially due to the transducers, and, in the future, these errors in the transducers will decrease [3]. With the decrease in the magnitude of errors in the measurements, the errors in the estimated bus admittance matrix through Algorithm 2.1 will also reduce.

As shown in Table 2.12, the errors of the algorithm also reduce when the magnitudes of variations in the loads increase. Although these variations are not in complete control of the power system operator, it is generally agreed upon that their magnitude will be greater for future power systems due to the increased participation of the prosumers and renewable

[17] If the regularization-term is not added to the optimization problem, the estimated bus admittance matrix will converge to the actual bus admittance matrix for the noise-less measurements. However, our algorithm uses the regularization term as the practical measurements always have error. Moreover, the regularization also offers many advantages as has already been mentioned in section 2.2.1. In addition, the magnitude of δ being used in our estimator is so small that for the case of no measurement errors the estimate obtained is extremely near to the actual bus admittance matrix.

sources in the system [3], [21].

For the cases of the systems considered in section 2.4, except for the IEEE 118-bus power system, the final value of the error is reduced to approximately 5% as shown in the tables and the plots of the section 2.4.

The final value of the error in the case of IEEE 118-bus case is approximately 10%. To further investigate this increased error, the error for all the columns, E_c, of the estimated bus admittance matrix, $\tilde{Y}_{bus}$, is shown in Figure 2.11.

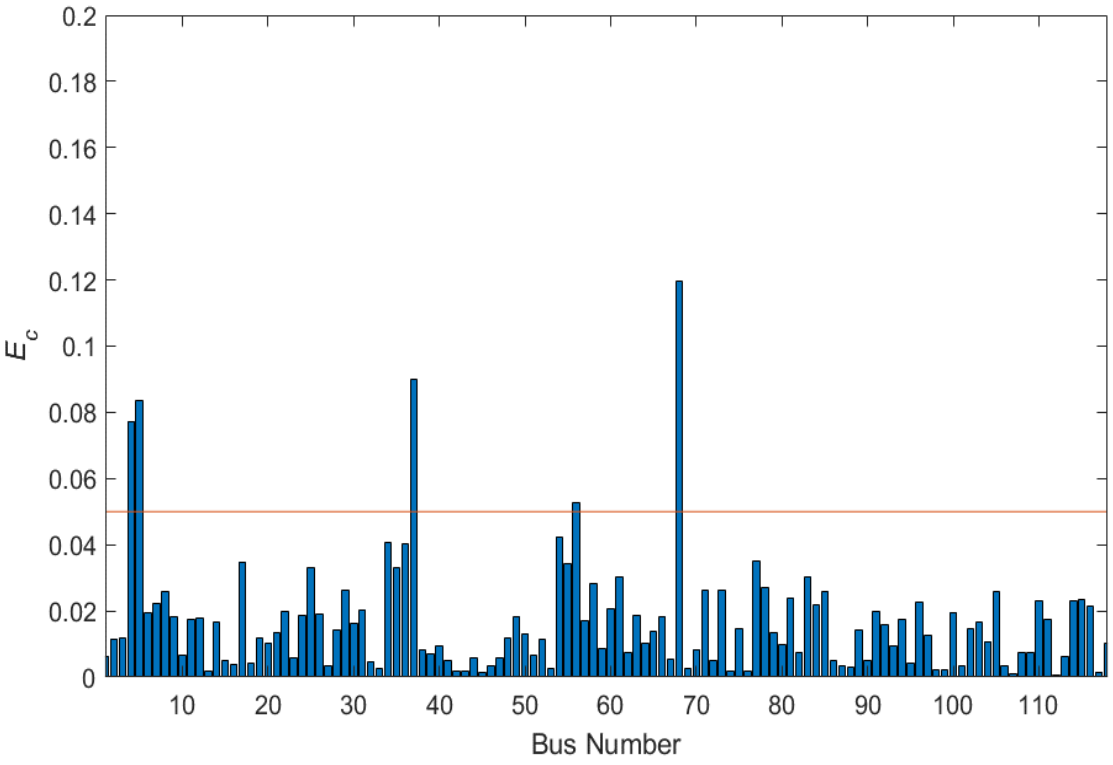

Figure 2.11 - Errors for the columns of the $\tilde{Y}_{bus}$ of IEEE 118-bus power system.

Almost all the buses have error less than 5% with a few exceptions. The buses for which the respective columns in the bus admittance matrix have errors sufficiently greater than 5% are shown in Table 2.13 with the corresponding errors.

Table 2.13 – Buses of the IEEE 118-bus power system for which the error > 5%

Bus Number	**4**	**5**	**37**	**56**	**68**
errors (%)	7.73	8.34	9.01	5.28	11.95

Further investigation into the columns of these buses of the estimated bus admittance matrix, $\tilde{Y}_{bus}$, show that only a few of the column entries have major contribution in the error. For example, the *absolute difference* between the actual bus admittance matrix, Y_{bus}, of the system and the estimated bus admittance matrix, $\tilde{Y}_{bus}$, for the columns of the buses mentioned in Table 2.13 are shown in Table 2.14.

The largest entries in the respective columns are highlighted. These entries correspond to specific branches of the power system. For example, the error in the columns of buses 4 and 5 is caused by the branch connecting buses 4 and 5. Similarly, the error in the column 68 of the bus admittance matrix is due the branch connecting bus 68 with bus 116. The errors are caused by the short impedance lines e.g. the impedance of the branch 68-116 is 0.00034+0.00405j p.u.

Table 2.14 – Columns of absolute errors of the entries of columns of the $\tilde{Y}_{bus}$ for which error > 5%

Columns number of the $\tilde{Y}_{bus}$									
4		**5**		**37**		**56**		**68**	
Bus No.	**Error**	**Bus No.**	**Error**	**Bus No.**	**Error**	**Bus No.**	**Error**	**Bus No.**	**Error**
5	9.6702	3	0.3508	33	0.3198	54	5.3478	65	6.4627
11	0.7541	4	13.8584	34	10.3831	55	3.9320	69	2.7943
-	-	6	0.4004	35	0.8709	57	9.8509	81	5.5104
-	-	8	0.9178	38	2.0567	58	0.2714	116	30.7229

-	-	11	0.9013	39	0.9758	59	0.1418	-	-
-	-	-	-	40	0.2168	-	-	-	-

For the algorithm in Figure 2.1 to converge near the actual bus admittance matrix, there must be enough variation in the boundary conditions of power system. This condition may not be satisfied if the system is lightly loaded as some of the buses, especially the buses connected with the short-impedance lines may cause problems.

One way this problem can be solved is by considering the branches causing the problems through the constraints in the optimization problem of equation 2.14. The problem is then modified as in equation 2.21[18] where the problematic branches are taken into account through the equality constraints

$$\begin{aligned} \tilde{Y}_{bus} = \ & \underset{\tilde{Y}_{bus}}{minimize} \ ||\tilde{r}\,||_f^2 \\ & s.t \\ & \tilde{Y}_{bus(r,s)} = \ -y_{r,s} \end{aligned} \tag{2.21}$$

where $y_{r,s}$ corresponds to the actual admittance of the branch with a relatively much larger error in its estimated admittance. The branch is connecting bus r to bus s. If there are more than one such branches, all can be accommodated in the similar manner through the equality constraints.

To validate the hypothesis that the increased error in the estimated bus admittance matrix can be eradicated through the constrained optimization problem 2.21, a test is performed on the IEEE 14-bus. The load at the bus 2 of the IEEE 14-bus power system is

[18] This modified formulation will serve as the basis of the next chapter.

reduced to a quarter of the nominal load and the simulation is performed on the updated system. As the buses 1 and 2 are connected through a relatively low impedance line, the final errors for the algorithms should increase. The errors in the estimation of the bus admittance matrix are plotted in Figure 2.12 and the values of the errors at a multiple set of measurements are shown in the Table 2.15.

As predicted, the errors of the algorithm have increased. That is, the errors for the case considered in section 2.4.1 are in the range of ~5%. Whereas, a decrease of load by a quarter at the bus 2 of the system has approximately doubled the errors (in the range of ~10%).

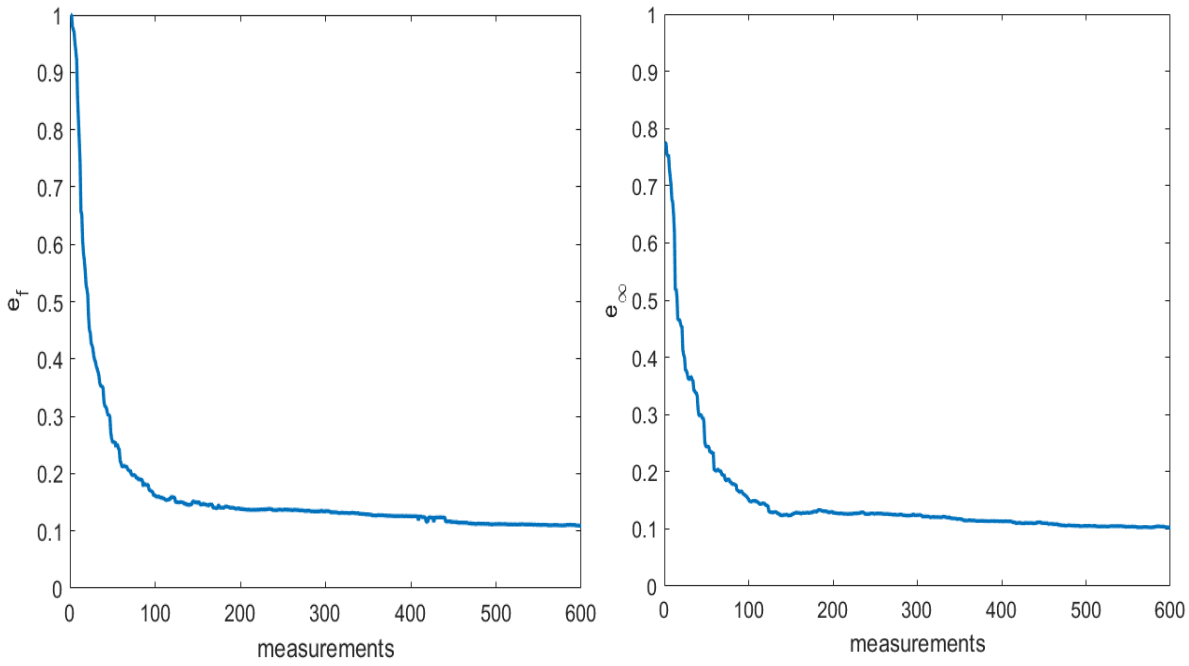

Figure 2.12 - Plot of the Algorithm 2.1 errors for the updated IEEE 14-bus power system.

The reason for this inceased error is that the buses 1 and 2 are joined by a low impedance line, and the decrease of the load at bus 2 has reduced the current flowing

through the low impedance line. Consequently, the voltage difference between the two buses has reduced for all the set of measurements. This reduction in the difference of volatges has brought the volatges of the buses 1 and 2 realtively closer. This nearness of the volatges has increased the condition number of the resulting volatge measurement matrix, and thus, the error in the estimated bus admittance matrix has increased.

Table 2.15 - Errors of the Algorithm 2.1 at various number of measurements for the updated IEEE 14-bus power system.

No. of sets of measurements	**100**	**200**	**300**	**400**	**500**	**600**
$\boldsymbol{e_f}$	0.1623	0.1378	0.1345	0.1256	0.1117	0.1090
$\boldsymbol{e_\infty}$	0.1514	0.1278	0.1241	0.1135	0.1051	0.1025

Therefore, the major cause of error in the bus admittance matrix estimated through Algorithm 2.1 will be the line connecting buses 1 and 2. To validate this statement, the errors for the various columns of the bus admittance matrix is shown in the Figure 2.13.

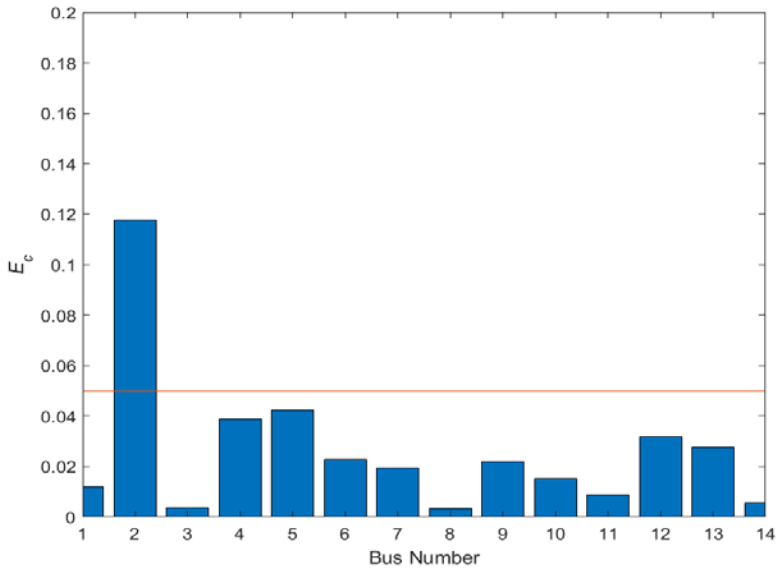

Figure 2.13 - Errors for the $\widetilde{Y}_{bus}$ columns for the updated case of IEEE 14-bus power system.

As hypothesized, the principal source of error is the column 2 of the bus admittance matrix. The *absolute error* for various entries of column 2 of the bus admittance matrix is mentioned in Table 2.16. The component with the largest error is the branch connecting the buses 1 and 2.

Table 2.16 – Errors for various entries of the 2nd column of the estimated bus admittance matrix

Bus No.	Error
1	2.2239
3	0.4997
4	0.6627
5	0.3223

Now if solve the optimization problem 2.21 for the IEEE 14-bus system under the updated load conditions with the admittance of the branch 1-2 as a constraint, the problem becomes

$$\begin{aligned} \tilde{Y}_{bus} = \underset{\acute{Y}_{bus}}{minimize}\ ||\acute{r}||_f^2 \\ s.t \\ \tilde{Y}_{bus(2,1)} = -y_{2,1} \end{aligned} \tag{2.22}$$

The errors in the solution of the problem 2.22 at various number of measurements is given in Table 2.17.

Table 2.17 - Errors at various number of measurements of IEEE 14-bus power system for the problem 2.22

No. of sets of measurements	**5n**	**10n**	**15n**	**20n**	**25n**
$\boldsymbol{e_f}$	0.0629	0.0481	0.0454	0.0422	0.0430
$\boldsymbol{e_\infty}$	0.0952	0.0692	0.0676	0.0549	0.0575

Table 2.17 shows that the error is again reduced to approximately 5% (as it was for the original base-load conditions). Therefore, the addition of the constraint in the optimization problem has resolved the issue of problematic branches. Although the issue of the problematic branch has been solved through the formulation 2.22, there are practical drawbacks in the formulation.

Firstly, the branches causing the problem cannot be known beforehand. That is, as the actual bus admittance matrix of the system is not known, the errors in the parameters of the components and the estimated bus admittance cannot be calculated, and, therefore, the problematic branches cannot be identified. Consequently, they cannot be included in the constraints of the optimization problem.

Secondly, the problem formulation 2.22 assumes that the parameters of the problematic branches are known perfectly without any errors and are, therefore, included as a hard constraint. This assumption of knowing the parameters with perfect accuracy is also unrealistic.

In reality, only the offline parameters of the components of power system are available. Therefore, only they can be used in the constraints instead of the actual parameters of components. As the offline parameters of the components are not extremely accurate, they should be included only as soft-constraints in the problem formulation instead of the hard-constraints[19] as is done in the problem formulation 2.22.

In the next chapter, these problematic issues of the optimization problem 2.22 are

[19] See section 3.3.

addressed through a new problem formulation.

CHAPTER 3. BUS ADMITTANCE MATRIX ESTIMATION ACCOMMODATING THE PRIOR INFORMATION

3.1 Introduction

In the previous chapter, no prior information regarding the parameters and the topology of the power system under consideration was used in the estimation of the corresponding bus admittance matrix. In this chapter, the algorithm proposed in the previous chapter is modified to take into account the prior available information. The prior information falls into two categories

i. Topology of the network.

ii. Admittance of the elements of power system.

As shown in section 1.4, any two buses i and j of a power system that are not directly connected through any component will result in a zero value in the corresponding entry of the bus admittance matrix. The structure of a power system is such that only a few of the buses are directly connected through some component. Moreover, there are many buses which are located so far apart that there is no possibility of their direct connection even in the case of a fault. Due to this intrinsic structure of power systems, node incidence matrices, and, therefore, the resulting bus admittance matrices are highly sparse. This fact can be considered in the problem formulation which will reduce the dimensions and therefore, the complexity of the resulting problem.

Additionally, the offline model-based parameters of power system elements can be used as an initial estimate for the algorithm. Although these parameters are derived during

the design of the elements, and the actual parameters may differ depending on the current operating condition of the element, they can serve as a good initial estimate in the algorithm.. Though not very accurate, offline parameters used as initial guess result in a faster solution of the estimation problem.

3.1.1 Prior Topology:

In this section, the objective function of the optimization problem, presented in the previous chapter, will be modified to accommodate the prior information about the topology of the power system This modification will result in the reduction of the complexity of the problem because of which the solution will require fewer steps and, accordingly, lesser time.

The bus admittance matrix, Y_{bus}, of a power system relates the bus voltage vector with the corresponding node injection current vector as

$$Y_{bus} v_{bus} = i_{bus} \tag{3.1}$$

where v_{bus} and i_{bus} are the complex vectors of buses' voltage phasors and buses' injection current phasors. The bus voltage matrix, V_{bus}, as defined in equation 2.2, is formed by appending the measurements of the voltage vectors taken at different time samples, and the bus injection current matrix, I_{bus}, defined in equation 2.3, is formed by appending the measurements of the injection current vectors at the corresponding time samples. If the measurements are ideal (i.e., without any noise), the two measurements matrices will be related through the bus admittance matrix as,

$$Y_{bus} V_{bus} = I_{bus} \tag{3.2}$$

Transposing the above equation results in

$$V_{bus}^{T} Y_{bus}^{T} = I_{bus}^{T} \tag{3.3}$$

The j^{th} column of V_{bus}^{T}, hereafter, represented by V_j consists of the voltage measurements at bus j for the consecutive 'm' time samples. Similarly, the j^{th} column of I_{bus}^{T}, henceforth, represented by I_j contains the measurements of the current injected into bus j of system for the corresponding 'm' time samples. If the j^{th} column of Y_{bus}^{T} is represented by Y_j, the equation corresponding to j^{th} column in equation 3.3 can be expressed as,

$$V_{bus}^{T} Y_j = I_j \tag{3.4}$$

As V_i is the i^{th}column of transposed voltage matrix, V_{bus}^{T}, the above equation can be also be expressed as[20],

$$\sum_{i=1}^{n} V_i \, Y_{ij} = I_j \tag{3.5}$$

where Y_{ij} is the i^{th} element of the vector, Y_j. Equation 3.5 expresses I_j simply as a linear combination of the columns of the transposed voltage matrix, V_{bus}^{T}. The coefficients of the linear combination are the elements of Y_j.

As previously mentioned, the bus admittance matrix, Y_{bus}, of a typical power system is highly sparse, most of the elements of Y_j will be zero. Therefore, many of the coefficients in the linear combination, $\sum_{i=1}^{n} V_i \, Y_{ij}$, will be zero, and the several

[20] A matrix-vector product can be seen as a linear combination of the columns of the matrix where the coefficients of the linear combination are the corresponding entries of the vector.

corresponding columns of V_{bus}^{T} will play no role in the formation of vector I_j. Taking out the columns that are being multiplied by zero, the dimension of the problem will reduce considerably.

If $L_j := \{index\ of\ buses\ directly\ connected\ with\ bus\ j\}$, then, without loss of generality, equation 3.5 can be effectively expressed as,

$$\sum_{i=L_j} V_i\, Y_{ij} = I_j \tag{3.6}$$

If $\hat{V}_j := [V_{L_j(1)} \mid V_{L_j(2)} \dots \dots . \mid V_{L_j(end)}]$ and $\hat{Y}_j$ is a column vector with only the non-zero elements of the j^{th} row of the bus admittance matrix, then equation 3.6 can be effectively expressed as a reduced equation,

$$\hat{V}_j \hat{Y}_j = I_j \tag{307}$$

where $\hat{V}_j$ is an $m \times L_j$ matrix, $\hat{Y}_j$ is an L_j-dimensional vector and I_j is an m-dimensional vector. Equation 3.7 will be satisfied only with the ideal measurements, but, for a practical system, phasor measurements will have some noise. Therefore, equation 3.7 will be satisfied only approximately as

$$\hat{V}_j \hat{Y}_j \approx I_j \tag{3.8}$$

$$\hat{V}_j \hat{Y}_j - I_j \approx 0 \tag{3.9}$$

In the approximate equation 3.9, the available data is the matrix $\hat{V}_j$ and the vector I_j (both of these will be available through phasor measurements), and the unknown is the vector,

$\hat{Y}_j$ (the reduced[21] j^{th} row of the bus admittance matrix expressed as a column vector). A reasonable criterion for the optimal $\hat{Y}_j$ is a small Euclidian norm of the residue vector, $\hat{r}_j \coloneqq \hat{V}_j\hat{Y}_j - I_j$.

Instead of the norm of the residual vector, its square can be used as the objective for minimization. The problem thus formulated will be equivalent as norm is a non-negative function and square function is monotonically increasing for non-negative real numbers. The updated expression will be

$$(\hat{V}_j\hat{Y}_j - I_j)^*(\hat{V}_j\hat{Y}_j - I_j) \approx 0 \tag{3.10}$$

Ideally, with error-free measurements, such a $\hat{Y}_j$ can be selected that the approximate equation 3.10 is perfectly satisfied. For practical noisy measurements, however, the equation will almost never, in probability, be satisfied perfectly. Therefore, our goal should be, instead, to solve the optimization problem

$$\underset{\hat{Y}_j}{minimize}\ (\hat{V}_j\hat{Y}_j - I_j)^*(\hat{V}_j\hat{Y}_j - I_j) \tag{3.11}$$

If $\hat{V}_{ki}$ represents the k^{th} component of the vector $\hat{V}_i$, and $\hat{Y}_{ij}$ represents the i^{th} component of the vector $\hat{Y}_j$, the expression in equation 3.11 is equivalent to

$$\underset{\hat{Y}_{ij}}{minimize} \sum_{k=1}^{m} \sum_{i=1}^{length(L_j)} \left(\hat{V}_{ki}\hat{Y}_{ij} - I_{kj}\right)^* \left(\hat{V}_{ki}\hat{Y}_{ij} - I_{kj}\right) \tag{3.12}$$

$$\underset{\hat{Y}_{ij}}{minimize} \sum_{k=1}^{m} \sum_{i=1}^{length(L_j)} ||\hat{V}_{ki}\hat{Y}_{ij} - I_{kj}||_2^2 \tag{3.13}$$

[21] Since only the non-zero elements of the j^{th} row of the bus admittance matrix are represented in $\hat{Y}_j$; that is, $\hat{Y}_j$ contains L_j number of entries.

3.1.2 Prior Parameters

If the off-line parameters, represented by the matrix $\hat{Y}^{in}$, are not much different from the actual parameters of the power system, they can serve as a good initial estimate. Moreover, the objective of the optimization problem should be such that the solution remains near the off-line parameters. A large discrepancy between an offline parameter and the corresponding measurement-based parameter can indicate an error in one of them. The identification of such a discrepancy can be used for the detection of a mistake in the offline parameter calculation or data entry. It can also identify a faulty instrument.

If $\hat{Y}_j^{in}$ is a column vector containing the parameters of the components connected to bus j, then the objective that ensures that the estimated parameters remain near the offline parameters can be roughly expressed as,

$$\hat{Y}_j \approx \hat{Y}_j^{in} \tag{3.14}$$

$$\hat{Y}_j - \hat{Y}_j^{in} \approx 0. \tag{3.15}$$

As mentioned previously for equation 3.9, a reasonable estimate for the j^{th} row of the bus admittance matrix can be similarly given by,

$$\underset{\hat{Y}_j}{minimize} \left(\hat{Y}_j - \hat{Y}_j^{in}\right)^* \left(\hat{Y}_j - \hat{Y}_j^{in}\right) \tag{3.16}$$

The objective in equation 3.16 is quadratic and can be equivalently expressed as

$$\underset{\hat{Y}_j}{minimize} \sum_{i}^{length(L_j)} \left(\hat{Y}_j - \hat{Y}_j^{in}\right)^* \left(\hat{Y}_j - \hat{Y}_j^{in}\right) \tag{3.17}$$

$$\underset{\hat{Y}_{ij}}{minimize} \quad \sum_{i}^{length(L_j)} ||\hat{Y}_{ij} - \hat{Y}_{ij}^{in}||_2^2 \tag{3.18}$$

3.2 Problem Formulation

Problems 3.13 and 3.18 are the minimization of two objective functions. The solution of the former accommodates only the measurements whereas the latter takes into account only the prior estimates. Since two distinct functions need to be minimized, the resulting problem is a bi-criterion optimization problem with the objective as a vector in $\mathbb{R}_+^2$ as,

$$\begin{aligned} O_j(\hat{Y}_j) := \begin{bmatrix} o_{1j}(\hat{Y}_j) \\ o_{2j}(\hat{Y}_j) \end{bmatrix} &:= \begin{bmatrix} (\hat{V}_j\hat{Y}_j - I_j)^*(\hat{V}_j\hat{Y}_j - I_j) \\ \left(\hat{Y}_j - \hat{Y}_j^{in}\right)^*\left(\hat{Y}_j - \hat{Y}_j^{in}\right) \end{bmatrix} \\ &= \begin{bmatrix} \sum_{k=1}^{m} \sum_{i=1}^{length(L_j)} ||\hat{V}_{ki}\hat{Y}_{ij} - I_{kj}||_2^2 \\ \sum_{i}^{length(L_j)} ||\hat{Y}_{ij} - \hat{Y}_{ij}^{in}||_2^2 \end{bmatrix} \end{aligned} \tag{3.19}$$

As both the objectives in O_j are convex, the minimization of the objective O_j is a convex vector-optimization problem. Unlike scalars (i.e., $\mathbb{R}$), vectors, mostly, are not compared through a linear ordering[22].

[22] A set S equipped with a linear ordering has the property that any two of its elements $x, y \in S$ must be related through only one of the relations : i) $x < y$; ii) $x > y$; or iii) $x = y$.

For the comparison of vectors, a proper cone[23] in which the optimization vector lies needs to be identified. The vector objective in equation 3.19 lies in the set of two-dimensional non-negative orthant ($\mathbb{R}_+^2$) which is a proper cone.

A standard way to solve such a vector-optimization problem is scalarization. In scalarization, a convex vector-optimization problem is transformed into a convex scalar-optimization problem. The scalar-optimization objective is obtained by taking an inner product of the objective, in a cone, with a vector in the corresponding dual cone[24]. As our objective is a vector in a self-dual cone $\mathbb{R}_+^2$, the objective of the corresponding scalarized optimization problem is obtained by taking a non-negative linear combination of the objectives of the vector optimization problem. Therefore, if $\lambda_j = \begin{bmatrix}\lambda_{1j} & \lambda_{2j}\end{bmatrix}^T; \lambda_{1j}, \lambda_{2j} \in \mathbb{R}_+$, then the scalarization of $O_j(\hat{Y}_j)$, expressed in equation 3.19, will result in the scalar objective function $\hat{O}_j(\lambda_j, \hat{Y}_j)$ as,

$$\hat{O}_j(\lambda_j, \hat{Y}_j) \coloneqq \lambda_j^T \cdot O_j(\hat{Y}_j) \tag{3.20}$$

$$\begin{aligned} \tilde{Y}_j(\lambda_j) &= \underset{\hat{Y}_j}{minimize}\ \hat{O}_j(\lambda_j, \hat{Y}_j) \\ &= \underset{\hat{Y}_j}{minimize}\ (\lambda_{1j} o_{1j} + \lambda_{2j} o_{2j}) \end{aligned} \tag{3.21}$$

[23] A set K is a cone if it satisfies the property of non-negative homogeneity; that is, if $x \in S$, then $ax \in S$ for all $a \geq 0$. A cone is a proper cone if it satisfies the following 4 properties.

i. It a closed set.
ii. It is a convex set.
iii. It is a pointed set
iv. It is full dimensional.

Every proper cone defines an ordering.

[24] A dual cone for a cone K is defined as the set $K^* = \{x \in K^* \mid x \cdot y \geq 0\ for\ all\ y \in K\}$

Both o_{1j} and o_{2j} are non-negative quadratic, and consequently, convex functions. Therefore, the objective function expressed in equation 3.21, a non-negative linear combination of o_{1j} and o_{2j}, is also convex.

3.3 Problem Solution:

The objective in equation 3.20 can also be written as

$$\tilde{Y}_j(\lambda_j) = \underset{\hat{Y}_j}{minimize} \;\; \lambda_j^T \cdot \begin{bmatrix} (\hat{V}_j\hat{Y}_j - I_j)^*(\hat{V}_j\hat{Y}_j - I_j) \\ (\hat{Y}_j - \hat{Y}_j^{in})^* (\hat{Y}_j - \hat{Y}_j^{in}) \end{bmatrix} \tag{3.22}$$

$$= \underset{\hat{Y}_{ij}}{minimize}\, \lambda_{1j} \left(\sum_{k=1}^{m} \sum_{i=1}^{length(L_j)} ||\hat{V}_{ki}\hat{Y}_{ij} - I_{kj}||_2^2 \right) + \lambda_{2j} \left(\sum_{i}^{length(L_j)} ||\hat{Y}_{ij} - \hat{Y}_{ij}^{in}||_2^2 \right)$$

In equation 3.22, the first expression in the parenthesis is taking into account the new measurements whereas the second one is ensuring that the resulting estimates of the parameters don't deviate much from the prior estimates. Roughly, the values of the scalars $\lambda_{1j}, \lambda_{2j} \in \mathbb{R}_+$ correspond to the importance given to each objective. For example, if the value of λ_{1j} is increased and the value of λ_{2j} is decreased, the solution will, most likely, update such that the resulting o_{1j} will decrease with an accompanying increase in o_{2j}.

This problem formulation can also be viewed in terms of a constrained-optimization problem. For example, if an extremely large value of λ_{2j} is selected compared to λ_{1j}, the solution thereby obtained will put almost all the emphasis in satisfying the constraint

$(\hat{Y}_{ij} - \hat{Y}_{ij}^{in} = 0)$. Such a problem formulation is equivalent to hard-constraint optimization problem

$$\underset{\hat{Y}_j}{minimize}\ (\hat{V}_j\hat{Y}_j - I_j)^*(\hat{V}_j\hat{Y}_j - I_j)$$

$$s.t.\ \hat{Y}_{ij} - \hat{Y}_{ij}^{in} = 0$$

Accommodating the constraints in the objective function, as is done in the Lagrangian function, turns a hard-constraint problem into a soft-constraint problem [61]. The problem 2.21 is a hard-constraint optimization problem whereas the problem in 3.22 can be regarded as a soft-constraint optimization problem.

The objective in equation 3.22 is a non-negative linear combination of the two non-negative quadratic functions. Therefore, it can be expressed as the least-squares approximate solution of the following system of equations [61],

$$\begin{bmatrix} \sqrt{\lambda_{1j}}\,.\,\hat{V}_j \\ \sqrt{\lambda_{2j}}\,.I \end{bmatrix}.\tilde{Y}_j = \begin{bmatrix} \sqrt{\lambda_{1j}}\,.\ I_j \\ \sqrt{\lambda_{2j}}\,.\ \hat{Y}_{ij}^{in} \end{bmatrix} \tag{3.23}$$

If $A_j := \begin{bmatrix} \sqrt{\lambda_{1j}}\,.\,\hat{V}_j \\ \sqrt{\lambda_{2j}}\,.I \end{bmatrix}$ and $B_j := \begin{bmatrix} \sqrt{\lambda_{1j}}\,.\ I_j \\ \sqrt{\lambda_{2j}}\,.\ \hat{Y}_{ij}^{in} \end{bmatrix}$, equation 3.23 can be expressed as,

$$A_j\tilde{Y}_j = B_j \tag{3.24}$$

In the next section, an algorithm is presented to find the solution $\tilde{Y}_j$ of the system of equations expressed in 3.24.

3.4 Algorithm 3.1

1) For each bus j, fill the array L_j with the bus numbers of the corresponding neighboring buses.
2) Select the rows from the bus voltage matrix, V_{bus}, corresponding to the entries in the array L_j. Append the resulting rows in ascending order of bus number and take the transpose of the resulting matrix to form the matrix, $\hat{V}_j$ with the dimensions $m \times L_j$.
3) Select the values of the scalars $\lambda_{1j}, \lambda_{2j} \in \mathbb{R}_+$ and form the matrix $A_j = \begin{bmatrix} \sqrt{\lambda_{1j}} \, . \, \hat{V}_j \\ \sqrt{\lambda_{2j}} \, . \, I \end{bmatrix}$ with dimension $(m + L_j) \times L_j$ and a vector $B_j = \begin{bmatrix} \sqrt{\lambda_{1j}} \, . \, I_j \\ \sqrt{\lambda_{2j}} \, . \, \hat{Y}_{ij}^{in} \end{bmatrix}$ of length $(m + L_j)$.
4) Evaluate the reduced QR factors of the matrix A_j, where Q is composed of orthogonal vectors (i.e., $Q^* Q = I$) and R is a square upper triangular matrix.
5) The solution of the systems of equations,

$$R \, \tilde{Y}_j = Q^* \, B_j \tag{3.25}$$

is solved for $\tilde{Y}_j$.

Note that at the end of this step all the non-zero entries of the bus admittance matrix have been obtained. Normally, the bus admittance matrix is stored in a sparse format with the values of the non-zero entries along with their position in the matrix. Therefore, the next two steps are not necessary; they are simply carried out for making comparison with the result of the Algorithm 2.1.

6) Let $S = \{x | x \epsilon \mathbb{N} \; and \; x \leq n\}$, then for the j^{th} column, find the complement of L_j in S i.e., ${L_j}^c \coloneqq S \backslash L_j$. For each value of j, extend the solution $\tilde{Y}_j$, found in step 5, by inserting zeros in the entries corresponding to the entries in ${L_j}^c$. This step will result in the columns of the estimated bus admittance matrix, $\tilde{Y}_{bus}$.

7) Append all the columns obtained in step 6 in ascending order to get the estimated bus admittance matrix, $\tilde{Y}_{bus}$.

The algorithm used for the simulation is illustrated as block diagram in Figure 3.1.

3.4.1 Complexity

The steps that dominate the computational complexity of the algorithm are steps 4 and 5. The bounds on the number of FLOPs needed to carry out these steps are mentioned below.

1) The QR factorization of the matrix A_j can be computed in $c_1\left(m + L_j\right) {L_j}^2$ operations where $c_1 \epsilon \mathbb{R}_{++}$.
2) The solution of $\hat{Y}_j$ in $R\,\hat{Y}_j = Q^* B_j$ can be computed in $c_2 {L_j}^2$ where $c_2 \epsilon \mathbb{R}_{+}$.

For a bus j, the total number of FLOPs needed to carry out the above-mentioned steps can be bounded by

$$Number\ of\ FLOPS\ for\ the\ computations\ of\ bus\ j \leq c_1\left(m + L_j\right) {L_j}^2 + c_2 {L_j}^2$$
$$= c_1 m {L_j}^2 + c_1 {L_j}^3 + c_2 {L_j}^2$$

In a typical power system, the average number of neighbouring buses is 1.5 – 2 [35]. That is, $L_j \ll m$. Therefore, $c_1 m {L_j}^2 + c_1 {L_j}^3 + c_2 {L_j}^2 \approx c_1 m {L_j}^2$.

In Algorithm 3.1, these steps need to be performed for all the buses of power system, the bound, therefore, on the total number of FLOPs can be given as,

$$number\ of\ FLOPs\ for\ the\ \text{Algorithm 3.1} \leq\ c_1 m \sum_{j=1}^{n} {L_j}^2$$

$$= c_1 m n^2 \sum_{j=1}^{n} \frac{{L_j}^2}{n^2}$$

$$= c_1 m n^2 L_{av}^2.$$

where $L_{av} (= \frac{1}{n}\sum_{j=1}^{n} L_j)$ is the average number of neighbouring buses in a power system. In a typical power system, L_{av} is in the range of 1.5-2 [35]. Therefore, L_{av}^2 can be accommodated in the constant, and the number of FLOPs for Algorithm 3.1 can be bounded by cmn^2 $(where\ c \coloneqq\ c_1 L_{av}^2)$. So the computational complexity of Algorithm 3.1 is $O(mn^2)$.

3.5 Experimental Results:

The algorithm is validated via simulations performed on various IEEE systems [66]. Simulations are performed in MATLAB using MATPOWER [67]. Slight modifications are made in the systems for the simulations.

For each new measurement, loads at all the buses are varied within $\sim 5\%$ of the nominal load. The difference in power, $\Delta P_G(t_k)$, between the total power generation at previous sampling time, $P_G(t_{k-1})$, and the sum of the updated total load at the current time, $P_L(t_k)$, with the system losses at previous sample, $P_{Loss}(t_{k-1})$, is distributed in all of the generators using participation factors according to the following equations

$$\Delta P_G(t_k) = P_L(t_k) + P_{Loss}(t_{k-1}) - P_G(t_{k-1}) \quad (3.26)$$

The additional power generated by the i^{th}generator at the k^{th}time sample is given by,

$$\Delta P_G^i(t_k) = \Delta P_G(t_k) \times PF^i \quad (3.27)$$

where, PF^i is the participation factor of the i^{th} generator defined as the ratio of the total MW capacity of the i^{th} generator to the sum of the total MW capacities of all the generators of the system.

Load flow analysis is then performed for the new system conditions. The residual power (difference between total generation and total consumption) of the system is provided by the slack-bus generator. The voltages and the injected current phasors are calculated at all the buses. Noise following a normal probability density function is added to all phasors to simulate phasor measurements. The algorithm mentioned in section 3.4 is used to evaluate the estimated bus admittance matrix, $\tilde{Y}_{bus}$.

The error matrix, ΔY_{bus}, is defined as

$$\Delta Y_{bus} = Y_{bus} - \tilde{Y}_{bus} \quad (3.28)$$

The accuracy and convergence of the algorithm is estimated [68] by

$$e_f = ||\Delta Y_{bus}||_f / ||Y_{bus}||_f \quad (3.29)$$

and

$$e_\infty = ||\Delta Y_{bus}||_\infty / ||Y_{bus}||_\infty \quad (3.30)$$

where f is representing the Frobenius norm and the ∞ is representing the infinity norm (the maximum value of the absolute row sum of a matrix). The magnitudes of the errors provide an estimate of the average error in the entries of the estimated matrix. For example,

if the errors, e_f and e_∞, are around 10%, then the average error in the entries of the estimated bus admittance matrix is also approximately 10%.

Note that the cases of power systems considered in this section are different from the cases considered in section 2.4. For the cases considered in this section, the magnitude of the variations in the loads connected to the systems is less than the magnitude of loads' variations considered in section 2.4. These changes are made to amplify the difference in performance of the algorithms. If the variations in the loads are large enough, as will be the case for future power systems, both the algorithms will produce accurate results.

The prior estimates of the parameters are generated by adding errors to the actual parameters of the system. The magnitude of the errors are such that the prior estimates represent the realistic value of the offline parameters; that is, within range of 25%-30% of the actual parameters [58].

3.5.1 IEEE 14-bus system:

A one-line diagram of the system is shown in Figure 2.2. The parameters and the connection information are provided in the appendix. Algorithms 2.1 and 3.1 are executed on the system. The errors at various numbers of measurements are tabulated in Table 3.1.

Table 3.1 - Errors of the algorithms at various number of measurements for the IEEE-14 bus power system

	No. of sets of measurements	**100**	**200**	**300**	**400**	**500**	**600**
Algorithm 2.1	e_f	0.1737	0.1294	0.1128	0.101	0.0929	0.0895
	e_∞	0.1599	0.1129	0.0938	0.0797	0.074	0.0709
Algorithm 3.1	e_f	0.1021	0.0807	0.0715	0.0645	0.0594	0.0568
	e_∞	0.0991	0.0753	0.0652	0.0568	0.0514	0.0494

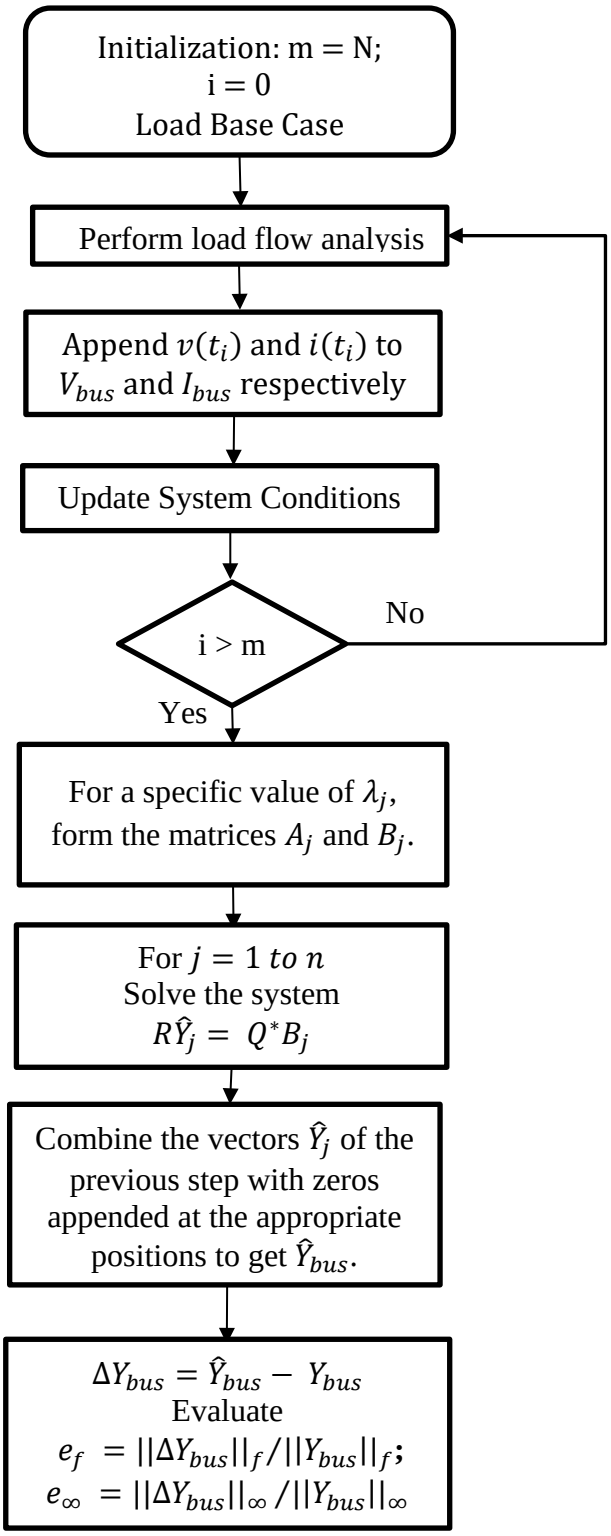

Figure 3.1 - The scheme used for the simulation of Algorithm 3.1

The errors for the algorithms are plotted in Figure 3.2. It is clear from the table and the figure that the Algorithm 3.1 has not only smaller errors but the algorithm is also converging to the estimated matrix in a relatively fewer number of measurements compared to the algorithm 2.1.

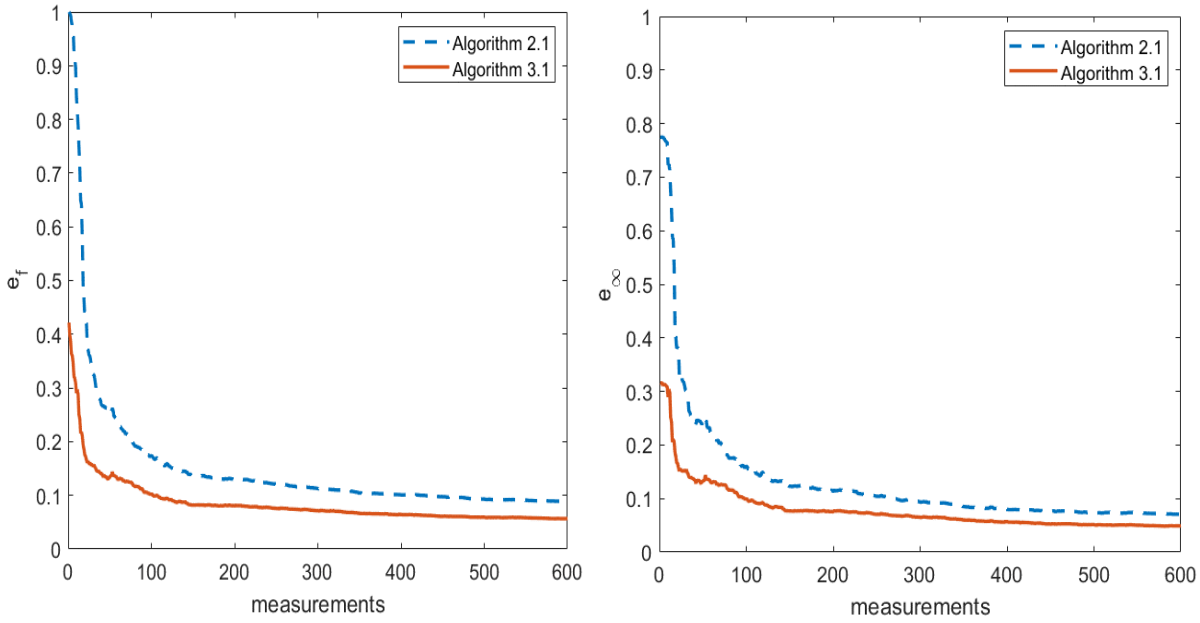

Figure 3.2 - Errors of the bus admittance matrices estimated through Algorithm 2.1 and Algorithm 3.1 for the IEEE 14-bus power system.

The actual bus admittance matrix and the estimated bus admittance matrix are mentioned in tables Table 3.2 and Table 3.3. Moreover, the parameters evaluated from the estimated bus admittance matrix are tabulated in Table 3.5 along with the errors. The histogram showing the number of estimated parameters within certain % error ranges is shown in Figure 3.3.

Based on the tables and the histogram, the performance of the algorithm 3.1 is much better than the performance of the algorithm 2.1.

Table 3.2 – Actual bus admittance matrix of the IEEE 14-bus power system.

Bus No	1	2	3	4	5	6	7	8	9	10	11	12	13	14
1	6.03 - 19.45i	-5.00 + 15.26i	-	-	-1.03 + 4.23i	-	-	-	-	-	-	-	-	-
2	-5.00 + 15.26i	9.52 - 30.27i	-1.14 + 4.78i	-1.69 + 5.12i	-1.70 + 5.19i	-	-	-	-	-	-	-	-	-
3	-	-1.14 + 4.78i	3.12 - 9.82i	-1.99 + 5.07i	-	-	-	-	-	-	-	-	-	-
4	-	-1.69 + 5.12i	-1.99 + 5.07i	10.51 - 38.65i	-6.84 + 21.58i	-	4.89i	-	1.86i	-	-	-	-	-
5	-1.03 + 4.23i	-1.70 + 5.19i	-	-6.84 + 21.58i	9.57 - 35.53i	4.26i	-	-	-	-	-	-	-	-
6	-	-	-	-	+ 4.26i	6.58 - 17.34i	-	-	-	-	-1.96 + 4.09i	-1.53 + 3.18i	-3.10 + 6.10i	-
7	-	-	-	4.89i	-	-	-19.55i	5.68i	9.09i	-	-	-	-	-
8	-	-	-	-	-	-	5.68i	- 5.68i	-	-	-	-	-	-
9	-	-	-	1.86i	-	-	9.09i	-	5.33 - 24.09i	-3.90 + 10.37i	-	-	-	-1.42 + 3.03i
10	-	-	-	-	-	-	-	-	-3.90 + 10.37i	5.78 - 14.77i	-1.88 + 4.40i	-	-	-
11	-	-	-	-	-	-1.96 + 4.09i	-	-	-	-1.88 + 4.40i	3.84 - 8.50i	-	-	-
12	-	-	-	-	-	-1.53 + 3.18i	-	-	-	-	-	4.01 - 5.43i	-2.49 + 2.25i	-
13	-	-	-	-	-	-3.10 + 6.10i	-	-	-	-	-	-2.49 + 2.25i	6.72 - 10.67i	-1.14 + 2.31i
14	-	-	-	-	-	-	-	-	-1.42 + 3.03i	-	-	-	-1.14 + 2.31i	2.56 - 5.34i

Table 3.3 – Bus admittance matrix of IEEE 14-bus power system estimated through Algorithm 2.1.

Bus No	1	2	3	4	5	6	7	8	9	10	11	12	13	14
1	5.86 - 18.88i	-4.6 + 14.53i	-	-	-1.17 + 4.03i	-	-	-	-	-	-	-	-	-
2	-4.76 + 14.5i	8.92 - 29.08i	-1.09 + 4.64i	-1.55 + 5.0i	-1.56 + 4.92i	-	-	-	-	-	-	-	-	-
3	-	-1.01 + 4.6i	3.08 - 9.79i	-1.93 + 4.83i	-	-	-	-	-	-	-	-	-	-
4	-	-1.71 + 5.08i	-1.9 + 4.95i	9.79 - 36.37i	-6.19 + 19.13i	-	-0.010 + 4.44i	-	-	-	-	-	-	-
5	-1.06 + 4.0i	-1.59 + 4.94i	-	-6.23 + 19.51i	9.0 - 32.87i	0.16 + 3.2i	-	-	-	-	-	-	-	-
6	-	-	-	-	0.14 + 3.78i	5.85 - 15.72i	-	-	-	-	-1.66 + 3.7i	-	-2.81 + 5.51i	-
7	-	-	-	-0.12 + 4.35i	-	-	0.090 - 18.48i	-0.060 + 5.24i	0.10 + 8.28i	-	-	-	-	-
8	-	-	-	-	-	-	-0.040 + 5.38i	0.030 - 5.53i	-	-	-	-	-	-
9	-	-	-	-	-	-	-0.010 + 8.25i	-	4.76 - 22.25i	-3.05 + 8.58i	-	-	-	-1.39 + 2.9i
10	-	-	-	-	-	-	-	-	-3.26 + 9.13i	4.86 - 13.25i	-1.51 + 3.85i	-	-	-
11	-	-	-	-	-	-1.77 + 3.63i	-	-	-	-1.54 + 3.87i	3.61 - 8.16i	-	-	-
12	-	-	-	-	-	-1.29 + 2.84i	-	-	-	-	-	3.77 - 5.01i	-2.41 + 2.04i	-
13	-	-	-	-	-	-2.8 + 5.45i	-	-	-	-	-	-2.42 + 1.97i	6.38 - 9.89i	-
14	-	-	-	-	-	-	-	-	-1.34 + 2.84i	-	-	-	-	2.54 - 5.27i

Table 3.4 – Bus admittance matrix of IEEE 14-bus power system estimated through Algorithm 3.1.

Bus No	1	2	3	4	5	6	7	8	9	10	11	12	13	14
1	5.94 - 19.26i	-4.79 + 14.54i	-	-	-0.91 + 3.88i	-	-	-	-	-	-	-	-	-
2	-4.81 + 14.97i	8.97 - 29.14i	-1.13 + 4.77i	-1.69 + 5.56i	-1.79 + 5.13i	-	-	-	-	-	-	-	-	-
3	-	-1.08 + 4.62i	3.11 - 9.82i	-1.89 + 4.88i	-	-	-	-	-	-	-	-	-	-
4	-	-1.59 + 5.05i	-1.98 + 5.08i	9.81 - 36.76i	-6.35 + 19.93i	-	-0.010 + 4.73i	-	-0.030 + 1.92i	-	-	-	-	-
5	-1.13 + 4.34i	-1.52 + 5.01i	-	-6.21 + 19.53i	9.1 - 33.26i	-0.050 + 4.14i	-	-	-	-	-	-	-	-
6	-	-	-	-	-0.060 + 4.08i	6.33 - 16.56i	-	-	-	-	-1.92 + 4.02i	-1.46 + 2.95i	-3.03 + 5.99i	-
7	-	-	-	-0.090 + 4.66i	-	-	0.090 - 18.72i	-0.020 + 5.64i	0.080 + 8.85i	-	-	-	-	-
8	-	-	-	-	-	-	-0.080 + 5.43i	0.020 - 5.64i	-	-	-	-	-	-
9	-	-	-	0.070 + 1.96i	-	-	-0.010 + 8.68i	-	5.1 - 23.3i	-3.39 + 9.44i	-	-	-	-1.43 + 3.0i
10	-	-	-	-	-	-	-	-	-3.68 + 9.78i	4.98 - 13.44i	-1.84 + 4.32i	-	-	-
11	-	-	-	-	-	-1.86 + 4.0i	-	-	-	-1.6 + 4.0i	3.75 - 8.34i	-	-	-
12	-	-	-	-	-	-1.39 + 2.79i	-	-	-	-	-	3.83 - 5.04i	-2.33 + 1.9i	-
13	-	-	-	-	-	-3.03 + 5.9i	-	-	-	-	-	-2.37 + 2.08i	6.47 - 10.08i	-1.12 + 2.29i
14	-	-	-	-	-	-	-	-	-1.48 + 2.99i	-	-	-	-1.1 + 2.2i	2.55 - 5.3i

Table 3.5 – Actual and estimated parameters of IEEE 14-bus power system.

Branch		Actual Impedance z_{ij}	Estimated Impedance $\tilde{z}_{ij}$		% error = $\left\|\frac{\tilde{z}_{ij}-z_{ij}}{z_{ij}}\right\| \times 100$ %	
bus i	bus j		Algorithm 2.1	Algorithm 3.1	Algorithm 2.1	Algorithm 3.1
1	2	0.0194+0.0592j	0.0211+0.0612j	0.0202+0.0605j	5.1199	3.3893
1	5	0.054+0.223i	0.0646+0.2328j	0.0589+0.2308j	3.6513	3.3023
2	3	0.047+0.198i	0.0495+0.2022j	0.0493+0.2003j	3.2978	1.8853
2	4	0.067+0.171i	0.0672+0.1762j	0.0680+0.1747j	2.2786	2.2352
2	5	0.0581+0.1763i	0.0597+0.1817j	0.0511+0.1748j	5.6055	1.4936
3	4	0.2045j	0.0017+0.2283j	0.0048+0.2144	3.6132	2.2489
4	5	0.5389j	0.0698+0.5052	0.0257+0.4989j	11.2509	8.4436
4	7	0.0133+0.0421j	0.0148+0.0461j	0.0144+0.0453j	6.9587	1.5013
4	9	0.0569+0.1739i	0.0593+0.1778j	0.0608+0.1720j	4.8567	1.9451
5	6	0.2349j	0.0080+0.2601j	0.0043+0.2425j	24.5235	3.5945
6	11	0.095+0.1989i	0.1032+0.2156j	0.0936+0.2014j	11.331	1.8939
6	12	0.1229+0.2558j	0.1350+0.2842j	0.1253+0.2715j	15.579	9.7567
6	13	0.0662+0.1303j	0.0708+0.1418j	0.0678+0.1333j	12.9366	3.218
7	8	0.11i	0.0012+0.1172j	0.0008+0.1135j	6.225	2.3666
7	9	0.1726i	0.0012+0.1172j	0.0008+0.1135j	11.1863	4.2738
9	10	0.0318+0.0845i	0.0385+0.0963j	0.0364+0.0902j	21.7371	11.692
9	14	0.0820+0.1921i	0.0909+0.2159j	0.0835+0.2019j	7.2512	0.9602
10	11	0.1229+0.2558j	0.1350+0.2842j	0.1253+0.2715j	14.4466	6.4999
12	13	0.2209+0.1999i	0.2388+0.2063j	0.2444+0.2076j	6.7167	8.4616
13	14	0.1709+0.3480i	0.1780+0.3641j	0.1741+0.3519j	6.9685	2.3609

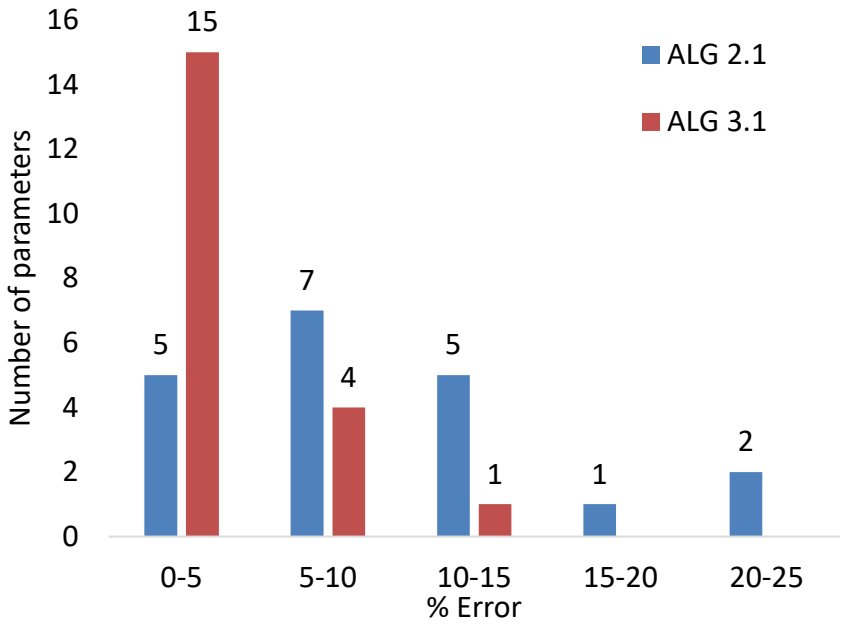

Figure 3.3 - Histogram of the errors in the parameters of IEEE 14-bus power estimated through Algorithm 2.1 and Algorithm 3.1.

3.5.2 IEEE 24-bus system

The algorithms of sections 2.3 and 3.4 are executed on the system and the errors at various numbers of measurements are tabulated in Table 3.6 and plotted in Figure 3.4.

Table 3.6 - Errors of the algorithm at various number of measurements for the IEEE 24-bus power system

	No. of sets of measurements	**100**	**200**	**300**	**400**	**500**	**600**
Original Problem	e_f	0.2202	0.1531	0.1334	0.124	0.1198	0.117
	e_∞	0.257	0.1647	0.1381	0.1255	0.1261	0.1262
Constrained problem	e_f	0.0857	0.0715	0.066	0.0617	0.0619	0.0607
	e_∞	0.0874	0.0718	0.0648	0.0601	0.0605	0.0594

The actual bus admittance matrix and the bus admittance matrices estimated through Algorithm 2.1 and Algorithm 3.1 are given in Table 3.8, Table 3.9 and Table 3.10 respectively.

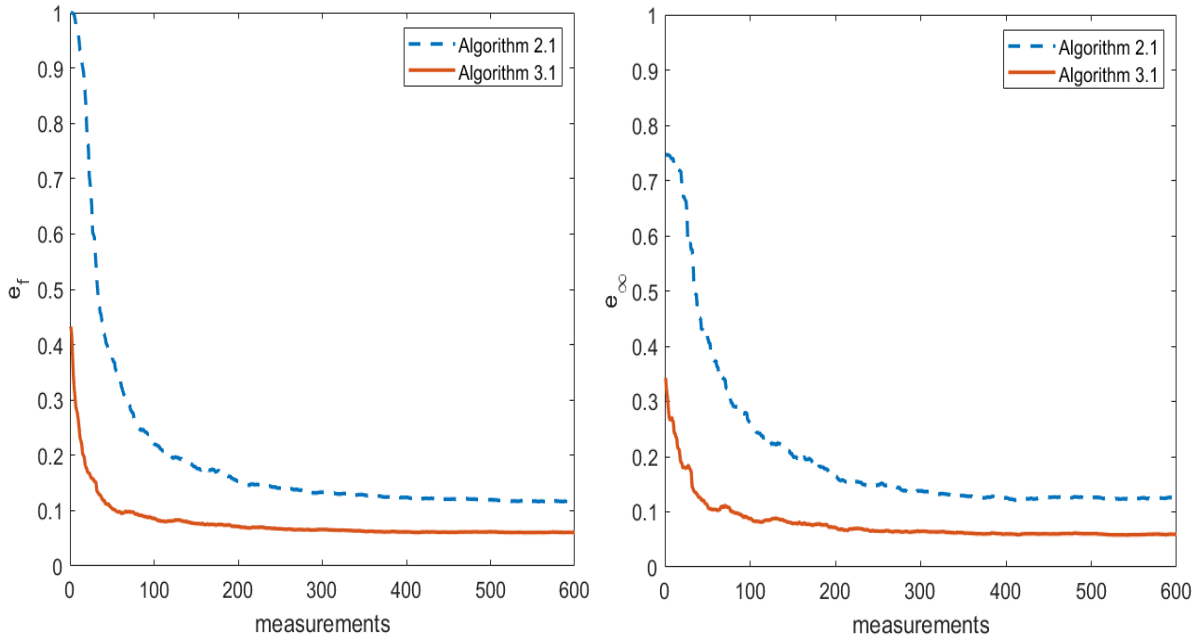

Figure 3.4 – Errors of Algorithm 2.1 and Algorithm 3.1 for the IEEE 24-bus power system.

Th actual and the estimated parameter of the IEEE 24-bus power system are tabulated in Table 3.7.

Table 3.7 - Actual and estimated parameters of IEEE 24-bus power system.

Branch		**Actual Impedance z_{ij}**	**Estimated Impedance**		**% error = $\left\|\frac{\tilde{z}_{ij}-z_{ij}}{z_{ij}}\right\| \times 100$ %**	
bus i	**bus j**		**Algorithm 2.1**	**Algorithm 3.1**	**Alg 2.1**	**Alg 3.1**
1	2	0.0026+0.0139i	0.0029+0.0161i	0.0028+0.0154i	15.4675	10.4288
1	3	0.0546+0.2112i	0.0555+0.2277i	0.055+0.212i	7.5646	0.396
1	5	0.0218+0.0845i	0.0231+0.0909i	0.0219+0.0842i	7.4785	0.309
2	4	0.0328+0.1267i	0.0375+0.1401i	0.0335+0.1283i	10.8221	1.372
2	6	0.0497+0.192i	0.0437+0.2048i	0.0476+0.1935i	7.1354	1.3247

3	9	0.0308+0.119i	0.0308+0.121i	0.0311+0.1191i	1.6523	0.2646
3	24	0.0024+0.0864i	0.0019+0.0884i	0.0023+0.0872i	2.34	0.9085
4	9	0.0268+0.1037i	0.0288+0.1055i	0.0272+0.1043i	2.4966	0.6839
5	10	0.0228+0.0883i	0.0226+0.0898i	0.023+0.0889i	1.7059	0.7081
6	10	0.0139+0.0605i	0.0141+0.0609i	0.0141+0.0606i	0.6713	0.4242
7	8	0.0159+0.0614i	0.0162+0.0616i	0.0161+0.0615i	0.5536	0.4173
8	9	0.0427+0.1651i	0.037+0.1672i	0.043+0.1657i	3.5354	0.4079
8	10	0.0427+0.1651i	0.0418+0.1682i	0.0432+0.1655i	1.8804	0.3602
9	11	0.0024+0.0864i	0.003+0.0905i	0.0025+0.0875i	4.7905	1.264
9	12	0.0024+0.0864i	0.0014+0.0977i	0.0027+0.0905i	13.0801	4.7172
10	11	0.0023+0.0856i	0.0029+0.0888i	0.0026+0.0866i	3.8087	1.271
10	12	0.0023+0.0856i	0.0019+0.0945i	0.0024+0.0897i	10.4461	4.8741
11	13	0.0061+0.0476i	0.0067+0.0494i	0.0059+0.0481i	3.9095	1.0684
11	14	0.0054+0.0418i	0.0052+0.043i	0.0053+0.0423i	2.8835	1.13
12	13	0.0061+0.0476i	0.0078+0.0536i	0.0066+0.0495i	12.9112	4.0199
12	23	0.0124+0.0966i	0.022+0.1082i	0.0122+0.1017i	15.5091	5.286
13	23	0.0111+0.0865i	0.0125+0.0917i	0.0131+0.0889i	6.1492	3.5949
14	16	0.005+0.0389i	0.0056+0.0438i	0.0055+0.0403i	12.6507	3.8594
15	16	0.0022+0.0173i	0.0033+0.0197i	0.0027+0.0181i	14.948	5.3569
15	21	0.0031+0.0245i	0.0041+0.0255i	0.0031+0.0247i	5.6902	0.8694
15	24	0.0067+0.0519i	0.0075+0.0548i	0.0068+0.0524i	5.7897	0.9591
16	17	0.0033+0.0259i	0.0043+0.03i	0.0043+0.0272i	16.3726	6.3249

16	19	0.003+0.0231i	0.0035+0.0275i	0.003+0.0243i	19.1642	5.2378
17	18	0.0018+0.0144i	0.0019+0.0155i	0.0019+0.0146i	7.8514	1.7634
17	22	0.0135+0.1053i	0.0146+0.1176i	0.0139+0.1047i	11.6621	0.6861
18	21	0.0017+0.013i	0.002+0.0147i	0.0017+0.0135i	13.8967	4.0256
19	20	0.0026+0.0198i	0.0037+0.0232i	0.0027+0.0209i	18.0689	5.8458
20	23	0.0014+0.0108i	0.002+0.013i	0.0017+0.0118i	21.3218	9.2849
21	22	0.0087+0.0678i	0.0148+0.0804i	0.0125+0.0735i	20.4629	9.9713

The histogram of the errors in the estimated parameters of the IEEE 24-bus power system for both the algorithms is shown in the Figure 3.5. From the figure, it is clear that the algorithm 3.1 is performing much better than the algorithm 2.1.

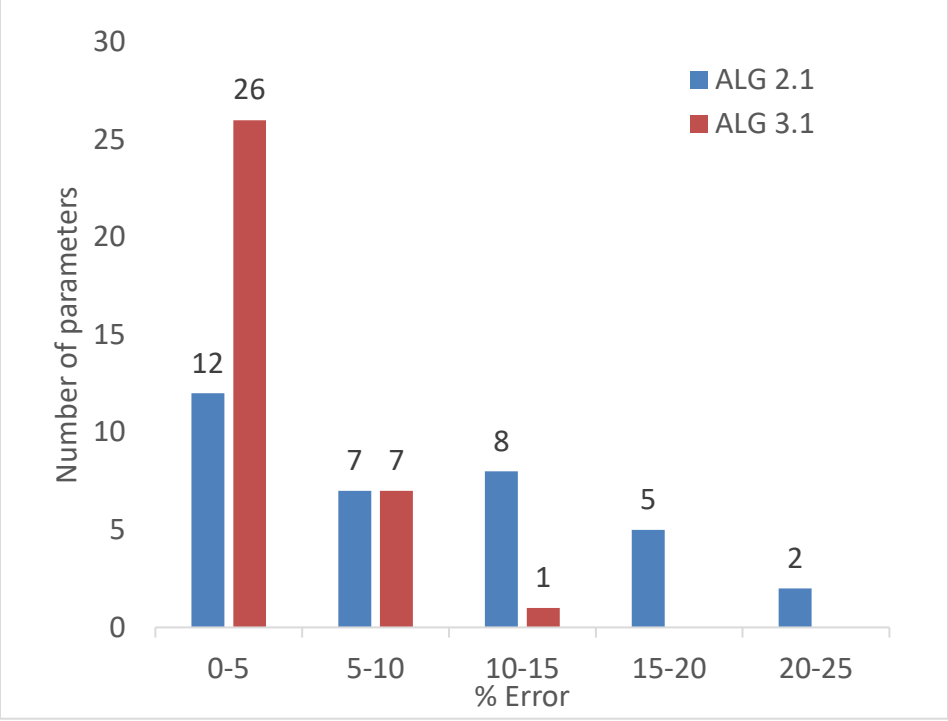

Figure 3.5 – Number of estimated parameters within various % error ranges.

Table 3.8 – Actual bus admittance matrix of IEEE 24-bus power system.

Bus No	1	2	3	4	5	6	7	8	9	10	11	12	13	14	15	16	17	18	19	20	21	22	23	24
1	17.01 - 84.77i	-13. + 69.51i	-1.15 + 4.44i	-	-2.86 + 11.1i	-	-	-	-	-	-	-	-	-	-	-	-	-	-	-	-	-	-	-
2	-13. + 69.51i	16.18 - 81.51i	-	-1.91 + 7.4i	-	-1.26 + 4.88i	-	-	-	-	-	-	-	-	-	-	-	-	-	-	-	-	-	-
3	-1.15 + 4.44i	-	3.49 - 23.5i	-	-	-	-	-	-2.04 + 7.88i	-	-	-	-	-	-	-	-	-	-	-	-	-	-	-0.32 + 11.56i
4	-	-1.91 + 7.4i	-	4.25 - 16.41i	-	-	-	-	-2.34 + 9.04i	-	-	-	-	-	-	-	-	-	-	-	-	-	-	-
5	-2.86 + 11.1i	-	-	-	5.6 - 21.69i	-	-	-	-	-2.74 + 10.62i	-	-	-	-	-	-	-	-	-	-	-	-	-	-
6	-	-1.26 + 4.88i	-	-	-	4.87 - 20.33i	-	-	-	-3.61 + 15.7i	-	-	-	-	-	-	-	-	-	-	-	-	-	-
7	-	-	-	-	-	-	3.95 - 15.25i	-3.95 + 15.26i	-	-	-	-	-	-	-	-	-	-	-	-	-	-	-	-
8	-	-	-	-	-	-	-3.95 + 15.26i	6.89 - 26.56i	-1.47 + 5.68i	-1.47 + 5.68i	-	-	-	-	-	-	-	-	-	-	-	-	-	-
9	-	-	-2.04 + 7.88i	-2.34 + 9.04i	-	-	-	-1.47 + 5.68i	6.46 - 44.99i	-	-0.32 + 11.56i	-0.32 + 11.56i	-	-	-	-	-	-	-	-	-	-	-	-
10	-	-	-	-	-2.74 + 10.62i	-3.61 + 15.7i	-	-1.47 + 5.68i	-	8.44 - 53.63i	-0.32 + 11.68i	-0.32 + 11.68i	-	-	-	-	-	-	-	-	-	-	-	-
11	-	-	-	-	-	-	-	-	-0.32 + 11.56i	-0.32 + 11.68i	6.34 - 67.93i	-	-2.65 + 20.67i	-3.04 + 23.53i	-	-	-	-	-	-	-	-	-	-
12	-	-	-	-	-	-	-	-	-0.32 + 11.56i	-0.32 + 11.68i	-	4.61 - 54.52i	-2.65 + 20.67i	-	-	-	-	-	-	-	-	-	-1.31 + 10.18i	-
13	-	-	-	-	-	-	-	-	-	-	-2.65 + 20.67i	-2.65 + 20.67i	6.76 - 52.52i	-	-	-	-	-	-	-	-	-	-1.46 + 11.37i	-
14	-	-	-	-	-	-	-	-	-	-	-3.04 + 23.53i	-	-	6.29 - 48.74i	-	-3.25 + 25.29i	-	-	-	-	-	-	-	-
15	-	-	-	-	-	-	-	-	-	-	-	-	-	-	14.84 - 115.81i	-7.23 + 56.88i	-	-	-	-	-5.16 + 40.15i	-	-	-2.45 + 18.95i
16	-	-	-	-	-	-	-	-	-	-	-	-	-	-3.25 + 25.29i	-7.23 + 56.88i	20.85 - 162.63i	-4.84 + 37.99i	-	-5.53 + 42.57i	-	-	-	-	-
17	-	-	-	-	-	-	-	-	-	-	-	-	-	-	-	-4.84 + 37.99i	14.59 - 115.56i	-8.55 + 68.38i	-	-	-	-1.2 + 9.34i	-	-
18	-	-	-	-	-	-	-	-	-	-	-	-	-	-	-	-	-8.55 + 68.38i	18.23 - 144.29i	-	-	-9.68 + 75.99i	-	-	-
19	-	-	-	-	-	-	-	-	-	-	-	-	-	-	-	-5.53 + 42.57i	-	-	11.93 - 92.15i	-6.4 + 49.68i	-	-	-	-
20	-	-	-	-	-	-	-	-	-	-	-	-	-	-	-	-	-	-	-6.4 + 49.68i	18.2 - 140.61i	-	-	-11.8 + 91.06i	-
21	-	-	-	-	-	-	-	-	-	-	-	-	-	-	-5.16 + 40.15i	-	-	-9.68 + 75.99i	-	-	16.71 - 130.42i	-1.86 + 14.51i	-	-
22	-	-	-	-	-	-	-	-	-	-	-	-	-	-	-	-	-1.2 + 9.34i	-	-	-	-1.86 + 14.51i	3.06 - 23.67i	-	-
23	-	-	-	-	-	-	-	-	-	-	-	-1.31 + 10.18i	-1.46 + 11.37i	-	-	-	-	-	-	-11.8 + 91.06i	-	-	14.57 - 112.38i	-
24	-	-	-0.32 + 11.56i	-	-	-	-	-	-	-	-	-	-	-	-2.45 + 18.95i	-	-	-	-	-	-	-	-	2.77 - 30.81i

Table 3.9 - Bus admittance matrix of IEEE 24-bus power system estimated through Algorithm 2.1.

Bus No	1	2	3	4	5	6	7	8	9	10	11	12	13	14	15	16	17	18	19	20	21	22	23	24
1	14.98 - 75.62i	-10.93 +60.14i	-0.86 + 4.16i	-	-2.5 + 10.46i	-	-	-	-	-	-	-	-	-	-	-	-	-	-	-	-	-	-	-
2	-11.02 +60.37i	14.13 - 72.5i	-	-1.61 + 6.69i	-	-0.99 + 4.63i	-	-	-	-	-	-	-	-	-	-	-	-	-	-	-	-	-	-
3	-1.16 + 4.14i	-	3.45 - 23.35i	-	-	-	-	-	-2.03 + 7.76i	-	-	-	-	-	-	-	-	-	-	-	-	-	-	-0.2 + 11.28i
4	-	-1.96 + 6.63i	-	4.24 - 16.26i	-	-	-	-	-2.34 + 8.89i	-	-	-	-	-	-	-	-	-	-	-	-	-	-	-
5	-2.76 + 10.21i	-	-	-	5.46 - 21.52i	-	-	-	-	-2.68 + 10.49i	-	-	-	-	-	-	-	-	-	-	-	-	-	-
6	-	-1. + 4.71i	-	-	-	4.85 - 20.28i	-	-	-	-3.6 + 15.58i	-	-	-	-	-	-	-	-	-	-	-	-	-	-
7	-	-	-	-	-	-	3.99 - 15.2i	-3.96 + 15.18i	-	-	-	-	-	-	-	-	-	-	-	-	-	-	-	-
8	-	-	-	-	-	-	-4. + 15.18i	6.9 - 26.45i	-1.16 + 5.7i	-1.24 + 5.63i	-	-	-	-	-	-	-	-	-	-	-	-	-	-
9	-	-	-1.92 + 7.76i	-2.47 + 8.75i	-	-	-	-1.37 + 5.7i	6.44 - 44.33i	-	-0.22 + 11.23i	0.17 + 10.09i	-	-	-	-	-	-	-	-	-	-	-	-
10	-	-	-	-	-2.59 + 10.45i	-3.63 + 15.61i	-	-1.55 + 5.57i	-	8.44 - 52.99i	-0.21 + 11.51i	-0.03 + 10.66i	-	-	-	-	-	-	-	-	-	-	-	-
11	-	-	-	-	-	-	-	-	-0.52 + 10.85i	-0.52 + 10.99i	5.98 - 66.32i	-	-2.78 + 19.72i	-2.8 + 22.99i	-	-	-	-	-	-	-	-	-	-
12	-	-	-	-	-	-	-	-	-0.47 + 10.38i	-0.38 + 10.5i	-	4.5 - 49.84i	-2.4 + 18.83i	-	-	-	-	-	-	-	-	-	-1.51 + 9.16i	-
13	-	-	-	-	-	-	-	-	-	-	-2.62 + 20.05i	-2.95 + 17.73i	6.76 - 51.07i	-	-	-	-	-	-	-	-	-	-1.29 + 10.48i	-
14	-	-	-	-	-	-	-	-	-	-	-2.76 + 22.84i	-	-	6.15 - 47.94i	-	-3.34 + 22.61i	-	-	-	-	-	-	-	-
15	-	-	-	-	-	-	-	-	-	-	-	-	-	-	15.56 - 111.03i	-8.22 + 48.66i	-	-	-	-	-6.96 + 38.28i	-	-	-2.44 + 17.51i
16	-	-	-	-	-	-	-	-	-	-	-	-	-	-2.36 + 22.3i	-8.48 + 50.28i	21.95 - 141.82i	-5.6 + 34.i	-	-3.61 + 36.28i	-0.27 + 3.5i	0.88 - 4.59i	-	0.4 - 3.16i	-
17	-	-	-	-	-	-	-	-	-	-	-	-	-	-	-	-3.81 + 31.2i	14.24 - 111.42i	-7.67 + 63.77i	-	-	-0.54 + 5.15i	-1.2 + 7.85i	-	-
18	-	-	-	-	-	-	-	-	-	-	-	-	-	-	-	-2.59 + 5.02i	-7.48 + 63.13i	16.98 - 135.37i	-	-	-8.98 + 65.01i	0.49 + 3.08i	-	-
19	-	-	-	-	-	-	-	-	-	-	-	-	-	-	-	-5.53 + 35.19i	-	-	11.51 - 87.03i	-7.89 + 41.16i	-	-	1.2 + 6.02i	-
20	-	-	-	-	-	-	-	-	-	-	-	-	-	-	-	-0.02 + 4.48i	-	-	-5.48 + 42.84i	17.84 - 120.13i	-	-	-12.72 + 74.44i	-
21	-	-	-	-	-	-	-	-	-	-	-	-	-	-	-5.39 + 38.12i	2.52 - 3.76i	-1.57 + 3.13i	-8.88 + 68.33i	-	-	17.3 - 118.78i	-2.48 + 11.03i	-0.14 - 3.61i	-
22	-	-	-	-	-	-	-	-	-	-	-	-	-	-	-	-	-0.87 + 8.89i	-	-	-	-1.95 + 13.04i	2.97 - 22.99i	-	-
23	-	-	-	-	-	-	-	-	-	-	-	-2.1 + 8.58i	-1.63 + 10.94i	-	-	0.06 - 3.19i	-	-	-1.12 + 4.55i	-10.15+ 75.38i	-	-	14.35 - 98.88i	-
24	-	-	-0.29 + 11.34i	-	-	-	-	-	-	-	-	-	-	-	-2.43 + 18.31i	-	-	-	-	-	-	-	-	2.68 - 30.23i

Table 3.10 – Bus admittance matrix of IEEE 24-bus power system estimated through Algorithm 3.1.

Bus No	1	2	3	4	5	6	7	8	9	10	11	12	13	14	15	16	17	18	19	20	21	22	23	24
1	15.8 - 78.51i	-11.65 + 62.96i	-1.15 + 4.44i	-	-2.82 + 11.04i	-	-	-	-	-	-	-	-	-	-	-	-	-	-	-	-	-	-	-
2	-11.68 +62.98i	14.68 - 75.02i	-	-1.91 + 7.36i	-	-1.24 + 4.88i	-	-	-	-	-	-	-	-	-	-	-	-	-	-	-	-	-	-
3	-1.14 + 4.41i	-	3.48 - 23.49i	-	-	-	-	-	-2.07 + 7.85i	-	-	-	-	-	-	-	-	-	-	-	-	-	-	-0.30 + 11.36i
4	-	-1.9 + 7.23i	-	4.24 - 16.34i	-	-	-	-	-2.36 + 8.95i	-	-	-	-	-	-	-	-	-	-	-	-	-	-	-
5	-2.96 + 11.2i	-	-	-	5.49 - 21.58i	-	-	-	-	-2.78 + 10.52i	-	-	-	-	-	-	-	-	-	-	-	-	-	-
6	-	-1.15 + 4.87i	-	-	-	4.86 - 20.33i	-	-	-	-3.67 + 15.58i	-	-	-	-	-	-	-	-	-	-	-	-	-	-
7	-	-	-	-	-	-	3.98 - 15.23i	-4.0 + 15.19i	-	-	-	-	-	-	-	-	-	-	-	-	-	-	-	-
8	-	-	-	-	-	-	-3.98 + 15.23i	6.92 - 26.44i	-1.46 + 5.66i	-1.5 + 5.64i	-	-	-	-	-	-	-	-	-	-	-	-	-	-
9	-	-	-2.04 + 7.87i	-2.33 + 9.01i	-	-	-	-1.47 + 5.64i	6.53 - 44.76i	-	-0.24 + 11.3i	-0.42 + 10.6i	-	-	-	-	-	-	-	-	-	-	-	-
10	-	-	-	-	-2.68 + 10.56i	-3.61 + 15.7i	-	-1.45 + 5.68i	-	8.61 - 53.25i	-0.28 + 11.38i	-0.33 + 10.73i	-	-	-	-	-	-	-	-	-	-	-	-
11	-	-	-	-	-	-	-	-	-0.42 + 11.54i	-0.41 + 11.69i	5.87 - 66.46i	-	-2.5 + 20.74i	-3.03 + 23.53i	-	-	-	-	-	-	-	-	-	-
12	-	-	-	-	-	-	-	-	-0.24 + 11.49i	-0.28 + 11.54i	-	4.49 - 50.15i	-2.7 + 20.73i	-	-	-	-	-	-	-	-	-	-1.15 + 9.96i	-
13	-	-	-	-	-	-	-	-	-	-	-2.54 + 20.25i	-2.59 + 19.i	6.77 - 52.54i	-	-	-	-	-	-	-	-	-	-1.65 + 10.69i	-
14	-	-	-	-	-	-	-	-	-	-	-2.8 + 23.06i	-	-	6.32 - 48.7i	-	-3.36 + 23.42i	-	-	-	-	-	-	-	-
15	-	-	-	-	-	-	-	-	-	-	-	-	-	-	15.24 - 114.71i	-8.21 + 51.99i	-	-	-	-	-4.86 + 39.77i	-	-	-2.41 + 18.64i
16	-	-	-	-	-	-	-	-	-	-	-	-	-	-3.29 + 25.27i	-7.61 + 56.08i	22.75 - 149.1i	-5.18 + 37.i	-	-5.25 + 41.81i	-	-	-	-	-
17	-	-	-	-	-	-	-	-	-	-	-	-	-	-	-	-6.16 + 34.7i	14.96 - 112.78i	-8.84 + 67.87i	-	-	-	-1.11 + 9.36i	-	-
18	-	-	-	-	-	-	-	-	-	-	-	-	-	-	-	-	-8.45 + 66.5i	17.98 - 141.21i	-	-	-9.72 + 72.72i	-	-	-
19	-	-	-	-	-	-	-	-	-	-	-	-	-	-	-	-4.9 + 39.16i	-	-	11.46 - 90.27i	-6.08 + 45.29i	-	-	-	-
20	-	-	-	-	-	-	-	-	-	-	-	-	-	-	-	-	-	-	-6.24 + 48.56i	17.35 - 126.92i	-	-	-12.17+ 84.68i	-
21	-	-	-	-	-	-	-	-	-	-	-	-	-	-	-5.21 + 39.89i	-	-	-9.12 + 73.35i	-	-	17.4 - 124.63i	-1.85 + 14.05i	-	-
22	-	-	-	-	-	-	-	-	-	-	-	-	-	-	-	-	-1.38 + 9.42i	-	-	-	-2.64 + 12.41i	2.96 - 23.21i	-	-
23	-	-	-	-	-	-	-	-	-	-	-	-1.17 + 9.42i	-1.58 + 11.32i	-	-	-	-	-	-	-11.41 +81.83i	-	-	15.05 - 105.26i	-
24	-	-	-0.30 + 11.56i	-	-	-	-	-	-	-	-	-	-	-	-2.45 + 18.9i	-	-	-	-	-	-	-	-	2.71 - 30.28i

3.5.3 IEEE 30-bus system

The values of the errors for the algorithms of sections 2.3 and 3.4 at various numbers of measurements are mentioned in Table 3.11.

Table 3.11 - Errors of the algorithm at various number of measurements for the IEEE 30-bus power system.

	No. of sets of measurements	**100**	**200**	**300**	**400**	**500**	**600**
Original Problem	e_f	0.1567	0.126	0.1169	0.1074	0.1009	0.0977
	e_∞	0.0985	0.0833	0.0801	0.0713	0.066	0.0622
Constrained problem	e_f	0.0779	0.0668	0.0623	0.0558	0.0537	0.0506
	e_∞	0.0581	0.0524	0.0495	0.0417	0.0392	0.0352

The algorithms of sections 2.3 and 3.4 are executed on the system and the errors are plotted in Figure 3.6.

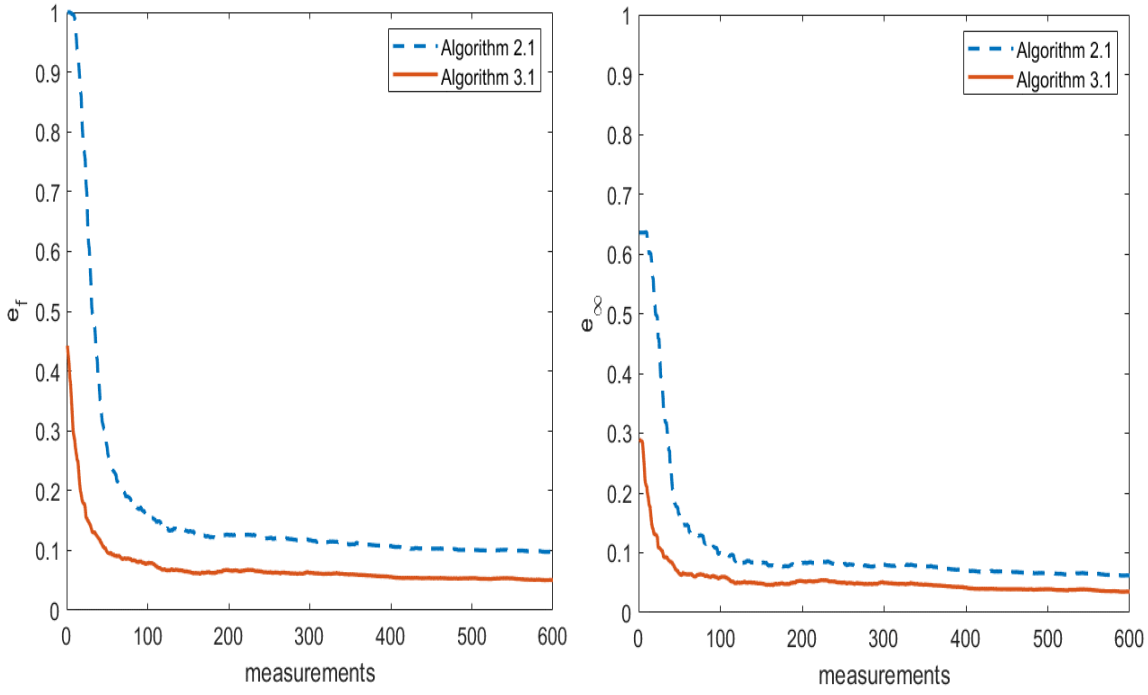

Figure 3.6 - Errors of Algorithm 2.1 and Algorithm 3.1 for the IEEE 30-bus power system.

3.5.4 IEEE 118-bus system

The algorithms of sections 2.3 and 3.4 are executed on the system. The values of the errors at various numbers of measurements are mentioned in Table 3.12.

Table 3.12 - Errors of the algorithm at various number of measurements for the IEEE-118 bus power system

	No. of sets of measurements	**100**	**200**	**300**	**400**	**500**	**600**
Original Problem	e_f	0.6622	0.1928	0.1439	0.1226	0.1111	0.1048
	e_∞	0.4992	0.1502	0.1203	0.1	0.0837	0.0777
Constrained problem	e_f	0.0876	0.0695	0.0616	0.0584	0.057	0.057
	e_∞	0.0676	0.053	0.0431	0.0407	0.0404	0.0412

The errors for the algorithms 2.1 and 3.1 are plotted in Figure 3.7.

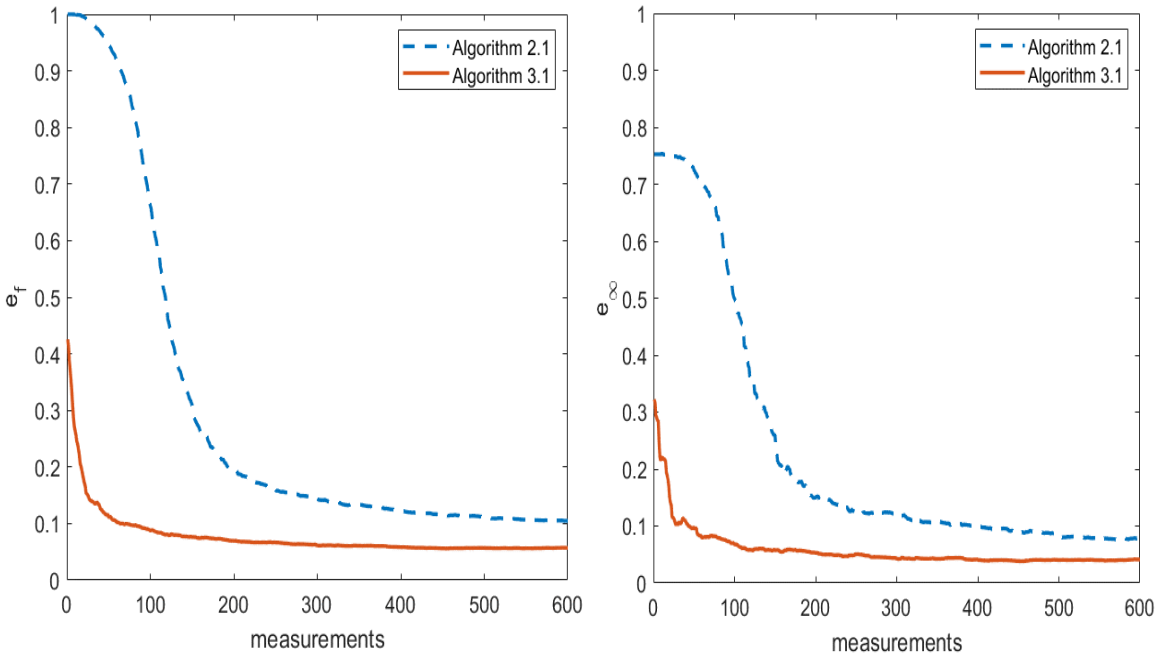

Figure 3.7 - Errors of Algorithm 2.1 and Algorithm 3.1 for the IEEE 24-bus power system.

3.6 Discussion

From the plots and tables of section 3.5, it is clear that the multi-objective algorithm of equation 3.19 performs much better than the algorithm of section 2.3. Therefore, whenever a reliable prior information is available, it should be used in the problem formulation.

Additionally, through the choice of $\lambda_j = \begin{bmatrix}\lambda_{1j} & \lambda_{2j}\end{bmatrix}^T$; $\lambda_{1j}, \lambda_{2j} \in \mathbb{R}_+$ in equation 3.21, the emphasis on the mutli-criterion objective of equation 3.19 can be changed. For example, if the parameters of the components are known with high accuracy, a relatively higher value of λ_{2j} should be used in the problem formulation. The problem solution thereby obtained will start and tend to stay near $\hat{Y}_j^{in}$as shown in the Figure 3.8.

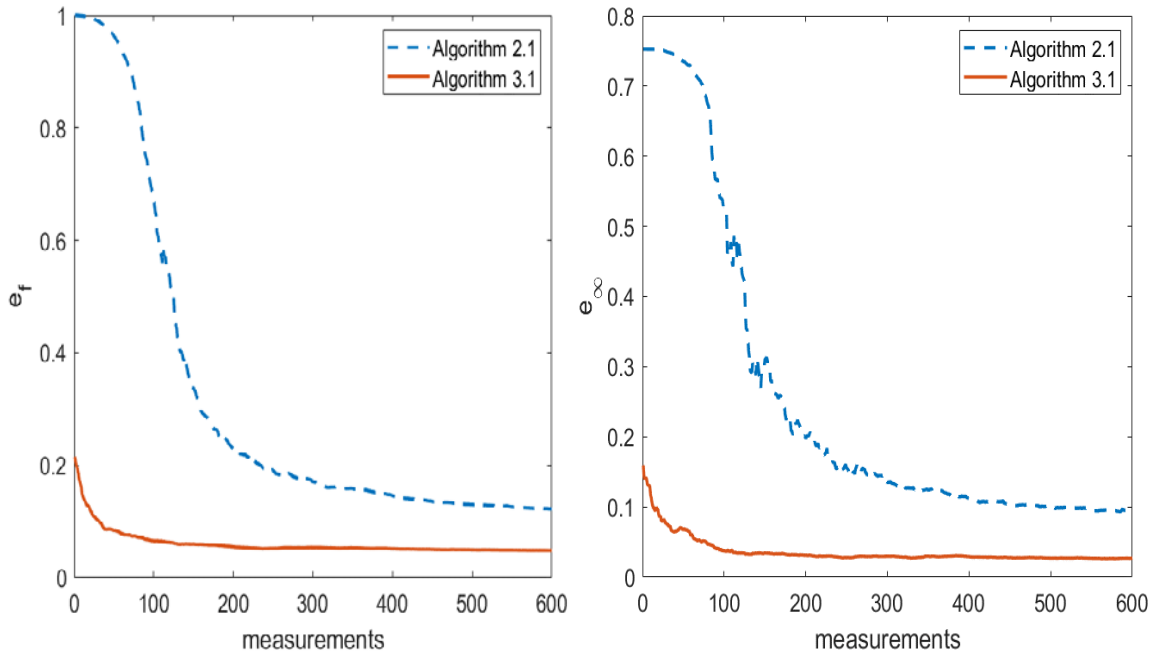

Figure 3.8 – Plot of the errors for Algorithm 3.1 for a relatively large value of λ_{2j}.

Moreover, the same concept can be extended even further. That is, in section 3.3, a two-dimensional λ_j is used for relative weighing of the two objectives o_{1j} and o_{2j} through scalarization. If the prior estimates of the parameters of the elements of power system connected with bus j, represented by $\hat{Y}_j^{in}$, are known with different accuracy, then instead of using the same scalar λ_{2j} for o_{2j}, a vector of the same dimension as o_{2j} can be used. The magnitude of each entry of the vector λ_{2j} will correspond to the confidence we have in the prior estimate of the respective component of the power system. The resulting inner product $\lambda_{2j} \cdot o_{j2} = \lambda_{2j,1} \cdot o_{12} + \lambda_{2j,2} \cdot o_{22} + \lambda_{2j,3} \cdot o_{32} \ldots \lambda_{2j,end} \cdot o_{2,end}$ will be used in problem formulation.

The algorithms presented in chapters 2 and chapter 3 assume that there are no faulty measurements. The errors considered in the measurements were measurement errors. In the next chapter, faulty measurements will be considered, and a robust algorithm will be introduced to cope with the faulty measurements.

CHAPTER 4. ROBUST ESTIMATION OF BUS ADMITTANCE MATRIX

One assumption on which the algorithms presented in the previous chapters are based is that there are no faulty measurements. In this chapter, this assumption will be relaxed, and a new estimator will be formulated that will be robust against the faulty measurements.

A specific percentage of the total number of measurements will be made faulty. The buses at which the measurements will be faulty will be chosen randomly. This scenario will model the noise in the communication channels. The algorithm will be compared with the algorithm presented in the previous chapter.

4.1 Mathematical Theory

In the previous chapter, the objective vector, $O_j(\hat{Y}_j)$, had two components o_{1j} and o_{2j} given as

$$O_j(\hat{Y}_j) := \begin{bmatrix} o_{1j}(\hat{Y}_j) \\ o_{2j}(\hat{Y}_j) \end{bmatrix} = \begin{bmatrix} (\hat{V}_j\hat{Y}_j - I_j)^*(\hat{V}_j\hat{Y}_j - I_j) \\ \left(\hat{Y}_j - \hat{Y}_j^{in}\right)^*\left(\hat{Y}_j - \hat{Y}_j^{in}\right) \end{bmatrix}$$

$$= \begin{bmatrix} \sum_{k=1}^{m} \sum_{i=1}^{length(L_j)} ||\hat{V}_{ki}\hat{Y}_{ij} - I_{kj}||_2^2 \\ \sum_{i}^{length(L_j)} ||\hat{Y}_{ij} - \hat{Y}_{ij}^{in}||_2^2 \end{bmatrix} \quad (4.1)$$

The first component is accommodating the measurements whereas the second part of the objective vector is considering the prior estimates. As the faulty measurements will have no effect on the second component of the objective, this part will be ignored in the

following discussion. If good prior estimates are available, they can later be added to form the optimization vector as was done in the previous chapter. In this chapter, the first part of the objective vector will be modified so that the estimator thereby obtained is robust against the faulty measurements.

The problem being addressed is the estimation of the parameters of a power system, given its topology, through phasor measurements where a certain percentage of the measurements are faulty. As presented in section 3.1.1, with the assumption of no faulty measurements, the following objective function was derived for the same problem

$$\underset{\hat{Y}_{ij}}{minimize} \sum_{k=1}^{m} \sum_{i=1}^{length(L_j)} ||\hat{V}_{ki}\hat{Y}_{ij} - I_{kj}||_2^2 \tag{4.2}$$

The objective in expression 4.2 is the sum of the squares of the Euclidian norm of the residuals, $\hat{V}_{ki}\hat{Y}_{ij} - I_{kj}$. As the square function increases disproportionally with the magnitude of the input, a measurement with a large residual will have a disproportionately large impact on the estimated vector, $\hat{Y}_{ij}$. Under the assumption of no faulty measurements, no individual measurement can have a relatively large residual. Rather, a measurement with a relatively large residual is often a faulty measurement.

The effect that a measurement with a large residual has on the solution can be modified by modifying the objective function. If, for example, an objective function that places relatively less emphasis on any outlier and consequently updates the variable in a relatively milder way is used in the optimization problem, then our objective function will be better able to cope with the faulty measurements. An ideal objective function with such

a property is shown in the Figure 4.1.

$$\varphi(x,t) = \begin{cases} |x|^2 & |x| \le t \\ t & |x| \ge t \end{cases} \tag{4.3}$$

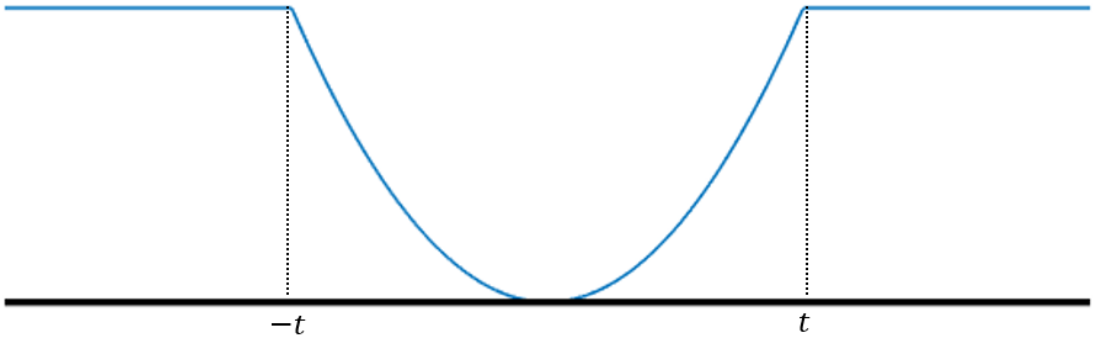

Figure 4.1 - $\varphi(x,t)$.

The function $\varphi(\cdot)$ will put zero emphasis on the measurements with residuals that are above the threshold value of t. Therefore, the solution of the optimization problem based on the function $\varphi(x,t)$ will not be affected by measurements with the corresponding residuals greater than t. However, solving optimization problem based on such a function will be difficult because the function is non-convex, and therefore, the resulting optimization problem

$$\underset{\hat{Y}_{ij}}{minimize} \sum_{k=1}^{m} \sum_{i}^{length(L_j)} \varphi\left(\hat{V}_{ki}\hat{Y}_{ij} - I_{kj}\right) \tag{4.4}$$

will also be non-convex, and therefore, cannot be guaranteed to solve in polynomial time [61].

If, however, a convex approximation of the function $\varphi(\cdot)$ is used instead, the resulting optimization will be convex. One such function, $\emptyset(\cdot)$ is given by

$$\emptyset(x,t) = \begin{cases} |x|^2 & |x| \le t \\ 2t|x| - t^2 & |x| \ge t \end{cases} \tag{4.5}$$

The function is plotted in Figure 4.2 along with the function x^2. Note that as the absolute value of the input argument increases, the difference between x^2 and $\emptyset(\cdot)$ is increasing with an increasing rate. The net result of this difference is that the function x^2 will put a disproportionate emphasis on the outliers relative to $\emptyset(\cdot)$. $\emptyset(\cdot)$ is the best convex approximation of $\varphi(\cdot)$ in the sense that epigraph[25] of $\emptyset(\cdot)$ will be a subset of any other convex approximation of $\varphi(\cdot)$. When the absolute value of the input is greater than the threshold (t), $\emptyset(\cdot)$ behaves linearly, and therefore, relatively less emphasis is placed on the outliers compared to x^2.

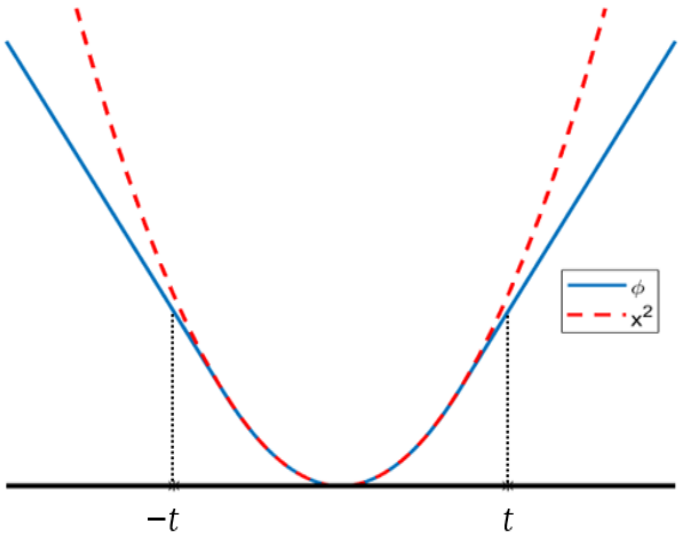

Figure 4.2 - $\emptyset(\cdot)$ and x^2.

Using $\emptyset(\cdot)$ in the optimization problem of 4.2 instead of the norm-square function results

[25] The epigraph of a function f : $\mathbb{R}^n \rightarrow \mathbb{R}$ is a set defined as epi $f = \{(x,t) \mid x \in dom\, f, f(x) \le t\}$. epi f is a subset of $\mathbb{R}^{n+1}$.

in the optimization problem

$$\underset{\hat{Y}_{ij}}{minimize} \sum_{k=1}^{m} \sum_{i}^{length(L_j)} \emptyset\left(\hat{V}_{ki}\hat{Y}_{ij} - I_{kj}\right) \tag{4.6}$$

4.2 Experimental Results

The algorithm is validated via simulations performed on various IEEE systems [66]. Simulations are performed in MATLAB using MATPOWER [67]. Slight modifications are made in the systems for the simulations.

For each new measurement, loads at all the buses are varied within $\sim 5\%$ of the nominal load. The difference in power, $\Delta P_G(t_k)$, between the total power generation at previous sampling time, $P_G(t_{k-1})$, and the sum of the updated total load at the current time, $P_L(t_k)$, with the system losses at previous sample, $P_{Loss}(t_{k-1})$, is distributed in all of the generators using participation factors according to the following equations

$$\Delta P_G(t_k) = P_L(t_k) + P_{Loss}(t_{k-1}) - P_G(t_{k-1}) \tag{4.7}$$

The additional power generated by the i^{th}generator at the k^{th}time sample is given by,

$$\Delta P_G^i(t_k) = \Delta P_G(t_k) \times PF^i \tag{4.8}$$

where, PF^i is the participation factor of the i^{th} generator defined as the ratio of the total MW capacity of the i^{th} generator to the sum of the total MW capacities of all the generators of the system.

Load flow analysis is then performed for the new system conditions. The residual power (difference between total generation and total consumption) of the system is

provided by the slack-bus generator. The voltages and the injected current phasors are calculated at all the buses. Noise following a normal probability density function is added to all the phasors to simulate measurements.

Some of the measurements in the data are made faulty. The time samples at which the faulty measurements occur are chosen randomly. The faults are simulated by taking samples from a Gaussian probability density function with a large standard deviation. The buses at which the faulty measurement occur are also selected randomly. This scenario is modeling the noisy communication channels. The setup used for the simulation is illustrated in Figure 4.3.

The error matrix, ΔY_{bus}, is defined as

$$\Delta Y_{bus} = Y_{bus} - \tilde{Y}_{bus} \tag{4.9}$$

The accuracy and convergence of the algorithm is estimated [68] by

$$e_f = ||\Delta Y_{bus}||_f / ||Y_{bus}||_f \tag{4.10}$$

and

$$e_\infty = ||\Delta Y_{bus}||_\infty / ||Y_{bus}||_\infty \tag{4.11}$$

where f is representing the Frobenius norm and the ∞ is representing the infinity norm (the maximum value of the absolute row sum of a matrix). The magnitudes of the errors provide an estimate of the average error in the entries of the estimated matrix. For example, if the errors, e_f and e_∞, are around 10%, then the average error in the entries of the estimated bus admittance matrix is also approximately 10%.

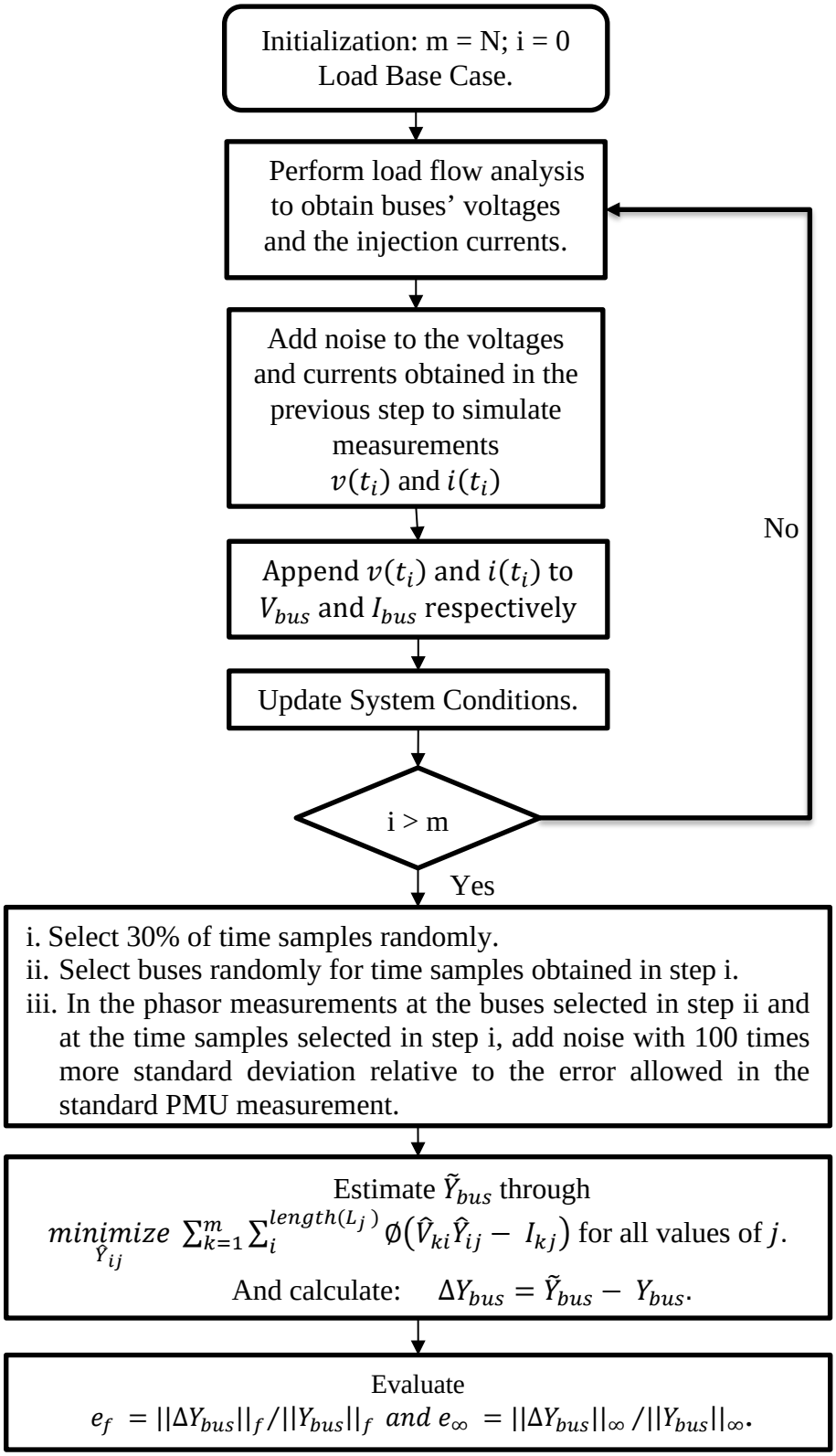

Figure 4.3 - Scheme used for the simulation of the robust algorithm.

4.2.1 IEEE 14-bus power system:

A one-line diagram of the system is shown in Figure 2.2. The parameters and the connection information are provided in the appendix. The algorithms based on equations 4.2 (original) and 4.6 (robust) are executed on the system and the errors are plotted in Figure 4.4.

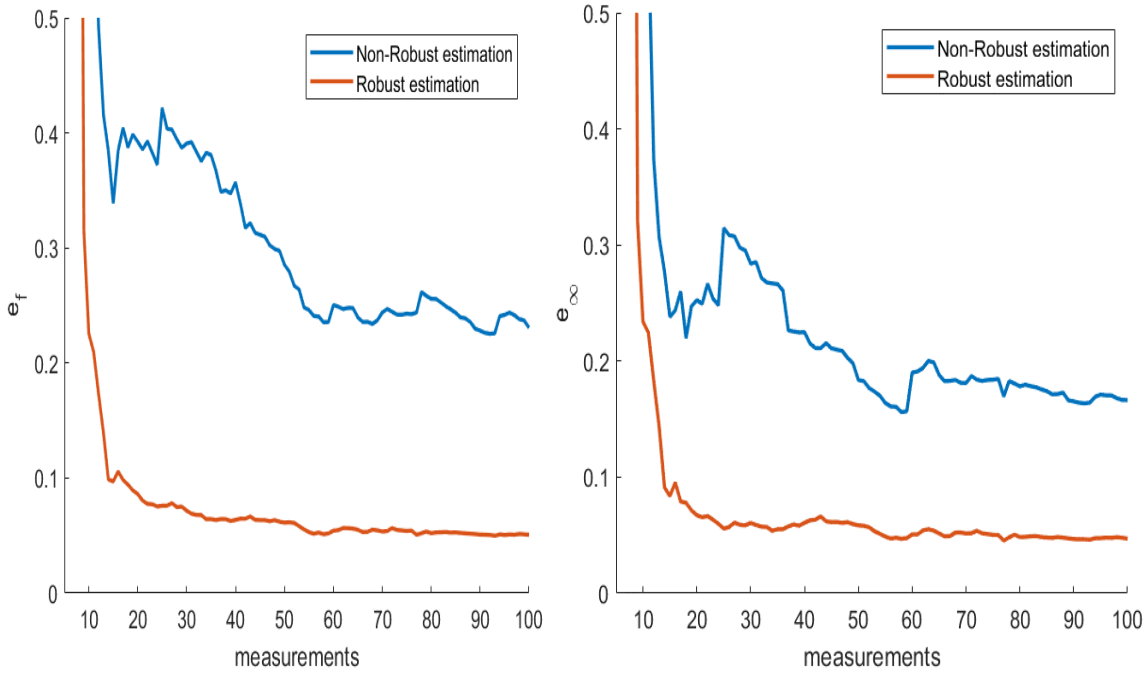

Figure 4.4 – Errors in the estimated bus admittance matrix of the non-robust and robust algorithm for IEEE 14-bus power system.

The values of the errors for the algorithms at various numbers of measurements are mentioned in Table 4.1. The actual bus admittance matrix along with the bus admittance matrix estimated through non-robust and robust algorithms are shown in the Tables 4.2, 4.3 and 4.4 respectively. The values of the parameters of the components of the power system are also mentioned in the Table 4.2. The histogram showing the number of estimated parameters within certain error ranges is shown in the Figure 4.5.

Table 4.1 – Errors in the estimated bus admittance matrices for the non-robust and robust algorithm for IEEE 14-bus power system.

	No. of sets of measurements	**20**	**40**	**60**	**80**	**100**
Non-robust estimation	e_f	0.3924	0.3570	0.2503	0.2558	0.2307
	e_∞	0.2525	0.2249	0.1901	0.1782	0.1664
Robust estimation	e_f	0.0862	0.0636	0.0542	0.0521	0.0506
	e_∞	0.0672	0.0607	0.0507	0.0484	0.0470

From the plots and the tables, it is clear that in the presence of faulty measurements, the performance of the non-robust algorithm is severely affected. The roust algorithm, however, has performed satisfactorily.

Table 4.2 - Actual and estimated parameters of IEEE 14-bus power system.

Branch		**Actual Impedance z_{ij}**	**Estimated Impedance $\tilde{z}_{ij}$**		**% error = $\left\|\frac{\tilde{z}_{ij}-z_{ij}}{z_{ij}}\right\| \times 100$ %**	
bus i	**bus j**		**Non-robust Algorithm**	**Robust Algorithm**	**Non-Robust Algorithm**	**Robust Algorithm**
1	2	0.0194+0.0592i	0.0169+0.0576i	0.0184+0.0599i	4.7829	2.0159
1	5	0.054+0.223i	0.0473+0.2021i	0.0428+0.2311i	9.5824	6.0176
2	3	0.047+0.198i	0.0412+0.1818i	0.045+0.1967i	8.44	1.1435
2	4	0.0581+0.1763i	0.1887+0.2268i	0.0786+0.1792i	75.4137	11.1526
2	5	0.0569+0.1739i	0.0222+0.1451i	0.0523+0.1617i	24.6723	7.1176
3	4	0.067+0.171i	0.0641+0.1966i	0.0627+0.1781i	14.0292	4.4843
4	5	0.0133+0.0421i	0.0156+0.0529i	0.0125+0.0445i	24.9342	5.7707
4	7	0.2045i	0.0069+0.2939i	0.0089+0.2363i	43.8432	16.1457
4	9	0.5389i	0.0174+0.2971i	0.0295+0.4408i	44.9922	19.0209

5	6	0.2349i	0.004+0.2447i	0.0031+0.2397i	4.5051	2.4205
6	11	0.095+0.1989i	0.1112+0.1868i	0.0965+0.1987i	9.1997	0.6992
6	12	0.1229+0.2558i	0.1+0.2977i	0.1202+0.2826i	16.816	9.4801
6	13	0.0662+0.1303i	0.0835+0.1305i	0.072+0.1295i	11.9088	4.0131
7	8	0.1762i	0.0067+0.1949i	0.0013+0.1809i	11.3313	2.8135
7	9	0.11i	0.001+0.1151i	0.0026+0.1117i	4.6717	2.824
9	10	0.0318+0.0845i	0.0234+0.0781i	0.0373+0.092i	11.6635	10.2445
9	14	0.1271+0.2704i	0.126+0.3854i	0.1204+0.2807i	38.4833	4.1052
10	11	0.0821+0.1921i	0.0573+0.1155i	0.0804+0.1963i	38.5199	2.1776
12	13	0.2209+0.1999i	0.0941+0.1244i	0.2148+0.2081i	49.5275	3.4364
13	14	0.1709+0.348i	0.1774+0.3745i	0.1833+0.362i	7.0206	4.8165

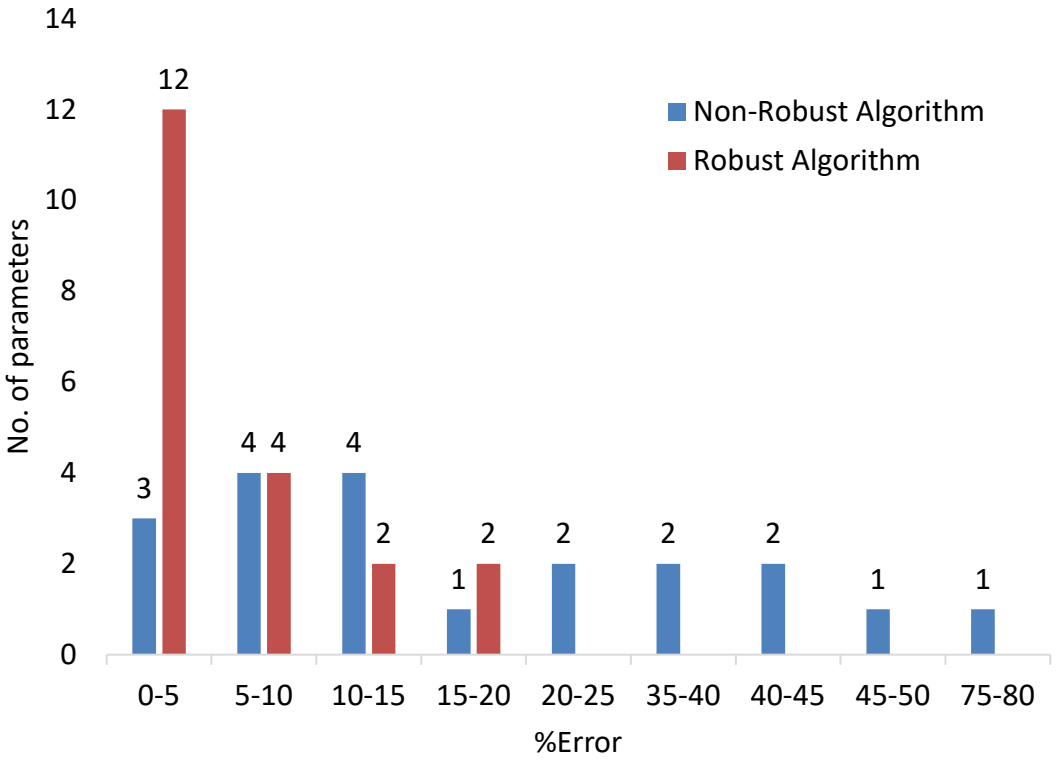

Figure 4.5 – Number of estimated parameters within various % error ranges for the IEEE 14-bus power system.

Table 4.3 – Actual Bus Admittance matrix of the IEEE 14-bus power system.

Bus No	1	2	3	4	5	6	7	8	9	10	11	12	13	14
1	6.03 - 19.45i	-5 + 15.26i	-	-	-1.03 + 4.23i	-	-	-	-	-	-	-	-	-
2	-5 + 15.26i	9.52 - 30.27i	-1.14 + 4.78i	-1.69 + 5.12i	-1.7 + 5.19i	-	-	-	-	-	-	-	-	-
3	-	-1.14 + 4.78i	3.12 - 9.82i	-1.99 + 5.07i	-	-	-	-	-	-	-	-	-	-
4	-	-1.69 + 5.12i	-1.99 + 5.07i	10.51 - 38.65i	-6.84 + 21.58i	-	4.89i	-	1.86i	-	-	-	-	-
5	-1.03 + 4.23i	-1.7 + 5.19i	-	-6.84 + 21.58i	9.57 - 35.53i	4.26i	-	-	-	-	-	-	-	-
6	-	-	-	-	4.26i	6.58 - 17.34i	-	-	-	-	-1.96 + 4.09i	-1.53 + 3.18i	-3.1 + 6.1i	-
7	-	-	-	4.89i	-	-	-19.55i	5.68i	9.09i	-	-	-	-	-
8	-	-	-	-	-	-	5.68i	5.68i	-	-	-	-	-	-
9	-	-	-	1.86i	-	-	9.09i	-	5.33 - 24.09i	-3.9 + 10.37i	-	-	-	-1.42 + 3.03i
10	-	-	-	-	-	-	-	-	-3.9 + 10.37i	5.78 - 14.77i	-1.88 + 4.4i	-	-	-
11	-	-	-	-	-	-1.96 + 4.09i	-	-	-	-1.88 + 4.4i	3.84 - 8.5i	-	-	-
12	-	-	-	-	-	-1.53 + 3.18i	-	-	-	-	-	4.01 - 5.43i	-2.49 + 2.25i	-
13	-	-	-	-	-	-3.1 + 6.1i	-	-	-	-	-	-2.49 + 2.25i	6.72 - 10.67i	-1.14 + 2.31i
14	-	-	-	-	-	-	-	-	-1.42 + 3.03i	-	-	-	-1.14 + 2.31i	2.56 - 5.34i

Table 4.4 - Bus admittance matrix of IEEE 14-bus system estimated through optimization problem 4.2 (Non-robust formulation).

Bus No	1	2	3	4	5	6	7	8	9	10	11	12	13	14
1	5.82 - 20.4i	-5.01 + 16.48i	-	-	-0.58 + 4.42i	-	-	-	-	-	-	-	-	-
2	-4.35 + 15.51i	8.97 - 31.74i	-1.3 + 5.07i	-1.27 + 4.62i	-2.43 + 4.09i	-	-	-	-	-	-	-	-	-
3	-	-1.07 + 5.39i	3.09 - 10i	-1.27 + 4.23i	-	-	-	-	-	-	-	-	-	-
4	-	-3.06 + 0.59i	-1.73 + 4.97i	6.72 - 32.66i	-5.72 + 17.34i	-	0.02 + 4.94i	-	-0.37 + 2.35i	-	-	-	-	-
5	-1.62 + 4.96i	0.37 + 9.38i	-	-4.56 + 17.44i	8.97 - 30.59i	0.03 + 3.68i	-	-	-	-	-	-	-	-
6	-	-	-	-	-0.17 + 4.49i	5.37 - 14.97i	-	-	-	-	-2.66 + 3.9i	-1.93 + 4.07i	-3.75 + 5.33i	-
7	-	-	-	0.14 + 1.86i	-	-	0.37 - 20.79i	0.49 + 4.07i	0.08 + 7.61i	-	-	-	-	-
8	-	-	-	-	-	-	-0.13 + 6.17i	-0.3 - 4.12i	-	-	-	-	-	-
9	-	-	-	-0.03 + 4.36i	-	-	-0.23 + 9.78i	-	4.52 - 20.33i	-4.68 + 16.19i	-	-	-	0.38 + 1.33i
10	-	-	-	-	-	-	-	-	-2.35 + 7.29i	7.32 - 22.72i	-4.34 + 7.42i	-	-	-
11	-	-	-	-	-	-2.05 + 4i	-	-	-	-2.56 + 6.48i	6.97 - 11.27i	-	-	-
12	-	-	-	-	-	-0.1 + 1.96i	-	-	-	-	-	8.57 - 10.93i	-1.06 + 3.35i	-
13	-	-	-	-	-	-3.21 + 5.54i	-	-	-	-	-	-6.67 + 6.87i	5.87 - 10.7i	-1.01 + 2.32i
14	-	-	-	-	-	-	-	-	-1.91 + 3.36i	-	-	-	-1.06 + 2.04i	0.55 - 3.66i

Table 4.5 - Bus admittance matrix estimated through optimization problem 4.6 (Robust formulation).

Bus No	1	2	3	4	5	6	7	8	9	10	11	12	13	14
1	5.75 - 19.48i	-4.72 + 15.22i	-	-	-0.43 + 4.12i	-	-	-	-	-	-	-	-	-
2	-4.63 + 15.3i	9.04 - 30.37i	-1.16 + 4.81i	-1.92 + 5.41i	-2.56 + 4.78i	-	-	-	-	-	-	-	-	-
3	-	-1.05 + 4.85i	3.11 - 9.84i	-1.58 + 4.93i	-	-	-	-	-	-	-	-	-	-
4	-	-2.19 + 3.95i	-1.94 + 5.06i	8.93 - 37.67i	-6.16 + 20.82i	-	0.01 + 4.67i	-	-0.09 + 1.93i	-	-	-	-	-
5	-1.12 + 4.25i	-1.06 + 6.42i	-	-5.54 + 20.82i	9.18 - 34.18i	-0.06 + 4.14i	-	-	-	-	-	-	-	-
6	-	-	-	-	-0.04 + 4.2i	6.53 - 16.74i	-	-	-	-	-1.99 + 4.1i	-1.37 + 3.21i	-3.24 + 5.75i	-
7	-	-	-	0.31 + 3.78i	-	-	-0.26 - 19.2i	0.12 + 5.36i	0.11 + 8.93i	-	-	-	-	-
8	-	-	-	-	-	-	-0.05 + 5.7i	-0.09 - 5.37i	-	-	-	-	-	-
9	-	-	-	-0.21+ 2.58i	-	-	0.31 + 8.96i	-	5.06 - 23i	-3.82 + 9.42i	-	-	-	-1.26 + 2.9i
10	-	-	-	-	-	-	-	-	-3.75 + 9.26i	5.51 - 13.65i	-1.87 + 4.49i	-	-	-
11	-	-	-	-	-	-1.97 + 4.04i	-	-	-	-1.7 + 4.24i	3.86 - 8.59i	-	-	-
12	-	-	-	-	-	-1.18 + 2.78i	-	-	-	-	-	3.88 - 5.57i	-2.29 + 2.29i	-
13	-	-	-	-	-	-3.32 + 6.05i	-	-	-	-	-	-2.51 + 2.36i	6.63 - 10.16i	-1.12 + 2.27i
14	-	-	-	-	-	-	-	-	-1.32 + 3.12i	-	-	-	-1.1 + 2.12i	2.38 - 5.17i

4.2.2 IEEE 24-bus power system:

The algorithms based on equations 4.2 (original) and 4.6 (robust) are executed on the system and the errors are plotted in Figure 4.6.

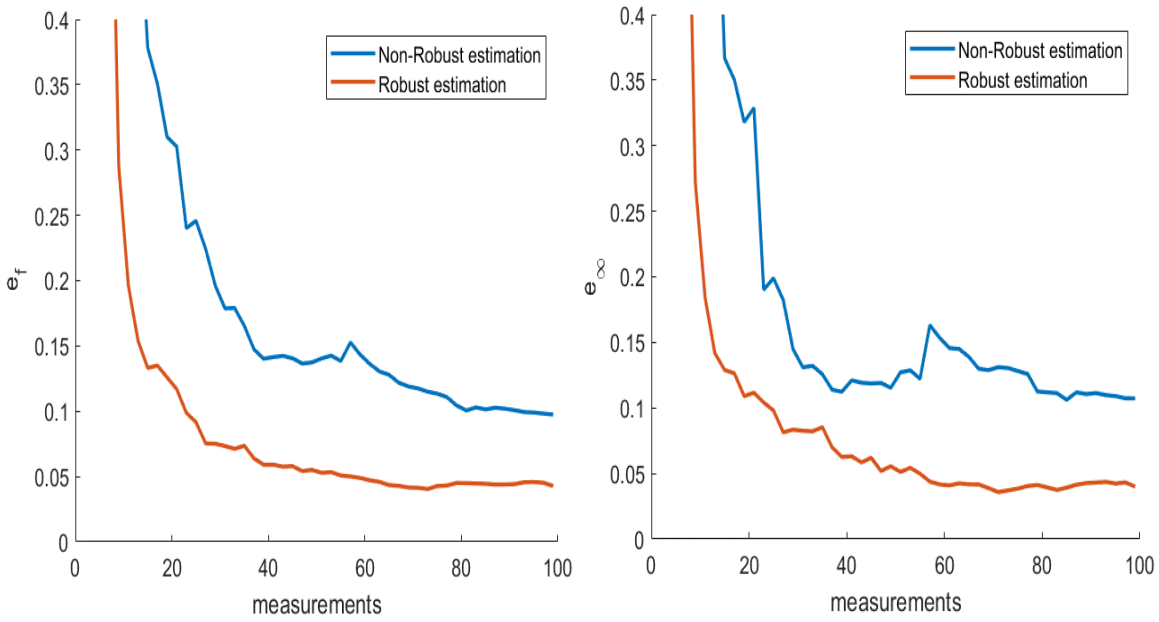

Figure 4.6 - Errors in the estimated bus admittance matrix of the non-robust and robust algorithm for IEEE 24-bus power system.

The values of the errors for the algorithms of at various numbers of measurements are mentioned in Table 4.6.

Table 4.6 - Errors in the estimated bus admittance matrix of the non-robust and robust algorithm for IEEE 24-bus power system.

	No. of sets of measurements	**20**	**40**	**60**	**80**	**100**
Non-robust estimation	e_f	0.3128	0.1414	0.1377	0.1030	0.0976
	e_∞	0.3439	0.1112	0.1455	0.1124	0.1073
Robust estimation	e_f	0.1271	0.0599	0.0451	0.0322	0.0437
	e_∞	0.1135	0.0647	0.0410	0.0391	0.0393

The actual bus admittance matrix of the IEEE 24-bus power system is mentioned in the Table 4.8. The bus admittance matrix of the system estimated through the non-robust algorithm is mentioned in Table 4.9 and the estimate of the matrix by the robust algorithm is mentioned in Table 4.10.

The actual parameters and the parameters estimated through the algorithms are mentioned in the table Table 4.7

Table 4.7 - Actual and estimated parameters of IEEE 24-bus power system.

Branch		**Actual Impedance z_{ij}**	**Estimated Impedance**		**% error = $\left\|\frac{\tilde{z}_{ij}-z_{ij}}{z_{ij}}\right\| \times 100$ %**	
Bus i	**Bus j**		**Non-robust estimation**	**Robust estimation**	**Non-robust algorithm**	**Robust Algorithm**
1	2	0.0026+0.0139i	0.0026+0.0136i	0.002+0.0147i	2.4004	7.1945
1	3	0.0546+0.2112i	0.0619+0.2192i	0.0521+0.2162i	4.9523	2.5687
1	5	0.0218+0.0845i	0.0144+0.0839i	0.0226+0.0837i	8.4862	1.3066
2	4	0.0328+0.1267i	0.0345+0.1145i	0.0331+0.1244i	9.4178	1.8094
2	6	0.0497+0.192i	0.0321+0.2015i	0.0484+0.1923i	10.0936	0.6669
3	9	0.0308+0.119i	0.0256+0.1176i	0.0305+0.1191i	4.4238	0.2705
3	24	0.0024+0.0864i	0.0045+0.0802i	0.0024+0.0863i	7.5542	0.1706
4	9	0.0268+0.1037i	0.0324+0.0914i	0.027+0.1039i	12.6347	0.2517
5	10	0.0228+0.0883i	0.0207+0.0829i	0.022+0.0885i	6.4174	0.8687
6	10	0.0139+0.0605i	0.0113+0.0583i	0.0129+0.0609i	5.4124	1.7534
7	8	0.0159+0.0614i	0.0142+0.0624i	0.0157+0.0616i	3.1239	0.4755

8	9	0.0427+0.1651i	0.0352+0.1645i	0.0431+0.1651i	4.4236	0.2582
8	10	0.0427+0.1651i	0.0449+0.1583i	0.0427+0.1649i	4.2196	0.1311
9	11	0.0024+0.0864i	0.0125+0.0909i	0.0036+0.0868i	12.8052	1.4508
9	12	0.0024+0.0864i	0.002+0.1015i	0.0025+0.0902i	17.4596	4.3723
10	11	0.0023+0.0856i	0.0029+0.0879i	0.0021+0.087i	2.7634	1.7313
10	12	0.0023+0.0856i	0.0125+0.1112i	0.0019+0.0891i	32.2016	4.1977
11	13	0.0061+0.0476i	0.0079+0.0495i	0.0072+0.0484i	5.4642	2.8293
11	14	0.0054+0.0418i	0.005+0.0428i	0.0058+0.0424i	2.6567	1.6598
12	13	0.0061+0.0476i	0.0113+0.0625i	0.0057+0.0492i	32.7972	3.383
12	23	0.0124+0.0966i	0.0236+0.1274i	0.0107+0.0996i	33.6161	3.5962
13	23	0.0111+0.0865i	0.0095+0.0928i	0.0125+0.0915i	7.4629	5.9729
14	16	0.005+0.0389i	0.0048+0.0413i	0.0045+0.0395i	6.1319	2.0589
15	16	0.0022+0.0173i	0.0021+0.0181i	0.0018+0.0178i	4.4352	3.6713
15	21	0.0031+0.0245i	0.0029+0.0248i	0.003+0.0246i	1.3756	0.8865
15	24	0.0067+0.0519i	0.006+0.0497i	0.0065+0.0528i	4.4505	1.8394
16	17	0.0033+0.0259i	0.0025+0.0271i	0.0024+0.027i	5.561	5.3872
16	19	0.003+0.0231i	0.0028+0.0243i	0.0023+0.0238i	5.3754	4.0846
17	18	0.0018+0.0144i	0.0012+0.0141i	0.0017+0.0144i	4.6053	0.5071
17	22	0.0135+0.1053i	-0.0154+0.1425i	0.007+0.1053i	44.4214	6.095
18	21	0.0017+0.013i	0.0009+0.0125i	0.0015+0.013i	6.4222	1.4477
19	20	0.0026+0.0198i	0.0021+0.0206i	0.0022+0.0205i	4.361	3.7231
20	23	0.0014+0.0108i	0.0013+0.0114i	0.0014+0.0114i	5.8859	5.7986
21	22	0.0087+0.0678i	0.0182+0.0679i	0.0124+0.0702i	13.9231	6.4081

The histogram showing the number of estimated parameters within certain error ranges are shown in the Figure 4.7.

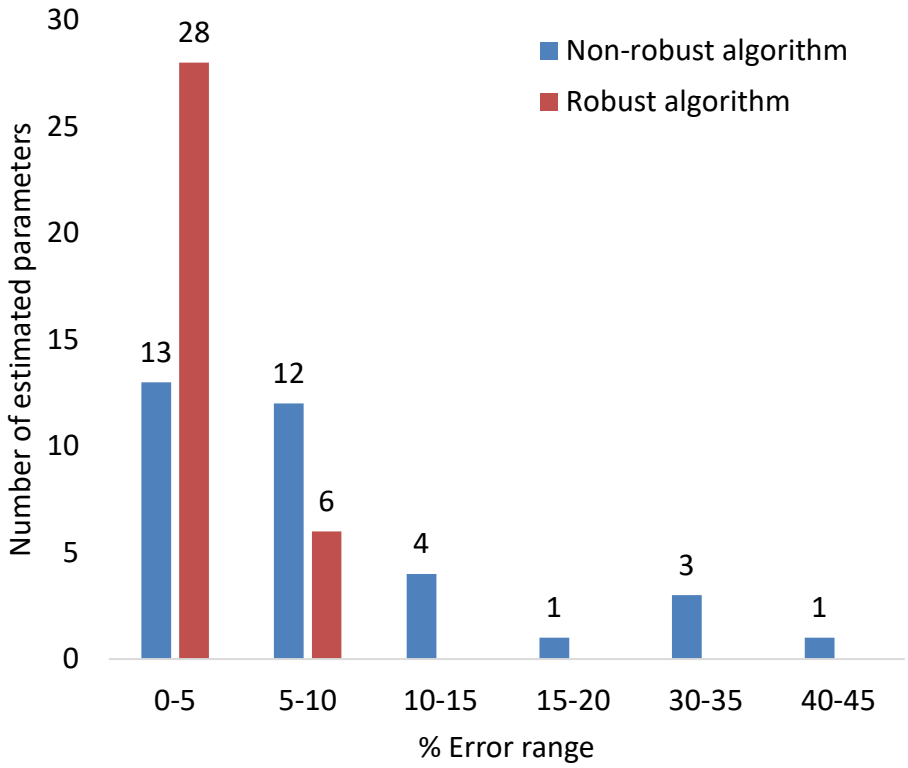

Figure 4.7 - Number of estimated parameters within various % error ranges for the IEEE 24-bus power system.

Again, as for the case of IEEE 14-bus power system, the performance of the non-robust algorithm is affected severely in the presence of the faulty measurements whereas the performance of the robust algorithm is largely unaffected.

The difference between the performance of the algorithms will increase with the increase in the magnitude of the errors in the faulty measurements. With a faulty measurement having a very large error, the estimate of the non-robust algorithm will be much more affected relative to the estimate obtained from the robust algorithm.

Table 4.8 – Actual bus admittance matrix of the IEEE 24-bus power system.

Bus No.	1	2	3	4	5	6	7	8	9	10	11	12	13	14	15	16	17	18	19	20	21	22	23	24
1	17.01 - 84.98i	-13 + 69.51i	-1.15 + 4.44i	-	-2.86 + 11.1i	-	-	-	-	-	-	-	-	-	-	-	-	-	-	-	-	-	-	-
2	-13 + 69.51i	16.18 - 81.72i	-	-1.91 + 7.4i	-	-1.26 + 4.88i	-	-	-	-	-	-	-	-	-	-	-	-	-	-	-	-	-	-
3	-1.15 + 4.44i	-	3.49 - 23.5i	-	-	-	-	-	-2.04 + 7.88i	-	-	-	-	-	-	-	-	-	-	-	-	-	-	-0.32 + 11.56i
4	-	-1.91 + 7.4i	-	4.25 - 16.41i	-	-	-	-	-2.34 + 9.04i	-	-	-	-	-	-	-	-	-	-	-	-	-	-	-
5	-2.86 + 11.1i	-	-	-	5.6 - 21.69i	-	-	-	-	-2.74 + 10.62i	-	-	-	-	-	-	-	-	-	-	-	-	-	-
6	-	-1.26 + 4.88i	-	-	-	4.87 - 20.33i	-	-	-	-3.61 + 15.7i	-	-	-	-	-	-	-	-	-	-	-	-	-	-
7	-	-	-	-	-	-	3.95 - 15.25i	-3.95 + 15.26i	-	-	-	-	-	-	-	-	-	-	-	-	-	-	-	-
8	-	-	-	-	-	-	-3.95 + 15.26i	6.89 - 26.56i	-1.47 + 5.68i	-1.47 + 5.68i	-	-	-	-	-	-	-	-	-	-	-	-	-	-
9	-	-	-2.04 + 7.88i	-2.34 + 9.04i	-	-	-	-1.47 + 5.68i	6.46 - 44.99i	-	-0.32 + 11.56i	-0.32 + 11.56i	-	-	-	-	-	-	-	-	-	-	-	-
10	-	-	-	-	-2.74 + 10.62i	-3.61 + 15.7i	-	-1.47 + 5.68i	-	8.44 - 53.63i	-0.32 + 11.68i	-0.32 + 11.68i	-	-	-	-	-	-	-	-	-	-	-	-
11	-	-	-	-	-	-	-	-	-0.32 + 11.56i	-0.32 + 11.68i	6.34 - 67.93i	-	-2.65 + 20.67i	-3.04 + 23.53i	-	-	-	-	-	-	-	-	-	-
12	-	-	-	-	-	-	-	-	-0.32 + 11.56i	-0.32 + 11.68i	-	4.61 - 54.52i	-2.65 + 20.67i	-	-	-	-	-	-	-	-	-	-1.31 + 10.18i	-
13	-	-	-	-	-	-	-	-	-	-	-2.65 + 20.67i	-2.65 + 20.67i	6.76 - 52.52i	-	-	-	-	-	-	-	-	-	-1.46 + 11.37i	-
14	-	-	-	-	-	-	-	-	-	-	-3.04 + 23.53i	-	-	6.29 - 48.74i	-	-3.25 + 25.29i	-	-	-	-	-	-	-	-
15	-	-	-	-	-	-	-	-	-	-	-	-	-	-	14.84 - 115.81i	-7.23 + 56.88i	-	-	-	-	-5.16 + 40.15i	-	-	-2.45 + 18.95i
16	-	-	-	-	-	-	-	-	-	-	-	-	-	-3.25 + 25.29i	-7.23 + 56.88i	20.85 - 162.63i	-4.84 + 37.99i	-	-5.53 + 42.57i	-	-	-	-	-
17	-	-	-	-	-	-	-	-	-	-	-	-	-	-	-	-4.84 + 37.99i	14.59 - 115.56i	-8.55 + 68.38i	-	-	-	-1.2 + 9.34i	-	-
18	-	-	-	-	-	-	-	-	-	-	-	-	-	-	-	-	-8.55 + 68.38i	18.23 - 144.29i	-	-	-9.68 + 75.99i	-	-	-
19	-	-	-	-	-	-	-	-	-	-	-	-	-	-	-	-5.53 + 42.57i	-	-	11.93 - 92.15i	-6.4 + 49.68i	-	-	-	-
20	-	-	-	-	-	-	-	-	-	-	-	-	-	-	-	-	-	-	-6.4 + 49.68i	18.2 - 140.61i	-	-	-11.8 + 91.06i	-
21	-	-	-	-	-	-	-	-	-	-	-	-	-	-	-5.16 + 40.15i	-	-	-9.68 + 75.99i	-	-	16.71 - 130.42i	-1.86 + 14.51i	-	-
22	-	-	-	-	-	-	-	-	-	-	-	-	-	-	-	-	-1.2 + 9.34i	-	-	-	-1.86 + 14.51i	3.06 - 23.67i	-	-
23	-	-	-	-	-	-	-	-	-	-	-	-1.31 + 10.18i	-1.46 + 11.37i	-	-	-	-	-	-	-11.8 + 91.06i	-	-	14.57 - 112.38i	-
24	-	-	-0.32 + 11.56i	-	-	-	-	-	-	-	-	-	-	-	-2.45 + 18.95i	-	-	-	-	-	-	-	-	2.77 - 30.81i

Table 4.9 - Bus admittance matrix of the IEEE 24-bus power system estimated through optimization problem 4.2 (Non-robust formulation).

Bus No.	1	2	3	4	5	6	7	8	9	10	11	12	13	14	15	16	17	18	19	20	21	22	23	24
1	15.35 - 86.66i	-15.51+ 71.78i	-1.53+ 4.11i	-	-1.58 + 11.21i	-	-	-	-	-	-	-	-	-	-	-	-	-	-	-	-	-	-	-
2	-11.95 + 70.4i	18.39 - 84.86i	-	-3.04 + 7.98i	-	-0.59 + 4.45i	-	-	-	-	-	-	-	-	-	-	-	-	-	-	-	-	-	-
3	-0.86 + 4.34i	-	4.04 - 23.06i	-	-	-	-	-	-1.74 + 8.35i	-	-	-	-	-	-	-	-	-	-	-	-	-	-	-0.79 + 13.36i
4	-	-1.79 + 8.03i	-	6.29 - 17.4i	-	-	-	-	-3.79 + 9.99i	-	-	-	-	-	-	-	-	-	-	-	-	-	-	-
5	-2.41 + 11.96i	-	-	-	3.73 - 22.4i	-	-	-	-	-3.52 + 11.51i	-	-	-	-	-	-	-	-	-	-	-	-	-	-
6	-	-0.95 + 5.23i	-	-	-	3.42 - 20.58i	-	-	-	-3.66 + 16.69i	-	-	-	-	-	-	-	-	-	-	-	-	-	-
7	-	-	-	-	-	-	3.77 - 15.65i	-3.15 + 14.78i	-	-	-	-	-	-	-	-	-	-	-	-	-	-	-	-
8	-	-	-	-	-	-	-3.78 + 15.72i	5.9 - 26.49i	-1.5 + 5.85i	-1.51 + 5.77i	-	-	-	-	-	-	-	-	-	-	-	-	-	-
9	-	-	-1.79 + 7.89i	-3.1 + 9.45i	-	-	-	-0.99 + 5.78i	8.58 - 47.78i	-	-0.3 + 10.77i	-1.54 + 6.26i	-	-	-	-	-	-	-	-	-	-	-	-
10	-	-	-	-	-2.15 + 11.22i	-2.78 + 16.36i	-	-1.81 + 5.93i	-	10.06 - 56.87i	-0.65 + 11.68i	-0.87 + 4.03i	-	-	-	-	-	-	-	-	-	-	-	-
11	-	-	-	-	-	-	-	-	-2.66 + 10.82i	-0.1 + 11.06i	6.79 - 65.75i	-	-3.5 + 19.41i	-2.23 + 23.25i	-	-	-	-	-	-	-	-	-	-
12	-	-	-	-	-	-	-	-	1.15 + 13.43i	-1.12 + 13.73i	-	6.4 - 23.56i	-2.53 + 22.14i	-	-	-	-	-	-	-	-	-	-1.62 + 10.77i	-
13	-	-	-	-	-	-	-	-	-	-	-2.79 + 19.99i	-3.05 + 8.87i	6.78 - 52.19i	-	-	-	-	-	-	-	-	-	-1.21 + 10.63i	-
14	-	-	-	-	-	-	-	-	-	-	-3.11 + 22.82i	-	-	5.19 - 48.28i	-	-2.63 + 22.68i	-	-	-	-	-	-	-	-
15	-	-	-	-	-	-	-	-	-	-	-	-	-	-	12.03 - 117.04i	-6.25 + 49.28i	-	-	-	-	-4.81 + 40.34i	-	-	-3.97 + 21.76i
16	-	-	-	-	-	-	-	-	-	-	-	-	-	-2.87 + 25.12i	-6.37 + 59.97i	18.08 - 144.59i	-1.93 + 39.4i	-	-5.05 + 42.32i	-	-	-	-	-
17	-	-	-	-	-	-	-	-	-	-	-	-	-	-	-	-4.72 + 33.84i	7.93 - 121.3i	-8.52 + 68.19i	-	-	-	3.8 + 4.5i	-	-
18	-	-	-	-	-	-	-	-	-	-	-	-	-	-	-	-	-3.48 + 72.61i	14.46 - 146.56i	-	-	-5.86 + 80.39i	-	-	-
19	-	-	-	-	-	-	-	-	-	-	-	-	-	-	-	-4.26 + 38.8i	-	-	10.17 - 91.49i	-4.75 + 47.02i	-	-	-	-
20	-	-	-	-	-	-	-	-	-	-	-	-	-	-	-	-	-	-	-5.14 + 49.28i	14.07 - 131.1i	-	-	-9.54 + 88.78i	-
21	-	-	-	-	-	-	-	-	-	-	-	-	-	-	-4.61 + 39.34i	-	-	-5.88 + 78.4i	-	-	15.89 - 128.84i	-2.2 + 19.07i	-	-
22	-	-	-	-	-	-	-	-	-	-	-	-	-	-	-	-	-2.3 + 9.36i	-	-	-	-5.18 + 8.41i	-0.77 - 23.05i	-	-
23	-	-	-	-	-	-	-	-	-	-	-	-1.19 + 4.41i	-0.98 + 10.7i	-	-	-	-	-	-	-9.39 + 84.23i	-	-	12.27 - 109.98i	-
24	-	-	-0.6 + 11.48i	-	-	-	-	-	-	-	-	-	-	-	-0.81 + 17.92i	-	-	-	-	-	-	-	-	4.99 - 35.35i

Table 4.10 - Bus admittance matrix of the IEEE 24-bus power system estimated through optimization problem 4.6 (Robust formulation).

Bus No.	1	2	3	4	5	6	7	8	9	10	11	12	13	14	15	16	17	18	19	20	21	22	23	24
1	11.42 - 82.02i	-10.93+ 66.79i	-1.16 + 4.41i	-	-2.84 + 11.04i	-	-	-	-	-	-	-	-	-	-	-	-	-	-	-	-	-	-	-
2	-7.28 + 66.49i	14.14 - 79.3i	-	-1.96 + 7.37i	-	-1.3 + 4.82i	-	-	-	-	-	-	-	-	-	-	-	-	-	-	-	-	-	-
3	-0.94 + 4.34i	-	3.51 - 23.46i	-	-	-	-	-	-2.03 + 7.87i	-	-	-	-	-	-	-	-	-	-	-	-	-	-	-0.29 + 11.6i
4	-	-2.04 + 7.65i	-	4.31 - 16.34i	-	-	-	-	-2.34 + 9.03i	-	-	-	-	-	-	-	-	-	-	-	-	-	-	-
5	-3.18 + 11.23i	-	-	-	5.54 - 21.61i	-	-	-	-	-2.59 + 10.68i	-	-	-	-	-	-	-	-	-	-	-	-	-	-
6	-	-1.16 + 4.96i	-	-	-	4.73 - 20.25i	-	-	-	-3.22 + 15.74i	-	-	-	-	-	-	-	-	-	-	-	-	-	-
7	-	-	-	-	-	-	3.91 - 15.23i	-3.86 + 15.26i	-	-	-	-	-	-	-	-	-	-	-	-	-	-	-	-
8	-	-	-	-	-	-	-3.9 + 15.25i	6.85 - 26.58i	-1.49 + 5.66i	-1.42 + 5.68i	-	-	-	-	-	-	-	-	-	-	-	-	-	-
9	-	-	-20 + 7.89i	-2.34 + 9.01i	-	-	-	-1.48 + 5.68i	6.5 - 44.92i	-	-0.51 + 11.49i	-0.39 + 10.59i	-	-	-	-	-	-	-	-	-	-	-	-
10	-	-	-	-	-2.71 + 10.59i	-3.43 + 15.66i	-	-1.52 + 5.69i	-	7.71 - 53.75i	-0.55 + 11.35i	-0.02 + 10.64i	-	-	-	-	-	-	-	-	-	-	-	-
11	-	-	-	-	-	-	-	-	-0.44 + 11.52i	-0.02 + 11.61i	7.38 - 66.69i	-	-3.05 + 20.03i	-3.04 + 23.35i	-	-	-	-	-	-	-	-	-	-
12	-	-	-	-	-	-	-	-	-0.22 + 11.57i	-0.45 + 11.78i	-	3.81 - 49.81i	-2.32 + 21.22i	-	-	-	-	-	-	-	-	-	-1.04 + 10.51i	-
13	-	-	-	-	-	-	-	-	-	-	-2.98 + 20.4i	-2.35 + 18.9i	6.53 - 51.82i	-	-	-	-	-	-	-	-	-	-1.67 + 10.73i	-
14	-	-	-	-	-	-	-	-	-	-	-3.33 + 22.99i	-	-	6.55 - 48.6i	-	-2.22 + 24.58i	-	-	-	-	-	-	-	-
15	-	-	-	-	-	-	-	-	-	-	-	-	-	-	13.39 - 115.29i	-4.92 + 53.87i	-	-	-	-	-4.8 + 40.29i	-	-	-2.48 + 18.94i
16	-	-	-	-	-	-	-	-	-	-	-	-	-	-3.45 + 25.37i	-6.35 + 57.33i	13.72 - 154.8i	-3.61 + 37.74i	-	-4.6 + 42.69i	-	-	-	-	-
17	-	-	-	-	-	-	-	-	-	-	-	-	-	-	-	-2.93 + 35.81i	12.63 - 116.32i	-8.84 + 68.25i	-	-	-	-0.06 + 8.92i	-	-
18	-	-	-	-	-	-	-	-	-	-	-	-	-	-	-	-	-7.63 + 68.82i	17.61 - 143.79i	-	-	-8.4 + 76.16i	-	-	-
19	-	-	-	-	-	-	-	-	-	-	-	-	-	-	-	-3.57 + 40.61i	-	-	9.26 - 92.47i	-5.68 + 46.83i	-	-	-	-
20	-	-	-	-	-	-	-	-	-	-	-	-	-	-	-	-	-	-	-4.68 + 49.86i	16.12 - 131.96i	-	-	-10.87 + 87i	-
21	-	-	-	-	-	-	-	-	-	-	-	-	-	-	-4.89 + 39.69i	-	-	-8.77 + 75.57i	-	-	15.74 - 129.42i	-2.34 + 14.35i	-	-
22	-	-	-	-	-	-	-	-	-	-	-	-	-	-	-	-	-1.21 + 9.99i	-	-	-	-2.54 + 13.29i	2.49 - 22.97i	-	-
23	-	-	-	-	-	-	-	-	-	-	-	-1.09 + 9.33i	-1.27 + 10.72i	-	-	-	-	-	-	-10.54 +85.29i	-	-	13.58 - 108.02i	-
24	-	-	-0.35 + 11.56i	-	-	-	-	-	-	-	-	-	-	-	-2.09 + 18.35i	-	-	-	-	-	-	-	-	2.77 - 30.81i

4.2.3 IEEE 30-bus power system:

The algorithms based on equations 4.2 (original) and 4.6 (robust) are executed on the system and the errors are plotted in the Figure 4.8.

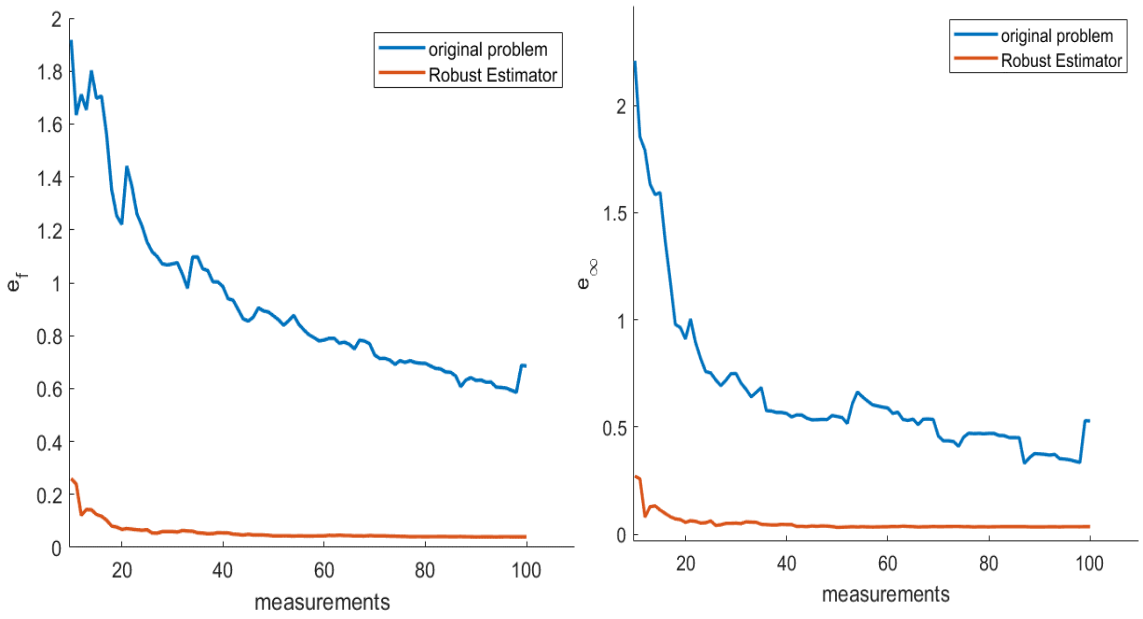

Figure 4.8 - Errors in the estimated bus admittance matrix of the non-robust and robust algorithm for the IEEE 30-bus power system.

The values of the errors for the algorithms of at various numbers of measurements are mentioned in the Table 4.11.

Table 4.11 - Errors of the algorithm at various number of measurements for the IEEE 30-bus power system.

	No. of sets of measurements	**10**	**25**	**40**	**55**	**70**	**85**
Non-robust estimation	e_f	1.2530	1.0972	0.8893	0.7755	0.6958	0.6057
	e_∞	0.9637	0.6618	0.5537	0.5308	0.4682	0.3522
Robust estimation	e_f	0.0767	0.0610	0.0456	0.0448	0.0406	0.0395
	e_∞	0.0680	0.0553	0.0355	0.0359	0.0343	0.0338

4.2.4 IEEE 118-bus power system

The algorithms based on equations 4.2 (original) and 4.6 (robust) are executed on the system and the errors are plotted in Figure 4.9.

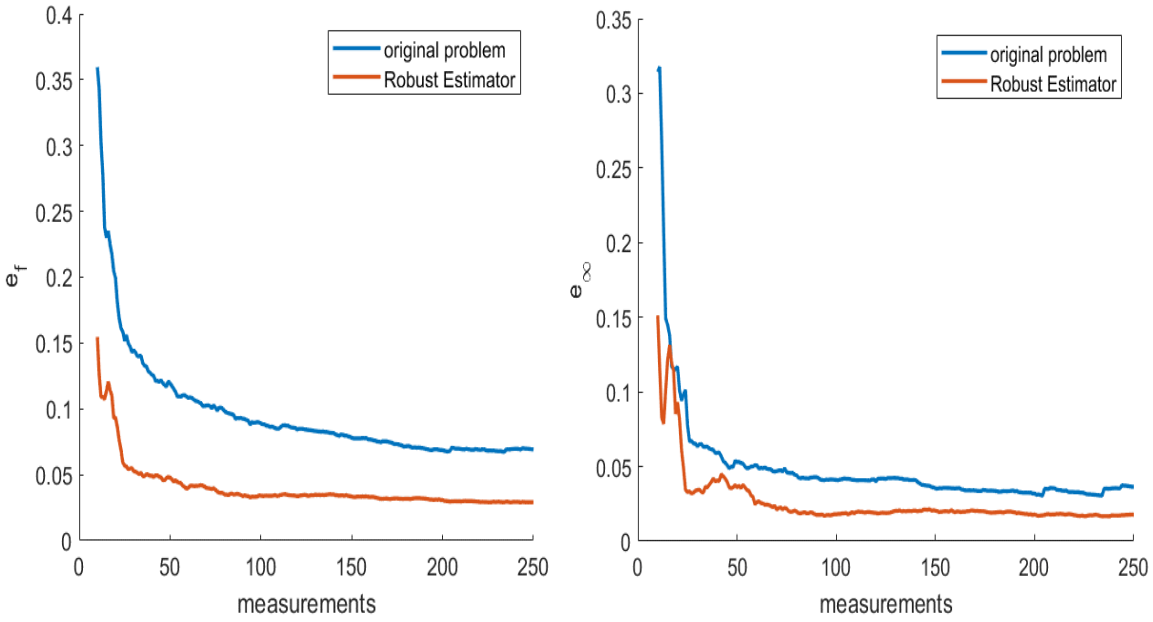

Figure 4.9 - Errors in the estimated bus admittance matrix of the non-robust and robust algorithm for IEEE 118-bus power system.

The values of the errors for the algorithms of sections 2.3 and 3.4 at various numbers of measurements are mentioned in Table 4.12.

Table 4.12 - Errors of the algorithm at various number of measurements for the IEEE 118-bus power system

	No. of sets of measurements	**10**	**50**	**90**	**130**	**170**	**210**
Non-robust estimation	e_f	0.2048	0.1094	0.0896	0.0817	0.0714	0.0693
	e_∞	0.1150	0.0508	0.0412	0.0410	0.0338	0.0330
Robust estimation	e_f	0.0930	0.0394	0.0342	0.0350	0.0317	0.0296
	e_∞	0.0852	0.0247	0.0180	0.0205	0.0192	0.0179

4.3 Detection of Faulty Instruments

In section 4.2 the communication channels have been assumed to be very noisy. Therefore, the buses at which the measurements were faulty were chosen randomly. However, if some set of communication channels or meters is defective, then there is a high probability that the measurements taken through them will be consistently faulty. In the following section, such a scenario will be considered, and the resulting solution will be discussed. Moreover, the detection of the faulty set will be discussed.

4.4 Experimental Results

All the experimental setup is essentially the same as the previous chapter with the exception a couple of preselected meters will consistently record faulty measurements. This scenario is modeling the faulty meters or faulty communication channels.

4.4.1 IEEE 14-bus power system

It is assumed that the phasor instruments at the buses 12 and 6 are faulty. The instruments at these locations are consistently recording faulty measurements. These faulty measurements are simulated by adding the samples of noise drawn from a probability density function with a large standard deviation.

The robust algorithm for the estimation of the bus admittance matrix is executed on the system and the residuals are plotted in the Figure 4.10. In the figure, the buses with a faulty instrument (i.e., buses 6 and 12) have relatively large residual. Bus 13 has a large residual due the faulty instrument at bus 12. Once the faulty instrument is removed the from bus number 12, the large residual of bus 13 will also reduce.

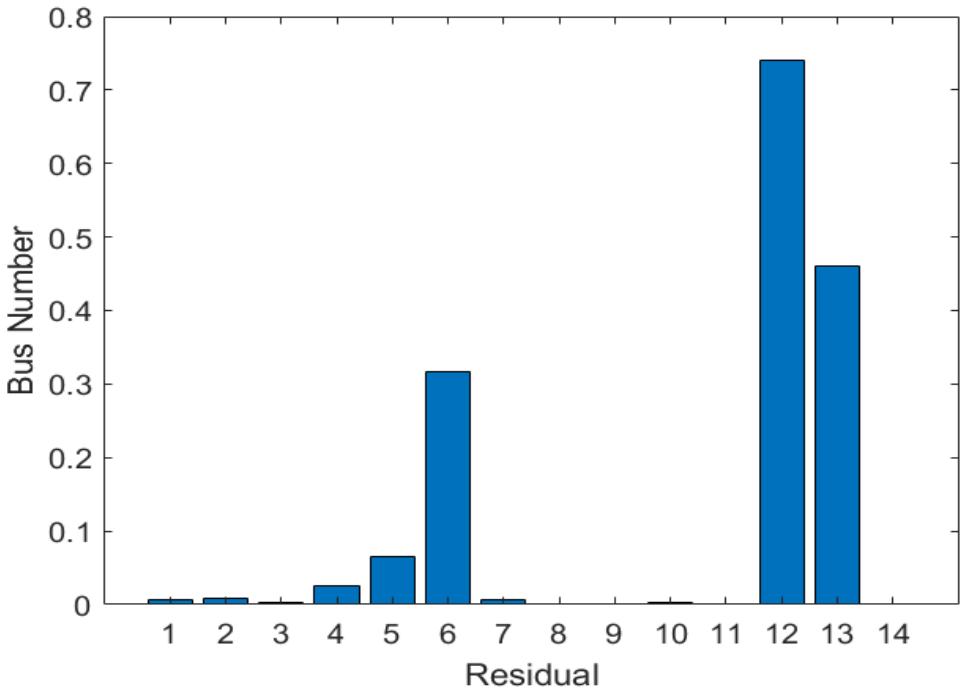

Figure 4.10 – Residuals of measurements taken at various buses of the IEEE 14-bus power system.

4.4.2 IEEE 24-bus power system

It is assumed that the phasor instruments at the buses 12 and 16 are faulty. The instruments at these locations are consistently recording faulty measurements. These faulty measurements are simulated by adding the samples of noise drawn from a probability density function with a large standard deviation.

The robust algorithm for the estimation of the bus admittance matrix is executed on the system and the residuals are plotted in the Figure 4.11. In the figure, the buses with a faulty instrument (i.e., buses 12 and 16) have relatively large residual. Once the faulty instrument is removed the from the bus number 16, the large residual of bus 19 will also reduce.

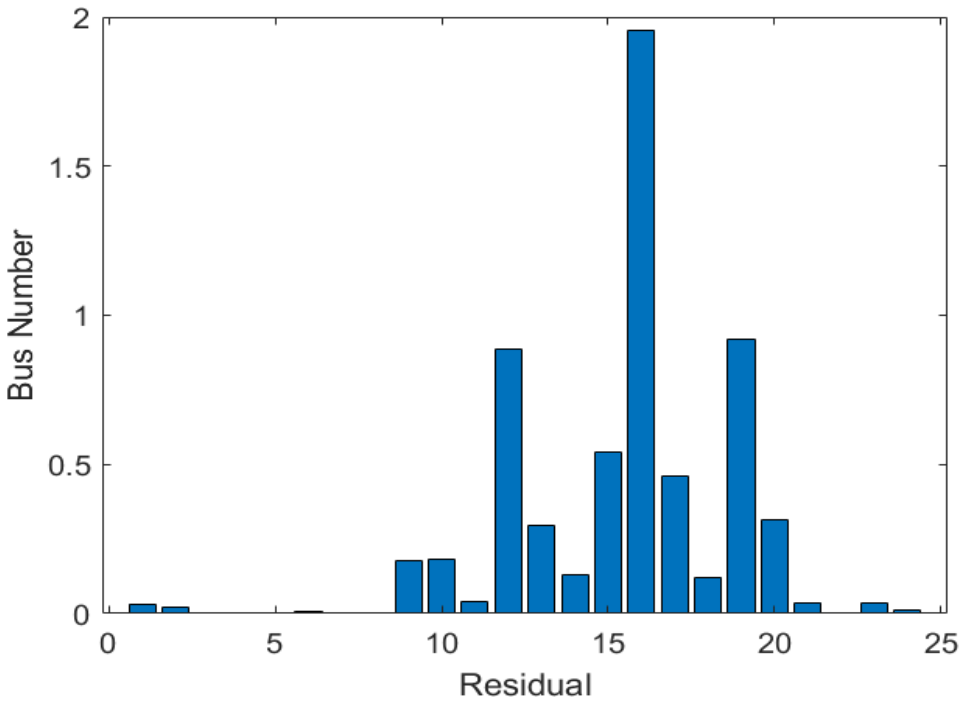

Figure 4.11 - Residuals of measurements taken at various buses of the IEEE 24-bus power system.

4.5 Discussion

Though the estimator based on the l_2-norm-square minimization works satisfactorily when the noise in the measurements are within the nominal bounds. Even if some of the measurements are faulty, the performance of the estimator does not degrade too much. If, however, the faulty measurements increase in number and magnitude the performance of the estimator is affected severely. This happens because the value of the cost function increases disproportionately with an increase in the magnitude of the input.

In the presence of many faulty measurements, the robust algorithm based on the objective function 4.6 using the $\emptyset(\cdot)$, defined in equation 4.5, as the cost function outperforms the l_2-estimator.

CHAPTER 5. ESTIMATION OF THE BUS IMPEDANCE MATRIX

5.1 Introduction

In this chapter a dual approach for the approximation of the network parameters will be presented. Instead of directly formulating the bus admittance matrix of a power system, the bus impedance matrix is formulated. Once the bus impedance matrix is formed, its triangular factors are used to evaluate the parameters of the power system.

The algorithm presented will be simulated on the test systems and the results are discussed.

5.2 Mathematical Theory

Voltages and currents of an $n+1$ bus power system (assuming one bus to be a reference) are related through an $n \times n$ bus impedance matrix as

$$v_{bus} - Z_{bus} i_{bus} = 0 \tag{5.1}$$

where v_{bus} is a complex-valued n-vector of actual bus voltages, and i_{bus} is a complex-valued n-vector of actual current injections at the respective buses. Voltage and current measurements taken at time t_i at bus j are $v_j(t_i)$ and $i_j(t_i)$ respectively. Buses' voltages and injection currents at time sample, t_i, are represented by $n - dimensional$ vectors, $v(t_i)$ and $i(t_i)$ respectively as, $v(t_i) \coloneqq [v_1(t_i)\ v_2(t_i)\ \dots v_n(t_i)]^T$ and $i(t_i) \coloneqq [i_1(t_i)\ i_2(t_i) \dots i_n(t_i)]^T$ where $^{\mathrm{T}}$ represents the transpose operation. The matrices V_{bus} and I_{bus} are $n \times m$ voltage and current measurement matrices defined as,

$$V_{bus} = [v(t_1) \mid v(t_2) \mid v(t_3) \ \ldots \ v(t_m)] \tag{5.2}$$

and

$$I_{bus} = [i(t_1) \mid i(t_2) \mid i(t_3) \ \ldots \ i(t_m)] \tag{5.3}$$

As all the phasor measurements will have some errors due to random measurement noise, V_{bus} and I_{bus} will be related as

$$V_{bus} - Z_{bus} I_{bus} \approx 0 \tag{5.4}$$

Defining r as the residual matrix,

$$r \coloneqq V_{bus} - Z_{bus} I_{bus} \tag{5.5}$$

where the magnitude of the elements in r will depend on the errors in the measurement matrices. In comparison to conventional measurements, phasor measurements have much better accuracy. Therefore, the errors in the measurements will be relatively much smaller. When the errors in the measurements are small, a reasonable estimate of the bus impedance matrix, $\tilde{Z}_{bus}$, can be obtained by using the Frobenius norm estimator [59] as,

$$\tilde{Z}_{bus} \coloneqq \underset{\tilde{Z}_{bus}}{minimize} \ ||(V_{bus} - \grave{Z}_{bus} I_{bus})||_f^2 \tag{5.6}$$

The solution of the optimization problem 5.6 is obtained by

$$\tilde{Z}_{bus} = V_{bus} \times I_{bus}^*(I_{bus} I_{bus}^*)^{-1} \tag{5.7}$$

As the solution of the optimization problem 5.6 assumes that the voltage measurements matrix is full rank. As mentioned previously in chapter 2, this assumption can be relaxed by resorting to the regularized optimization problem.

$$\tilde{Z}_{bus} \coloneqq \underset{\tilde{Z}_{bus}}{minimize}\ ||(\ V_{bus} - \ \grave{Z}_{bus} I_{bus}\ )||_f^2 + \ \delta||\grave{Z}_{bus}||_f^2 \tag{5.8}$$

Due to the addition of the regulation term, the solution of the optimization is always guaranteed, regularization of the optimization problem can be justified for various reasons as mentioned in section 2.3.

The solution of the resulting problem is

$$\tilde{Z}_{bus} = \ V_{bus} \times I_{bus}^{*}(I_{bus} I_{bus}^{*} \ + \ \delta\ I)^{-1} \tag{5.9}$$

Additionally, as the measurements are received sequentially, so Sherman-Morrison-Woodbury identity,

$$(A + UCV)^{-1} = \ A^{-1} - A^{-1}U(C^{-1} + VA^{-1}U)^{-1}VA^{-1} \tag{5.10}$$

can be used to reduce the computations for the evaluation of the matrix $(I_{bus} I_{bus}^{*} + \ \delta\ I)^{-1}$. Since for our system, each new measurement updates the matrix by rank 1, therefore, the identity in equation 5.10 transforms as

$$\left(I_{bus,q} I_{bus,q}^{*}\right)^{-1} = \ \left(I_{bus,q-1} I_{bus,q-1}^{*} + \ i_{bus,q} i_{bus,q}^{*}\ \right)^{-1} \tag{5.11}$$

where, $i_{bus,q}$ is the current measurement vector at the q^{th} time sample and $I_{bus,q-1}$ and $I_{bus,q}$ are the current matrices up until $(q-1)^{th}$ and q^{th} time sample. Therefore, using these values, the Sherman-Morrison-Woodbury identity, mentioned in equation 5.10, can be used to evaluate $\left(I_{bus,q} I_{bus,q}^{*}\right)^{-1}$ as

$$\left(I_{bus,q} I_{bus,q}^{*}\right)^{-1} = \left(I_{bus,q-1} I_{bus,q-1}^{*}\ \right)^{-1} - \left(I_{bus,q-1} I_{bus,q-1}^{*}\ \right)^{-1} i_{bus,q}\ \times$$

$$\left(1 + i_{bus,q}^{*}\left(I_{bus,q-1} I_{bus,q-1}^{*}\ \right)^{-1} i_{bus,q}\right)^{-1} i_{bus,q}\left(I_{bus,q} I_{bus,q}^{*}\right)^{-1}$$

To initialize the algorithm, matrix A in 5.10 must be invertible, but A can not be invertible until n linear independent measurements have been obtained. To solve this problem, the algorithm can be initialized by using δI as A for the first iteration. The detailed algorithm for the solution, $\tilde{Z}_{bus}$, expressed in equation 5.9 for the optimization problem of equation 5.8 is as follows.

5.2.1 Algorithm 5.1

1. Initialize a matrix G as $G_0^{-1} \coloneqq \delta I$.
2. For each new measurement $i_{bus,k}$, evaluate

$$G_k^{-1} = \; G_{k-1}^{-1} - G_{k-1}^{-1} i_{bus,k} \left(1 + i_{bus,k}^{*} G_{k-1}^{-1} i_{bus,k}\right)^{-1} i_{bus,k}^{*} G_{k-1}^{-1} \, .$$

3. Evaluate

$$\tilde{Z}_{bus}^{k} = \; V_{bus,k} \times I_{bus,k}^{*} G_k^{-1}.$$

Once the algorithm has converged, the bus impedance matrix of a given power system will be available through which the Thevenin impedance and the transfer impedances of the power system can be derived.

5.3 Experimental Results

The algorithm is validated via simulations performed on IEEE systems [66]. Simulations are performed in MATLAB using MATPOWER [67]. Slight modifications are made in the systems for the simulations.

For each new measurement, loads at all the buses are varied within $\pm 10\%$ of the nominal load. The difference in power, $\Delta P_G(t_k)$, between the total power generation at

previous sampling time, $P_G(t_{k-1})$, and the sum of the updated total load at the current time, $P_L(t_k)$, with the system losses at previous sample, $P_{Loss}(t_{k-1})$, is distributed in all of the generators using participation factors according to the following equations

$$\Delta P_G(t_k) = P_L(t_k) + P_{Loss}(t_{k-1}) - P_G(t_{k-1}) \tag{5.12}$$

The additional power generated by the i^{th}generator at the k^{th}time sample is given by,

$$\Delta P_G^i(t_k) = \Delta P_G(t_k) \times PF^i \tag{5.13}$$

where, PF^i is the participation factor of the i^{th} generator defined as the ratio of the total MW capacity of the i^{th} generator to the sum of the total MW capacities of all the generators of the system.

Load flow analysis is then performed for the new system conditions. The residual power (difference between total generation and total consumption) of the system is provided by the slack bus generator at bus 1. The voltages and the injected current phasors are calculated at all the buses. Noise following a normal probability density function is added to all phasors to simulate phasor measurements.

The error matrix, ΔZ_{bus}, is defined as

$$\Delta Z_{bus} = Z_{bus} - \tilde{Z}_{bus} \tag{5.14}$$

The accuracy and convergence of the algorithm is estimated [68] by

$$E_f = ||\Delta Z_{bus}||_f / ||Z_{bus}||_f \tag{5.15}$$

and

$$E_\infty = ||\Delta Z||_\infty / ||\mathrm{Z}||_\infty \tag{5.16}$$

where f is representing the Frobenius norm and the ∞ is representing the infinity norm (the maximum value of the absolute row sum of a matrix).

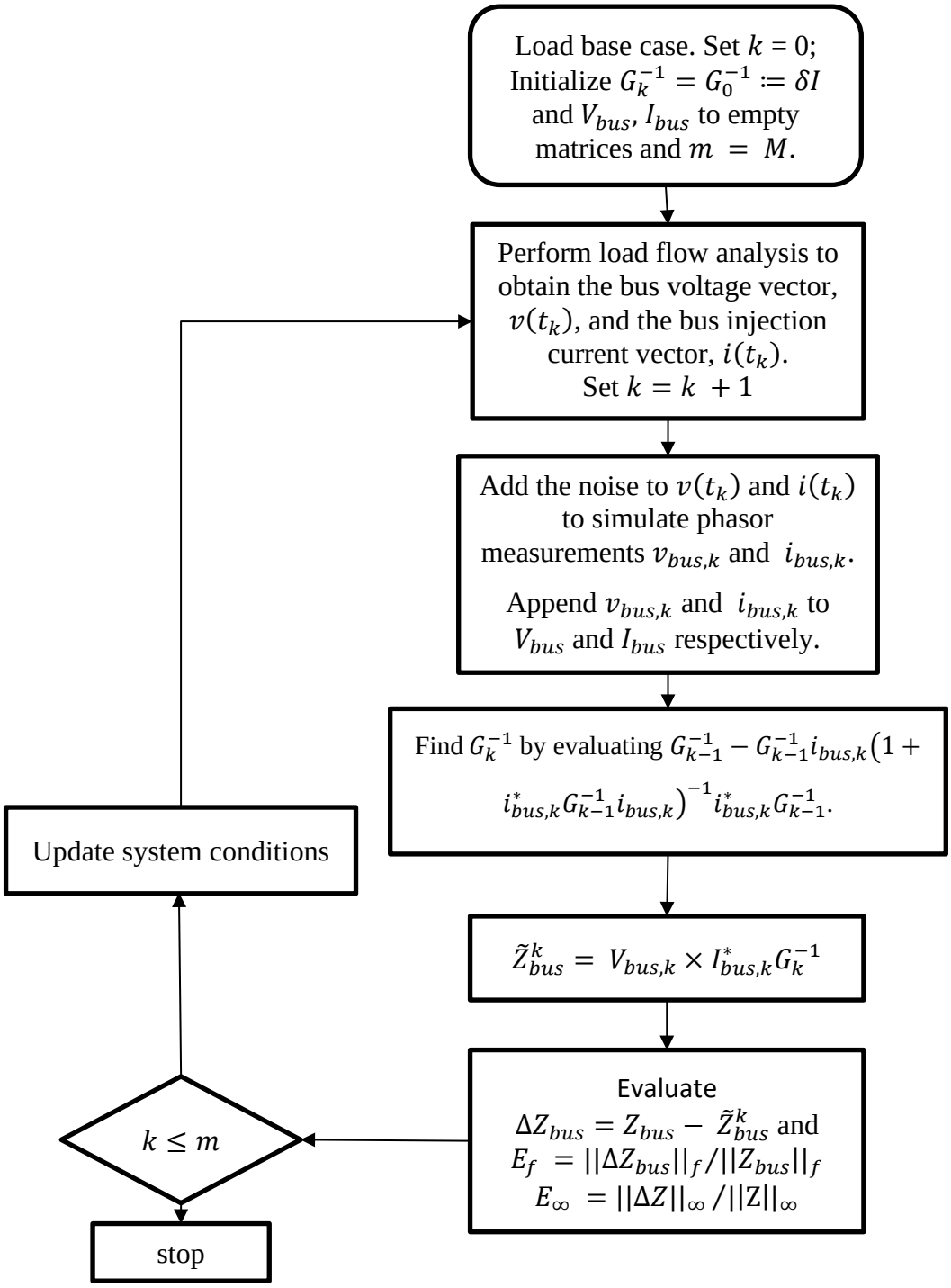

Figure 5.1 – The scheme used for the simulation of the Algorithm 5.1 for the estimation of the bus impedance matrix of a power system.

5.3.1 IEEE 14-bus system

A one-line diagram of the system is shown in Figure 2.2. The parameters and the connection information are provided in the appendix. The algorithm of section 5.2.1 is executed on the system and the errors are tabulated in Table 5.1.

Table 5.1 - Errors in the bus impedance matrix estimated through Algorithm 5.1 at various number of measurements for the IEEE 14-bus power system.

No. of sets of measurements	**50**	**100**	**150**	**200**	**250**	**300**	**350**
$\boldsymbol{e_f}$	0.09645	0.03706	0.02078	0.01568	0.01389	0.01128	0.00955
$\boldsymbol{e_\infty}$	0.09481	0.03643	0.02043	0.01542	0.01365	0.01108	0.00938

The errors, E_f and E_∞, for the algorithm 5.1 are plotted in the Figure 5.1. The actual bus impedance matrix and the bus impedance matrix estimated through the algorithm is shown in the Table 5.2 and Table 5.3 respectively. The Thevenin impedances of the system are mentioned the Table 5.3.

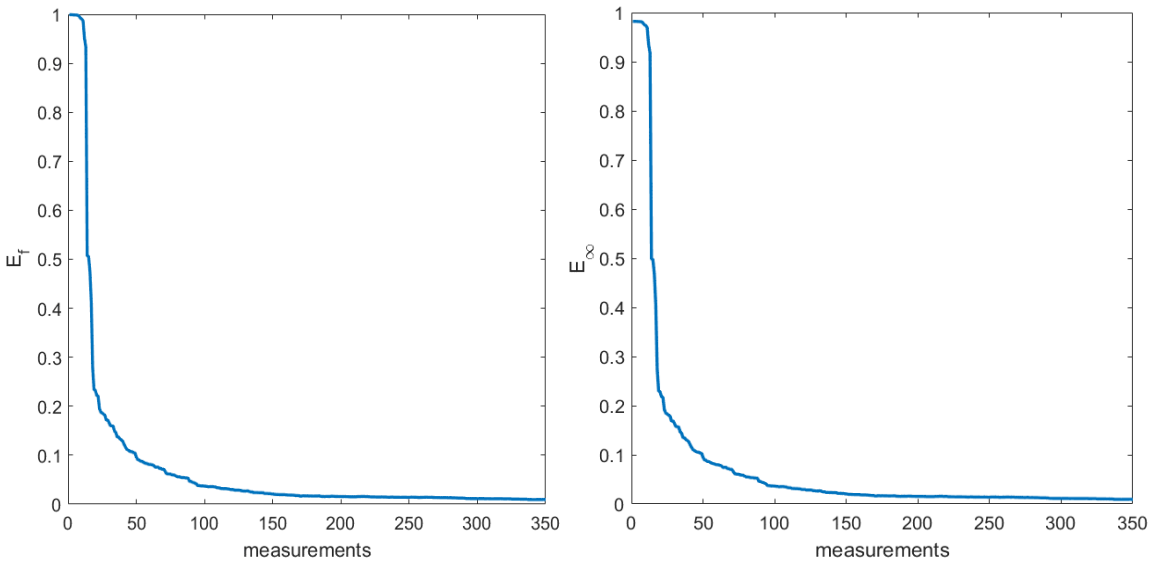

Figure 5.2 – Plot of the errors in the bus impedance matrix estimated through Algorithm 5.1 for the IEEE 14-bus power system.

Table 5.2 -Actual Bus impedance Matrix of the IEEE 14-bus power system.

Bus No	1	2	3	4	5	6	7	8	9	10	11	12	13	14
1	0.0162-2.2442i	0.0049-2.2811i	-0.001-2.3052i	-0.0049-2.3148i	-0.001-2.3026i	-0.0024-2.4706i	-0.0044-2.4344i	-0.0044-2.4344i	-0.0041-2.47i	-0.0038-2.4701i	-0.0031-2.4703i	-0.0026-2.4706i	-0.0027-2.4705i	-0.0035-2.4702i
2	0.0049-2.2811i	0.0094-2.2684i	0.0018-2.2978i	-0.0043-2.3121i	-0.0016-2.3032i	-0.0029-2.4701i	-0.0038-2.4323i	-0.0038-2.4323i	-0.0036-2.4681i	-0.0034-2.4685i	-0.0031-2.4693i	-0.0029-2.47i	-0.0029-2.4698i	-0.0033-2.4689i
3	-0.001-2.3052i	0.0018-2.2978i	0.027-2.2158i	-0.0031-2.306i	-0.0028-2.3067i	-0.004-2.4704i	-0.0028-2.4278i	-0.0028-2.4278i	-0.0026-2.4646i	-0.0028-2.4656i	-0.0033-2.4679i	-0.0039-2.4699i	-0.0037-2.4695i	-0.0031-2.4667i
4	-0.0049-2.3148i	-0.0043-2.3121i	-0.0031-2.306i	0.003-2.2896i	-2.2985i	-0.0003-2.4585i	0.0033-2.4122i	0.0033-2.4122i	0.0034-2.4496i	0.0029-2.4512i	0.0014-2.4548i	-0.0001-2.4578i	0.0003-2.4572i	0.0021-2.4529i
5	-0.001-2.3026i	-0.0016-2.3032i	-0.0028-2.3067i	-2.2985i	0.0074-2.2738i	0.0061-2.4444i	0.001-2.4148i	0.001-2.4148i	0.0015-2.4488i	0.0023-2.448i	0.0041-2.4462i	0.0058-2.4447i	0.0054-2.445i	0.0032-2.4471i
6	-0.0024-2.4706i	-0.0029-2.4701i	-0.004-2.4704i	-0.0003-2.4585i	0.0061-2.4444i	0.0188-2.4535i	-0.007-2.5402i	-0.007-2.5402i	-0.0106-2.5541i	-0.0064-2.5364i	0.005-2.4958i	0.0178-2.461i	0.0138-2.4679i	-0.0003-2.5165i
7	-0.0044-2.4344i	-0.0038-2.4323i	-0.0028-2.4278i	0.0033-2.4122i	0.001-2.4148i	-0.007-2.5402i	0.0079-2.4021i	0.0079-2.4021i	0.0103-2.4782i	0.0079-2.4892i	0.0012-2.5142i	-0.0065-2.5356i	-0.0041-2.5313i	0.0043-2.5014i
8	-0.0044-2.4344i	-0.0038-2.4323i	-0.0028-2.4278i	0.0033-2.4122i	0.001-2.4148i	-0.007-2.5402i	0.0079-2.4021i	0.0079-2.2259i	0.0103-2.4782i	0.0079-2.4892i	0.0012-2.5142i	-0.0065-2.5356i	-0.0041-2.5313i	0.0043-2.5014i
9	-0.0041-2.47i	-0.0036-2.4681i	-0.0026-2.4646i	0.0034-2.4496i	0.0015-2.4488i	-0.0106-2.5541i	0.0103-2.4782i	0.0103-2.4782i	0.0139-2.4643i	0.0105-2.4801i	0.001-2.5163i	-0.0098-2.5474i	-0.0064-2.5412i	0.0054-2.4979i
10	-0.0038-2.4701i	-0.0034-2.4685i	-0.0028-2.4656i	0.0029-2.4512i	0.0023-2.448i	-0.0064-2.5364i	0.0079-2.4892i	0.0079-2.4892i	0.0105-2.4801i	0.0351-2.4205i	0.0161-2.4773i	-0.0058-2.5322i	-0.0036-2.5283i	0.0046-2.5012i
11	-0.0031-2.4703i	-0.0031-2.4693i	-0.0033-2.4679i	0.0014-2.4548i	0.0041-2.4462i	0.005-2.4958i	0.0012-2.5142i	0.0012-2.5142i	0.001-2.5163i	0.0161-2.4773i	0.055-2.3887i	0.0049-2.4973i	0.0043-2.4987i	0.0023-2.5087i
12	-0.0026-2.4706i	-0.0029-2.47i	-0.0039-2.4699i	-0.0001-2.4578i	0.0058-2.4447i	0.0178-2.461i	-0.0065-2.5356i	-0.0065-2.5356i	-0.0098-2.5474i	-0.0058-2.5322i	0.0049-2.4973i	0.1073-2.3239i	0.0278-2.426i	0.006-2.4944i
13	-0.0027-2.4705i	-0.0029-2.4698i	-0.0037-2.4695i	0.0003-2.4572i	0.0054-2.445i	0.0138-2.4679i	-0.0041-2.5313i	-0.0041-2.5313i	-0.0064-2.5412i	-0.0036-2.5283i	0.0043-2.4987i	0.0278-2.426i	0.058-2.3908i	0.021-2.4755i
14	-0.0035-2.4702i	-0.0033-2.4689i	-0.0031-2.4667i	0.0021-2.4529i	0.0032-2.4471i	-0.0003-2.5165i	0.0043-2.5014i	0.0043-2.5014i	0.0054-2.4979i	0.0046-2.5012i	0.0023-2.5087i	0.006-2.4944i	0.021-2.4755i	0.085-2.3359i

Table 5.3 – Bus impedance matrix estimated through Algorithm 5.1.

Bus No	1	2	3	4	5	6	7	8	9	10	11	12	13	14
1	0.019-2.2227i	0.0024-2.2599i	-0.0008-2.2825i	-0.0042-2.2912i	-0.0017-2.2841i	-0.0018-2.4484i	-0.0051-2.4123i	-0.0043-2.4077i	-0.0044-2.4454i	-0.0004-2.45i	-0.0057-2.4487i	-0.0196-2.4521i	-0.0037-2.441i	-0.0082-2.4451i
2	0.0074-2.2609i	0.0068-2.2484i	0.002-2.2764i	-0.0034-2.2898i	-0.0023-2.286i	-0.002-2.4487i	-0.0044-2.4112i	-0.0032-2.4072i	-0.0035-2.4449i	0.0009-2.4494i	-0.0052-2.449i	-0.0234-2.4542i	-0.0036-2.4414i	-0.008-2.4454i
3	0.0023-2.2835i	-2.2764i	0.0276-2.1929i	-0.0017-2.2821i	-0.0031-2.2879i	-0.0033-2.4475i	-0.0031-2.4052i	-0.0013-2.4007i	-0.0022-2.4397i	0.0021-2.4444i	-0.0053-2.4462i	-0.0226-2.4514i	-0.0044-2.4392i	-0.007-2.4416i
4	-0.002-2.2938i	-0.0067-2.2913i	-0.0027-2.2839i	0.0038-2.2665i	-0.0004-2.2805i	0.0001-2.4365i	0.0028-2.3905i	0.0051-2.3863i	0.0038-2.4254i	0.007-2.4313i	-0.0004-2.4337i	-0.0183-2.4399i	-0.0005-2.4279i	-0.0018-2.4284i
5	0.0023-2.2806i	-0.0032-2.2816i	-0.002-2.2837i	0.0013-2.2746i	0.0068-2.255i	0.0071-2.4214i	0.0009-2.392i	0.0023-2.3881i	0.002-2.4235i	0.0058-2.4275i	0.0022-2.4244i	-0.0146-2.4264i	0.0047-2.4151i	-0.0006-2.4216i
6	-0.0001-2.4503i	-0.0057-2.45i	-0.004-2.4489i	0.0003-2.4361i	0.0046-2.4275i	0.0198-2.4323i	-0.0082-2.5191i	-0.0076-2.515i	-0.0113-2.5306i	-0.0029-2.5174i	0.0026-2.4757i	-0.0003-2.4445i	0.0129-2.4393i	-0.0049-2.4928i
7	-0.0011-2.4138i	-0.0061-2.4118i	-0.0021-2.4059i	0.0048-2.3894i	0.0007-2.3971i	-0.0061-2.5184i	0.0078-2.3807i	0.0091-2.3766i	0.0106-2.4542i	0.0131-2.4695i	-0.0014-2.4938i	-0.0246-2.5177i	-0.0045-2.5023i	0.0001-2.4773i
8	-0.0008-2.4137i	-0.0057-2.4118i	-0.0019-2.4059i	0.0049-2.3893i	0.0009-2.3971i	-0.0056-2.5184i	0.008-2.3801i	0.0087-2.2003i	0.0105-2.4544i	0.0128-2.469i	-0.0005-2.4937i	-0.0235-2.518i	-0.0047-2.5017i	0.0005-2.4771i
9	-0.0012-2.4479i	-0.0059-2.4464i	-0.0022-2.4414i	0.0043-2.4254i	0.001-2.4299i	-0.0096-2.5308i	0.0091-2.4552i	0.0109-2.4514i	0.0136-2.4392i	0.0146-2.4598i	-0.0015-2.4946i	-0.0298-2.5284i	-0.007-2.511i	0.001-2.4723i
10	-0.0008-2.4484i	-0.0058-2.447i	-0.0023-2.4428i	0.0039-2.4274i	0.0018-2.4294i	-0.0056-2.514i	0.0077-2.4667i	0.0096-2.4623i	0.0107-2.4553i	0.0401-2.4001i	0.014-2.4556i	-0.0231-2.5135i	-0.0047-2.498i	0.0003-2.4763i
11	-0.0001-2.4488i	-0.0055-2.4479i	-0.003-2.4451i	0.0023-2.431i	0.0036-2.4275i	0.0058-2.473i	-0.0001-2.4915i	0.001-2.4874i	0.0009-2.4915i	0.0198-2.4568i	0.0532-2.3674i	-0.0152-2.4784i	0.0035-2.4685i	-0.0022-2.4837i
12	0.0005-2.4494i	-0.005-2.4492i	-0.0034-2.4477i	0.0013-2.4347i	0.0051-2.4268i	0.019-2.4392i	-0.0074-2.5137i	-0.005-2.5094i	-0.0093-2.523i	-0.0007-2.5115i	0.0031-2.4764i	0.0901-2.3064i	0.0276-2.3966i	0.0014-2.47i
13	0.0006-2.4484i	-0.0051-2.448i	-0.0031-2.4463i	0.0013-2.433i	0.0053-2.4259i	0.0148-2.4447i	-0.0044-2.5083i	-0.0031-2.5044i	-0.0061-2.5158i	0.0012-2.507i	0.0019-2.4768i	0.0071-2.4077i	0.0583-2.3604i	0.0163-2.4499i
14	-0.0005-2.4486i	-0.0056-2.4476i	-0.0029-2.444i	0.003-2.4292i	0.0025-2.4287i	0.0001-2.4935i	0.0037-2.479i	0.0049-2.4751i	0.0052-2.4732i	0.009-2.4808i	0.0001-2.4872i	-0.0117-2.4759i	0.0201-2.4454i	0.0802-2.3106i

Table 5.4 – Actual Thevenin impedances of the IEEE 14-bus power system along with the impedances estimated through Algorithm 5.1

Bus i	Thevenin Impedance		% Error
	Actual	Computed	
1	0.0162 - 2.2442i	0.019 - 2.2227i	0.9625
2	0.0094 - 2.2684i	0.0068 - 2.2484i	0.8883
3	0.027 - 2.2158i	0.0276 - 2.1929i	1.0343
4	0.003 - 2.2896i	0.0038 - 2.2665i	1.008
5	0.0074 - 2.2738i	0.0068 - 2.255i	0.8248
6	0.0188 - 2.4535i	0.0198 - 2.4323i	0.8666
7	0.0079 - 2.4021i	0.0078 - 2.3807i	0.8908
8	0.0079 - 2.2259i	0.0087 - 2.2003i	1.1542
9	0.0139 - 2.4643i	0.0136 - 2.4392i	1.0195
10	0.0351 - 2.4205i	0.0401 - 2.4001i	0.8686
11	0.055 - 2.3887i	0.0532 - 2.3674i	0.8929
12	0.1073 - 2.3239i	0.0901 - 2.3064i	1.0546
13	0.058 - 2.3908i	0.0583 - 2.3604i	1.2692
14	0.085 - 2.3359i	0.0802 - 2.3106i	1.1

The histogram showing the number of estimated parameters falling within certain error ranges is shown in the histogram of Figure 5.3. It is clear from the figure that none of the estimated parameters has errors > 2%, and most of the estimated parameters have error < 1%.

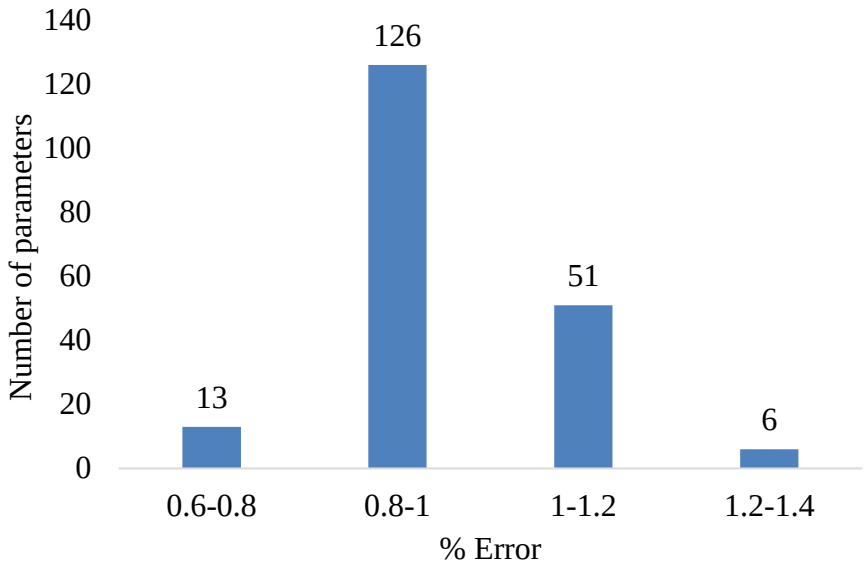

Figure 5.3 - Number of estimated Z_{bus} elements within various % error ranges for the IEEE 14-bus power system.

5.3.2 IEEE 24-bus system

The parameters and the connection information are provided in the appendix. The algorithm of section 5.2.1 is executed on the system and the errors at various measurements are tabulated in Table 5.5.

Table 5.5 - Errors in the bus impedance matrix estimated through Algorithm 5.1 at various number of measurements for the IEEE 24-bus power system.

No. of sets of measurements	**50**	**100**	**150**	**200**	**250**	**300**
e_f	0.01088	0.00523	0.00376	0.00302	0.00293	0.00237
e_∞	0.01006	0.00474	0.00336	0.00268	0.00263	0.00203

The actual bus impedance matrix and the estimated bus impedance matrix of the IEEE 24-bus power system are mentioned in the Table 5.6 and Table 5.7 respectively. The actual and the estimated Thevenin impedances of the IEEE 24-bus power system are mentioned in the Table 5.8. The errors of the algorithm are plotted in the Figure 5.4.

Table 5.6 – Actual bus impedance matrix of the IEEE 24-bus power system.

Bus No	1	2	3	4	5	6	7	8	9	10	11	12	13	14	15	16	17	18	19	20	21	22	23	24
1	0.0117-0.1914i	0.0105-0.1975i	-0.0003-0.2358i	0.0039-0.2218i	0.0052-0.2166i	0.0005-0.2345i	-0.0017-0.2431i	-0.0017-0.243i	-0.0013-0.241i	-0.0015-0.2425i	-0.0015-0.243i	-0.0015-0.2425i	-0.0018-0.245i	-0.0021-0.2473i	-0.0024-0.2502i	-0.0024-0.2505i	-0.0027-0.2523i	-0.0027-0.2525i	-0.0025-0.2505i	-0.0024-0.2499i	-0.0027-0.2524i	-0.0029-0.2543i	-0.0024-0.2493i	-0.0011-0.2426i
2	0.0105-0.1975i	0.0118-0.1905i	-0.0005-0.2372i	0.0045-0.2184i	0.0046-0.2198i	0.0008-0.2329i	-0.0017-0.2429i	-0.0017-0.2428i	-0.0013-0.2405i	-0.0015-0.2427i	-0.0015-0.243i	-0.0015-0.2425i	-0.0018-0.2451i	-0.0021-0.2475i	-0.0024-0.2507i	-0.0025-0.2508i	-0.0028-0.2527i	-0.0028-0.2529i	-0.0025-0.2507i	-0.0025-0.2501i	-0.0028-0.2529i	-0.003-0.2547i	-0.0024-0.2495i	-0.0013-0.2433i
3	-0.0003-0.2358i	-0.0005-0.2372i	0.0101-0.1842i	-0.0003-0.2339i	-0.0011-0.2426i	-0.0022-0.2492i	-0.0012-0.2411i	-0.0012-0.241i	0.0001-0.2304i	-0.0017-0.2491i	-0.0001-0.2352i	-0.0003-0.2362i	-0.0002-0.2368i	0.0008-0.2342i	0.0026-0.2291i	0.0017-0.2325i	0.0018-0.2331i	0.0019-0.2327i	0.0011-0.2349i	0.0006-0.2364i	0.002-0.2322i	0.0017-0.2343i	0.0003-0.2369i	0.0065-0.2103i
4	0.0039-0.2218i	0.0045-0.2184i	-0.0003-0.2339i	0.0175-0.1648i	0.0015-0.2328i	-0.0004-0.2405i	-0.2353i	-0.2351i	0.0015-0.2241i	-0.0009-0.2438i	-0.2358i	0.0001-0.2353i	-0.0003-0.2379i	-0.0007-0.2406i	-0.0013-0.2444i	-0.0012-0.2443i	-0.0015-0.2462i	-0.0015-0.2464i	-0.0012-0.244i	-0.0011-0.2432i	-0.0015-0.2464i	-0.0018-0.2482i	-0.0009-0.2425i	-0.0005-0.2382i
5	0.0052-0.2166i	0.0046-0.2198i	-0.0011-0.2426i	0.0015-0.2328i	0.0139-0.1818i	0.0006-0.2328i	-0.0006-0.2393i	-0.0006-0.2392i	-0.0008-0.2427i	0.0002-0.2333i	-0.0006-0.2404i	-0.0005-0.2397i	-0.0009-0.2425i	-0.0014-0.2458i	-0.002-0.2504i	-0.0019-0.2499i	-0.0022-0.252i	-0.0023-0.2523i	-0.0019-0.2494i	-0.0017-0.2484i	-0.0023-0.2523i	-0.0025-0.2541i	-0.0016-0.2476i	-0.0013-0.2451i
6	0.0005-0.2345i	0.0008-0.2329i	-0.0022-0.2492i	-0.0004-0.2405i	0.0006-0.2328i	0.0113-0.1874i	-0.0006-0.2396i	-0.0005-0.2395i	-0.0011-0.246i	0.0007-0.2306i	-0.0006-0.2414i	-0.0005-0.2405i	-0.0009-0.2436i	-0.0016-0.2475i	-0.0025-0.2531i	-0.0023-0.2523i	-0.0026-0.2545i	-0.0027-0.2549i	-0.0021-0.2515i	-0.0019-0.2502i	-0.0027-0.255i	-0.0029-0.2567i	-0.0018-0.2492i	-0.0021-0.2493i
7	-0.0017-0.2431i	-0.0017-0.2429i	-0.0012-0.2411i	-0.2353i	-0.0006-0.2393i	-0.0006-0.2396i	0.0383-0.0884i	0.0224-0.1498i	0.0015-0.2282i	0.0006-0.2349i	0.0006-0.2345i	0.0008-0.2337i	0.0003-0.2366i	-0.0003-0.2403i	-0.0012-0.2456i	-0.001-0.2449i	-0.0013-0.247i	-0.0014-0.2473i	-0.0008-0.2441i	-0.0006-0.2429i	-0.0014-0.2474i	-0.0016-0.2491i	-0.0005-0.242i	-0.0009-0.2416i
8	-0.0017-0.243i	-0.0017-0.2428i	-0.0012-0.241i	-0.2351i	-0.0006-0.2392i	-0.0005-0.2395i	0.0224-0.1498i	0.0224-0.1497i	0.0016-0.2281i	0.0007-0.2348i	0.0007-0.2344i	0.0008-0.2335i	0.0004-0.2365i	-0.0002-0.2402i	-0.0011-0.2454i	-0.001-0.2447i	-0.0013-0.2468i	-0.0013-0.2472i	-0.0008-0.244i	-0.0006-0.2428i	-0.0014-0.2473i	-0.0016-0.249i	-0.0004-0.2418i	-0.0009-0.2415i
9	-0.0013-0.241i	-0.0013-0.2405i	0.0001-0.2304i	0.0015-0.2241i	-0.0008-0.2427i	-0.0011-0.246i	0.0015-0.2282i	0.0016-0.2281i	0.0039-0.21i	-0.0002-0.2439i	0.0014-0.2292i	0.0015-0.2286i	0.0012-0.2312i	0.0007-0.2342i	-0.0001-0.2385i	0.2381i	-0.0003-0.2401i	-0.0003-0.2403i	0.0001-0.2377i	0.0003-0.2368i	-0.0003-0.2404i	-0.0005-0.2421i	0.0005-0.236i	0.0003-0.2332i
10	-0.0015-0.2425i	-0.0015-0.2427i	-0.0017-0.2491i	-0.0009-0.2438i	0.0002-0.2333i	0.0007-0.2306i	0.0006-0.2349i	0.0007-0.2348i	-0.0002-0.2439i	0.0021-0.2232i	0.0005-0.2372i	0.0006-0.2361i	0.0002-0.2394i	-0.0005-0.2436i	-0.0015-0.2499i	-0.0013-0.2488i	-0.0016-0.2511i	-0.0017-0.2515i	-0.0011-0.2478i	-0.0009-0.2464i	-0.0017-0.2517i	-0.0019-0.2534i	-0.0007-0.2452i	-0.0014-0.2473i
11	-0.0015-0.243i	-0.0015-0.243i	-0.0001-0.2352i	-0.2358i	-0.0006-0.2404i	-0.0006-0.2414i	0.0006-0.2345i	0.0007-0.2344i	0.0014-0.2292i	0.0005-0.2372i	0.0021-0.2071i	0.0006-0.2245i	0.001-0.2188i	0.0009-0.2175i	-0.0003-0.2282i	-0.0001-0.2264i	-0.0004-0.2288i	-0.0004-0.2293i	-0.0001-0.2267i	0.2264i	-0.0005-0.2295i	-0.0007-0.231i	0.0001-0.2259i	-0.0002-0.2287i
12	-0.0015-0.2425i	-0.0015-0.2425i	-0.0003-0.2362i	0.0001-0.2353i	-0.0005-0.2397i	-0.0005-0.2405i	0.0008-0.2337i	0.0008-0.2335i	0.0015-0.2286i	0.0006-0.2361i	0.0006-0.2245i	0.0023-0.2046i	0.0011-0.217i	-0.2281i	-0.0006-0.2321i	-0.0005-0.2306i	-0.0008-0.2329i	-0.0008-0.2334i	-0.0001-0.2274i	0.0002-0.2243i	-0.0008-0.2336i	-0.001-0.2351i	0.0004-0.2222i	-0.0005-0.2315i
13	-0.0018-0.245i	-0.0018-0.2451i	-0.0002-0.2368i	-0.0003-0.2379i	-0.0009-0.2425i	-0.0009-0.2436i	0.0003-0.2366i	0.0004-0.2365i	0.0012-0.2312i	0.0002-0.2394i	0.001-0.2188i	0.0011-0.217i	0.0033-0.2002i	0.0004-0.2235i	-0.0003-0.229i	-0.0001-0.2271i	-0.0004-0.2295i	-0.0004-0.23i	0.0003-0.224i	0.0007-0.2209i	-0.0005-0.2303i	-0.0007-0.2317i	0.0009-0.2189i	-0.0003-0.2298i
14	-0.0021-0.2473i	-0.0021-0.2475i	0.0008-0.2342i	-0.0007-0.2406i	-0.0014-0.2458i	-0.0016-0.2475i	-0.0003-0.2403i	-0.0002-0.2402i	0.0007-0.2342i	-0.0005-0.2436i	0.0009-0.2175i	-0.2281i	0.0004-0.2235i	0.0039-0.1958i	0.0013-0.2166i	0.0017-0.2138i	0.0014-0.2164i	0.0013-0.2171i	0.0012-0.2179i	0.0008-0.221i	0.0012-0.2175i	0.0011-0.2187i	0.0006-0.2223i	0.0008-0.2211i
15	-0.0024-0.2502i	-0.0024-0.2507i	0.0026-0.2291i	-0.0013-0.2444i	-0.002-0.2504i	-0.0025-0.2531i	-0.0012-0.2456i	-0.0011-0.2454i	-0.0001-0.2385i	-0.0015-0.2499i	-0.0003-0.2282i	-0.0006-0.2321i	-0.0003-0.229i	0.0013-0.2166i	0.0042-0.1954i	0.0029-0.2051i	0.0032-0.2032i	0.0034-0.2018i	0.002-0.2123i	0.0012-0.2181i	0.0036-0.2003i	0.0033-0.203i	0.0008-0.2209i	0.0029-0.2061i
16	-0.0024-0.2505i	-0.0025-0.2508i	0.0017-0.2325i	-0.0012-0.2443i	-0.0019-0.2499i	-0.0023-0.2523i	-0.001-0.2449i	-0.001-0.2447i	0.2381i	-0.0013-0.2488i	-0.0001-0.2264i	-0.0005-0.2306i	-0.0001-0.2271i	0.0017-0.2138i	0.0029-0.2051i	0.0034-0.2014i	0.0031-0.2042i	0.003-0.205i	0.0024-0.2091i	0.0016-0.2152i	0.0029-0.2056i	0.0028-0.2066i	0.0012-0.2182i	0.0019-0.2134i
17	-0.0027-0.2523i	-0.0028-0.2527i	0.0018-0.2331i	-0.0015-0.2462i	-0.0022-0.252i	-0.0026-0.2545i	-0.0013-0.247i	-0.0013-0.2468i	-0.0003-0.2401i	-0.0016-0.2511i	-0.0004-0.2288i	-0.0008-0.2329i	-0.0004-0.2295i	0.0014-0.2164i	0.0032-0.2032i	0.0031-0.2042i	0.0051-0.1885i	0.0046-0.1929i	0.002-0.2118i	0.0012-0.2179i	0.0041-0.1966i	0.0043-0.1949i	0.0008-0.2209i	0.0021-0.2124i
18	-0.0027-0.2525i	-0.0028-0.2529i	0.0019-0.2327i	-0.0015-0.2464i	-0.0023-0.2523i	-0.0027-0.2549i	-0.0014-0.2473i	-0.0013-0.2472i	-0.0003-0.2403i	-0.0017-0.2515i	-0.0004-0.2293i	-0.0008-0.2334i	-0.0004-0.23i	0.0013-0.2171i	0.0034-0.2018i	0.003-0.205i	0.0046-0.1929i	0.0055-0.1856i	0.002-0.2126i	0.0012-0.2185i	0.0047-0.1918i	0.0045-0.1937i	0.0008-0.2215i	0.0022-0.2114i
19	-0.0025-0.2505i	-0.0025-0.2507i	0.0011-0.2349i	-0.0012-0.244i	-0.0019-0.2494i	-0.0021-0.2515i	-0.0008-0.2441i	-0.0008-0.244i	0.0001-0.2377i	-0.0011-0.2478i	-0.0001-0.2267i	-0.0001-0.2274i	0.0003-0.224i	0.0012-0.2179i	0.002-0.2123i	0.0024-0.2091i	0.002-0.2118i	0.002-0.2126i	0.004-0.1964i	0.0029-0.205i	0.0019-0.213i	0.0018-0.2142i	0.0023-0.2094i	0.0012-0.2187i
20	-0.0024-0.2499i	-0.0025-0.2501i	0.0006-0.2364i	-0.0011-0.2432i	-0.0017-0.2484i	-0.0019-0.2502i	-0.0006-0.2429i	-0.0006-0.2428i	0.0003-0.2368i	-0.0009-0.2464i	0.2264i	0.0002-0.2243i	0.0007-0.2209i	0.0008-0.221i	0.0012-0.2181i	0.0016-0.2152i	0.0012-0.2179i	0.0012-0.2185i	0.0029-0.205i	0.004-0.1958i	0.0011-0.219i	0.001-0.2202i	0.0033-0.2014i	0.0007-0.2229i
21	-0.0027-0.2524i	-0.0028-0.2529i	0.002-0.2322i	-0.0015-0.2464i	-0.0023-0.2523i	-0.0027-0.255i	-0.0014-0.2474i	-0.0014-0.2473i	-0.0003-0.2404i	-0.0017-0.2517i	-0.0005-0.2295i	-0.0008-0.2336i	-0.0005-0.2303i	0.0012-0.2175i	0.0036-0.2003i	0.0029-0.2056i	0.0041-0.1966i	0.0047-0.1918i	0.0019-0.213i	0.0011-0.219i	0.0053-0.1873i	0.0047-0.1924i	0.0007-0.2219i	0.0024-0.2103i
22	-0.0029-0.2543i	-0.003-0.2547i	0.0017-0.2343i	-0.0018-0.2482i	-0.0025-0.2541i	-0.0029-0.2567i	-0.0016-0.2491i	-0.0016-0.249i	-0.0005-0.2421i	-0.0019-0.2534i	-0.0007-0.231i	-0.001-0.2351i	-0.0007-0.2317i	0.0011-0.2187i	0.0033-0.203i	0.0028-0.2066i	0.0043-0.1949i	0.0045-0.1937i	0.0018-0.2142i	0.001-0.2202i	0.0047-0.1924i	0.0098-0.1533i	0.0005-0.2232i	0.0021-0.2127i
23	-0.0024-0.2493i	-0.0024-0.2495i	0.0003-0.2369i	-0.0009-0.2425i	-0.0016-0.2476i	-0.0018-0.2492i	-0.0005-0.242i	-0.0004-0.2418i	0.0005-0.236i	-0.0007-0.2452i	0.0001-0.2259i	0.0004-0.2222i	0.0009-0.2189i	0.0006-0.2223i	0.0008-0.2209i	0.0012-0.2182i	0.0008-0.2209i	0.0008-0.2215i	0.0023-0.2094i	0.0033-0.2014i	0.0007-0.2219i	0.0005-0.2232i	0.0039-0.1967i	0.0004-0.2248i
24	-0.0011-0.2426i	-0.0013-0.2433i	0.0065-0.2103i	-0.0005-0.2382i	-0.0013-0.2451i	-0.0021-0.2493i	-0.0009-0.2416i	-0.0009-0.2415i	0.0003-0.2332i	-0.0014-0.2473i	-0.0002-0.2287i	-0.0005-0.2315i	-0.0003-0.2298i	0.0008-0.2211i	0.0029-0.2061i	0.0019-0.2134i	0.0021-0.2124i	0.0022-0.2114i	0.0012-0.2187i	0.0007-0.2229i	0.0024-0.2103i	0.0021-0.2127i	0.0004-0.2248i	0.0071-0.1736i

Table 5.7 – Bus Impedance matrix of the IEEE-24 bus power system estimated through Algorithm 5.1.

Bus No	1	2	3	4	5	6	7	8	9	10	11	12	13	14	15	16	17	18	19	20	21	22	23	24
1	0.0115-0.191i	0.0108-0.1971i	-0.0002-0.2354i	0.0042-0.2214i	0.0053-0.2159i	0.0007-0.2343i	-0.0017-0.2427i	-0.0015-0.2428i	-0.0012-0.2405i	-0.0012-0.242i	-0.0018-0.2425i	-0.0018-0.2431i	-0.0016-0.2447i	-0.0021-0.2469i	-0.0022-0.2501i	-0.0025-0.2503i	-0.0026-0.252i	-0.0026-0.2522i	-0.0025-0.2502i	-0.0021-0.2497i	-0.0023-0.2522i	-0.0034-0.2539i	-0.0022-0.2491i	-0.0013-0.242i
2	0.0106-0.1968i	0.0121-0.1898i	-0.0001-0.2366i	0.0044-0.2176i	0.0044-0.2188i	0.0012-0.2323i	-0.0017-0.2422i	-0.0013-0.2423i	-0.001-0.2398i	-0.0011-0.2419i	-0.0014-0.2427i	-0.0013-0.2429i	-0.0015-0.2445i	-0.0019-0.2469i	-0.0023-0.2502i	-0.0022-0.2506i	-0.0026-0.2522i	-0.0025-0.2524i	-0.0026-0.2503i	-0.0024-0.2496i	-0.0023-0.2524i	-0.0031-0.2547i	-0.0022-0.2488i	-0.0008-0.2426i
3	-0.0005-0.2353i	-0.0006-0.2368i	0.0099-0.1837i	-0.0004-0.2332i	-0.0016-0.2419i	-0.0024-0.2488i	-0.0016-0.2406i	-0.0015-0.2407i	0.2298i	-0.0018-0.2486i	-0.0004-0.235i	-0.0009-0.2368i	-0.0003-0.2364i	0.0007-0.2338i	0.0025-0.2287i	0.0015-0.2322i	0.0017-0.2327i	0.0018-0.2322i	0.0009-0.2346i	0.0002-0.236i	0.0021-0.2318i	0.001-0.2339i	0.0002-0.2365i	0.0071-0.2101i
4	0.004-0.221i	0.005-0.2177i	-0.0002-0.2332i	0.0175-0.164i	0.0016-0.2317i	-0.0003-0.24i	0.0001-0.2346i	0.0001-0.2346i	0.0019-0.2234i	-0.0006-0.243i	0.0003-0.2353i	-0.2359i	0.2373i	-0.0005-0.24i	-0.0011-0.2438i	-0.001-0.2438i	-0.0012-0.2456i	-0.0013-0.2458i	-0.0012-0.2434i	-0.0011-0.2426i	-0.0011-0.2459i	-0.0021-0.2474i	-0.0007-0.2418i	-0.0003-0.2371i
5	0.0053-0.2163i	0.0046-0.2195i	-0.0012-0.2423i	0.0012-0.2324i	0.0139-0.1812i	0.0007-0.2326i	-0.001-0.2389i	-0.0005-0.2389i	-0.0008-0.2422i	0.0004-0.2329i	-0.0008-0.2402i	-0.0011-0.2402i	-0.0009-0.2423i	-0.0014-0.2455i	-0.0019-0.2503i	-0.002-0.25i	-0.0023-0.2518i	-0.0022-0.252i	-0.0018-0.2493i	-0.0019-0.2482i	-0.0021-0.2521i	-0.0026-0.2541i	-0.0018-0.2473i	-0.0018-0.2443i
6	0.0008-0.234i	0.0011-0.2325i	-0.002-0.2488i	-0.2401i	0.0004-0.2321i	0.0113-0.1871i	-0.0005-0.2392i	-0.0002-0.2392i	-0.0006-0.2455i	0.0011-0.2301i	-0.0006-0.2411i	0.2411i	-0.0007-0.2433i	-0.0015-0.2471i	-0.0024-0.2529i	-0.0023-0.2521i	-0.0024-0.2543i	-0.0025-0.2546i	-0.0022-0.2512i	-0.0018-0.25i	-0.0023-0.2549i	-0.0032-0.2568i	-0.0019-0.2486i	-0.0025-0.2486i
7	-0.0019-0.2426i	-0.0015-0.2426i	-0.0014-0.2407i	-0.0005-0.2346i	-0.0007-0.2386i	-0.0009-0.2393i	0.0381-0.088i	0.0223-0.1494i	0.0015-0.2277i	0.0007-0.2344i	0.0003-0.2343i	0.0006-0.2341i	0.0003-0.2362i	-0.0005-0.2398i	-0.0012-0.2453i	-0.0013-0.2446i	-0.0014-0.2467i	-0.0015-0.2469i	-0.001-0.2438i	-0.0005-0.2427i	-0.0013-0.2471i	-0.0019-0.249i	-0.0006-0.2415i	-0.0013-0.2412i
8	-0.0021-0.2425i	-0.0017-0.2425i	-0.0015-0.2406i	-0.0004-0.2346i	-0.0009-0.2386i	-0.0009-0.2391i	0.0221-0.1495i	0.022-0.1495i	0.0013-0.2275i	0.0004-0.2343i	0.001-0.2344i	-0.2339i	0.0002-0.2361i	-0.0006-0.2397i	-0.0013-0.2452i	-0.0012-0.2446i	-0.0016-0.2465i	-0.0015-0.2468i	-0.0011-0.2437i	-0.0008-0.2425i	-0.0014-0.2469i	-0.0024-0.2483i	-0.0009-0.2414i	-0.0013-0.2407i
9	-0.0013-0.2403i	-0.0009-0.24i	-0.2298i	0.0017-0.2234i	-0.0011-0.2418i	-0.0011-0.2456i	0.0016-0.2277i	0.0017-0.2277i	0.004-0.2093i	-0.0001-0.2433i	0.0012-0.2289i	0.0019-0.2289i	0.0013-0.2307i	0.0006-0.2336i	-0.2381i	-0.2377i	-0.0003-0.2395i	-0.0002-0.2398i	0.0002-0.2373i	0.0001-0.2363i	-0.0001-0.2399i	-0.0011-0.2416i	0.0005-0.2354i	-0.0001-0.2324i
10	-0.0014-0.2419i	-0.0015-0.2421i	-0.0019-0.2486i	-0.0009-0.2432i	0.0002-0.2324i	0.0005-0.2302i	0.0008-0.2344i	0.0007-0.2344i	-0.0001-0.2433i	0.0021-0.2225i	0.0006-0.2367i	0.0008-0.2366i	0.0003-0.2389i	-0.0005-0.2431i	-0.0014-0.2495i	-0.0015-0.2484i	-0.0016-0.2507i	-0.0016-0.251i	-0.0011-0.2473i	-0.0008-0.2458i	-0.0014-0.2513i	-0.0026-0.2527i	-0.0006-0.2448i	-0.0009-0.2465i
11	-0.0018-0.2425i	-0.0018-0.2427i	-0.0003-0.2349i	-0.0003-0.2354i	-0.001-0.2397i	-0.0009-0.2411i	0.0004-0.2342i	0.0003-0.2343i	0.0012-0.2288i	0.0002-0.2368i	0.0019-0.207i	0.0005-0.2253i	0.0007-0.2184i	0.0006-0.2171i	-0.0004-0.228i	-0.0006-0.2263i	-0.0007-0.2284i	-0.0007-0.2289i	-0.0005-0.2263i	-0.0003-0.2261i	-0.0005-0.2291i	-0.0012-0.231i	-0.0001-0.2255i	-0.0004-0.2283i
12	-0.0013-0.2421i	-0.0013-0.2421i	-0.0002-0.2359i	0.0004-0.2346i	-0.0004-0.2389i	-0.0003-0.2401i	0.0007-0.2332i	0.0011-0.2331i	0.0017-0.228i	0.001-0.2356i	0.0007-0.2242i	0.002-0.205i	0.0013-0.2166i	0.0001-0.2277i	-0.0005-0.2319i	-0.0005-0.2304i	-0.0006-0.2327i	-0.0007-0.233i	0.0001-0.2272i	0.0003-0.224i	-0.0003-0.2334i	-0.0013-0.2349i	0.0005-0.2219i	-0.0006-0.2308i
13	-0.0022-0.2444i	-0.0021-0.2445i	-0.0004-0.2363i	-0.0007-0.2372i	-0.0012-0.2415i	-0.0012-0.2431i	-0.236i	0.0002-0.236i	0.001-0.2305i	0.0002-0.2386i	0.001-0.2183i	0.0012-0.2177i	0.0033-0.1996i	0.0002-0.2229i	-0.0003-0.2285i	-0.0003-0.2267i	-0.0004-0.229i	-0.0006-0.2294i	0.0002-0.2236i	0.0007-0.2204i	-0.0003-0.2298i	-0.0007-0.2316i	0.0007-0.2183i	-0.0006-0.2289i
14	-0.0025-0.247i	-0.0023-0.2473i	0.0005-0.2341i	-0.0012-0.2404i	-0.0017-0.2452i	-0.0018-0.2474i	-0.0004-0.2402i	-0.0006-0.2402i	0.0004-0.234i	-0.0007-0.2434i	0.0007-0.2175i	-0.0008-0.2287i	0.0002-0.2233i	0.0035-0.1955i	0.0011-0.2165i	0.0014-0.2137i	0.0011-0.2163i	0.0011-0.2169i	0.0007-0.2178i	0.0007-0.2208i	0.001-0.2172i	0.0003-0.2185i	0.0003-0.2222i	0.0008-0.2208i
15	-0.0025-0.2501i	-0.0023-0.2505i	0.0025-0.229i	-0.0012-0.244i	-0.0019-0.2497i	-0.0026-0.2531i	-0.0014-0.2455i	-0.0012-0.2454i	-0.0001-0.2382i	-0.0016-0.2497i	-0.0006-0.2281i	-0.0012-0.2326i	-0.0003-0.2289i	0.0014-0.2165i	0.0042-0.1954i	0.0029-0.205i	0.0032-0.2031i	0.0034-0.2016i	0.0018-0.2123i	0.0012-0.218i	0.0037-0.2003i	0.0027-0.2029i	0.0006-0.2207i	0.0029-0.2056i
16	-0.0022-0.25i	-0.0023-0.2505i	0.0016-0.2322i	-0.0018-0.2442i	-0.0021-0.2493i	-0.0024-0.2521i	-0.0013-0.2446i	-0.001-0.2444i	-0.0001-0.2377i	-0.0013-0.2484i	-0.0001-0.2261i	-0.0011-0.2313i	-0.0001-0.2268i	0.0015-0.2134i	0.0029-0.2048i	0.0031-0.2011i	0.003-0.2039i	0.003-0.2047i	0.0022-0.2088i	0.0016-0.2149i	0.003-0.2053i	0.0018-0.2062i	0.001-0.2179i	0.0022-0.2128i
17	-0.0026-0.2519i	-0.0026-0.2524i	0.0018-0.2329i	-0.0018-0.2461i	-0.0023-0.2513i	-0.0024-0.2542i	-0.0018-0.2469i	-0.0014-0.2467i	-0.0001-0.2396i	-0.0016-0.2507i	-0.0005-0.2284i	-0.0011-0.2336i	-0.0003-0.2292i	0.0014-0.2162i	0.0034-0.2031i	0.0029-0.204i	0.0051-0.1883i	0.0047-0.1926i	0.0019-0.2117i	0.0011-0.2177i	0.0043-0.1964i	0.0032-0.1945i	0.0008-0.2206i	0.0018-0.2119i
18	-0.0026-0.2517i	-0.0027-0.2524i	0.0019-0.2322i	-0.0017-0.2459i	-0.0023-0.2515i	-0.0028-0.2545i	-0.0015-0.2468i	-0.0013-0.2466i	-0.0003-0.2396i	-0.0017-0.2509i	-0.0007-0.2289i	-0.0013-0.2341i	-0.0004-0.2296i	0.0011-0.2166i	0.0033-0.2014i	0.003-0.2047i	0.0044-0.1924i	0.0055-0.1851i	0.0017-0.2122i	0.0009-0.2182i	0.0048-0.1913i	0.0038-0.1933i	0.0005-0.2211i	0.002-0.2106i
19	-0.0029-0.2497i	-0.0026-0.25i	0.001-0.2342i	-0.0014-0.2431i	-0.0021-0.2483i	-0.0023-0.2508i	-0.0011-0.2435i	-0.001-0.2434i	0.0003-0.2368i	-0.0012-0.247i	-0.0001-0.2262i	-0.0006-0.228i	0.0003-0.2234i	0.001-0.2173i	0.0019-0.2118i	0.0023-0.2086i	0.0018-0.2111i	0.0019-0.2119i	0.0037-0.1959i	0.0027-0.2044i	0.0021-0.2124i	0.0012-0.2136i	0.0022-0.2087i	0.0015-0.2176i
20	-0.0028-0.2495i	-0.0029-0.2498i	0.0001-0.2361i	-0.002-0.243i	-0.0026-0.248i	-0.0026-0.2501i	-0.001-0.2427i	-0.0011-0.2427i	-0.0002-0.2363i	-0.0013-0.2459i	-0.0004-0.2263i	-0.0005-0.2249i	0.0003-0.2206i	0.0001-0.2206i	0.0008-0.2177i	0.0014-0.2151i	0.0007-0.2174i	0.0008-0.2181i	0.0022-0.2048i	0.0036-0.1956i	0.0006-0.2184i	0.0003-0.2199i	0.0028-0.201i	0.0003-0.2223i
21	-0.003-0.2521i	-0.0029-0.2525i	0.002-0.2317i	-0.0014-0.2456i	-0.0025-0.2516i	-0.0028-0.2547i	-0.0014-0.247i	-0.0014-0.247i	-0.0005-0.24i	-0.0017-0.2512i	-0.0009-0.2295i	-0.0017-0.2344i	-0.0006-0.23i	0.0012-0.2171i	0.0035-0.2001i	0.0029-0.2054i	0.0039-0.1963i	0.0046-0.1914i	0.0017-0.2128i	0.0009-0.2188i	0.0054-0.187i	0.0044-0.1922i	0.0003-0.2215i	0.0027-0.2094i
22	-0.003-0.2537i	-0.0029-0.2541i	0.0017-0.2338i	-0.002-0.2477i	-0.0028-0.2534i	-0.003-0.2565i	-0.0019-0.2487i	-0.0017-0.2486i	-0.0005-0.2414i	-0.0019-0.2529i	-0.001-0.2307i	-0.0023-0.2358i	-0.0007-0.2313i	0.0009-0.2183i	0.0032-0.2026i	0.0026-0.2063i	0.0042-0.1945i	0.0044-0.1932i	0.0015-0.2139i	0.0008-0.2198i	0.0047-0.192i	0.01-0.1531i	0.0005-0.2227i	0.0021-0.2122i
23	-0.0028-0.2491i	-0.0024-0.2492i	0.0001-0.2368i	-0.0012-0.2421i	-0.0019-0.2471i	-0.0021-0.2492i	-0.001-0.2418i	-0.0006-0.2417i	0.0003-0.2357i	-0.0008-0.245i	-0.0002-0.2259i	-0.0001-0.2233i	0.0008-0.2187i	0.0004-0.2222i	0.0006-0.2208i	0.0011-0.2184i	0.0007-0.2207i	0.0005-0.2212i	0.002-0.2093i	0.0029-0.2013i	0.0006-0.2216i	0.0004-0.2233i	0.0037-0.1966i	0.0002-0.2242i
24	-0.0014-0.2419i	-0.0014-0.2428i	0.0064-0.2098i	-0.0008-0.2376i	-0.0014-0.2441i	-0.0022-0.2488i	-0.001-0.241i	-0.0011-0.2411i	0.0002-0.2325i	-0.0015-0.2466i	-0.0007-0.2283i	-0.0017-0.2318i	-0.0004-0.2292i	0.0006-0.2206i	0.0028-0.2057i	0.0019-0.2129i	0.0021-0.212i	0.0022-0.2108i	0.0008-0.2183i	0.0007-0.2223i	0.0024-0.2098i	0.0014-0.2121i	0.0002-0.2243i	0.0075-0.173i

Table 5.8 – Actual Thevenin impedances of the IEEE 24-bus power system along with the impedances estimated through Algorithm 5.1.

Bus No.	Thevenin Impedance		% Error
	Actual	Computed	
1	0.0117 - 0.1914i	0.0115 - 0.191i	0.248
2	0.0118 - 0.1905i	0.0121 - 0.1898i	0.401
3	0.0101 - 0.1842i	0.0099 - 0.1837i	0.2714
4	0.0175 - 0.1648i	0.0175 - 0.164i	0.4772
5	0.0139 - 0.1818i	0.0139 - 0.1812i	0.3335
6	0.0113 - 0.1874i	0.0113 - 0.1871i	0.1371
7	0.0383 - 0.0884i	0.0381 - 0.088i	0.454
8	0.0224 - 0.1497i	0.022 - 0.1495i	0.2918
9	0.0039 - 0.21i	0.004 - 0.2093i	0.3337
10	0.0021 - 0.2232i	0.0021 - 0.2225i	0.306
11	0.0021 - 0.2071i	0.0019 - 0.207i	0.0926
12	0.0023 - 0.2046i	0.002 - 0.205i	0.2494
13	0.0033 - 0.2002i	0.0033 - 0.1996i	0.2752
14	0.0039 - 0.1958i	0.0035 - 0.1955i	0.2149
15	0.0042 - 0.1954i	0.0042 - 0.1954i	0.022
16	0.0034 - 0.2014i	0.0031 - 0.2011i	0.1978
17	0.0051 - 0.1885i	0.0051 - 0.1883i	0.0939
18	0.0055 - 0.1856i	0.0055 - 0.1851i	0.2728
19	0.004 - 0.1964i	0.0037 - 0.1959i	0.2891
20	0.004 - 0.1958i	0.0036 - 0.1956i	0.2358
21	0.0053 - 0.1873i	0.0054 - 0.187i	0.1548
22	0.0098 - 0.1533i	0.01 - 0.1531i	0.2015
23	0.0039 - 0.1967i	0.0037 - 0.1966i	0.0991
24	0.0071 - 0.1736i	0.0075 - 0.173i	0.4247

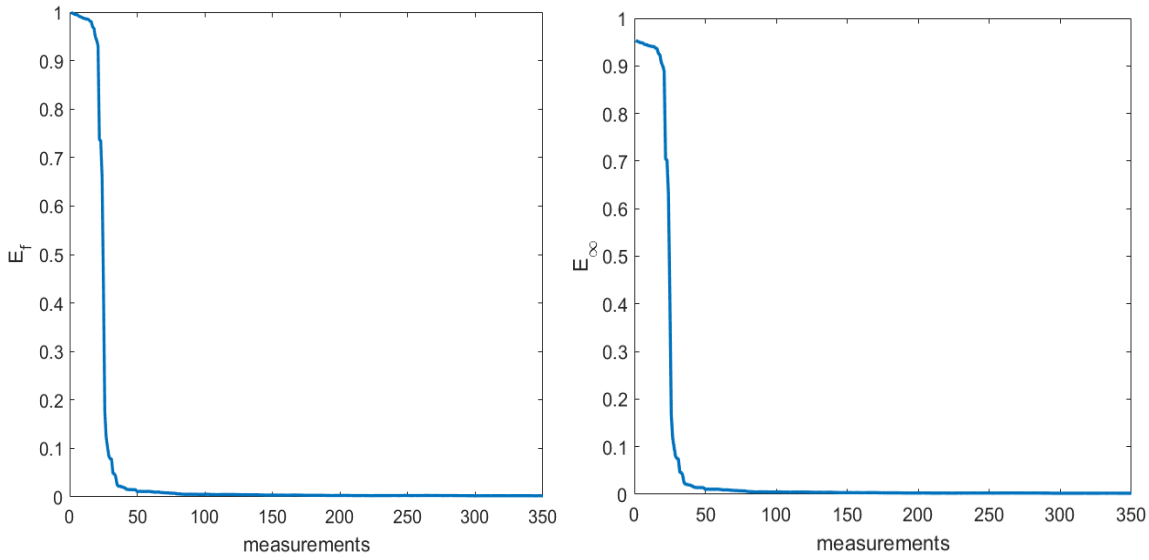

Figure 5.4 – Errors in the bus impedance matrix estimated through Algorithm 5.1 for the IEEE 24-bus power system.

The histogram showing the number of estimated parameters falling within certain error ranges is shown in the histogram of Figure 5.5. All the estimated impedances have errors less than 1%.

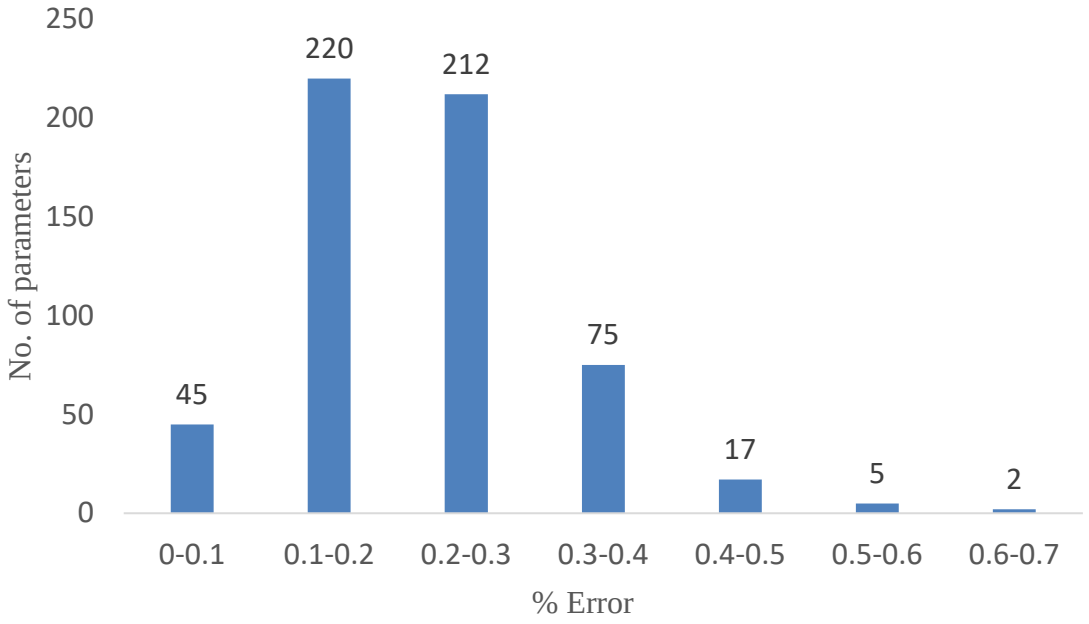

Figure 5.5 - Number of estimated parameters within various % error ranges for the IEEE 14-bus power system.

5.3.3 IEEE 30-bus system

The system has generators connected at buses 1, 2, 22, 27, 23 and the slack bus as 13. The system has 41 branches and 30 buses. The parameters and the connection information are provided in the appendix. The algorithm of the 5.2.1 is executed on the system and the errors are plotted in Figure 5.6.

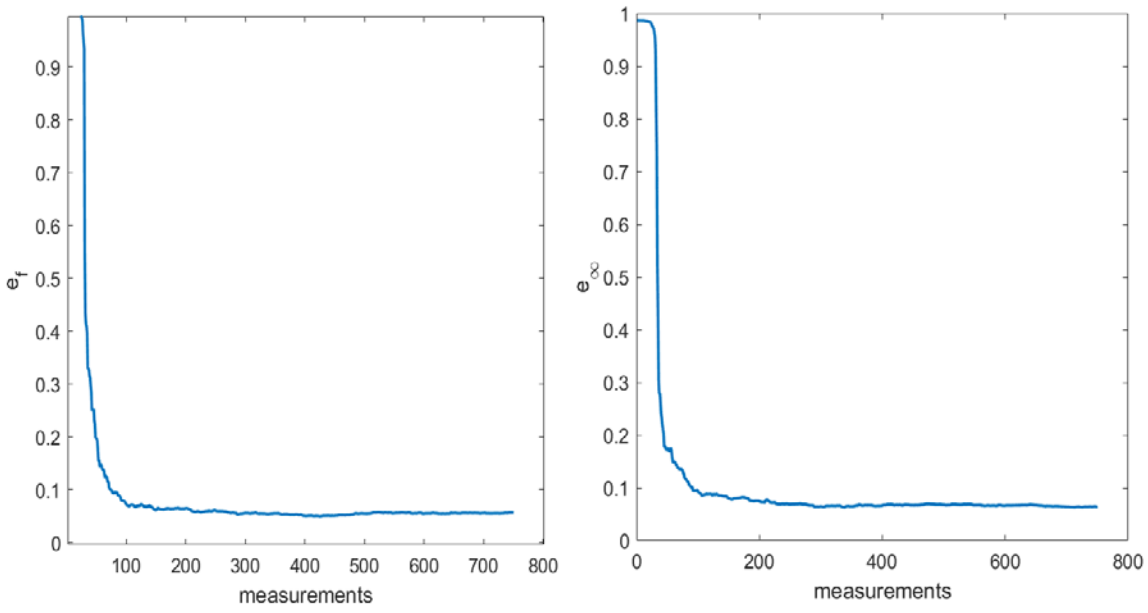

Figure 5.6 – Plot of the errors in the bus impedance matrix estimated through Algorithm 5.1 for the IEEE 30-bus power system.

The values of error at various number of measurements is tabulated in Table 5.9.

Table 5.9 - Errors in the bus impedance matrix estimated through Algorithm 5.1 at various number of measurements for the IEEE 30-bus power system.

No. of sets of measurements	**50**	**150**	**250**	**350**	**450**	**550**	**650**	**750**
e_f	0.2089	0.0725	0.0650	0.0702	0.0677	0.0639	0.0627	0.0630
e_∞	0.2062	0.0716	0.0642	0.0693	0.0669	0.0631	0.0619	0.0622

5.3.4 IEEE 118-bus system

The system has generators connected at 54 of its buses and the slack bus number is 69. The system has 186 branches and 118 buses. The parameters and the connection information are provided in the appendix.

The algorithm of the section 5.2.1 is executed on the system and the errors are plotted in Figure 5.7.

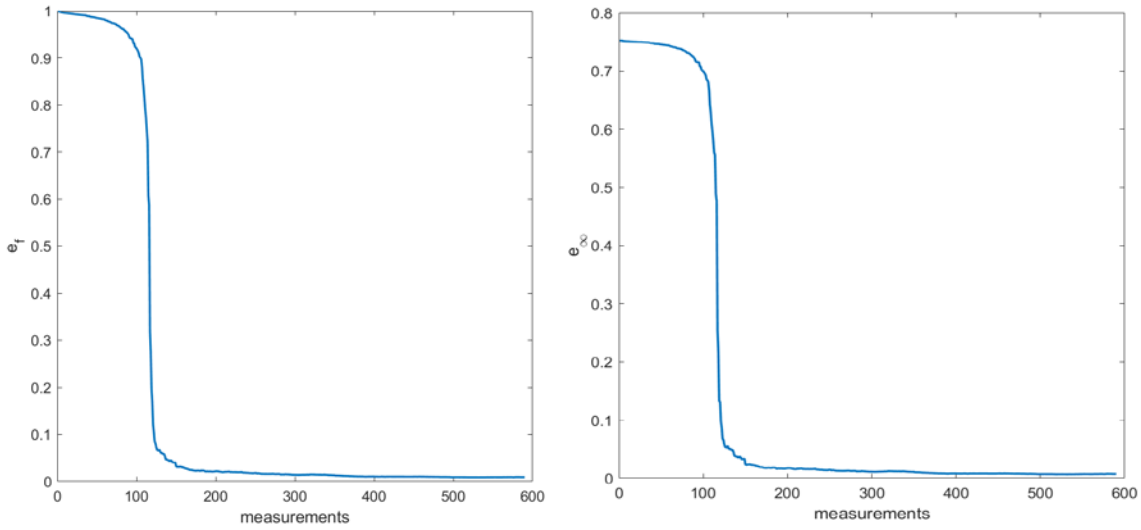

Figure 5.7 - Plot of the errors in the bus impedance matrix estimated through Algorithm 5.1 for the IEEE 118-bus power system.

The values of errors at various number of measurements are tabulated in Table 5.10.

Table 5.10 - Errors in the bus impedance matrix estimated through Algorithm 5.1 at various number of measurements for the IEEE 118-bus power system.

No. of sets of measurements	**50**	**150**	**250**	**350**	**450**	**550**
e_f	0.9845	0.0321	0.0176	0.0131	0.0101	0.0089
e_∞	0.7456	0.0246	0.0143	0.0108	0.0081	0.0070

5.4 Estimation of network parameters using Z_{bus}

Once the estimate of the bus impedance matrix is obtained, the parameters of the components of the corresponding power system can be obtained through the evaluation of the columns of the bus admittance matrix by using the triangular factors. The detailed steps are mentioned below

1. Evaluate the LU factors of the bus impedance matrix.
2. To evaluate the i^{th} column of the bus admittance matrix, solve the system $LUx = e_i$ by following steps
    i. Solve $Ly = e_i$ for y.
    ii. Solve $Ux = y$ for x.

The x obtained in the last step corresponds to the i^{th} column of the bus admittance matrix. In the following example the parameters of the branches connected with the bus 75 of the IEEE 118-bus power system are evaluated by using the above algorithm, and the result is tabulated in the Table 5.11.

Table 5.11 – Computed and actual admittances of the branches connected with bus 75 of IEEE 118-bus power system

Branches	Admittances		$\%\ \mathbf{error} = \frac{\mathbf{abs}(\acute{y}_{ij} - y_{ij})}{\mathbf{abs}(y_{ij})} \times 100$
	Computed ($\acute{y}_{ij}$)	Actual (y_{ij})	
75-69	2.3747 - 7.3973i	2.4509 - 7.3831i	0.9974
75-70	2.2612 - 6.3534i	1.9712 - 6.4939i	4.7485
75-74	6.6881 -22.5628i	6.8347 -22.5599i	0.6218
75-77	1.1776 - 4.5516i	1.3793 - 4.5878i	4.2777

75-118	5.5664 -19.1163i	5.7452 -19.0581i	0.9444

5.5 Discussion

The approach of the current chapter is preferable if no prior estimates of the parameters of the elements of a power system is used. The algorithm converges quickly in comparison to the algorithm presented in chapter 2 of the thesis. The reason for the faster convergence is that the variations in the currents flowing in power system branches due to changes in loads are larger compared to the variations in the voltages of the buses. Therefore, the condition number of the current measurement matrix is smaller compared to the voltage measurement matrix. This reduced condition number of the matrix that needs to be inverted results in more accurate results. If, however, good prior estimates of the parameters of a power system are available then by introducing the constraints or by using the vector optimization technique, presented in the chapter 3, the results with the same accuracy can be obtained.

As mentioned previously, one major application of the elements of a bus impedance matrix is the settings of the relays in the underlying power system. Therefore, if somehow the elements of the bus impedance matrix required for the settings of the corresponding relays are available at each bus, they can be used for the settings of the corresponding relays. For this purpose, a decentralized and distributed algorithm, that can update the elements of the bus impedance matrix with changes in the corresponding power system is better suited. In the next chapter, such an algorithm is presented.

CHAPTER 6. DECENTRALIZED ESTIMATION OF THE BUS IMPEDANCE MATRIX OF A POWER SYSTEM

6.1 Introduction

In this chapter, a distributed and decentralized scheme is presented for the estimation of the bus impedance matrix, Z_{bus} of a power system. The entries of Z_{bus} are used for performing various analyses (such as the contingency analysis and the fault analysis) in power system operations. Therefore, an accurate estimation of the bus impedance matrix is highly desired as the results from the fault analysis (the accuracy of which depends on the accuracy of the bus impedance matrix) are used in setting the relays of the power system.

The relays should be set in such a manner that the objectives of power system protection are satisfied. The main objectives of power system protection are selectivity, sensitivity and dependability [70]. Selectivity is the ability to take out only the minimum possible part of a power system for fault clearance, sensitivity is the capability to detect even the smallest of faults, and dependability is the ability of a protection system to act only if there is an actual fault (while neglecting all the temporary faults) on the power system. The current methods used for the settings of relays are such that sometimes the objectives of the power system protection are compromised [23].

The current method for the Z_{bus} evaluation uses the off-line models of the power system components. Such methods can cause errors [21] in the calculated elements of the Z_{bus}. These errors can then propagate into the results of the fault analysis that are used in the settings of the relays of the power system. The relays' settings are decided offline by

simulating the power system under a number of loading conditions for various system configurations [23]. Various faults are applied and the offline Z_{bus} is used to calculate the fault currents, and the worst-case fault is then used to set the relays. Once the relays are set, they are seldom updated to accommodate the actual state of the system [23]. These practices can sometimes result in settings that do not meet the objectives of the power system protection under certain conditions due to their inability to accommodate the changes in the power system.

The objectives of power system protection can be better satisfied if the settings of the relays are evaluated and decided using the measurement-based Z_{bus}. The measurement-based Z_{bus} will model a power system in its current operating condition, unlike the offline approach (currently used) which neglects any variability in the parameter values of power system components by using their offline values.

In this chapter, a measurement-based method for the estimation the bus impedance matrix is proposed. The method uses an iterative technique to converge to the Z_{bus} in a distributed and decentralized way. Such an approach is preferable for a complex systems like power systems [20], [71]. By utilizing the proposed technique, the measurement-based entries of the Z_{bus} will be available in near real-time at the respective buses which can be used by the corresponding relays to update their settings. Through these updated settings, the relays will be able to meet the objectives of power system protection in a better way.

The underlying theory and the proposed algorithm are presented in the section 6.2. The convergence of the algorithm is shown in section 6.3 where the algorithm is tested on various IEEE power systems.

6.2 Mathematical Theory

The basis of the proposed method is the Jacobi algorithm [34] for solving a system of equations, such as

$$Ax = b; \qquad A \in C^{n\times n}, \qquad x, b \in C^{n}. \tag{6.1}$$

Assuming an initial guess, x^{o} for the solution, the Jacobi algorithm iteratively solves for x by successively substituting the values of the components of x in

$$x_i^k = \frac{1}{a_{ii}}\left(b_i - \sum_{j=1\ j\neq i}^{n} a_{ij}x_j^{k-1}\right) \ ; \quad i = 1\ to\ n \tag{6.2}$$

where, x_i^k is the i^{th} component of the vector x at the k^{th} iteration, and a_{ii} is the i^{th} diagonal entry of the matrix, A. The solution (if it exists) to equation 6.1 is obtained by successively substituting the values of x in equation 6.2 from the previous iteration until convergence.

Note that the Jacobi algorithm lends itself quite naturally to parallel implementation because the evaluation of the components of x in equation 6.2 is not dependent on the sequencing of the equations [71].

As the Jacobi method is an iterative process, the system of equations to being solved needs to satisfy certain conditions for the iterations in equation 6.2 to converge. The necessary and sufficient conditions for the method to converge is that the matrix A should be absolutely-diagonally dominant; A is absolutely-diagonally dominant if its elements satisfy the condition,

$$|a_{ii}| > \sum_{j=1\ j\neq i}^{n} |a_{ij}| \ ; \ i = 1\ to\ n. \tag{6.3}$$

The iterations in equation 6.2 can be written in a compact matrix form as,

$$x^{k+1} = Px^k + D^{-1}b \tag{6.4}$$

where, $D = diag(A)$ and $P = D^{-1}(D - A)$. Modifying equation 6.1 for n systems of equations results in,

$$AX = B\ ; \qquad A, X, B \in C^{n \times n} \tag{6.5}$$

Note that all of the entries in equation 6.5 are square matrices of the dimension n. Updating equation 6.4 for the systems of equation 6.5 results in,

$$X^{k+1} = PX^k + D^{-1}B \tag{6.6}$$

The converged X in equation 6.6 is the solution (if it exists) to equation 6.5. Substituting the identity matrix for B in equation 6.5 gives,

$$AX = I\ ;\ \ A, X, I \in R^{n \times n} \tag{6.7}$$

where, I is the identity matrix. Then, the equation 6.6 will be updated as,

$$X^{k+1} = PX^k + D^{-1} \tag{6.8}$$

where P and D are the same as defined in equation 6.4. The fixed-point solution of equation 6.8, if it exists, will be the inverse of A. Replacing the matrix A by the Y_{bus} in equation 6.7 will update P to $D^{-1}(D - Y_{bus})$ and D to $diag(Y_{bus})$ in equation 6.8. As mentioned before, equation 6.8 is guaranteed to converge if the matrix, Y_{bus} is absolutely-diagonally dominant. The bus admittance matrix of a typical power system does not satisfy this condition [72]; however, under normal operating conditions, a power system is fully

connected[26], and therefore, the corresponding Y_{bus} is irreducible[27]. If the matrix is irreducible, then the condition for the convergence of the Jacobi iterations can be relaxed [62] to $|y_{ii}| \geq \sum_{j=1\ j\neq i}^{n} |y_{ij}|; i = 1\ to\ n$. The non-strict inequality should hold for at least one of the values of i. The charging capacitance of transmission lines are ignored in the fault calculations [35]. If the charging capacitance of the lines are ignored, as is done in our algorithm, the resulting bus impedance matrix will satisfy the equality condition for the convergence of iterations. If the impedances of the generators are modeled in a power system (as required in the fault calculations), then the inequality part of the condition is satisfied by at least one bus in the resulting Y_{bus} of the power system and the iterations of equation 6.8 will converge.

The converged result will be equal to the bus impedance matrix of the power system since Z_{bus} is the inverse of Y_{bus}. Therefore, from equation 6.8,

$$Z_{bus}^{k+1} = PZ_{bus}^{k} + D^{-1} \tag{6.9}$$

where $P = D^{-1}(D - Y_{bus})$ and $D = diag(Y_{bus})$. Note that the columns of the bus impedance matrix can be evaluated from equation 6.9 as

$$z_{bus,i}^{k+1} = Pz_{bus,i}^{k} + D^{-1}I_i \quad ; \quad i = 1\ to\ n \tag{6.10}$$

where, $z_{bus,i}$ is the i^{th} column of Z_{bus} and I_i is the i^{th} column of the identity matrix.

[26] A network (or graph) is fully connected if each node can be accessed through every other node by traversing along its branches (edges).

[27] A matrix A is irreducible [62] if there exists no permutation matrix P such that $P^T AP = \begin{bmatrix} X & Y \\ 0 & Z \end{bmatrix}$; where X and Z are both square.

If the system does not undergo a change, the matrices P and D^{-1} are defined only at the start of the iterations and remain unaltered thereafter. Therefore, the iterations for the columns of Z_{bus} in equation 6.10 can be carried out independently from one another. Owing to the decoupling of the equations, Z_{bus} can be evaluated in the time required to solve a single set of equations, provided we have enough processors.

For the implementation of the proposed algorithm, it is assumed that the voltage and current phasors are measured at all of the buses of the power system. It is noteworthy that in current power systems, these phasors are not measured at all of the buses. However, after taking into account the advantages of such measurements [36] and the impetus to install more PMUs [49], this assumption is likely to hold for future power systems [3].

Additionally, PMUs need not be installed at each bus of the power system for such an assumption to hold, as almost all modern relays also have the capability to measure voltage and current phasors [21], [32], [56]. Therefore, if these capabilities of the relays are put to use, then this assumption can hold even for many of the power systems currently in use.

The proposed strategy also assumes that each bus of the power system has an equipment to communicate with neighboring buses. Many modern numerical relays have this capability [21]. Additionally, each bus is also assumed to be equipped with a device that can store data and perform elementary calculations. Such devices have already been presented in [73], [74] where their economic and technical viabilities have been discussed. Moreover, in [75], they were used to better utilize the capacity of transmission lines by assessing their real-time condition. The combination of devices which provide the

abovementioned functions (of measurements, storage, elementary calculation and communication with adjoining devices) will be hereafter called an Intelligent Electronic Device (IED) [3].

Using their phasor measurements, the IEDs at the adjoining buses can calculate the admittance of the components connecting the buses as demonstrated in [12]. The results from these calculations are then stored in the respective IEDs. These admittance calculations are repeated after some pre-specified time interval and the results will replace the previous values stored in the IEDs only if the change in admittance is above a certain threshold. Each bus of the power system is identified by a unique number which is called its bus number. The connection information for each bus (the bus numbers of its neighboring buses) will also be stored in the IEDs. Given the connection information and the impedances of elements, the P and D matrices can be calculated and stored by the IEDs.

Note that P and D are highly sparse matrices and should be stored using sparsity techniques in order to reduce the storage requirements in the IEDs. Once stored, the matrices are updated whenever a change occurs in the power system. Any change in the power system will be communicated from the IEDs at the buses where the update took place, to the neighboring IEDs which will update their matrices and communicate the updates to their neighboring IEDs. This process will continue until all of the IEDs have the updated matrices. Given the P and D matrices, IED at each bus will carry out the iterations in equation 6.10. Once the iterations have been performed, the IED at each bus will have the corresponding column of the bus impedance matrix.

6.3 Experimental Results

The proposed algorithm is validated for various IEEE systems. Small modifications are performed on the test cases for simulation purposes e.g., the admittances of generators were absent in the test cases, so typical values of the generator admittances [35] are used in the updated cases. Equation 6.10 is implemented by the IED at each of the buses of the power system. The zero vector is used for the initialization of the columns of the bus impedance matrix in all the IEDs. The iterations are performed using equation 6.10 and the latest result is stored over the $z_{bus,i}$ of the previous iteration. Errors are calculated as the ratio of the Euclidean norm of the difference between the columns of the calculated and the actual bus impedance matrix to the Euclidian norm of the actual respective column of the bus impedance matrix i.e.,

$$error_i = \frac{||z_{bus,i}^{actual} - z_{bus,i}^{calculated}||_2}{|z_{bus,i}^{actual}||_2}$$

where $error_i$ is the error in the estimation of the i^{th} column of the bus impedance matrix.

6.3.1 IEEE 14-bus power system

The convergence behavior of the algorithm at all the 14 buses of the system is shown in Figure 6.1. As is evident in the figure, the errors in all the calculated bus impedance matrix columns recue to zero within 50 iterations. Initially, the convergence is rapid so that the error is reduced to 10% within first 25 iterations.

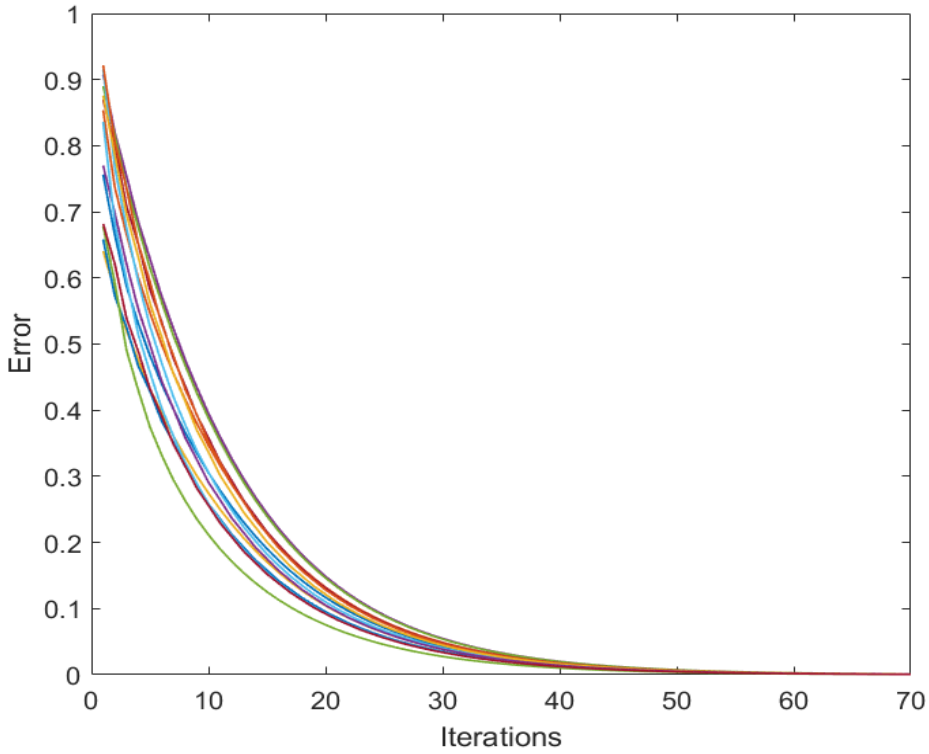

Figure 6.1 - Convergence of the columns of Z_{bus} at various buses for the IEEE 14-bus system.

6.3.2 IEEE 30-bus power system

The proposed algorithm is also validated for IEEE 30-bus system. The system has 41 branches and 6 generators connected at buses 1, 2, 5, 8, 11, 13.

The convergence of the algorithm is shown for all the buses in Figure 6.2. As is evident from the figure, the errors at the buses have converged to near zero within 200 iterations. Intially, the rate of convergenc is very rapid as the errors are reduced to 10% within first 100 iterations.

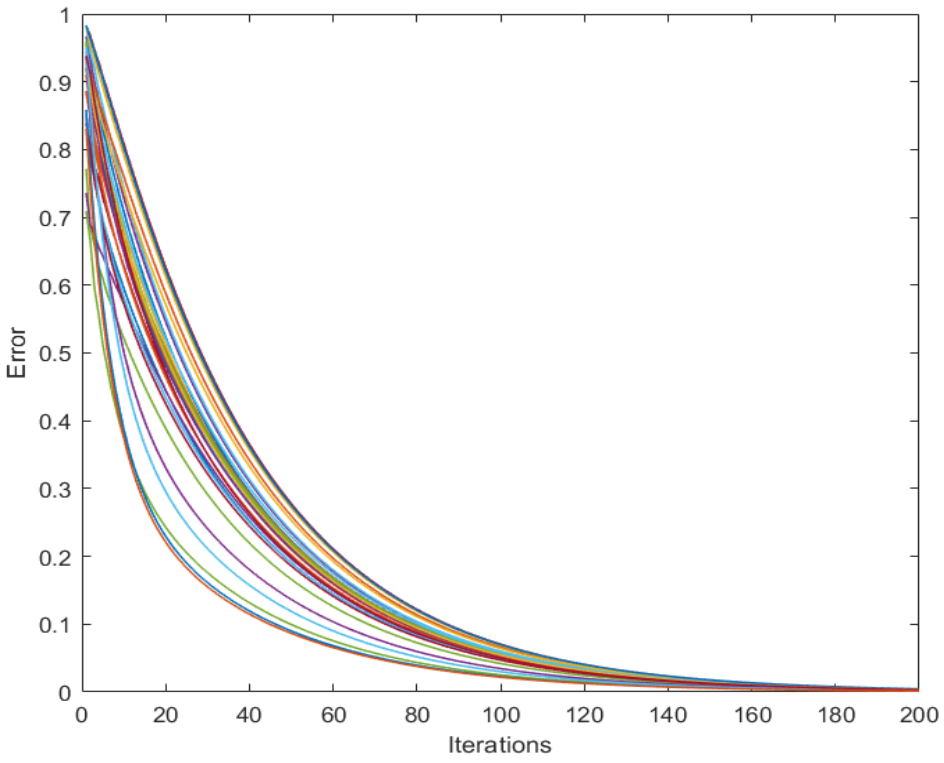

Figure 6.2 - Convergence of columns of Z_{bus} at various buses for IEEE 30-bus system.

6.3.3 IEEE 118-bus power system

The proposed algorithm is also validated for the IEEE 118-bus system. The system has 186 branches and 54 generators connected at various buses. The buses for which the iterations of the algorithm are plotted are bus 1, bus 6, bus 11 ….. bus 116 (i.e. buses are selected with the increment of 5). The convergence of the algorithm for the selected buses is shown through the plot in Figure 6.3. The plot of rest of the buses follow the same course. The error for all the buses falls below 1% within 100 iterations.

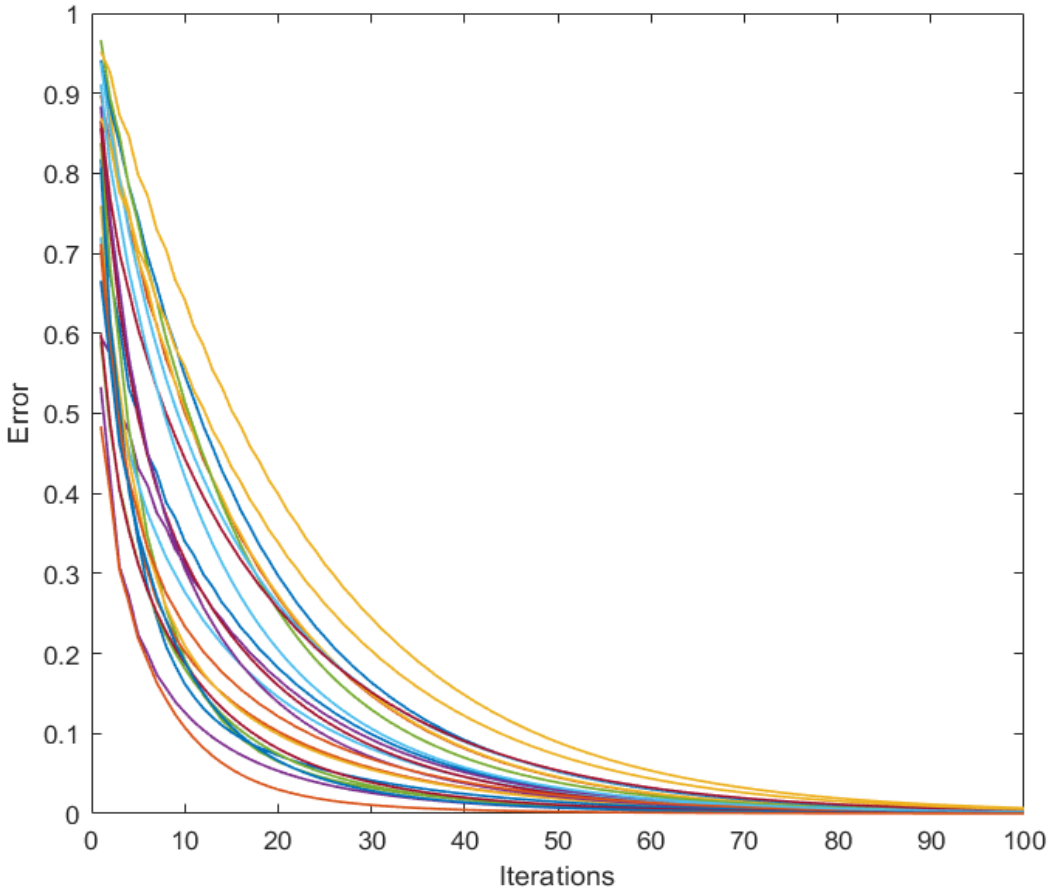

Figure 6.3 - Convergence of columns of Z_{bus} at various buses for IEEE 118-bus system

6.3.4 IEEE 300-bus power system

The proposed algorithm is also validated for the IEEE 300-bus system. The system has 411 branches and 69 generators connected at various buses. The buses for which the iterations of the algorithm are plotted are bus 1, bus 6, bus 11 ….. bus 299 (i.e. buses are selected with the increment of 5). The convergence of the algorithm for the selected buses is shown through the plot in Figure 6.4. The plot of rest of the buses follow the same course. The error for all the buses falls below 1% within 1000 iterations. The errors for all the buses fall under 10% within first half of the iterations.

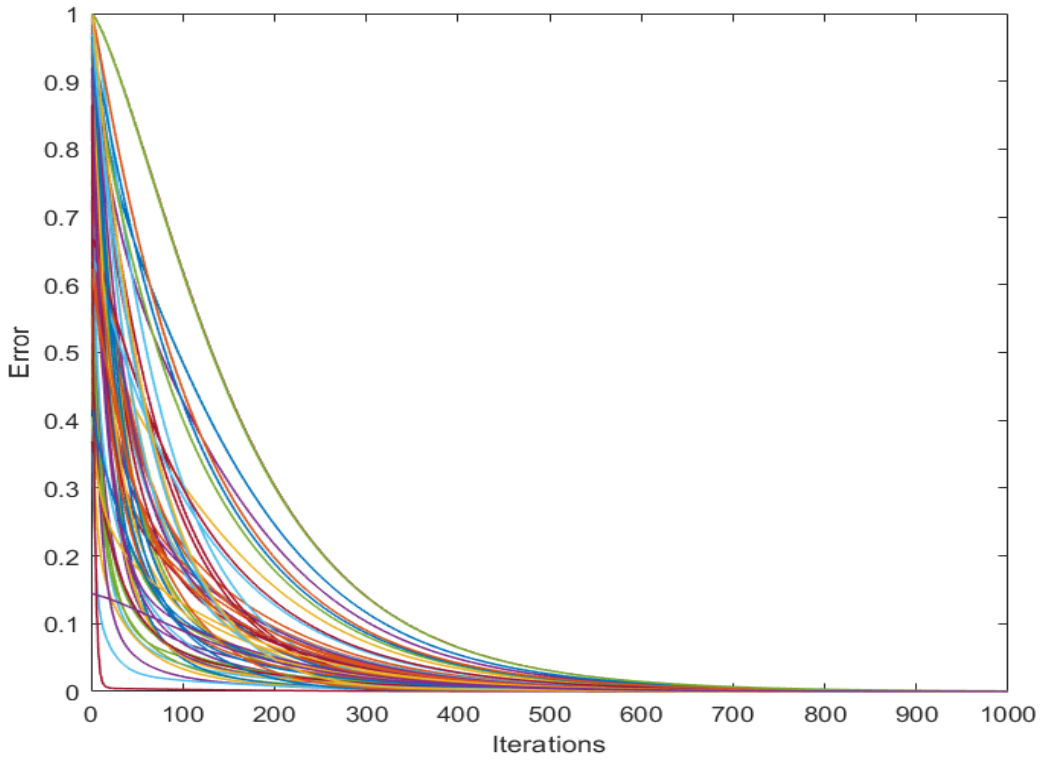

Figure 6.4 - Convergence of columns of Z_{bus} at various buses for IEEE 300-bus system

6.4 Approximation of Thevenin impedances using local information

Although the algorithm as presented will work well for any power system, for bigger systems the communication of the updates at any bus to the far-off buses will be present many practical problems. For example, if a change occurs at one side of a power system, to communicate this information to the bus at the other side of the system, the information will be transmitted through many of the buses and even if the path of shortest delay is used, it will take a considerable amount of time for a practical system. Moreover, in a typical power system there are many changes taking place simultaneously; therefore, communicating all the updates to all the buses will be infeasible.

To overcome this practical difficulty, we can make use of the observation that any

change in a power system results in a significant update only in the corresponding neighboring section of the respective bus impedance matrix.

So even if the changes in a network at any bus are not communicated to the far-off buses, the errors in the resulting calculated columns of the bus impedance matrix will not be much affected. The hypothesis is tested on the IEEE 118 and IEEE 300-bus power systems.

6.5 Experimental Results

At any bus, the calculations are initially performed using only the information from the neighboring buses (tier-1 buses). The Thevenin impedance thus calculated is compared with the actual value of the Thevenin impedance. If the relative error is more than 5%, the calculations are repeated with an additional tier.

This procedure is repeated until the final error is below the threshold of 5%. The plot in the Figure 6.5 shows the trace of the errors for all the 118 buses. It is evident that the errors in all the Thevenin impedances fall below 5% within 100 iterations.

The average number of tiers a bus needed to communicate for achieving the error threshold is 2.9322. The frequency histogram of the various number of tiers for the IEEE 118-bus system is shown in the Figure 6.6.

The average number of buses needed to be communicated for the 5% error in the case of IEEE-118 bus power system is 22. The corresponding histogram showing the number of buses to be communicated with is shown in the Figure 6.7.

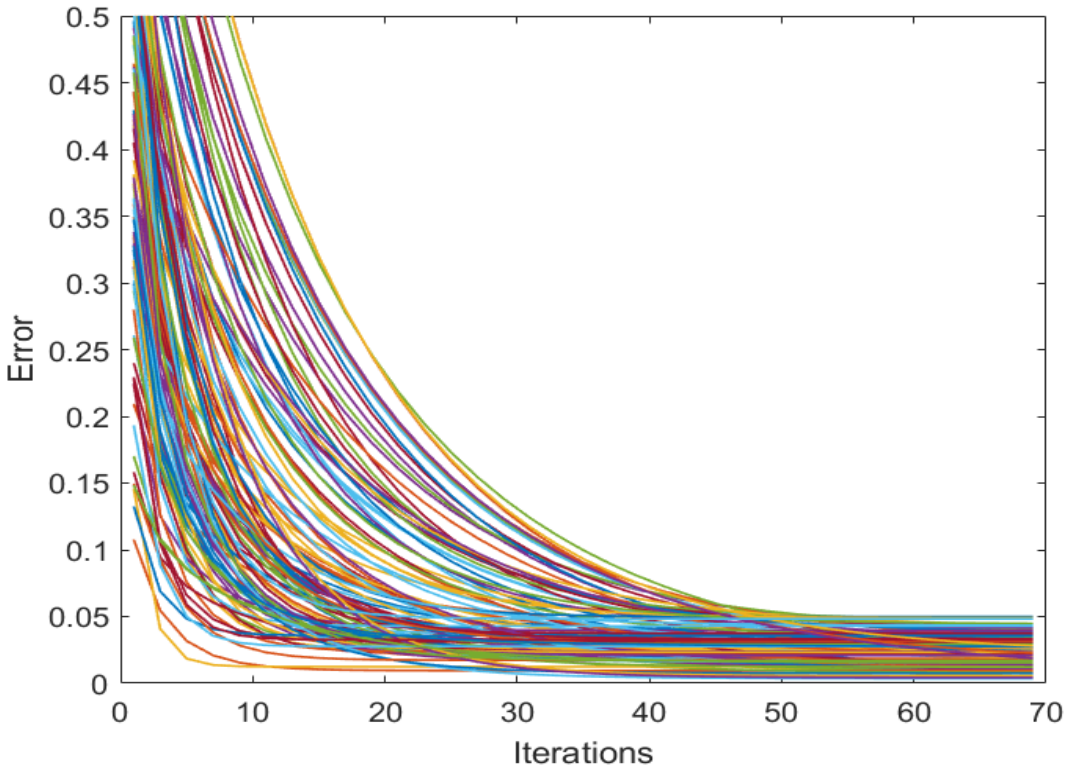

Figure 6.5 - Convergence of columns of Z_{bus} at various buses for IEEE 118-bus system

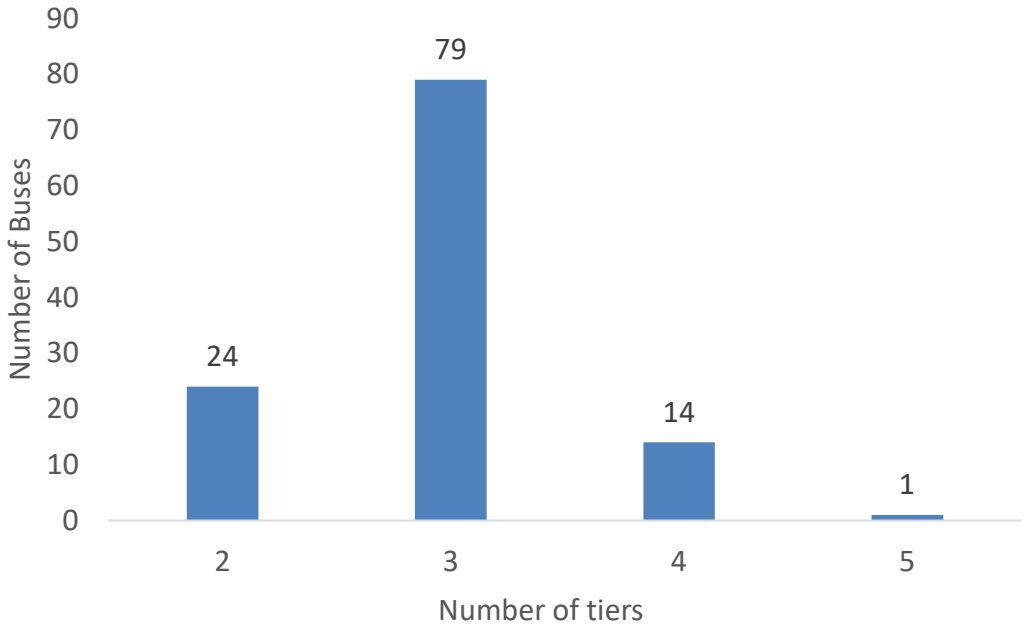

Figure 6.6 – Frequency histogram of the number of tiers for 5% error for IEEE 118-bus system

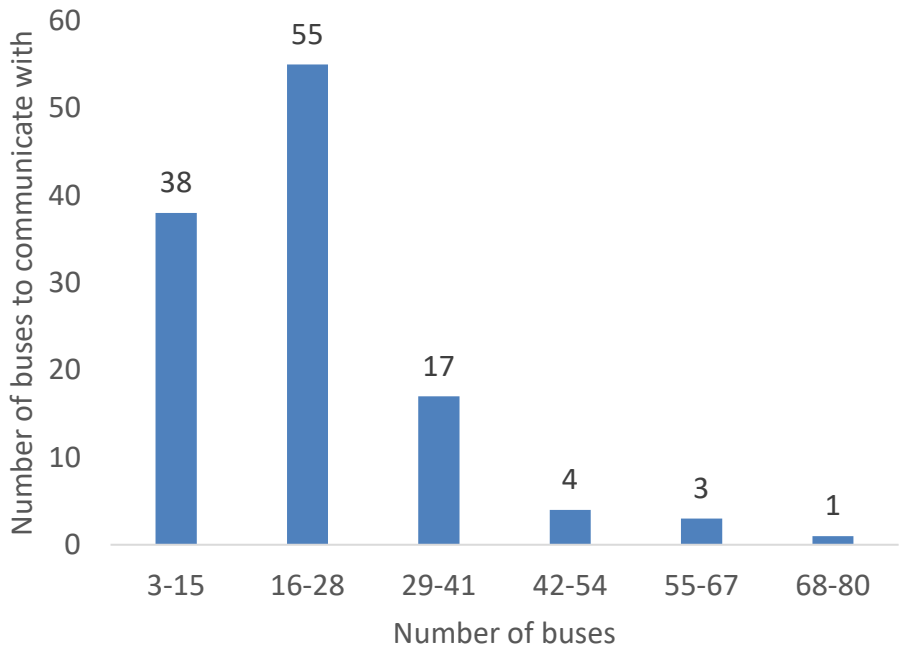

Figure 6.7 – Frequency histogram of the number of buses to be communicated with for 5% error in the IEEE 118-bus system.

The procedure is also repeated for the IEEE-300 power system. Figure 6.8 shows the convergence of the error to the threshold of 5%. Errors for the all the buses has reduced below the threshold within 700 iterations.

The number of tiers a bus needed to communicate to for achieving the error threshold is 4.6. The frequency histogram of the of the various number of tiers for the IEEE 300-bus system is shown in the Figure 6.9.

The average number of buses needed to be communicated for the 5% error in the case of IEEE-300 bus power system is 41. The corresponding histogram showing the number of buses to be communicated with is shown in the Figure 6.10.

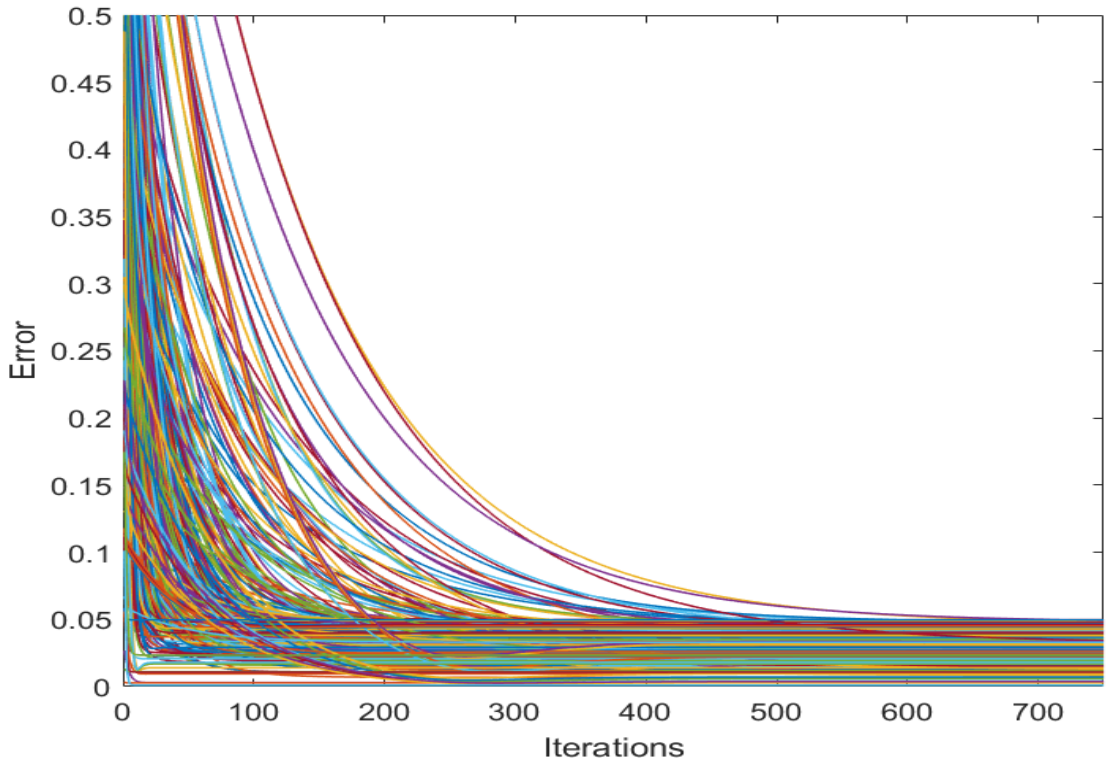

Figure 6.8 - Convergence of the columns of Z_{bus} at various buses for IEEE 300-bus system

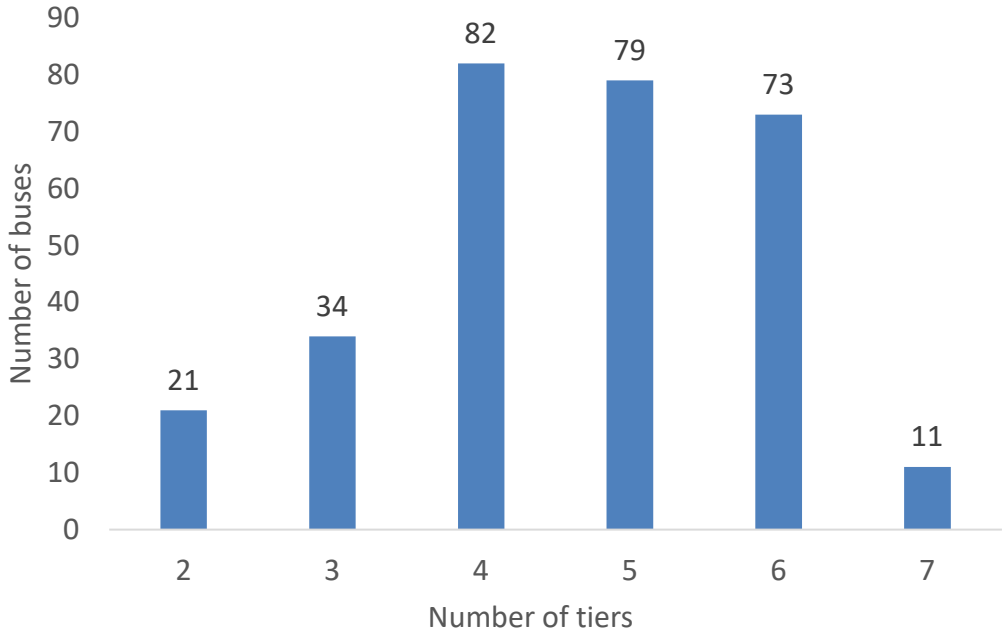

Figure 6.9 – Frequency histogram of the number of tiers for 5% error for IEEE 300-bus system.

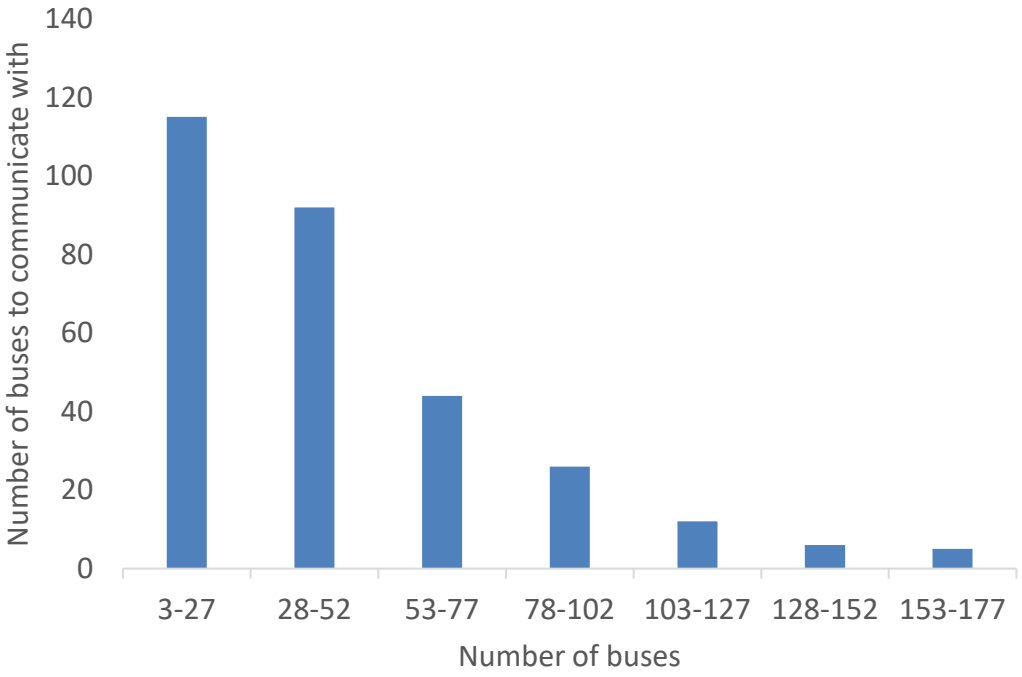

Figure 6.10 – Frequency histogram of the number of buses to be communicated with for 5% error in the IEEE 300-bus system.

6.6 Discussion

From the plots of the section 6.3, it is clear that the columns at the buses of power systems converge to the corresponding columns of the bus impedance matrix. Once the algorithm converges to the columns of the Z_{bus}, the converged result can be used for the settings of the relays. The relays set in such a manner will protect the system in a better way.

CHAPTER 7. CONCLUSION AND FUTURE WORK

In this chapter the concluding remarks regarding the research are presented. The contribution of the research and the ideas regarding the future work are discussed as well. In the future, power systems will be using small-capacity renewable and distributed sources of power unlike the large-capacity conventional thermal power sources. This paradigm shift in the operation of power systems will reduce the pollution produced by the conventional thermal power plants, but it will also introduce many new technical challenges in power system operations. One such major challenge will be the increased magnitude of variations introduced in the power systems due to the addition of renewable sources.

To accommodate such variations while maintaining a reliable operation of a power system, a new set of tools will be required for power system operations. These set of tools should have the ability to accommodate, in real-time, any changes taking place in the power system. The framework suited for such tools is measurement-based as any changes in the power system are reflected in the measurements taken by the instruments. So, the measurement-based tools will be able to accommodate any such changes. Therefore, the results of the analysis and design based on such tools will be more reliable than the model-based offline tools, currently in use.

In the thesis, various measurement-based algorithms are presented. Firstly, the Algorithm 2.1 is presented which uses only the measurements from PMUs to estimate the bus admittance matrix of a power system. The algorithm assumes that the phasor measurements are available, and the underlying power system has sufficient variations in

the boundary conditions (load and generation). Although these variations are not under complete control of a power system operator, it is agreed upon that their magnitude will increase for future power systems. If the assumptions are met, the algorithm will converge near to the actual bus admittance matrix. The Algorithm 2.1 relies only on the measurements from the PMUs and does not consider any prior information about the topology of the system and the parameters of the elements. From the estimated bus admittance matrix, the topology and the parameters of the power system can be estimated.

When the variations in the boundary conditions of a power system are small, there may be some buses (most likely attached through a low-impedance line) in a power system whose voltages are not sufficiently independent. The existence of such buses can cause the problem for the Algorithm 2.1. In the future, however, the variations in the boundary conditions of a power system is likely to increase due to the prevalence of renewable sources. And, therefore, the application of the Algorithm 2.1 will produce satisfactory results. If, however, due to some reason, the variations in the boundary conditions of a power system are small so that the algorithm does not produce an accurate result, then the problem can be addressed by taking into account the prior estimates of the problematic branches, as is done in Algorithm 3.1.

Algorithm 3.1 accommodates any prior information regarding the topology and the elements' parameters. Therefore, the resulting computational complexity of the problem reduces, and the algorithm converges to the actual bus admittance matrix of the system by ensuring that estimated parameters do not deviate much from the prior information about the parameters. The Algorithm 2.1 and the Algorithm 3.1 work fine as long as the faulty measurements are below a certain threshold. If, however, the faulty measurements are

above a certain threshold the results are affected adversely. If the data contains the faulty measurements, it is better to use the robust estimator instead.

In chapter 4, a robust estimator is used instead and through the simulations it is shown that the algorithm outperforms the algorithm of the previous chapter in the presence of faulty measurements.

The Algorithms presented up until fourth chapter are estimating the bus admittance matrix. As long as the assumptions of the algorithms are satisfied, the results will be satisfactory. The primary assumption is that there are enough variations in the loading conditions of the system so that the gram matrix of the voltage matrix is well-conditioned. With the increase in the variability and the increase in the accuracy of measuring devices, this assumption will, most likely, hold for future power system.

For large power systems, there will be proportionally more low impedance lines. These low impedance lines coupled with no or very small variations in the load can cause problems. However, as the current distributes itself such that it follows the path of least impedance, the current variations in the low impedance lines of the power system will be comparatively higher than the other lines in the power system[28]. Therefore, there will be a few lines in the power system that may cause problem in the convergence of the algorithm. One way the problem caused by these lines can be addressed is by accommodating these lines in the prior estimates part of the estimation problem.

[28] The low impedance of the lines, per se, is not problematic. It the combination of low impedance coupled with little or no variations in the line currents that cause problem.

In the algorithm 5.2.1, a dual approach for the estimation of the parameters through the evaluation of the bus impedance matrix of a power system is presented. The problems presented by the algorithm 2.2.1 may be solved by using this dual approach as the matrix that needs to be inverted has a reduced condition number. The parameters are estimated by using the triangular factors of the bus impedance matrix.

Lastly, in chapter 6, a decentralized and distributed algorithm based on the Jacobi iterations is presented for the estimation of the bus impedance matrix. The results available in the intelligent electronic devices (IEDs) can be used for the settings of the relays. The relays set in such a manner will better meet the objectives of power system protection.

7.1 Applications of the work

The algorithms presented in the current work can be used for various applications in the operation and analysis of power system. Some of the applications are mentioned below.

7.1.1 Estimation of the parameters of the elements of a power system

If the assumptions are met, the algorithms presented in the thesis can be used to estimate the parameters of the elements of power system components. These estimates will be more accurate and consider the current operating conditions of the element and system.

7.1.2 Estimation of the topology of the power system

The algorithms presented can also be used to estimates the topology of the network. For example, if the status of some branch of a power system is not known, then its admittance estimated through the algorithms can be used to check whether the branch is in or out of circuit.

7.1.3 Early detection of the aging elements of a power system

Usually, the impedance of a component of a power system changes from their nominal value range when they are about to fail. This change in the value of the parameter, estimated by the algorithm, can be used to detect the component that is likely to fail in near future.

7.1.4 Adaptive settings of the relays

Currently, the relays are set offline in a static manner. That is the offline models of the power systems are used for deciding the relays setting, and once the relays are set, they are seldom updated to adapt the current operating condition of the system. The algorithm presented in chapter 6 can be used to dynamically set the relays using the online parameters of the elements of power systems. The relays set in such a manner will better meet the objectives of power system protection.

7.2 Future work and extensions

The work presented in the thesis has followed a general framework. With a set of assumptions, an objective function was formulated for each estimation problem. The objective function formulated was such that it conformed to certain beliefs about the system and measurements.

Using the same framework, various extensions of the estimation problem can be formulated. Some of the modification are listed below

7.2.1 L_1- Norm minimization

In future power systems, some of the elements will be switched frequently for the reliable and economic operation and to avoid the congestion. If the prior estimates of the admittances of such components are included in the objective function through L_2 −norm, then they will cause the resulting residual to increase when they will be switched out of the circuit. A better way to include such type of components in the objective will be through L_1 − norm.

So, a possible objective function, for such power systems, can be a combination of the two objective functions. The first one based on the L_2-norm minimization for the components that are supposed to be in the power system all the time. Whereas the second one based on the L_1-norm minimization for the components that are more likely to switch to ensure an efficient and reliable operation of power system.

7.2.2 Recursive QR Factorization

In the thesis, QR factorization has been used for the estimation of the matrices. Though modern computers are fast, and the required calculations can be performed in a manageable time, the computations, and therefore the resulting time, can be reduced by using the recursive QR factorization.

Depending on the size of the system, only a specific number of measurements are required to the estimate of the bus admittance matrix. Let us assume that this number is p. The number of measurements in the matrices is kept equal to p by deleting the oldest

measurement whenever a new set of measurement is received. This procedure will keep the size of the measurement matrices equal to $n \times p$.

As after the arrival of each new set of measurements, the measurement matrices will be only slightly updated, there is no need to carry out the complete QR factorization of the matrix. Instead, the QR factors of the updated matrix can be easily obtained by performing a small number of operations on the factors of the previous matrix by using the recursive QR factorization.

7.2.3 Online convex optimization

In the thesis, a robust estimator is used for the estimation of the power system matrix. The algorithm works in the batch mode and assumes all the measurements have been received before it is run. A possible future extension can be to estimate the matrices by using the online convex optimization.

7.2.4 Total least squares

In the thesis, the errors in the coefficient matrix of the optimization problem are considered using the regularization. Another way to take this into account is by using the error in the variable model, also known as total least squares.

APPENDIX

The appendix contains the parameter information of various IEEE power systems used in validating the algorithms of the thesis.

a) IEEE 14-BUS POWER SYSTEM

Bus		Impedance (pu)		
From	**To**	**R**	**X**	**B**
1	2	0.01938	0.05917	0.0528
1	5	0.05403	0.22304	0.0492
2	3	0.04699	0.19797	0.0438
2	4	0.05811	0.17632	0.034
2	5	0.05695	0.17388	0.0346
3	4	0.06701	0.17103	0.0128
4	5	0.01335	0.04211	0
4	7	0	0.20912	0
4	9	0	0.55618	0
5	6	0	0.25202	0
6	11	0.09498	0.1989	0
6	12	0.12291	0.25581	0
6	13	0.06615	0.13027	0
7	8	0	0.17615	0
7	9	0	0.11001	0
9	10	0.03181	0.0845	0
9	14	0.12711	0.27038	0
10	11	0.08205	0.19207	0
12	13	0.22092	0.19988	0
13	14	0.17093	0.34802	0

b) IEEE 23-BUS POWER SYSTEM

Bus		Impedance (pu)		
From	**To**	**R**	**X**	**B**
1	2	0.0026	0.0139	0.4611
1	3	0.0546	0.2112	0.0572
1	5	0.0218	0.0845	0.0229
2	4	0.0328	0.1267	0.0343
2	6	0.0497	0.192	0.052
3	9	0.0308	0.119	0.0322
3	24	0.0023	0.0839	0
4	9	0.0268	0.1037	0.0281
5	10	0.0228	0.0883	0.0239
6	10	0.0139	0.0605	2.459
7	8	0.0159	0.0614	0.0166
8	9	0.0427	0.1651	0.0447
8	10	0.0427	0.1651	0.0447
9	11	0.0023	0.0839	0
9	12	0.0023	0.0839	0
10	11	0.0023	0.0839	0
10	12	0.0023	0.0839	0
11	13	0.0061	0.0476	0.0999
11	14	0.0054	0.0418	0.0879
12	13	0.0061	0.0476	0.0999
12	23	0.0124	0.0966	0.203
13	23	0.0111	0.0865	0.1818
14	16	0.005	0.0389	0.0818
15	16	0.0022	0.0173	0.0364
15	21	0.0063	0.049	0.103
15	21	0.0063	0.049	0.103

15	24	0.0067	0.0519	0.1091
16	17	0.0033	0.0259	0.0545
16	19	0.003	0.0231	0.0485
17	18	0.0018	0.0144	0.0303
17	22	0.0135	0.1053	0.2212
18	21	0.0033	0.0259	0.0545
18	21	0.0033	0.0259	0.0545
19	20	0.0051	0.0396	0.0833
19	20	0.0051	0.0396	0.0833
20	23	0.0028	0.0216	0.0455
20	23	0.0028	0.0216	0.0455
21	22	0.0087	0.0678	0.1424

c) IEEE 30-BUS POWER SYSTEM

Bus		**Impedance (pu)**		
From	**To**	**R**	**X**	**B**
1	2	0.02	0.06	0.03
1	3	0.05	0.19	0.02
2	4	0.06	0.17	0.02
3	4	0.01	0.04	0
2	5	0.05	0.2	0.02
2	6	0.06	0.18	0.02
4	6	0.01	0.04	0
5	7	0.05	0.12	0.01
6	7	0.03	0.08	0.01
6	8	0.01	0.04	0
6	9	0	0.21	0
6	10	0	0.56	0

9	11	0	0.21	0
9	10	0	0.11	0
4	12	0	0.26	0
12	13	0	0.14	0
12	14	0.12	0.26	0
12	15	0.07	0.13	0
12	16	0.09	0.2	0
14	15	0.22	0.2	0
16	17	0.08	0.19	0
15	18	0.11	0.22	0
18	19	0.06	0.13	0
19	20	0.03	0.07	0
10	20	0.09	0.21	0
10	17	0.03	0.08	0
10	21	0.03	0.07	0
10	22	0.07	0.15	0
21	22	0.01	0.02	0
15	23	0.1	0.2	0
22	24	0.12	0.18	0
23	24	0.13	0.27	0
24	25	0.19	0.33	0
25	26	0.25	0.38	0
25	27	0.11	0.21	0
28	27	0	0.4	0
27	29	0.22	0.42	0
27	30	0.32	0.6	0
29	30	0.24	0.45	0
8	28	0.06	0.2	0.02
6	28	0.02	0.06	0.01

d) IEEE 118-BUS POWER SYSTEM

Bus		Impedance (pu)		
From	**To**	**R**	**X**	**B**
1	2	0.0303	0.0999	0.0254
1	3	0.0129	0.0424	0.01082
4	5	0.00176	0.00798	0.0021
3	5	0.0241	0.108	0.0284
5	6	0.0119	0.054	0.01426
6	7	0.00459	0.0208	0.0055
8	9	0.00244	0.0305	1.162
8	5	0	0.0267	0
9	10	0.00258	0.0322	1.23
4	11	0.0209	0.0688	0.01748
5	11	0.0203	0.0682	0.01738
11	12	0.00595	0.0196	0.00502
2	12	0.0187	0.0616	0.01572
3	12	0.0484	0.16	0.0406
7	12	0.00862	0.034	0.00874
11	13	0.02225	0.0731	0.01876
12	14	0.0215	0.0707	0.01816
13	15	0.0744	0.2444	0.06268
14	15	0.0595	0.195	0.0502
12	16	0.0212	0.0834	0.0214
15	17	0.0132	0.0437	0.0444
16	17	0.0454	0.1801	0.0466
17	18	0.0123	0.0505	0.01298
18	19	0.01119	0.0493	0.01142
19	20	0.0252	0.117	0.0298
15	19	0.012	0.0394	0.0101

20	21	0.0183	0.0849	0.0216
21	22	0.0209	0.097	0.0246
22	23	0.0342	0.159	0.0404
23	24	0.0135	0.0492	0.0498
23	25	0.0156	0.08	0.0864
26	25	0	0.0382	0
25	27	0.0318	0.163	0.1764
27	28	0.01913	0.0855	0.0216
28	29	0.0237	0.0943	0.0238
30	17	0	0.0388	0
8	30	0.00431	0.0504	0.514
26	30	0.00799	0.086	0.908
17	31	0.0474	0.1563	0.0399
29	31	0.0108	0.0331	0.0083
23	32	0.0317	0.1153	0.1173
31	32	0.0298	0.0985	0.0251
27	32	0.0229	0.0755	0.01926
15	33	0.038	0.1244	0.03194
19	34	0.0752	0.247	0.0632
35	36	0.00224	0.0102	0.00268
35	37	0.011	0.0497	0.01318
33	37	0.0415	0.142	0.0366
34	36	0.00871	0.0268	0.00568
34	37	0.00256	0.0094	0.00984
38	37	0	0.0375	0
37	39	0.0321	0.106	0.027
37	40	0.0593	0.168	0.042
30	38	0.00464	0.054	0.422
39	40	0.0184	0.0605	0.01552
40	41	0.0145	0.0487	0.01222

40	42	0.0555	0.183	0.0466
41	42	0.041	0.135	0.0344
43	44	0.0608	0.2454	0.06068
34	43	0.0413	0.1681	0.04226
44	45	0.0224	0.0901	0.0224
45	46	0.04	0.1356	0.0332
46	47	0.038	0.127	0.0316
46	48	0.0601	0.189	0.0472
47	49	0.0191	0.0625	0.01604
42	49	0.0715	0.323	0.086
42	49	0.0715	0.323	0.086
45	49	0.0684	0.186	0.0444
48	49	0.0179	0.0505	0.01258
49	50	0.0267	0.0752	0.01874
49	51	0.0486	0.137	0.0342
51	52	0.0203	0.0588	0.01396
52	53	0.0405	0.1635	0.04058
53	54	0.0263	0.122	0.031
49	54	0.073	0.289	0.0738
49	54	0.0869	0.291	0.073
54	55	0.0169	0.0707	0.0202
54	56	0.00275	0.00955	0.00732
55	56	0.00488	0.0151	0.00374
56	57	0.0343	0.0966	0.0242
50	57	0.0474	0.134	0.0332
56	58	0.0343	0.0966	0.0242
51	58	0.0255	0.0719	0.01788
54	59	0.0503	0.2293	0.0598
56	59	0.0825	0.251	0.0569
56	59	0.0803	0.239	0.0536

55	59	0.04739	0.2158	0.05646
59	60	0.0317	0.145	0.0376
59	61	0.0328	0.15	0.0388
60	61	0.00264	0.0135	0.01456
60	62	0.0123	0.0561	0.01468
61	62	0.00824	0.0376	0.0098
63	59	0	0.0386	0
63	64	0.00172	0.02	0.216
64	61	0	0.0268	0
38	65	0.00901	0.0986	1.046
64	65	0.00269	0.0302	0.38
49	66	0.018	0.0919	0.0248
49	66	0.018	0.0919	0.0248
62	66	0.0482	0.218	0.0578
62	67	0.0258	0.117	0.031
65	66	0	0.037	0
66	67	0.0224	0.1015	0.02682
65	68	0.00138	0.016	0.638
47	69	0.0844	0.2778	0.07092
49	69	0.0985	0.324	0.0828
68	69	0	0.037	0
69	70	0.03	0.127	0.122
24	70	0.00221	0.4115	0.10198
70	71	0.00882	0.0355	0.00878
24	72	0.0488	0.196	0.0488
71	72	0.0446	0.18	0.04444
71	73	0.00866	0.0454	0.01178
70	74	0.0401	0.1323	0.03368
70	75	0.0428	0.141	0.036
69	75	0.0405	0.122	0.124

74	75	0.0123	0.0406	0.01034
76	77	0.0444	0.148	0.0368
69	77	0.0309	0.101	0.1038
75	77	0.0601	0.1999	0.04978
77	78	0.00376	0.0124	0.01264
78	79	0.00546	0.0244	0.00648
77	80	0.017	0.0485	0.0472
77	80	0.0294	0.105	0.0228
79	80	0.0156	0.0704	0.0187
68	81	0.00175	0.0202	0.808
81	80	0	0.037	0
77	82	0.0298	0.0853	0.08174
82	83	0.0112	0.03665	0.03796
83	84	0.0625	0.132	0.0258
83	85	0.043	0.148	0.0348
84	85	0.0302	0.0641	0.01234
85	86	0.035	0.123	0.0276
86	87	0.02828	0.2074	0.0445
85	88	0.02	0.102	0.0276
85	89	0.0239	0.173	0.047
88	89	0.0139	0.0712	0.01934
89	90	0.0518	0.188	0.0528
89	90	0.0238	0.0997	0.106
90	91	0.0254	0.0836	0.0214
89	92	0.0099	0.0505	0.0548
89	92	0.0393	0.1581	0.0414
91	92	0.0387	0.1272	0.03268
92	93	0.0258	0.0848	0.0218
92	94	0.0481	0.158	0.0406
93	94	0.0223	0.0732	0.01876

94	95	0.0132	0.0434	0.0111
80	96	0.0356	0.182	0.0494
82	96	0.0162	0.053	0.0544
94	96	0.0269	0.0869	0.023
80	97	0.0183	0.0934	0.0254
80	98	0.0238	0.108	0.0286
80	99	0.0454	0.206	0.0546
92	100	0.0648	0.295	0.0472
94	100	0.0178	0.058	0.0604
95	96	0.0171	0.0547	0.01474
96	97	0.0173	0.0885	0.024
98	100	0.0397	0.179	0.0476
99	100	0.018	0.0813	0.0216
100	101	0.0277	0.1262	0.0328
92	102	0.0123	0.0559	0.01464
101	102	0.0246	0.112	0.0294
100	103	0.016	0.0525	0.0536
100	104	0.0451	0.204	0.0541
103	104	0.0466	0.1584	0.0407
103	105	0.0535	0.1625	0.0408
100	106	0.0605	0.229	0.062
104	105	0.00994	0.0378	0.00986
105	106	0.014	0.0547	0.01434
105	107	0.053	0.183	0.0472
105	108	0.0261	0.0703	0.01844
106	107	0.053	0.183	0.0472
108	109	0.0105	0.0288	0.0076
103	110	0.03906	0.1813	0.0461
109	110	0.0278	0.0762	0.0202
110	111	0.022	0.0755	0.02

110	112	0.0247	0.064	0.062
17	113	0.00913	0.0301	0.00768
32	113	0.0615	0.203	0.0518
32	114	0.0135	0.0612	0.01628
27	115	0.0164	0.0741	0.01972
114	115	0.0023	0.0104	0.00276
68	116	0.00034	0.00405	0.164
12	117	0.0329	0.14	0.0358
75	118	0.0145	0.0481	0.01198
76	118	0.0164	0.0544	0.01356

References

[1] A. J. Wood, B. F. Wollenberg, and G. B. Sheblé, *Power Generation Operation and Control*, 3rd ed. Wiley-Interscience, 2013.

[2] N. Smit, J . J. (Fac. of Electr. Eng., Mathematics & Comput. Sci., Delft Univ. of Technol., "Trends in Emerging Technologies in Power Systems," in *International Conference on Future Power Systems*, 2005.

[3] F. Li *et al.*, "Smart transmission grid: Vision and framework," *IEEE Trans. Smart Grid*, vol. 1, no. 2, pp. 168–177, 2010.

[4] A. Osmani, J. Zhang, V. Gonela, and I. Awudu, "Electricity generation from renewables in the United States: Resource potential, current usage, technical status, challenges, strategies, policies, and future directions," *Renewable and Sustainable Energy Reviews*, vol. 24. Pergamon, pp. 454–472, 01-Aug-2013.

[5] M. Pipattanasomporn, M. Willingham, and S. Rahman, "Implications of on-site distributed generation for commercial/industrial facilities," *IEEE Trans. Power Syst.*, vol. 20, no. 1, pp. 206–212, Feb. 2005.

[6] M. H. Nazari, Z. Costello, M. J. Feizollahi, S. Grijalva, and M. Egerstedt, "Distributed Frequency Control of Prosumer-Based Electric Energy Systems," *IEEE Trans. Power Syst.*, vol. 29, no. 6, pp. 2934–2942, 2014.

[7] T. F. Garrity, "Innovation and trends for future electric power systems," in *2009 Power Systems Conference: Advance Metering, Protection, Control, Communication, and Distributed Resources, PSC 2009*, 2009, pp. 253–260.

[8] L. Bird, M. Milligan, and D. Lew, "Integrating Variable Renewable Energy: Challenges and Solutions," *NREL/TP-6A20-60451*, no. September, p. 14, 2013.

[9] EPRI, "Electric Power System Flexibility: Challenges and Opportunities," 2016.

[10] E. Hillberg *et al.*, "Flexibility needs in the future power system," 2019.

[11] M. I. Alizadeh, M. Parsa Moghaddam, N. Amjady, P. Siano, and M. K. Sheikh-El-Eslami, "Flexibility in future power systems with high renewable penetration: A review," *Renewable and Sustainable Energy Reviews*, vol. 57. Elsevier Ltd, pp. 1186–1193, 01-May-2016.

[12] E. Kabalci, "Power system flexibility and resiliency," in *Power Systems*, Springer, Berlin, Heidelberg, 2019, pp. 81–100.

[13] S. R. Salkuti, "Congestion management using optimal transmission switching," *IEEE Syst. J.*, vol. 12, no. 4, 2018.

[14] K. W. Hedman, S. S. Oren, and R. P. O'Neill, "A review of transmission switching and network topology optimization," in *IEEE Power and Energy Society General Meeting*, 2011, pp. 1–7.

[15] B. Kocuk, S. S. Dey, and X. A. Sun, “New Formulation and Strong MISOCP Relaxations for AC Optimal Transmission Switching Problem,” *IEEE Trans. Power Syst.*, vol. 32, no. 6, pp. 4161–4170, Nov. 2017.

[16] K. W. Hedman, R. P. O’Neill, E. B. Fisher, and S. S. Oren, “Optimal Transmission Switching With Contigency Analysis,” *IEEE Trans. power Deliv.*, vol. 24, pp. 1576–1577, 2009.

[17] Z. Dong and P. Zhang, *Emerging techniques in power system analysis*. Springer, Berlin, Heidelberg, 2009.

[18] A. Atputharajah and T. K. Saha, “Power system blackouts - literature review,” in *ICIIS 2009 - 4th International Conference on Industrial and Information Systems 2009, Conference Proceedings*, 2009, pp. 460–465.

[19] Y. K. Wu, S. M. Chang, and Y. L. Hu, “Literature Review of Power System Blackouts,” in *Energy Procedia*, 2017, vol. 141, pp. 428–431.

[20] F. F. Wu, K. Moslehi, and A. Bose, “Power system control centers: Past, present, and future,” in *Proceedings of the IEEE*, 2005, vol. 93, no. 11, pp. 1890–1908.

[21] I. D. Kim and R. K. Aggarwal, “A study on the on-line measurement of transmission line impedances for improved relaying protection,” *Int. J. Electr. Power Energy Syst.*, 2006.

[22] A. Abur and A. G. Expósito, *Power System State Estimation: Theory and Implementation*. 2004.

[23] A. G. Phadke, P. Wall, L. Ding, and V. Terzija, “Improving the performance of power system protection using wide area monitoring systems,” *J. Mod. Power Syst. Clean Energy*, vol. 4, no. 3, pp. 319–331, 2016.

[24] U.S.-Canada Power System Outage Task Force, “Final Report on the August 14, 2003 Blackout in the United States and Canada: Causes and Recommendations,” 2004.

[25] J. L. Crassidis and J. L. Junkins, *Optimal Estimation of Dynamic Systems*, 2nd ed. Chapman & Hall/CRC Applied Mathematics & Nonlinear Science, 2011.

[26] A. G. Phadke, “Synchronized phasor measurements ~ a historical overview,” in *Proceedings of the IEEE Power Engineering Society Transmission and Distribution Conference*, 2002.

[27] F. Aminifar, M. Fotuhi-Firuzabad, A. Safdarian, A. Davoudi, and M. Shahidehpour, “Synchrophasor Measurement Technology in Power Systems: Panorama and State-of-the-Art,” *IEEE Access*, vol. 2, pp. 1607–1628, 2014.

[28] Y. Du and Y. Liao, “On-line estimation of transmission line parameters, temperature and sag using PMU measurements,” *Electr. Power Syst. Res.*, vol. 93, pp. 39–45, 2012.

[29] J. C. N. Pantoja, A. Olarte, and H. Díaz, “Simultaneous estimation of exciter, governor and synchronous generator parameters using phasor measurements,” *9th Int. 2014 Electr. Power Qual. Supply Reliab. Conf. PQ 2014 - Proc.*, pp. 43–49, 2014.

[30] M. Saadeh, M. Alsarray, and R. McCann, “Estimation of the bus admittance matrix for transmission systems from synchrophasor data,” in *Proceedings of the IEEE Power Engineering Society Transmission and Distribution Conference*, 2016, vol. 2016-July.

[31] Y. C. Chen, A. D. Dominguez-Garcia, and P. W. Sauer, “Measurement-based estimation of linear sensitivity distribution factors and applications,” *IEEE Trans. Power Syst.*, vol. 29, no. 3, pp. 1372–1382, 2014.

[32] Y. C. Chen, S. Member, A. D. Domínguez-garcía, P. W. Sauer, and L. Fellow, “A Sparse Representation Approach to Online Estimation of Power System Distribution Factors,” *IEEE Trans. Power Syst*, vol. 30, no. 4, pp. 1727–1738, 2015.

[33] X. Zhao, H. Zhou, D. Shi, H. Zhao, C. Jing, and C. Jones, “On-line PMU-based transmission line parameter identification,” *CSEE J. Power Energy Syst.*, vol. 1, no. 2, pp. 68–74, 2015.

[34] J. E. Chadwick, “How a smarter grid could have prevented the 2003 U.S. cascading blackout,” in *2013 IEEE Power and Energy Conference at Illinois, PECI 2013*, 2013, pp. 65–71.

[35] J. J. Grainger and W. D. Stevenson, *Power system analysis*. McGraw-Hill Education, 1994.

[36] J. De La Ree, V. Centeno, J. S. Thorp, and A. G. Phadke, “Synchronized phasor measurement applications in power systems,” *IEEE Trans. Smart Grid*, vol. 1, no. 1, pp. 20–27, 2010.

[37] S. (NDR) Nuthalapati, Ed., *Power System Grid Operation Using Synchrophasor Technology*. Springer International Publishing AG, 2019.

[38] A. G. Phadke and K. J. Karimi, “Real time voltage-phasor measurements for static state estimation,” *IEEE Trans. Power Appar. Syst.*, 1985.

[39] A. G. Phadke, J. S. Thorp, and K. J. Karimi, “State estimation with phasor measurements,” *IEEE Trans. Power Syst.*, 1986.

[40] D. Kosterev, “Hydro turbine-governor model validation in pacific northwest,” *IEEE Trans. Power Syst.*, 2004.

[41] Z. Huang, P. Du, D. Kosterev, and S. Yang, “Generator dynamic model validation and parameter calibration using phasor measurements at the point of connection,” *IEEE Trans. Power Syst.*, 2013.

[42] L. Fan, Z. Miao, and Y. Wehbe, “Application of dynamic state and parameter estimation techniques on real-world data,” *IEEE Trans. Smart Grid*, 2013.

[43] P. Overholt, D. Kosterev, J. Eto, S. Yang, and B. Lesieutre, “Improving reliability through better models: Using synchrophasor data to validate power plant models,” *IEEE Power Energy Mag.*, 2014.

[44] J. Ma, D. Han, W. J. Sheng, R. M. He, C. Y. Yue, and J. Zhang, “Wide area measurements-based model validation and its application,” *IET Gener. Transm. Distrib.*, 2008.

[45] J. A. Jiang, J. Z. Yang, Y. H. Lin, C. W. Liu, and J. C. Ma, “An adaptive PMU based fault detection/location technique for transmission lines part I: Theory and algorithms,” *IEEE Trans. POWER Deliv.*, vol. 15, no. 2, pp. 486–493, 2000.

[46] J. E. Tate and T. J. Overbye, “Line outage detection using phasor angle measurements,” *IEEE Trans. Power Syst.*, 2008.

[47] M. M. Adibi and N. Martins, “Impact of power system blackouts,” in *IEEE Power and Energy Society General Meeting*, 2015, pp. 1–15.

[48] N. A. E. R. C. Federal Energy Regulatory Commission, “Arizona-Southern California Outages on September 8, 2011 Causes and Recommendations,” 2011.

[49] U.S. Department of Energy, “Synchrophasor Technologies and their Deployment in the Recovery Act Smart Grid Programs,” 2013.

[50] M. Kezunovic, S. Meliopoulos, V. Venkatasubramanian, and V. Vittal, *Application of Time-Synchronized Measurements in Power System Transmission Networks*. Power Electronics and Power Systems, Springer, 2014.

[51] R. F. Nuqui and A. G. Phadke, “Phasor measurement unit placement techniques for complete and incomplete observability,” *IEEE Trans. Power Deliv.*, vol. 20, no. 4, pp. 2381–2388, Oct. 2005.

[52] W. Yuill, A. Edwards, S. Chowdhury, and S. P. Chowdhury, “Optimal PMU placement: A comprehensive literature review,” in *IEEE Power and Energy Society General Meeting*, 2011.

[53] V. Madani *et al.*, “PMU placement considerations - A roadmap for optimal PMU placement,” in *2011 IEEE/PES Power Systems Conference and Exposition, PSCE 2011*, 2011.

[54] B. K. Saha Roy, A. K. Sinha, and A. K. Pradhan, “An optimal PMU placement technique for power system observability,” *Int. J. Electr. Power Energy Syst.*, vol. 42, no. 1, pp. 71–77, Nov. 2012.

[55] N. M. Manousakis, G. N. Korres, and P. S. Georgilakis, “Taxonomy of PMU placement methodologies,” *IEEE Trans. Power Syst.*, vol. 27, no. 2, pp. 1070–1077, May 2012.

[56] E. O. Schweitzer, D. E. Whitehead, and G. Zweigle, “Practical synchronized phasor solutions,” in *2009 IEEE Power and Energy Society General Meeting, PES ’09*, 2009, pp. 1–8.

[57] G. Benmouyal, E. O. Schweitzer, and A. Guzmán, “Synchronized phasor measurement in protective relays for protection, control, and analysis of electric power systems,” *Annu. Conf. Prot. Relay Eng.*, pp. 419–450, 2004.

[58] G. L. Kusic and D. L. Garrison, “Measurement of transmission line parameters from SCADA data,” in *IEEE PES Power Systems Conference and Exposition, 2004.*, pp. 344–349.

[59] B. Stephen and L. Vandenberghe, *Introduction to Applied Linear Algebra – Vectors, Matrices, and Least Squares*. Cambridge University Press, 2018.

[60] G. H. Golub and C. F. Van Loan, *Matrix Computations*, Fourth edi. Johns Hopkins University Press, 2012.

[61] S. Boyd and L. Vandenberghe, *Convex Optimization*. Cambridge University Press, 2004.

[62] G. Dahlquist and Å. Björck, *Numerical Methods in Scientific Computing Volume II*. 2008.

[63] loyd N. Trefethen and D. B. III, *Numerical Linear Algebra*. SIAM: Society for Industrial and Applied Mathematics.

[64] T. K. Moon and W. C. Stirling, *Mathematical Methods and Algorithms for Signal Processing*. Pearson, 1999.

[65] T. H. Cormen, C. E. Leiserson, R. L. Rivest, and C. Stein, *Introduction to Algorithms*, 3rd Editio. The MIT Press, 2009.

[66] “Power Systems Test Case Archive.” [Online]. Available: https://www2.ee.washington.edu/research/pstca/pf14/pg_tca14bus.htm. [Accessed: 24-Apr-2018].

[67] R. D. Zimmerman, C. E. Murillo-Sanchez, and R. J. Thomas, “MATPOWER: Steady-State Operations, Planning, and Analysis Tools for Power Systems Research and Education,” *IEEE Trans. Power Syst.*, vol. 26, no. 1, pp. 12–19, 2011.

[68] S. Blackford, *LAPACK Users’ Guide*, Third Edit. SIAM, 1999.

[69] A. Papoulis and S. Unnikrishna Pillai, *Probability, Random Variables and Stochastic Processes*, 4th ed. McGraw-Hill Europe, 2002.

[70] S. R. B. PAITHANKAR, Y.G., *Fundamentals of Power System Protection*, Second edi. 2013.

[71] D. P. Bertsekas and J. N. Tsitsiklis, *Parallel and Distributed Computation: Numerical Methods*, 1st editio. Athena Scientific, 1989.

[72] A. Keyhani, *Design of smart power grid renewable energy systems*. Wiley, 2011.

[73] Y. Yang, F. Lambert, and D. Divan, “A Survey on Technologies for Implementing Sensor Networks for Power Delivery Systems,” in *2007 IEEE Power Engineering*

Society General Meeting, 2007, pp. 1–8.

[74] Yi Yang, D. Divan, R. G. Harley, and T. G. Habetler, “Power line sensornet - a new concept for power grid monitoring,” *2006 IEEE Power Eng. Soc. Gen. Meet.*, vol. 0250, p. 8 pp., 2006.

[75] Y. Yang, D. Divan, G. Harley, and T. G. Habetler, “Design and Implementation of Power Line Sensornet for Overhead Transmission Lines,” *Ieee*, vol. 0250, pp. 1–8, 2009.

[76] K. E. Martin *et al.*, “Exploring the IEEE standard C37.118-2005 synchrophasors for power systems,” *IEEE Trans. Power Deliv.*, vol. 23, no. 4, pp. 1805–1811, 2008.